NASA Tech Briefs

National Aeronautics and
Space Administration

September/October 1986
Volume 10 Number 5

Pioneering the Space Frontier:

The Report of the National Commission on Space

In space: looking back to look forward.

What can the nature and origin of the universe tell us about the future of Earth? To help answer that question, we make craft and instruments for traveling billions of miles in space and seeing as far as 15 billion years back in time. Martin Marietta was the integrator and builder of two Viking landers, which sent back remarkable photos of the surface of Mars, examined soil samples, and studied Martian weather and seismic activity. For the Voyagers we provided instrumentation that reported on electromagnetic activity near Jupiter and Saturn—Voyager 2 went on to Uranus, some 2 billion miles from Earth. That was nine years after launch; next destination, Neptune, in 1989. These are but a few results of Martin Marietta's ability to create survivable, mystery-solving craft and their instruments—from concept through mission completion.

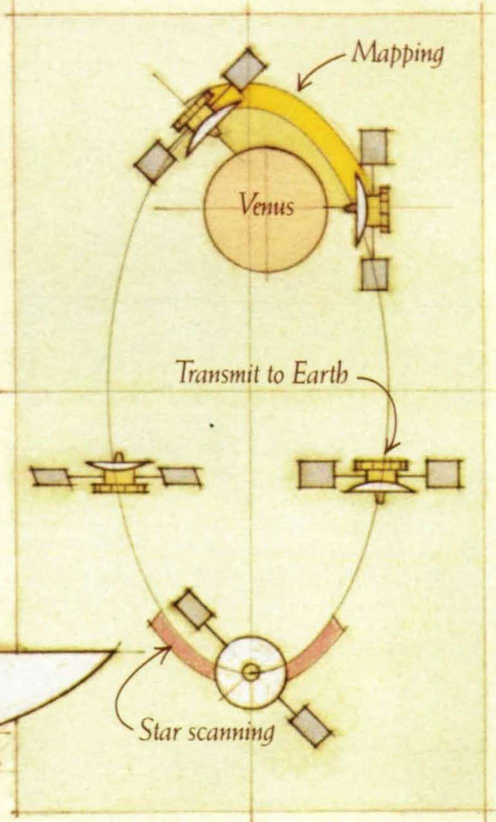

Orbit and orientation

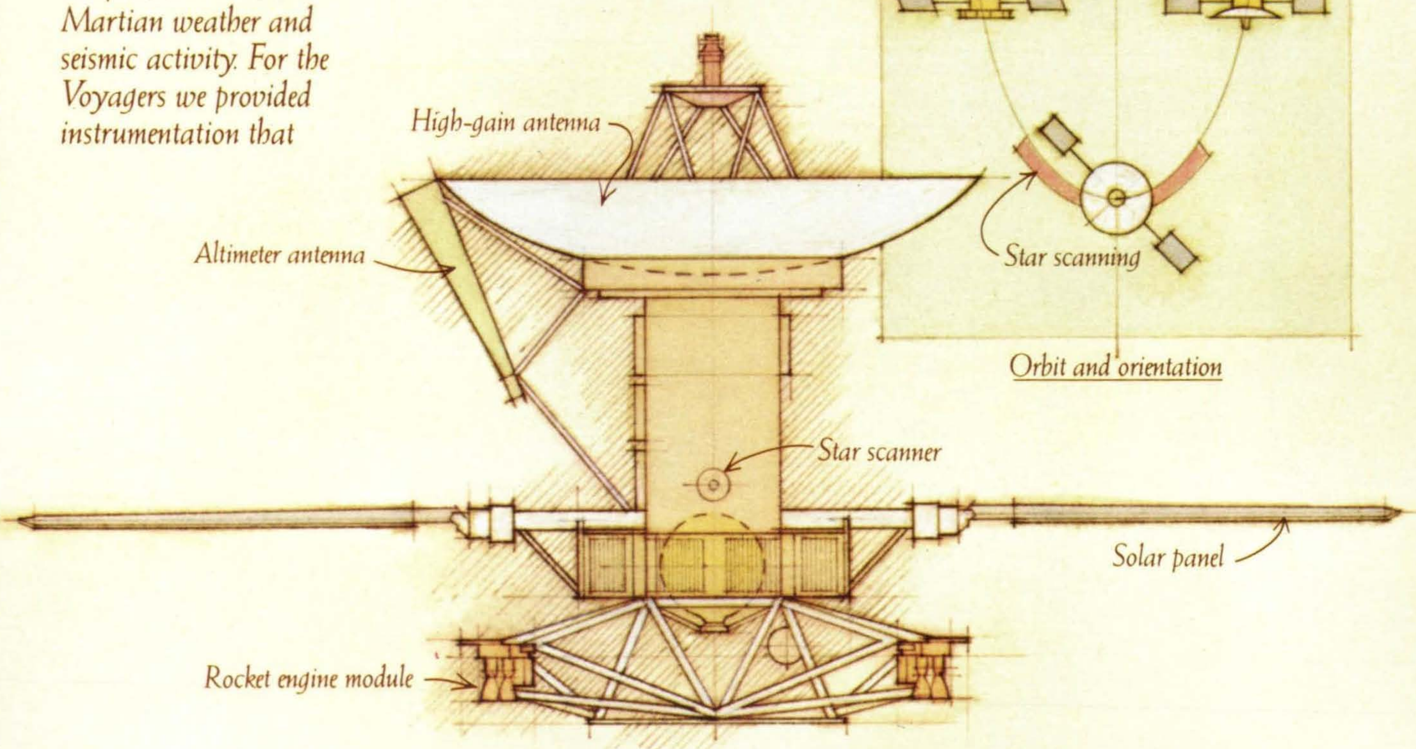

Magellan Spacecraft

Mission: map Venus.

From orbit, Magellan's radar will penetrate the planet's thick, gaseous cloud cover and send back photo-like images of nearly 90% of its surface. Our role: design, integrate, build and test the craft.

Viewing the infant universe.

For the Hubble Space Telescope we are providing the Faint Object Spectrograph (FOS), which will see objects up to 15 billion light-years away. Since the universe is estimated to be 18-20 billion years old, astronomers will witness events close to its birth.

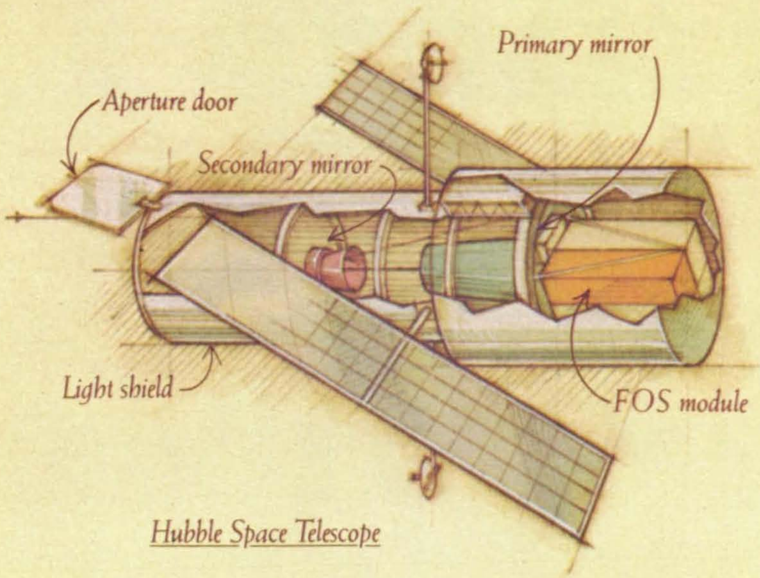

Hubble Space Telescope

The fine points of fine pointing.

Precisely controlled, space-spanning energy delivery and collection systems create difficult pointing and retargeting challenges, which we can now simulate. This new lab is working toward the precision to zero in on a football-size object 3,000 miles away, in support of the Strategic Defense Initiative research program.

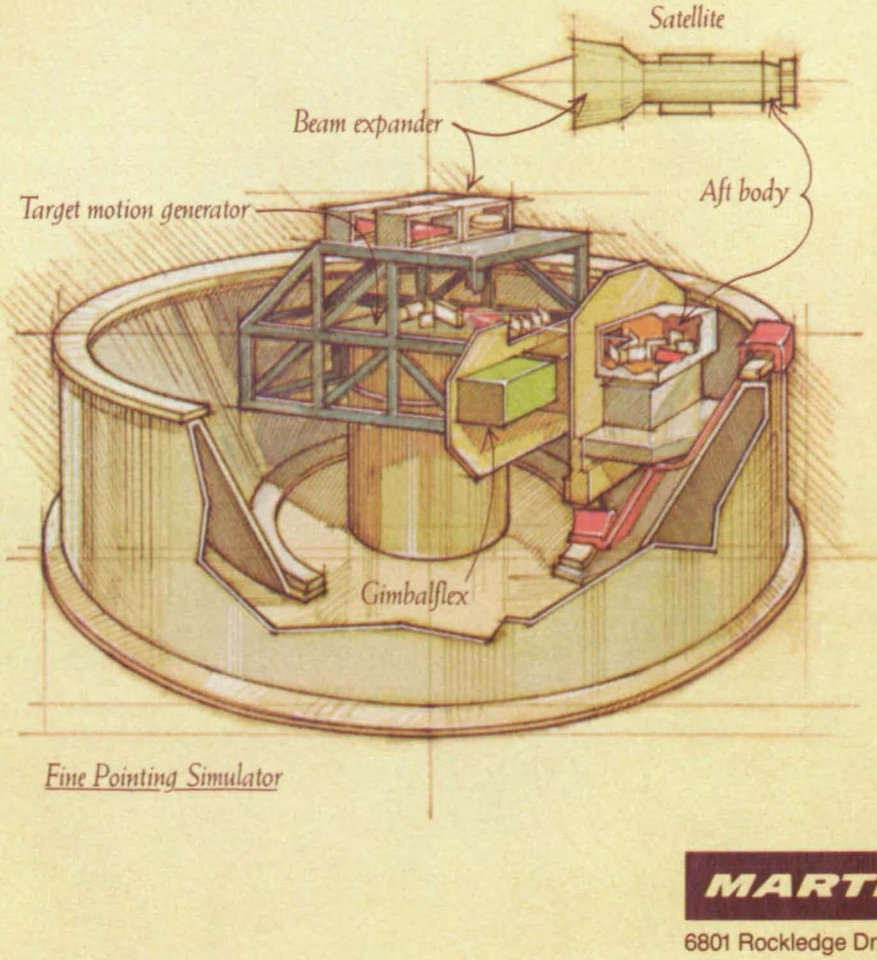

Fine Pointing Simulator

The challenge of transferring fluids in space is being met

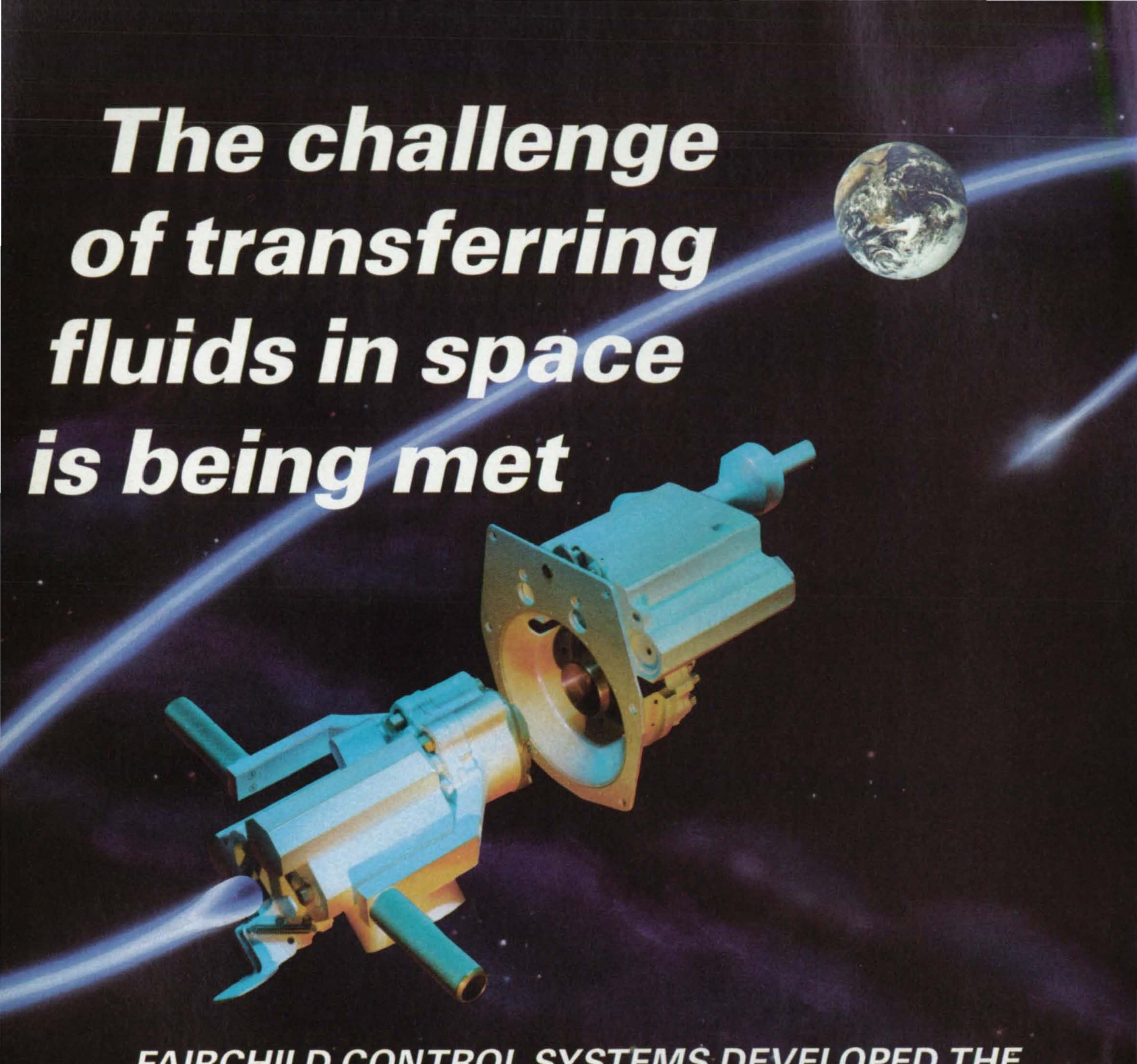

FAIRCHILD CONTROL SYSTEMS DEVELOPED THE STANDARDIZED SPACECRAFT REFUELING COUPLING

Until now, the useful life of a spacecraft has been limited by the quantity of propellant and other consumables on board at launch. At Fairchild today, that's being changed. The first steps toward indefinite spacecraft utility are being taken through the development of the Standardized Refueling Coupling. Under the auspices of the NASA Johnson Space Center, Fairchild is working to make spacecraft serviceability a reality. The Standardized Refueling Coupling will allow payloads like TRW's Gamma Ray Observatory to be resupplied with hydrazine in orbit. Designed to be safe for manual servicing, the Standardized Refueling Coupling is easily adapted to automated operation. If your future involves serviceable spacecraft, contact Fairchild Control Systems Company to learn how the Standardized Refueling Coupling can make the future happen.

FAIRCHILD
CONTROL SYSTEMS COMPANY

Fairchild Control Systems Company
1800 Rosecrans Avenue
Manhattan Beach, California 90266
Tel: (213) 643-9222
Telex: 910-325-6216

NASA Tech Briefs
National Aeronautics and Space Administration

SEPTEMBER/OCTOBER 1986
Volume 10 Number 5

BPA

Special Features and Departments

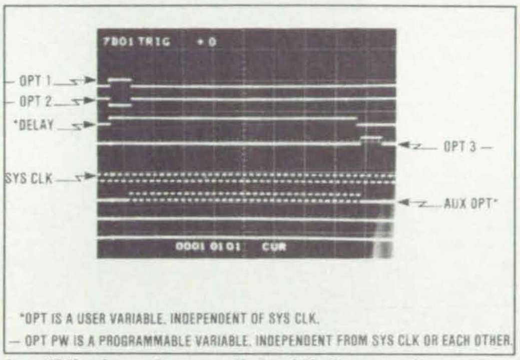

In "Mission Aecomplished," learn about one engineer's proven approach to his design problems. Shown here is the timing diagram to Joseph King's multiple output sequencing controller, described on page 131.

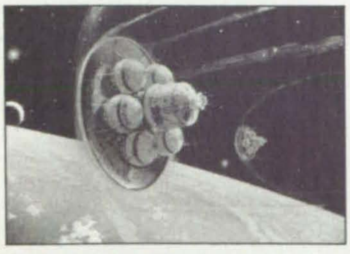

ARTIST: ROBERT McCALL, COPYRIGHT 1986, BANTAM BOOKS, INC.

Transfer vehicles slowing down in the earth's upper atmosphere as they return to the future Space Station. A large ceramic disk serves as the aerobrake. Behind the disk are six propellant tanks and a cylindrical crew module.

The Report of the National Commission on Space, reviewed in this issue, predicts exciting developments in space during the next half-century . . . page 10.

Technical Section Thumb Index

Thumb Index Technical Section

NASA Tech Briefs, ISSN 0145-319X, copyright © 1986 in U.S., is published bi-monthly by Associated Business Publications, Inc., 41 E. 42nd St., New York, NY 10017-5391. The copyrighted information does not include the individual Tech Briefs which are supplied by NASA. Editorial, sales, production and circulation offices at 41 E. 42nd Street, New York, NY 10017-5391. Subscriptions for non-qualified subscribers in the U.S., Panama Canal Zone, and Puerto Rico, $50.00 for 1 year; $100.00 for 2 years; $150 for 3 years. Single copies $15.00. Remit by check, draft, postal or express orders. Other remittances at sender's risk. Address all communications for subscriptions or circulation to NASA Tech Briefs, 41 E. 42nd Street, New York, NY 10017-5391. Application to mail at second-class postage rates is pending at New York, NY 10017 and additional mailing offices.

POSTMASTER: please send address changes to NASA Tech Briefs, 41 E. 42nd Street, Suite 921, New York, NY 10017-5391.


A GREAT
SOLUTION
DOESN'T HAVE
TO BE
COMPLICATED

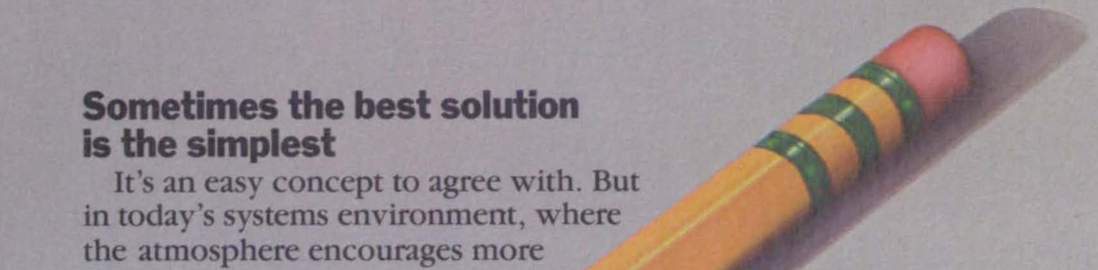

Sometimes the best solution is the simplest

It's an easy concept to agree with. But in today's systems environment, where the atmosphere encourages more complex and costly solutions, it's being increasingly overlooked.

Grumman Data Systems is trying to reverse that trend. Our information processing systems deliver optimum performance at the lowest life-cycle cost, yet they remain simple and user-friendly.

In C³I, CIM, computerized test, engineering and scientific, and management information systems, we've established an enviable record for building systems that are both cost effective and responsive to the user's needs.

To accomplish this, we've become leaders in advanced research and development in such areas as networking, computer graphics, machine intelligence, fault tolerant, command support systems, and the Ada software language.

A measure of our success comes from having an unbiased point of view. We have nationwide facilities that support our customers with total services that include information processing services, multi-vendor hardware and software maintenance, training, data base and micrographic publishing, and facilities management.

Our reputation for solving complex problems—simply—has made us the fastest growing division of the Grumman Corporation. For further information about any of our capabilities, contact Wesley R. Stout, Director, Technical Services at (516) 682-8500.

Grumman Data Systems

CUSTOM SOLUTIONS
for Managing Information

GRUMMAN®

Circle Reader Action No. 363

® A registered trademark of Grumman Corporation

NASA Tech Briefs

National Aeronautics and Space Administration

BPA

NASA Tech Briefs:

Published by .... **Associated Business Publications**
Editor-in-Chief/Publisher .... **Bill Schnirring**
Managing Editor .... **R.J. Laer**
Associate Editor .... **Leo D. Kluger**
Assistant Editor .... **Elena Nacanther**
Technical Advisor .... **Dr. Robert E. Waterman**
Art Director .... **Melanie Gottlieb**
Assistant Art Director .... **Michelle Schmitz**
Production Manager .... **Rita Nothaft**
Traffic Manager .... **Joe Pramberger**
Circulation Manager .... **Anita Weissman**
Fulfillment Manager .... **Elizabeth Kuzio**
Controller .... **Neil B. Rose**

Technical Staff:
Briefs prepared for National Aeronautics and Space Administration by **Logical Technical Services Corp.**, NY, NY
Technical Editor .... **Ted Selinsky**
Art Director .... **Ernest Gillespie**
Managing Editor .... **Theron Cole, Jr.**
Administrator .... **Elizabeth Texeira**
Chief Copy Editor .... **Pamela Touboul**
Staff Editors .... **James Boyd, Larry Grunberger, Jordan Randjelovich, George Watson**
Graphics .... **Luis Martinez, Huburn Profitt, Joe Renzler**
Editorial & Production .... **Lorne Bullen, Leonard Dalfino, Bill Little Frank Ponce, Ivonne Valdes,**

NASA:
NASA Tech Briefs are provided by the National Aeronautics and Space Administration, Technology Transfer Division, Washington, DC:
Administrator .... **Dr. James C. Fletcher**
Assistant Administrator for Commercial Programs ... **Isaac T. Gillam IV**
Director Technology Utilization Division ... **Henry J. Clarks**
Publications Manager .... **Leonard A. Ault**

Associated Business Publications
41 East 42nd Street, Suite 921
New York, NY 10017-5391
(212) 490-3999
President .... **Bill Schnirring**
Executive Vice President .... **Frank Nothaft**
Vice President—Sales .... **Wayne Pierce**
Vice President .... **Patricia Neri**

Advertising:

New York Office: (212) 490-3999
Vice President—Sales .... **Wayne Pierce**
Sales Manager .... **Robin DuCharme**
Account Executive .... **Dick Soule**
Account Executive .... **Carol-Lynne Cox**
Account Executive .... **Fred Bousquet**
Advertising Assistant .... **Erving Dockery, Jr.**

Los Angeles Office: (213) 477-5866

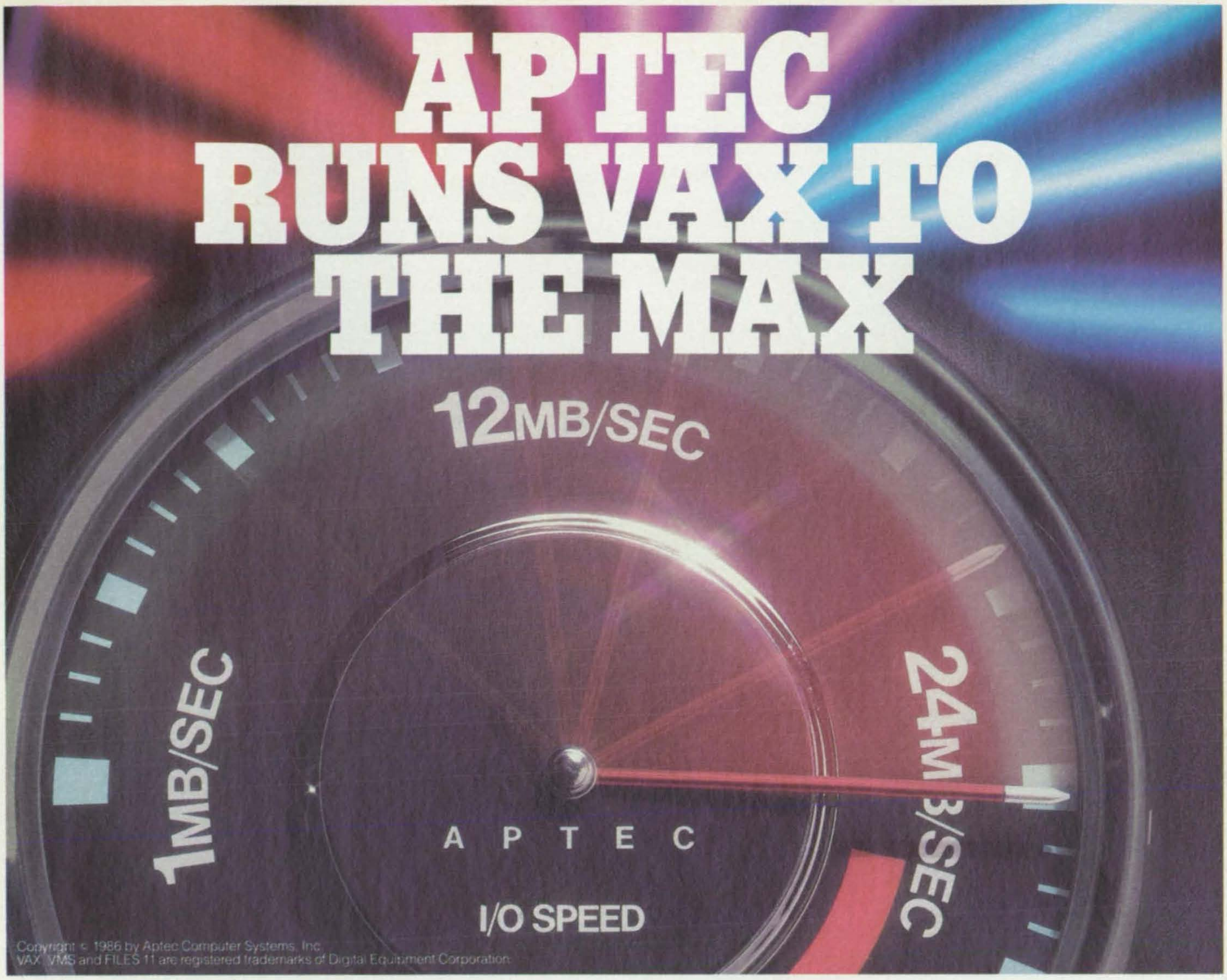

Aptec Computer Systems
P.O. Box 6750
Portland, OR 97228-6750
(503) 626-9000 Telex 467167

Editorial Notebook

The National Commission on Space

The cover story this month is a synopsis of the President's Commission on Space's predictions for the next 50 years. The possibilities are staggering. The great leaps we have made in the past 50 years will be dwarfed by what happens in the next, and technology as always will not only be the driving force, but also one of the major end results.

I hope you'll find the article interesting, and I hope too that it will move you to buy the report, read it, and then let your elected representatives know how you feel about it. It is my personal opinion as a private citizen that this is the time to support a national effort to pioneer the space frontier. In constant dollars NASA funding is approximately half of what it was during the Apollo days.

As I sat down to write this editorial notebook, I noticed that *The New York Times Magazine* had a feature story on the billions of dollars of benefits, and the technological break-throughs that will in all probability accrue through SDI. It is a continual irritant to me that publications like *TNYT* can somehow be aware of the possibilities in SDI, yet are simultaneously able to ignore the reality of the successful transfer of technology that NASA has already achieved. I almost used the phrase, "It has never ceased to amaze me," but that would not only have been hackneyed, but untrue. I have unfortunately long since become inured to the situation.

Under the heading of errata, in our article on KSC last issue, we mentioned that the "crawler-transporter weighs a whopping 3½ million tons." Well, it's heavy, but it doesn't whop quite that hard. The crawler weighs 6 million pounds, the orbiter launch platform another 8 million pounds, and the Orbiter, including the SRBs, but excluding the liquid fuel for the main engine which is pumped in at the launch site, weighs 3 million pounds, for a grand total of seventeen million pounds. Perhaps this and Palmdale's instant relocation was due to the fact that we did so much with mirrors in that issue. (See Letters, page 127.) □

A possible joint U.S./Soviet unmanned Mars mission is envisioned here, with the U.S. providing a prospector to collect soil samples, and the Soviets providing the spacecraft to return them to Earth. Below: An unmanned spacecraft leaving the solar system. In the foreground is Pluto, in the background, its moon Charon.

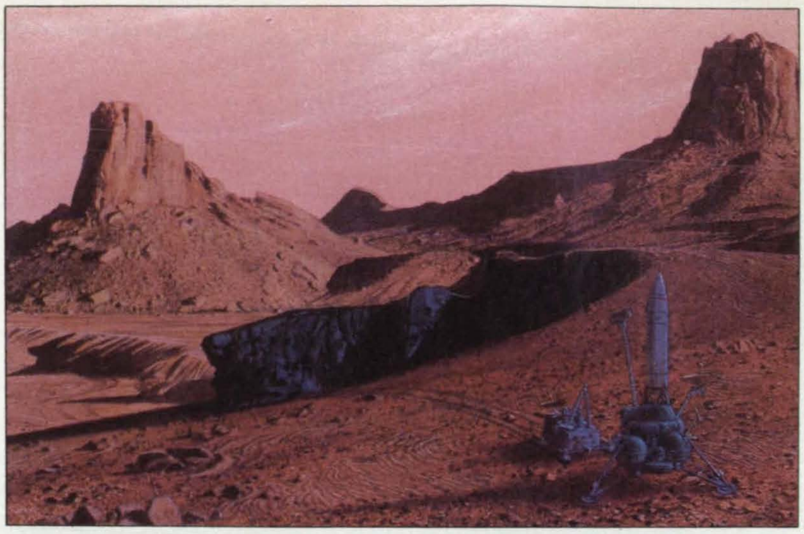

DATELINE 2035:

The Report of the National Commission on Space

ARTIST: RON MILLER. COPYRIGHT 1986, BANTAM BOOKS, INC.

Fifty years. Depending on your point of view, it can constitute a lifetime or pass in the blink of an eye. Looking back, it is the measure of recent history, the heart of the twentieth century, the post-modern era; looking ahead, it is the future, the threshold of a new millennium, and the inspiration for ongoing speculation by a new breed of social scientist, the futurist.

In the Space Age, the future tends to attract more attention than the past, so it is fitting that Congress, in 1984, commissioned a study to map civilian space goals for the next fifty years. But ironically, "Pioneering the Space Frontier," the report of the National Commission on Space, appeared at almost the same time as the Rogers commission report on the Challenger accident. Without a doubt, the Rogers commission report garnered the lion's share of public attention and focused it firmly in the uncertain present.

Historians and futurists alike view the the Challenger accident as a critical juncture in the United States space program. Because one of the functions of history is to put crisis in perspective, the Rogers commission report is essentially a historical document. On the other ►

hand, the report of the National Commission on Space, which was practically complete prior to the Challenger accident, is in the wake of Challenger perhaps even more futuristic than its authors intended.

In any event, the report of the National Commission on Space, whose timing has been called alternately "ghastly" and "fortuitous," and whose content has been labeled "ambitious," is a 211-page compendium of civilian space strategies and goals for the 21st century. The report was prepared by the fifteen distinguished members of the National Commission on Space, chaired by Dr. Thomas O. Paine, former NASA administrator and former president of Northrop Corporation. The commission's recommendations were based in part on a series of fifteen public forums held in cities throughout the U.S. during 1985. Over 1800 people attended these forums, and most took advantage of the opportunity to present their personal points of view to the commission.

Bantam Books published the report in late May and it is currently available in bookstores nationwide for $14.95. Here we've highlighted some of the report's recommendations for a bold 21st-century civilian space program.

The View From Here

"To lead the exploration and development of the space frontier, advancing science, technology and enterprise, and building institutions and systems that make accessible vast new resources and support human settlements beyond Earth orbit, from the highlands of the Moon to the plains of Mars." That, in brief, is the recommendation of the National Commission on Space to Congress and the President regarding what should be the goals of the nation's space program in the 21st century. To accomplish these goals, the commission recommends an approach based on three mutually-supportive thrusts: space science, space exploration and settlement, and the development of space enterprises. The report stresses that the success of this approach hinges on a commitment to the research and development of enabling technologies, particularly a space transportation system that ensures low-cost and regular access to space.

In the commission's view, the next generation space transportation system should be comprised of two different types of launch vehicles, one optimized for cargo and therefore very low-cost, and the other possessing a manned capability for less frequent launches at a higher cost. The cargo-carrying vehicle would evolve from current shuttle technology, and the passenger vehicle would be either an aerospace plane or an advanced rocket system. The commission recommends that a final decision on which manned option to pursue should be made only after preliminary R&D on both vehicles has been completed.

With regard to private sector involvement in the space transportation system, the commission, again citing the cost-cutting factor, urges that the next generation space vehicles be developed by the government but designed for eventual operation by the private sector.

Once a reliable space transportation system is in place, the commission foresees the paving of a highway to space, where a network of outposts will be established to enable long-term and in-depth space exploration and eventual settlement. Key to this plan is an Earth spaceport, which would be a follow-on to the international space station. Like the space station, the spaceport would be based on a modular design concept and located in low-earth orbit. It would be the first space airport, a transport node where spaceships could be berthed, cargo could be stored and passengers could disembark. ►

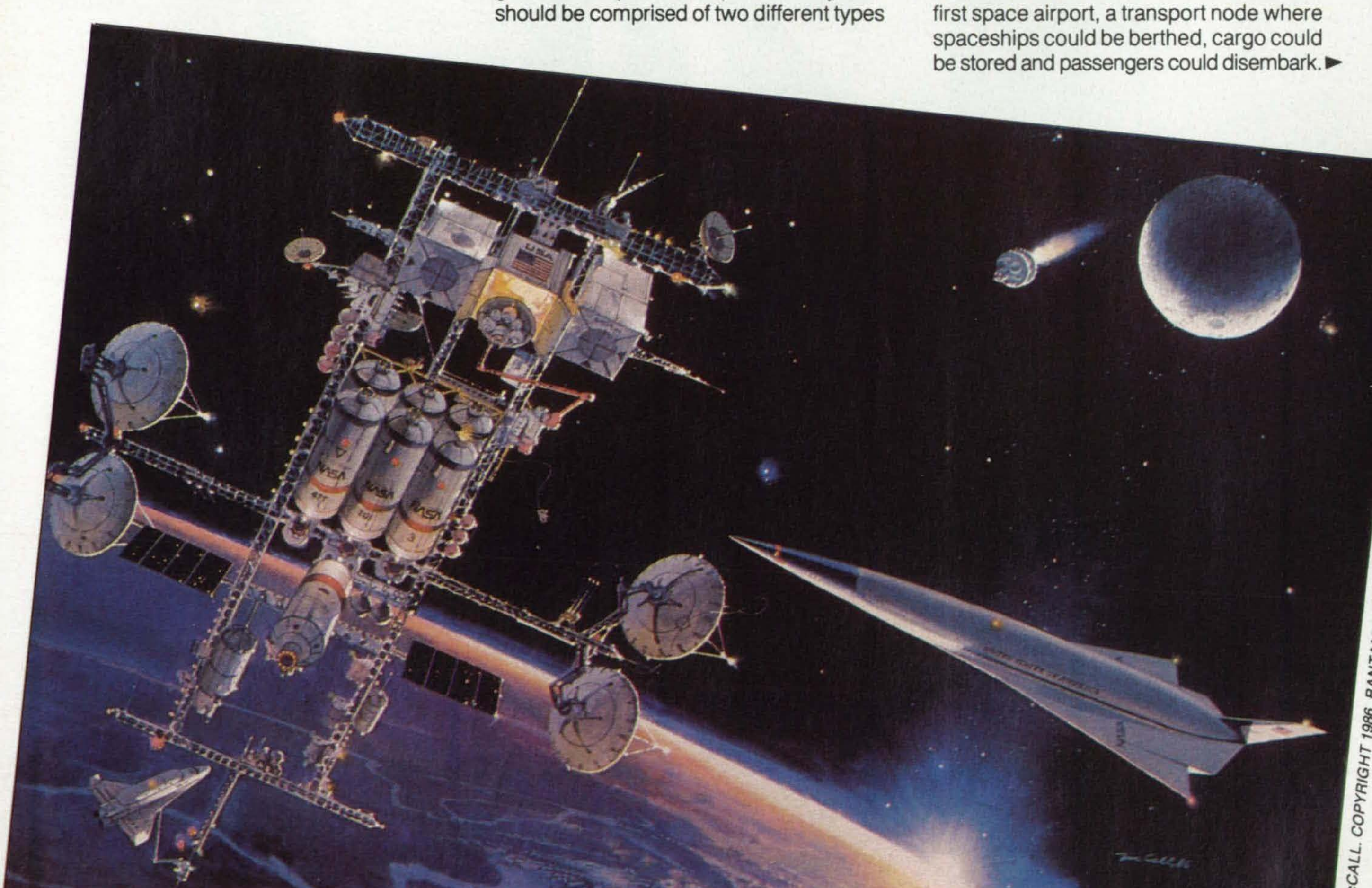

In the foreground is an aerospace plane approaching the Earth Spaceport. The Spaceport is receiving material from an unpiloted Cargo Transport Vehicle in the lower left-hand corner. A Transfer Vehicle is returning to the Spaceport from the moon.

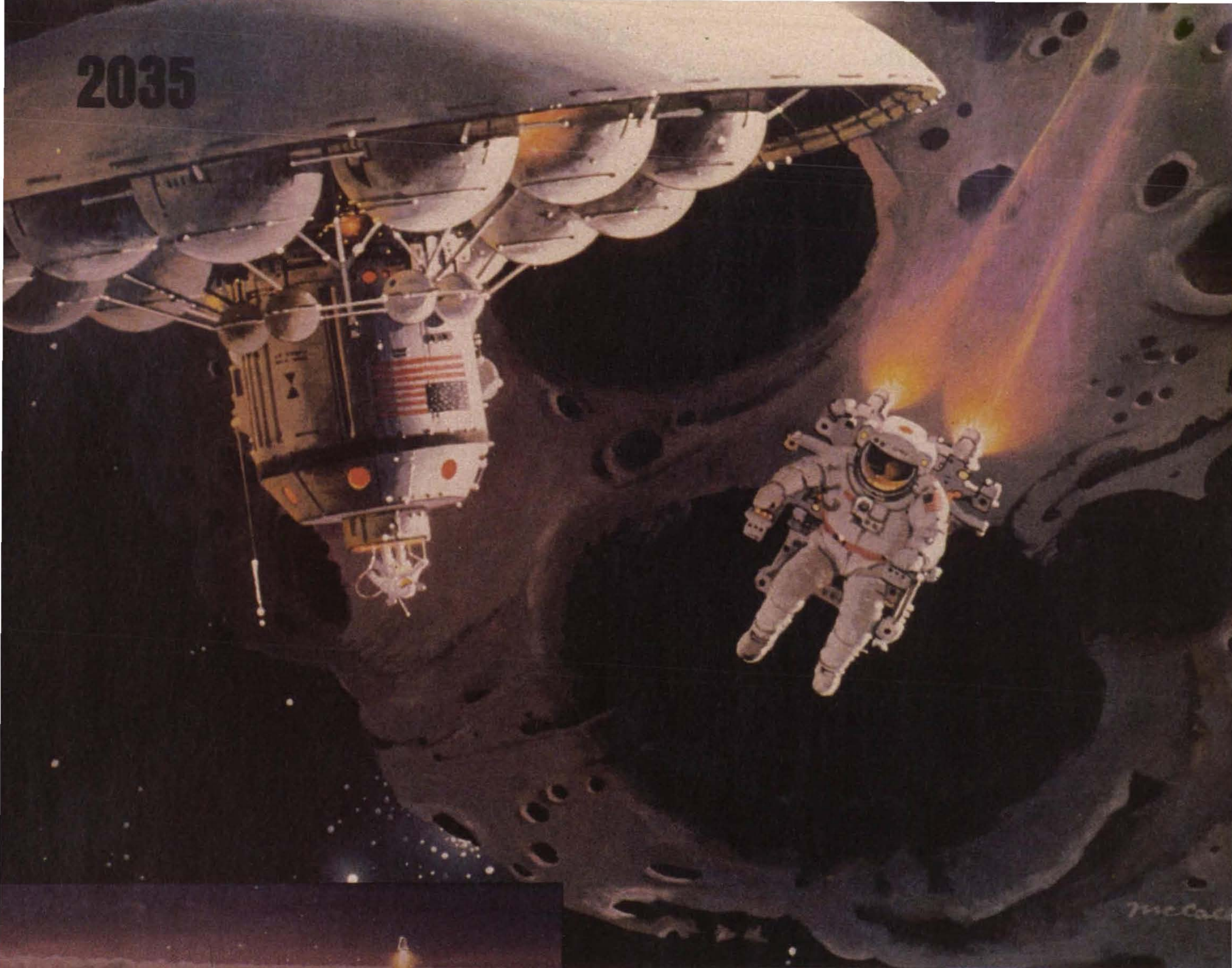

ARTIST: ROBERT McCALL. COPYRIGHT 1986, BANTAM BOOKS, INC.

Top: ***An astronaut leaves a transfer vehicle for a closer look at an asteroid. A Mars settlement in the 21st century.***

The commission envisions locating other spaceports in lunar orbit, at the L1 libration point between the earth and the moon, and perhaps eventually in orbit around Mars.

Establishing a network of spaceports would provide bases from which manned exploration missions and eventual settlements on both the moon and Mars could be launched. Prior to this, the commission's report suggests a series of advanced space science missions to complete the surveys and sampling missions begun by the Ranger, Surveyor and Viking spacecraft, and Apollo astronauts.

The commission recommends that the U.S. send a robotic lunar prospector to the moon to conduct a low-orbit survey of the entire surface of the moon, especially its polar regions. It also recommends lunar probe missions to drive penetrators into the lunar surface for further analysis of lunar material. Then, the report states, "it will be time for people to return to the moon . . . not only for brief expeditions, but for longer, systematic explorations; eventually, we should come to stay . . . establishing human-tended lunar surface outposts, primarily for a variety of scientific studies."

The View from There

Beyond the moon, the commission has singled out Mars and its moons, Phobos and Deimos, for scientific and eventual manned exploration. It recommends that the U.S. launch a sample return mission to the red planet early in the 21st century, and mentions a manned follow-up mission as a candidate for an international endeavor linking the U.S. and Soviet space programs.

Asteroids should also be investigated, according to the report, to determine what mineral resources they may yield to 21st century space prospectors. A number of accessible earth-crossing asteroids have already been identified by astronomers, and there is evidence to suggest that ►

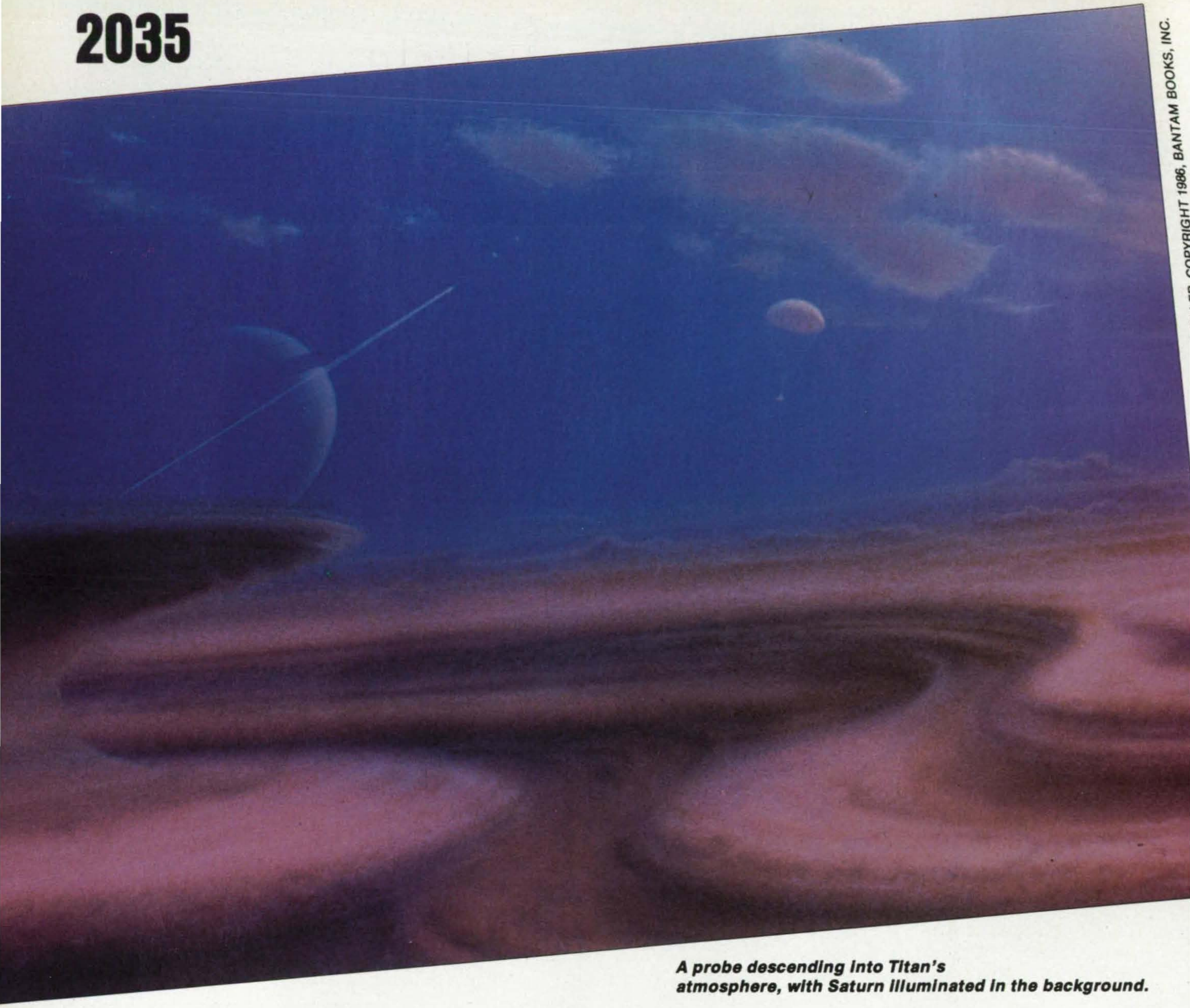

A probe descending into Titan's atmosphere, with Saturn illuminated in the background.

some of them may contain carbon, nitrogen and hydrogen. The report urges the expansion of the search for readily-accessible asteroids and robotic prospector missions to selected asteroids.

The fact that space is an as yet untapped source of natural resources and raw materials becomes important in light of the third of the commission's three recommendations: developing space-based commercial enterprises. Also, in order to sustain human outposts and settlements in space, the commission strongly recommends that long earth-based lines of supply be eschewed in favor of "living off the land" in space.

According to the report, there are three categories of space enterprise that will be viable in the world of 2035: supporting industries on earth, space industries with markets on earth and space industries with markets in space. Privately owned launch vehicles, facilities and related support services, such as maintenance, repair, fuel and communications are examples of supporting industries on earth.

A few examples of space industries with markets on earth currently exist, chief among them the satellite communications industry. Remote sensing, which facilitates the observation and management of crops and mineral, water and wildlife resources, is another potentially viable space industry now developing markets on earth. And microgravity materials processing and manufacturing are other potential space-based industries whose possibilities are already being examined by a number of earth-based companies. Solar power satellites capable of intercepting solar energy and transmitting it to earth are also being assessed in terms of their economic and technical feasibility.

Space industries with markets in space is still a speculative category at this point, but speculations abound. Mining raw materials on the moon, asteroids and on the moons of Mars, and then purifying these materials for use as propellants and in space-based manufacturing and construction is the approach suggested by the commission's report.

Such a brief overview of the report of the National Commission on Space does not really do justice to its far-ranging, well thought-out and ultimately visionary recommendations. In spite of its often heavy-handed, textbook style, the report is well organized and well illustrated. The ideas it presents are fascinating and its strategies based on evolutionary steps sound feasible.

Predicting the future is an age-old human activity, but systematically plotting its course is a relatively new, perhaps even Space Age, development. And considering the uncertainties that surround the nation's space program at present, it's certainly heartening to know that the future is still within our far-reaching grasp. □


WYLE
NASA


THE WORLD'S FASTEST SEMICONDUCTOR...
BUILT FROM THE ATOMS UP.

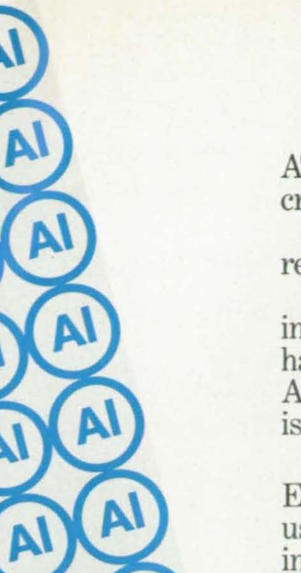

AT&T is building semiconductor crystals atomic layer by atomic layer.

The reason? To help electrons reach their full potential.

In our world of rapidly increasing information needs, the more data we have, the faster it has to be processed. And today, the key to faster processing is faster electrons.

Speed Is Of The Essence

Electrons in silicon—the most widely used material in the semiconductor industry—move quickly. But not quickly enough for many increasingly sophisticated applications, like real-time speed and image processing.

Now, silicon has just about reached its electron speed limit. For faster electrons to meet special needs, new materials are the key—new materials, not found in nature, built from the atoms up.

Going Flat Out With Atoms

Tailor-making new materials uses a form of atomic spray painting called Molecular Beam Epitaxy (MBE).

Invented and perfected by AT&T Bell Laboratories scientists, MBE creates ultra-thin, extraordinarily uniform films of selected elements. To prevent contamination, individual layers are sprayed onto a substrate in a vacuum containing 100 billion times fewer atoms than in the earth's normal atmosphere.

Finished films are uniformly flat to plus or minus one atom in depth.

Electrons That Move Like Rockets

In one application, AT&T constructed material using crystal layers of gallium aluminum arsenide and gallium arsenide. The gallium arsenide was kept pure, while the gallium aluminum arsenide layer was seeded, or doped, with carefully controlled impurities—sources of needed electrons.

These electrons are drawn in droves to the face of the pure layer. Here, unimpeded by impurities, electrons can rocket across the transistor's gate at 20 million centimeters per second—almost three times as fast as in today's silicon semiconductors.

Spray painting with atoms.

Using this new material, AT&T scientists collaborated with colleagues at Cornell University to set a transistor speed record. The device switched a logic circuit on and off in 5.8 picoseconds (trillionths of a second)—that's 170,000,000,000 times in a single second.

Putting The Future On The Beam

Molecular Beam Epitaxy has also enabled Bell Labs to produce a semiconductor that replaces electricity with... light.

Built of 2,500 precise, alternate layers of gallium arsenide and gallium aluminum arsenide, the chip contains four photonic switches that are turned on and off by light beams, much the way electronic transistors are activated by electrical charges.

This light switch presages a day when optical computers will process information 1,000 times faster than present electronic computers. A day brought closer by AT&T's layered technology.

AT&T publishes a magazine called PROTO, a report to managers on how AT&T technologies are being used in advanced communications products and services.

For a free copy of PROTO, write: PROTO Circulation Manager, AT&T Bell Laboratories, Box B, 1L-404, 101 John F. Kennedy Parkway, Short Hills, New Jersey 07078.

AT&T

The right choice.

New Product Ideas

New Product Ideas are just a few of the many innovations described in this issue of *NASA Tech Briefs* and having promising commercial applications. Each is discussed further on the referenced page in the appropriate section in this issue. If you are interested in developing a product from these or other NASA innovations, you can receive further technical information by requesting the TSP referenced at the end of the full-length article or by writing the Technology Utilization Office of the sponsoring NASA center (see page 29). NASA's patent-licensing program to encourage commercial development is described on page 29.

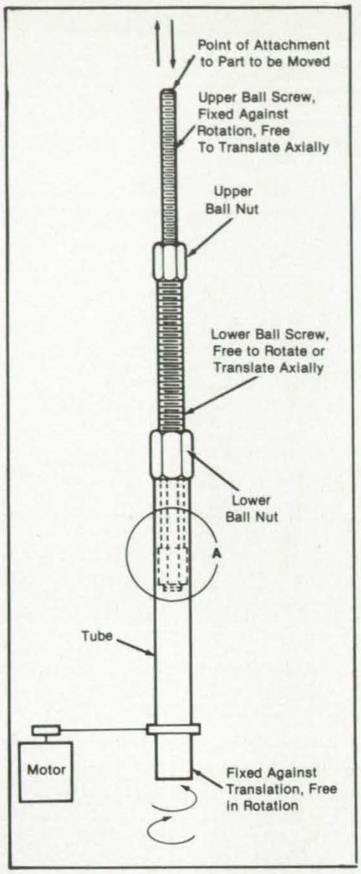

Shock-Absorbent Ball-Screw Mechanism

An actuator containing two ball screws in series employs Belleville springs to reduce impact loads, thereby increasing its life expectancy. The mechanism uses Belleville springs as the shock-absorbing elements because Belleville springs have a good energy-to-volume ratio and are easily stacked to attain any stiffness and travel. In addition to the two ball screws, the mechanism employs two ball nuts, a tube, and a drive motor (see figure). When the tube is rotated, the lower screw rotates or translates, thereby translating the upper screw axially so that it raises or lowers a part attached to the upper tip of the mechanism. A set of three springs within the lower screw of the ball-screw mechanism absorbs the impacts that result when the parts reach their upper and lower limits of movement. (See page 110.)

Tandem-Mirror Ion Source

A tandem-mirror ion source uses electrostatic and magnetic fields to keep electrons in the ionization chamber and to assure a uniform output beam having low divergence in energy and angle. The improved ion source, which produces a beam of ions at any kinetic energy from 1 to 1,000 eV, could be useful in studies of the surface properties of materials, surface etching, deposition, and the development of plasma-diagnostic instrumentation.
(See page 63.)

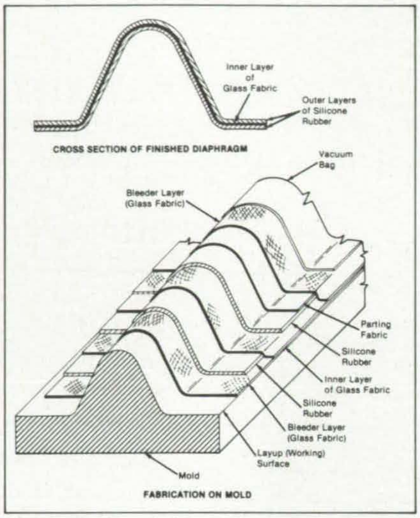

Flexible Diaphragm Withstands Extreme Temperatures

Durable, simple, versatile, and relatively inexpensive to manufacture, a diaphragm seal retains flexibility throughout the temperature range of −200 to +600 °F (−129 to +316 °C). The diaphragm, which consists of a glass-fabric layer sandwiched between two silicone-rubber layers, should be suitable for refrigeration seals, autoclaves, storage lockers, and other sealing applications subjected to extreme temperature differentials.
(See page 122.)

Polyimide Film of Increased Tear Strength

A high-temperature linear aromatic polyimide with improved resistance to tearing is made by a new process that incorporates an elastomer into the polyimide. Linear aromatic condensation polyimides are materials of prime choice for use as films and coatings where durability at temperatures in the range of 200 to 300 °C is required. However, the tendency of these films to tear upon impact limits their usefulness in certain applications. It is anticipated that elastomer-containing polyimide film with improved toughness will prove useful for applications where resistance to tearing and long-term thermal stability are necessary.
(See page 85.)

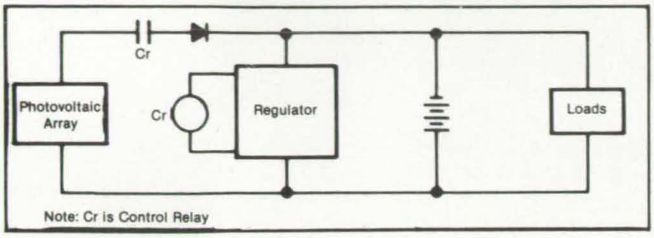

Voltage Regulators for Photovoltaic Systems

Two simple circuits were developed to provide voltage regulation for high-voltage (i.e., □75 volts) and low-voltage (i.e.,• volts) photovoltaic/battery power systems. The use of these circuits results in a voltage regulator that is small, low-cost, and reliable, with very low power dissipation. The circuit shown in the figure is a regulator for high-voltage systems. It performs as an astable oscillator with a duty cycle derived from the system voltage. Adjustments in the nominal operating voltage are controlled by the potentiometer and by use of zener diodes of different voltage ratings. A light-emitting diode (LED) in the circuit provides a visual indication that the circuit is switching on and off. A single regulator may be used to control a small array, or several regulators may be used in parallel to control independent sections of a large array.

(See page 34.)

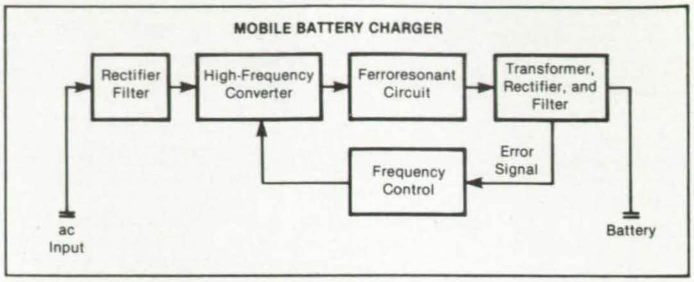

Ferroresonant Flux-Coupled Battery Charger

A portable battery charger operates at about 20kHz to take advantage of the relatively low weight and low acoustical noise of ferroresonant circuits operating in this frequency range. The charger can be split into a stationary unit connected to a powerline and a mobile unit connected to a battery or other load. Power would be transferred to the mobile unit by magnetic coupling between mating transformer halves. This is an advantage where sparking at an electrical connection might pose an explosion hazard or where the operator is disabled and cannot manipulate a plug into a wall outlet. Likely applications for the charger include wheelchairs and robots.

(See page 30.)

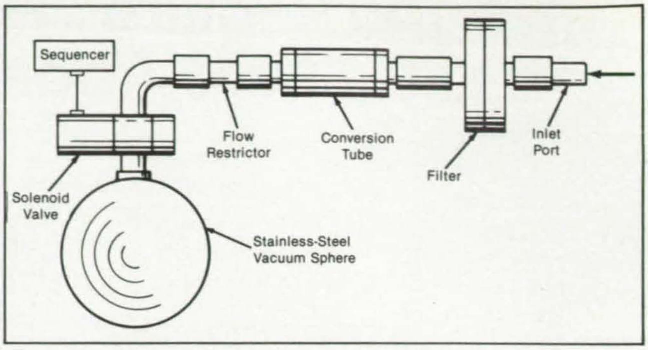

Batch Gas-Sampling System

A sampler collects a designated substance contained in the air and stabilizes it for later chemical analysis. The device can be used for concentrations ranging from a few parts per million to 100 percent. Activated by a sequencer, a solenoid valve opens, and gas from the surroundings is immediately drawn by the vacuum in a stainless-steel sphere into an inlet port, where particles are trapped in a filter. The gas continues into a conversion tube, where the component of interest reacts with the appropriate reagant and is changed into a stable compound in proportion to its concentration. At the end of a preset collection period or when the vacuum is exhausted, the sequencer closes the valve. The conversion tube, with its content, is then sent to a laboratory for analysis.

(See page 82.)

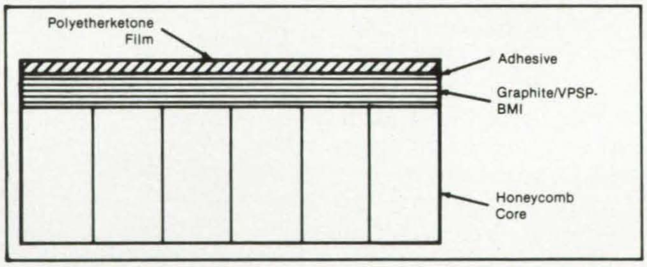

Lightweight, Fire-Resistant Graphite Composites

Aircraft safety could be improved with interior paneling made of a new laminate with good thermophysical properties. Featuring a lightweight graphite composite (graphite with a blend of vinyl polystyrylpyridine and bismaleimide, VPSP-BMI), the laminate resists heat and flame more effectively and produces much less smoke in fire than do the commonly used epoxy-resin-containing laminates. In addition, the new laminates have processing and curing parameters comparable to those of the epoxy/glass composites, making their manufacturing costs lower than those of such other high-temperature and fire-resistant resins as the polymides.

(See page 74.)

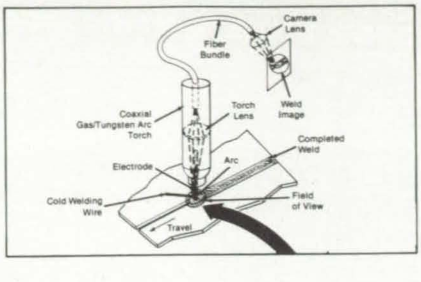

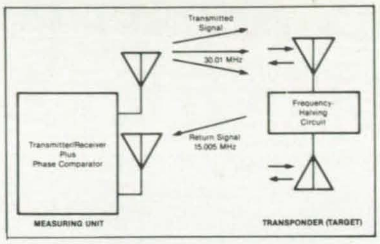

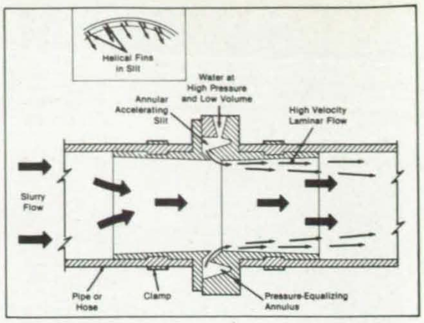

Robotic Vision for Welding

Protected within a welding-torch body, a lens and fiber-optic bundle give a robot a closeup view — along the axis of the welding electrode — of a weld in progress, without interfering with the workpiece or hindering tool movement. Relayed to a video camera on the robot manipulator frame, the detailed weld image is analyzed in real time by a control computer, which guides the robot and adjusts such parameters as the welding current and the feed of welding wire into the weld.

(See page 121.)

Transponder System for High-Frequency Ranging

A transponder system uses the phase difference between transmitted and reflected high-frequency radio waves to measure the distance to a target. To suppress spurious measurements of reflections from objects near the target at the transmitted frequency and its harmonics, the transponder at the target generates a return signal at half the transmitted frequency. The system should be useful in such applications as surveying, the docking of ships, and short-range navigation.

(See page 54.)

Flow Injector Would Keep Slurry From Settling

A proposed ring nozzle may help to prevent the choking of short-haul slurry pipelines. The ring nozzle helps to prevent blockages by enabling the injection of extra water or other fluid to increase the flow near the wall. A relatively small volume of water at high pressure is accelerated through an annular slit into the pipe (see figure), forming a laminar-flow boundary layer that entrains a large volume of slurry. Helical fins in the accelerating slit impart a rotation to the injected and entrained flows, thereby enhancing the ability to prevent settling of the slurry particles.

(See page 112.)

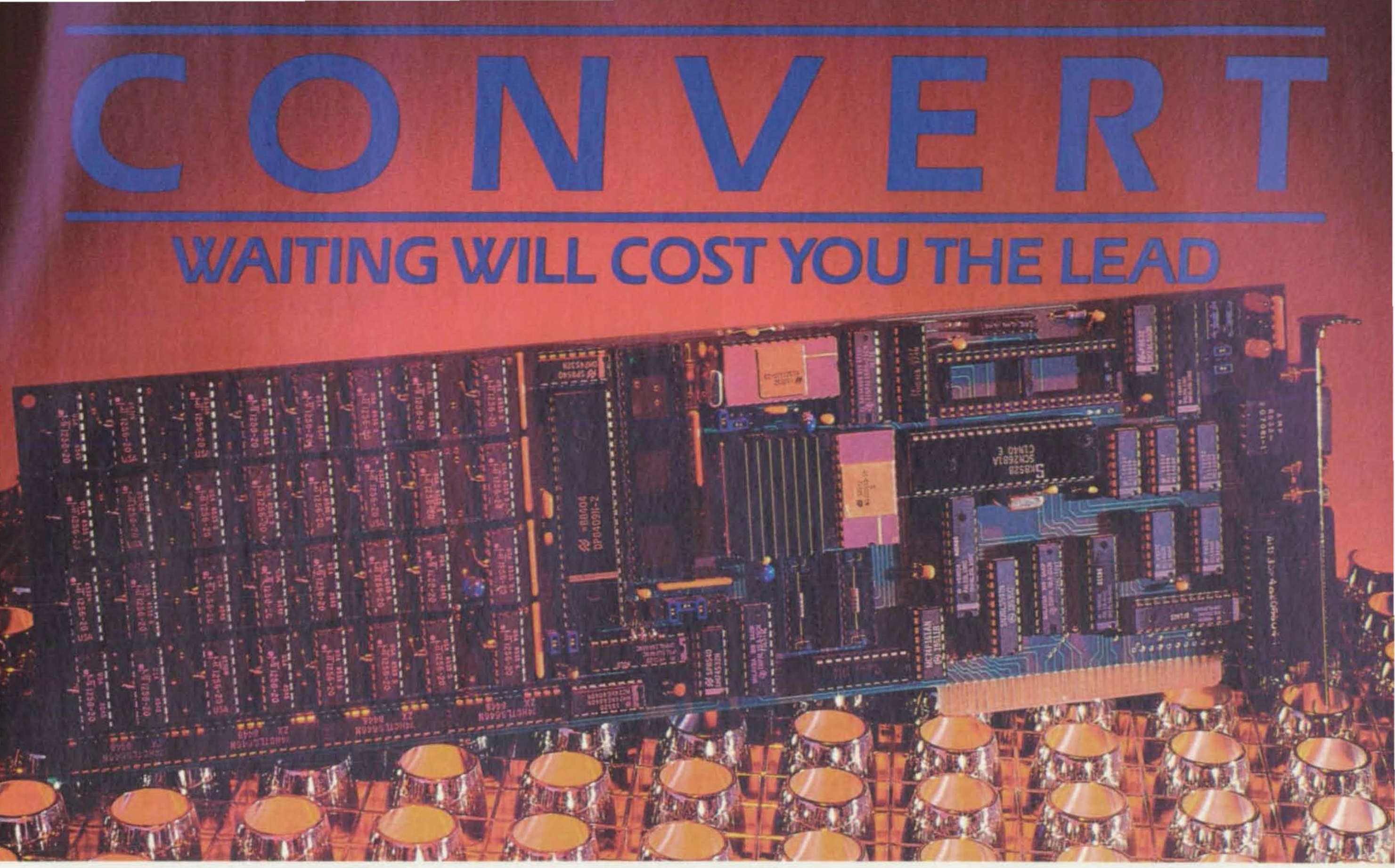

Turn your PC into a powerful 32-bit Super-Mini.

When your PC runs 35 times faster, you outrun the competition. Tired of playing runner-up? Plug a **PM™** model **DSI-32 Co-Processor** into your personal computer. And easily outrun any XT, AT…even many VAX's.

A completely self-contained 32-bit computer—with floating point processor—on a single PC board, the **PM™** converts any IBM/PC into a powerful Super-Mini that runs at an incredible 10 MHz, with no wait states. Across the board, it's the fastest board for the money, putting the power and performance of a $150,000 computer in your lap… *for a hundredth of the price!*

Simple to install, in minutes it's up and running compatibly with your standard PC MS/DOS system, without retraining or file conversion. You can port scientific or commercial applications without recoding or restructuring your software to fit Intel's architecture. And you can choose either MS/DOS or Unix at will, without commiting your system to either one.

Why lag behind? Call the 800 number below for a no-risk trial of the **PM™**. And convert your personal computer to a *Personal Mini*. It'll make a convert out of *you.*

- Operates in any PC/XT/AT or compatible.
- Takes only one slot.
- Has National Semiconductor's 32032 processor and 32081 math co-processor both running at 10 Mhz.
- Optional MMU and ICU provide for true demand paging virtual memory up to 15 megabytes.
- DSI memory full 32 bit bus with 1/2/4/8 megabytes on board
- DSI-MS/DOS environment has access to all devices on PC bus.
- The PC's 8088/86/286, used concurrent, handle all I/O and leaves DSI-32 to run uninterrupted.
- Port, mini and mainframe source programs in minutes.
- Includes assembler, linker, and debugger and full documentation.
- Supported by C, Pascal and Fortran-77 compilers ported for Vax/VMS compatibility.
- Two level hardware implemented software protection, custom arrangements negotiable.
- Two serial ports up to 38k baud.
- Hardware and software support for 1 year. Extended hardware/software support available.
- Try our board NOW for no-risk, 30 day Money Back Evaluation Period.

Sieve Benchmark

N*	IBM XT	IBM AT	VAX 750	VAX 780	DSI-32
20,000	35.30	8.13	6.11	3.04	4.52
40,000	351.50	99.71	13.13	6.38	9.07

Float Benchmark

40,000	11.46	17.71	.83	.50	.80

Unix Benchmarks

	DSI-32	VAX 780	VAX 750
O.S. Overhead	3.88	4.4	7.0
C Compiler Test	.55	1.0	1.7
Sieve of Eratosthenes	1.93	1.7	2.4

ECOTECH, INC.
COMPUTER SYSTEMS
3711 35th Street, N.W.
Washington, D.C. 20016
202 244-3858

800 826-2189

Circle Reader Action No. 440

HOW YOU CAN BENEFIT FROM NASA's TECHNOLOGY UTILIZATION SERVICES

If you're a regular reader of TECH BRIEFS, then you're already making use of one of the low- and no-cost services provided by NASA's Technology Utilization (TU) Network. But a TECH BRIEFS subscription represents only a fraction of the technical information and applications/engineering services offered by the TU Network as a whole. In fact, when all of the components of NASA's Technology Utilization Network are considered, TECH BRIEFS represents the proverbial tip of the iceberg.

On the following pages, we've outlined NASA's TU Network—named the participants, described their services, and listed the individuals you can contact for more information relating to your specific needs. We encourage you to make use of the information, access, and applications services offered by NASA's Technology Utilization Network. You can save time and money by doing so.

HOW YOU CAN UTILIZE NASA'S Industrial Applications Centers

A nationwide network offering a broad range of technical services, including computerized access to over 100 million documents worldwide.

You can contact NASA's network of Industrial Applications Centers (IACs) for assistance in solving a specific technical problem or meeting your information needs. The "user friendly" IACs are staffed by technology transfer experts who provide computerized information retrieval from one of the world's largest banks of technical data. Nearly 500 computerized data bases, ranging from NASA's own data base to Chemical Abstracts and INSPEC, are accessible through the nine IACs, which are located throughout the nation. The IACs also offer technical consultation services and/or linkage with other experts in the field.

You can obtain more information about these services by calling or writing the nearest IAC. User fees are charged for IAC information services.

Aerospace Research Applications Center (ARAC)
Indianapolis Center for Advanced Research
611 N. Capitol Avenue
Indianapolis, IN 46204
Dr. F. Timothy Janis, Director
(317) 262-5003

Kerr Industrial Applications Center (KIAC)
Southeastern Oklahoma State University
Station A, Box 2584
Durant, OK 74701
Tom J. McRorey, Director
(405) 924-6822

NASA Industrial Applications Center
823 William Pitt Union
University of Pittsburgh
Pittsburgh, PA 15260
Paul A. McWilliams, Executive Director
(412) 624-5211

NASA/Southern Technology Applications Center
State University System of Florida
307 Weil Hall
Gainesville, FL 32611
J. Ronald Thornton, Director
(904) 392-6760

NASA/UK Technology Applications Center
University of Kentucky
109 Kinkead Hall
Lexington, KY 40506-0057
William R. Strong, Director
(606) 257-6322

NERAC, Inc.
Mansfield Professional Park
Storrs, CT 06268
Daniel U. Wilde, President
(203) 429-3000

North Carolina Science and Technology Research Center (NC/STRC)
Post Office Box 12235
Research Triangle Park, NC 27709
J. Graves Vann, Jr., Acting Director
(919) 549-0671

Technology Application Center (TAC)
University of New Mexico
Albuquerque, NM 87131
Stanley A. Morain, Director
(505) 277-3622

NASA Industrial Applications Center (WESRAC)
University of Southern California
Research Annex
3716 South Hope Street
Room 200
Los Angeles, CA 90007
Radford G. King, Acting Director
(213) 743-6132
(800) 642-2872 (CA only)
(800) 872-7477 (toll-free US)

If you represent a public sector organization with a particular need, you can contact NASA's Application Team for technology matching and problem solving assistance. Staffed by professional engineers from a variety of disciplines, the Application Team works with public sector organizations to identify and solve critical problems with existing NASA technology.

Technology Application Team
Research Triangle Institute
P.O. Box 12194
Research Triangle Park, NC 27709
Doris Rouse, Director
(919) 541-6980

A SHORTCUT TO SOFTWARE:

COSMIC®

An economical source of computer programs developed by NASA & other gov't. agencies.

Software developed by the U.S. government may be applicable to your needs. To tap this valuable resource, contact COSMIC, NASA's Computer Software Management and Information Center. Approximately 1400 computer programs and related documentation comprise the current library. New and updated programs are announced regularly in NASA Tech Briefs' Computer Programs section, and COSMIC publishes an annual software catalog.

More information about COSMIC's services can be obtained by calling or writing:

COSMIC®
Computer Services Annex
University of Georgia
Athens, GA 30602
John A. Gibson, Director
(404) 542-3265

HOW YOU CAN ACCESS TECHNOLOGY TRANSFER SERVICES AT NASA FIELD CENTERS:

Technology Utilization Officers & Patent Counsels

Each NASA Field Center has designated a Technology Utilization Officer and a Patent Counsel to facilitate technology transfer between NASA and the private sector.

If you need further information about new technologies presented in NASA Tech Briefs, you should request the Technical Support Package (TSP) that accompanies the brief. In the event that a TSP is not available, you can contact the Technology Utilization Officer at the NASA Field Center that sponsored the research. He can arrange for expert assistance in applying the technology by putting you in touch with the people who developed it.

If you want additional information about the patent status of a particular technology or are interested in licensing a NASA invention, contact the Patent Counsel at the NASA Field Center that sponsored the research. Be sure to refer to the NASA reference number at the end of the tech brief.

Ames Research Center
Technology Utilization Officer:
Laurance A. Milov
Mail Code 204-10
Moffett Field, CA 94035
(415) 694-5761
Patent Counsel:
Darrell G. Brekke
Mail Code 200-11
Moffett Field, CA 94035
(415) 694-5104

Goddard Space Flight Center
Technology Utilization Officer:
Donald S. Friedman
Mail Code 702-1
Greenbelt, MD 20771
(301) 286-6242
Patent Counsel:
John O. Tresansky
Mail Code 204
Greenbelt, MD 20771
(301) 286-7351

Lyndon B. Johnson Space Center
Technology Utilization Officer:
Dean C. Glenn
Mail Code AL32
Houston, TX 77058
(713) 483-3809
Patent Counsel:
Marvin F. Matthews
Mail Code AL3
Houston, TX 77058
(713) 483-4871

John F. Kennedy Space Center
Acting Technology Utilization Officer: Thomas M. Hammond
Mail Stop PT-TPO-A
Kennedy Space Center, FL 32899
(305) 867-3017
Patent Counsel:
James O. Harrell
Mail Code PT-PAT
Kennedy Space Center, FL 32899
(305) 867-2544

Langley Research Center
Technology Utilization Officer:
John Samos
Mail Stop 139A
Hampton, VA 23665
(804) 865-3281
Patent Counsel:
Howard J. Osborn
Mail Code 279
Hampton, VA 23665
(804) 865-3725

Lewis Research Center
Technology Utilization Officer:
Daniel G. Soltis
Mail Stop 7-3
21000 Brookpark Road
Cleveland, OH 44135
(216) 433-5567
Patent Counsel:
Gene E. Shook
Mail Code 60-2
21000 Brookpark Road
Cleveland, OH 44135
(216) 433-5753

Jet Propulsion Laboratory
Technology Utilization Manager:
Norman L. Chalfin
Mail Stop 201-110
4800 Oak Grove Drive
Pasadena, CA 91109
(818) 354-2240

NASA Resident Office-JPL
Technology Utilization Officer:
Gordon S. Chapman
Mail Stop 180-801
4800 Oak Grove Drive
Pasadena, CA 91109
(818) 354-4849
Patent Counsel:
Paul F. McCaul
Mail Code 180-801
4800 Oak Grove Drive
Pasadena, CA 91109
(818) 354-2734

George C. Marshall Space Flight Center
Technology Utilization Officer:
Ismail Akbay
Code AT01
Marshall Space Flight Center, AL 35812
(205) 544-2223
Patent Counsel:
Leon D. Wofford, Jr.
Mail Code CC01
Marshall Space Flight Center, AL 35812
(205) 544-0014

National Space Technology Laboratories
Technology Utilization Officer:
Robert M. Barlow
Code GA-10
NSTL Station, MS 39529
(601) 688-1929

NASA Headquarters
Technology Utilization Officer:
Leonard A. Ault
Code IU
Washington, DC 20546
(202) 453-1920
Assistant General Counsel for Patent Matters: Robert F. Kempf
Code GP
Washington, DC 20546
(202) 453-2424

IF YOU HAVE A QUESTION...

NASA Scientific & Technical Information Facility

If you have a general or specific question about NASA's Technology Utilization Network or its services and documents, you can contact the STI facility for assistance. The STI staff can answer your questions, supply documents and provide referrals to meet your needs. You can use the feedback card in this issue to contact STI directly.

NASA Scientific and Technical Information Facility

Technology Utilization Office
P.O. Box 8757
BWI Airport, MD 21240
Walter M. Heiland, Manager
(301) 859-5300, Ext. 242, 243

Electronic Components & Circuits

Hardware, Techniques, and Processes

Books & Reports

Computer Programs

Ferroresonant Flux-Coupled Battery Charger

A high power frequency keeps design weight low.

NASA's Jet Propulsion Laboratory, Pasadena, California

A portable battery charger operates at about 20 kHz to take advantage of the relatively low weight and low acoustical noise of ferroresonant circuits operating in this frequency range. The charger can be split into a stationary unit connected to a powerline and a mobile unit connected to a battery or other load, as shown in Figure 1. Power would be transferred to the mobile unit by magnetic coupling between mating transformer halves. This is an advantage where sparking at an electrical connection might pose an explosion hazard or where the operator is disabled and cannot manipulate a plug into a wall outlet. Likely applications for the charger include wheelchairs and robots.

The circuit (see Figure 2) includes a series inductor in the tuned tank circuit of a ferroresonant saturating transformer. The series inductor allows the input voltage and power to vary over a wider range than is allowable with capacitor tuning alone, while keeping down the temperature rise of the saturating transformer.

The output voltage of the saturating transformer at a given frequency is hard limited to the value at the saturating flux. Since the transformer is operated in saturation, powerline voltage transients have little effect on the output. The output voltage is adjusted by varying the frequency, inasmuch as the output of a saturating transformer is approximately proportional to the frequency.

The output voltage is sampled by voltage divider R_1, R_2 and compared with a reference voltage representing the desired output. The resulting error voltage controls the output of a light-emitting diode in an optocoupler (which is used for electrical isolation). The optocoupler output is, in effect, a varying frequency-controlling resistance connected to the power-supply oscillator. The frequency is increased or decreased to decrease the size of the error voltage; that is, to bring the output voltage back toward the desired value whenever it has strayed due to a powerline voltage change or load change.

Toroidal transformer cores are used because they have the requisite high permeabilities and square hysteresis loops. For reliability and repeatable performance, the temperature rise of the core must be minimized. The cores are therefore mounted di-

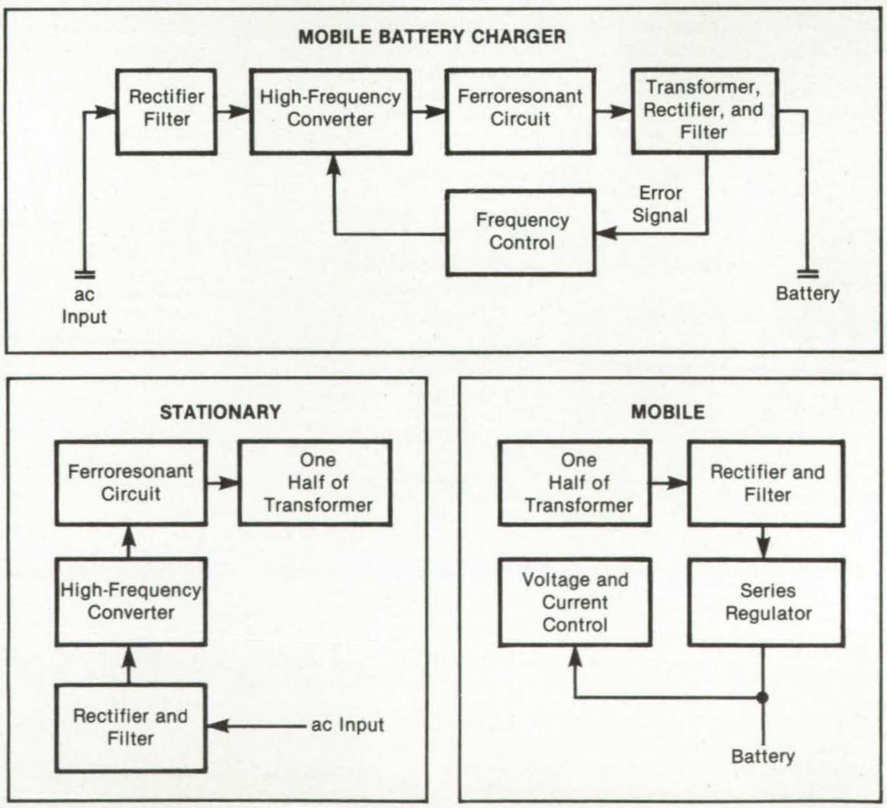

Figure 1. The **Battery Charger** could be built as a mobile unit or as a stationary unit plus a mobile unit that is brought to the stationary unit for charging.

IN A MATTER OF SECONDS, THE NEW TEK 2467 CAN SAVE WEEKS OF TROUBLESHOOTING.

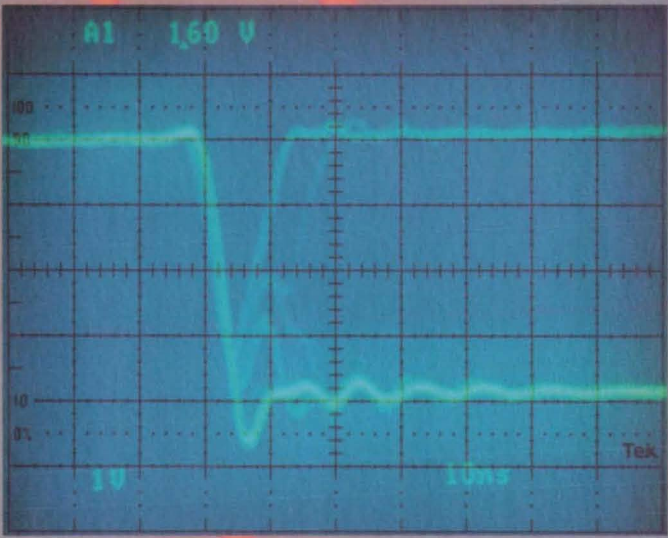

Now. See what you've always needed to see with a portable scope. (Above) Tek's new 2467 Transient Intensifying Oscilloscope, with its exclusive microchannel-plate CRT, highlights the infrequent metastability of a flip-flop output. (Below) The same metastability is invisible on a conventional high-speed scope.

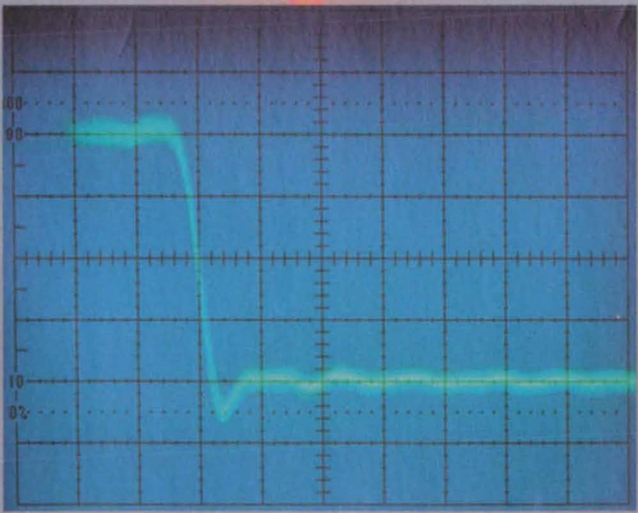

Don't be stymied by elusive glitches, pulses and single-shot events.

Our new 350 MHz Transient Intensifying Oscilloscope reveals invisible signals that escape detection by any other portable instrument. An approximate 100-fold increase in *visual* writing rate translates high-speed, single-shot phenomena and low-repetition-rate signals into easily-seen displays—in normal room light and at sweep speeds as fast as 500 ps/div.

Discover marginal conditions you don't even know exist. Now designers and test engineers can quickly identify circuit or system faults caused by infrequent metastability, asynchronous noise, crosstalk or erratic timing-margin violations—even if they occur only once in a million normal operations.

Not only can you shorten time to market, you can deliver more reliable new products.

To see the Tek 2467 in action, or to order, contact your Tek Sales Engineer. Or call the Tek National Marketing Center, 1-800-426-2200. In Oregon, call collect, (503) 627-9000.

To rent a Tek 2467 for a trial evaluation, contact an authorized Tektronix rental company:

Continental Resources, Inc.
(800) 323-2401 Nationwide
(312) 860-5991 Illinois

Electro Rent Corporation
(800) 423-2337 Nationwide
(800) 232-2173 California

General Electric Company
(800) GE-RENTS

GENSTAR Rental Electronics, Inc.
(800) 227-8409 Nationwide
(800) 331-3440 California

McGrath RentCorp
(415) 568-8866

Telogy, Inc.
(800) T-E-L-O-G-Y-Inc.

U.S. Instrument Rentals, Inc.
(800) 824-2873

Tektronix®
COMMITTED TO EXCELLENCE

Circle Reader Action No. 359

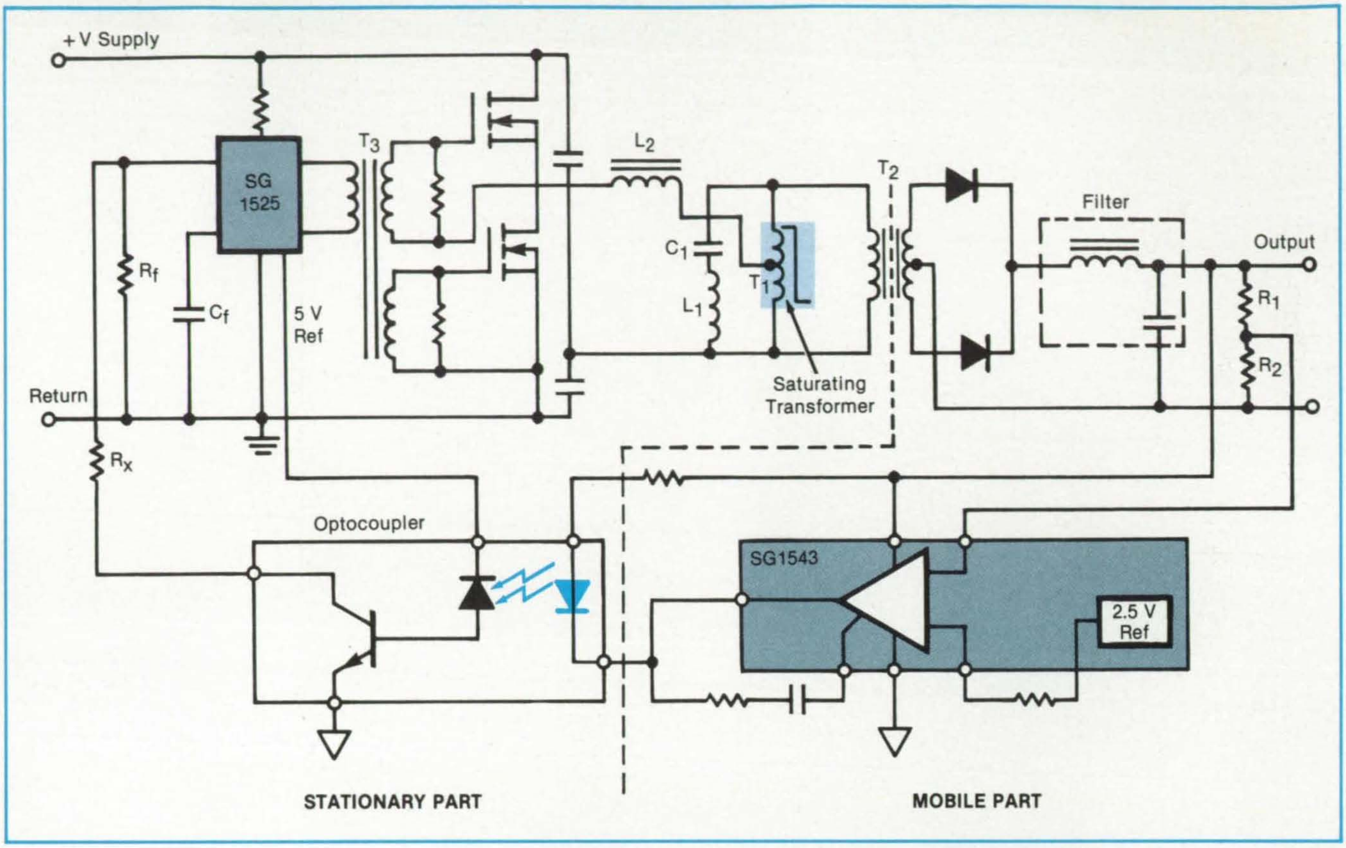

Figure 2. The **Charger Circuit** includes a lightweight ferroresonant saturating transformer. The circuit operates at about 20 kHz so that lightweight magnetic-coupling and output-filtering components can be used.

rectly in heat-sinking metal brackets that conduct heat away from cores and windings. Each winding surrounds its core and bracket. This kind of design ensures good heat sinking with reduced size and weight.

This work was done by Colonel W. T. McLyman of Caltech for **NASA's Jet Propulsion Laboratory**. *For further information, Circle 88 on the TSP Request Card.*

Inquiries concerning rights for the commercial use of this invention should be addressed to the Patent Counsel, NASA Resident Office-JPL [see page 29]. Refer to NPO-16530.

GaAs Semi-Insulating Layer for a GaAs Device

Damaging thermal stresses at cryogenic temperatures would be greatly reduced.

NASA's Jet Propulsion Laboratory, Pasadena, California

In an improved design for a GaAs electronic device or integrated circuit designed to operate at cryogenic temperatures, the customary SiO_2 insulating layer is replaced by a semi-insulating layer of GaAs. The thermal expansions of the device and the covering layer therefore match closely, and thermal stresses caused by immersion in a cryogenic chamber are nearly eliminated.

Conventionally, a layer of doped SiO_2 in the form of borosilicate or phosphosilicate glass is deposited on the GaAs by pyrolytic deposition. Because of the difference in thermal expansion between the SiO_2 and the GaAs, severe thermal stresses are developed especially at the periphery of openings in the SiO_2 layer as the device is cooled from the deposition temperature or from room temperature to the operating temperature of 20 to 77 K. The interfacial stresses concentrate at the edges of the holes that are etched in the SiO_2 layer in the course of device fabrication, with consequent damage to the GaAs device.

In the new fabrication process, the semi-insulating layer of GaAs is grown epitaxially on the semiconducting GaAs of the device. The device is subsequently processed in a manner similar to that of the SiO_2. With negligible variations caused by doping, the crystal lattice and thermal expansion of the two GaAs layers match closely at all temperatures.

The electrical resistivity of the semi-insulating GaAs (10^{12} ohm-cm) is not as great as that of SiO_2 (10^{17} ohm-cm), but apparently it is sufficient for the intended application. Chromium doping might increase the resistivity. In devices that have to operate at high frequency, a more serious disadvantage lies in the fact that the dielectric constant of the semi-insulating GaAs is 12, while that of SiO_2 is only 3.8. The relatively high dielectric constant will give rise to higher shunt displacement-current leakage.

This work was done by Greg Sherrill and Robert J. Mattauch of the University of Virginia for **NASA's Jet Propulsion Laboratory**. *For further information, Circle 80 on the TSP Request Card.*

Inquiries concerning rights for the commercial use of this invention should be addressed to the Patent Counsel, NASA Resident Office — JPL [see page 29]. Refer to NPO-16394.

Voltage Regulators for Photovoltaic Systems

Two small, inexpensive regulator circuits consume little power.

Lewis Research Center, Cleveland, Ohio

Two simple circuits were developed to provide voltage regulation for high-voltage (i.e., >75 volts) and low-voltage (i.e., <36 volts) photovoltaic/battery power systems. The use of these circuits results in a voltage regulator that is small, low-cost, and reliable, with very low power dissipation.

A simple oscillator circuit can control photovoltaic-array current to regulate system voltage and control battery charging. The circuit senses the battery (and system) voltage and adjusts the array current to keep the battery voltage from exceeding a maximum voltage (determined by the number and type of battery cells). The oscillator circuit combined with a power-control device forms a complete regulator (see top parts of Figures 1 and 2).

The regulator switches the photovoltaic array on and off at a rate inversely proportional to the battery voltage. If the battery voltage is lower than the low voltage limit, the circuit turns on the array full time. If the battery voltage is above the high voltage limit, the circuit turns off the array. The circuit switches the array on and off periodically if the battery voltage is between these two voltage limits. The duty cycle (ratio of the time on to the times on plus off) of this switching action is varied, according to the battery (system) voltage, to vary the average array current. This action then keeps the battery voltage at or below the high voltage limit.

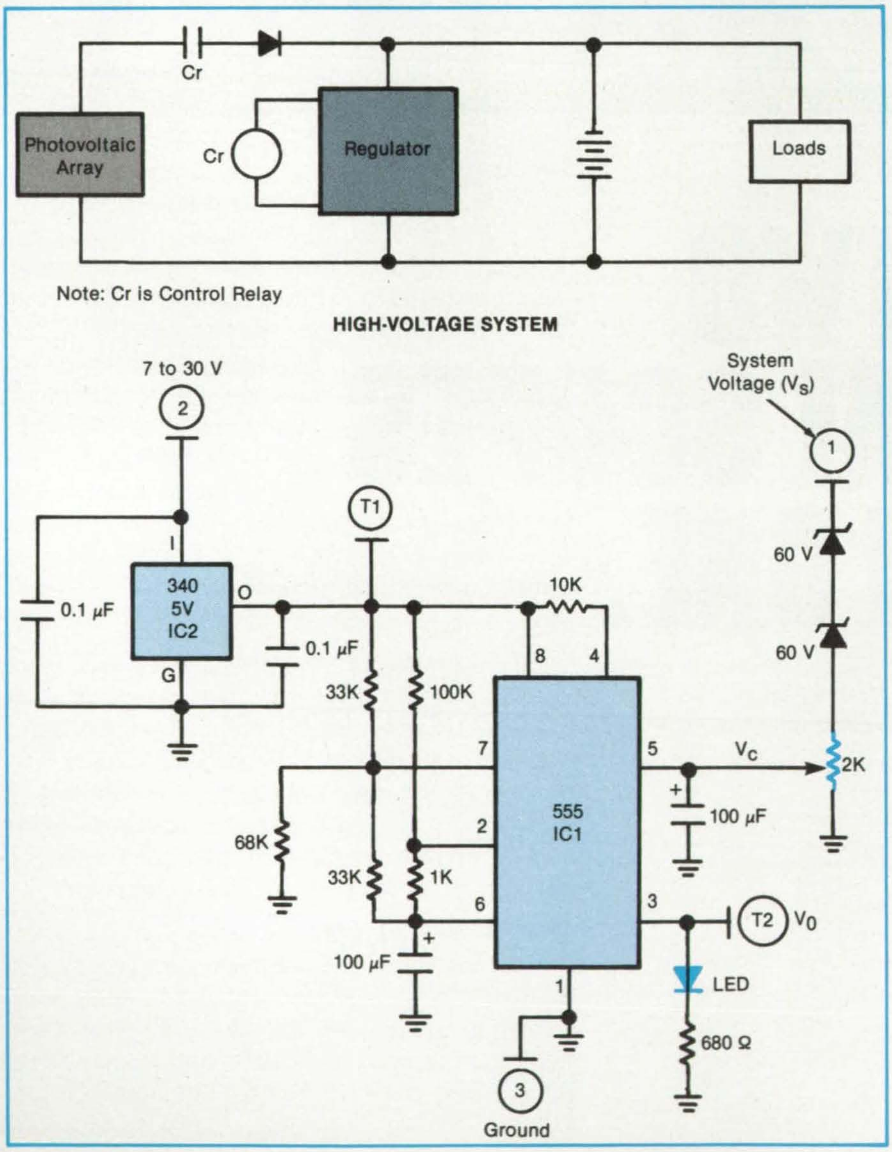

Figure 1. A **Regulator for High-Voltage Systems,** shown in more detail on the circuit diagram, performs as an astable oscillator. Its duty cycle is derived from the system voltage. Adjustments in the nominal operating voltage are controlled by the potentiometer and by use of zener diodes with different voltage ratings.

The circuit shown in Figure 1 is used for high-voltage systems (i.e., >75 volts). The oscillator circuit incorporates an oscillator/timer integrated circuit IC_1, type 555. With the external components, the circuit is configured as an astable oscillator with a period of approximately 5 seconds. The duty cycle of the output is controlled by the voltage at pin 5 of IC_1, which is derived from the system voltage.

The nominal operating voltage of the circuit can be changed in two ways. For large-scale adjustments (>3 percent), the zener diodes can be replaced with those having different voltage ratings. For finer adjustments and calibrations, the 2-kilohm potentiometer can be adjusted. With the two 60-volt zener diodes in Figure 2, this regulator is used in a 120-volt dc (nominal) system.

The circuit shown in Figure 2 is used for low-voltage systems (i.e., <36 volts). The oscillator circuit incorporates a commercial pulse-width-modulated switching circuit, type ZN1066, IC_2. IC_2 consists of (along with other functional elments) a comparator and an oscillator. The output of IC_2 is a 0.5-Hz switching waveform, with the duty cycle of the waveform being a linear function of the system voltage. The nominal operating voltage of the circuit can be changed in two ways. For major changes in voltage range, such as for operation at 6, 12, or 24 volts, several component values need to be changed. For small adjustments such as calibrations, the potentiometer is adjusted.

A light-emitting diode (LED) in each circuit provides a visual indication that the circuit is switching on and off. A single high- or low-voltage regulator may be used to control a small array (see Figure 1), or several regulators may be used in parallel to control independent sections of a large array. The high-voltage system can utilize multiple high-voltage regulators: Multiple regulators tend to smooth the total array current to minimize the effects of switching transients. For higher power applications, the power-switch section may be replaced with a circuit of higher power capabilities, or it may be used to control a larger relay or transistor.

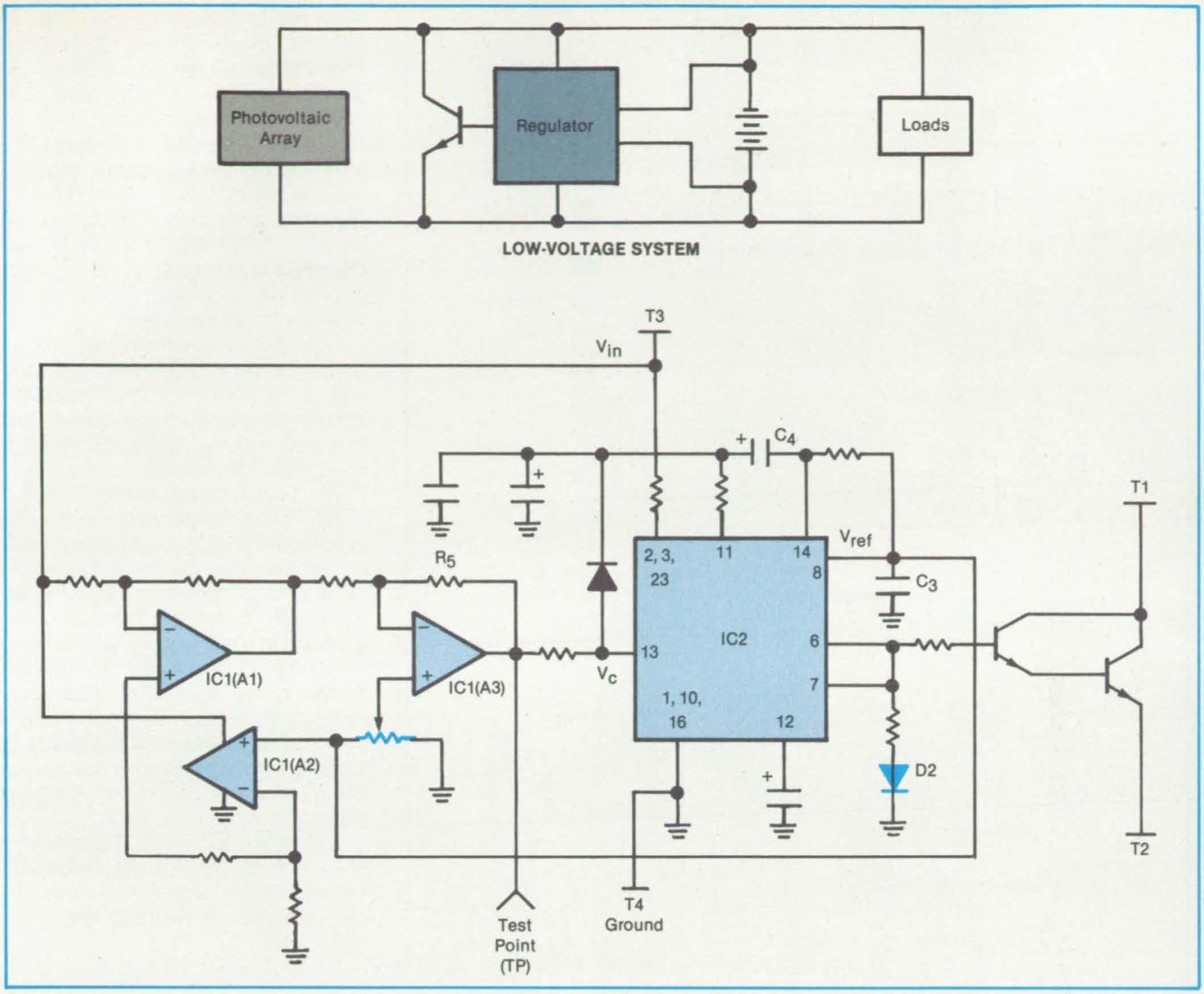

Figure 2. A **Regulator for Low-Voltage Systems,** shown in more detail on the circuit diagram, uses a commercial switching circuit as an oscillator. Small adjustments in the nominal operating voltage are controlled by the potentiometer; larger adjustments require changes in values of several components.

This work was done by Richard DeLombard of **Lewis Research Center.** *Further information may be found in NASA TM-83625 [N84-25926/NSP], "Low Frequency Switching Voltage Regulators for Terrestrial Photovoltaic Systems."*

Copies may be purchased [prepayment required] from the National Technical Information Service, Springfield, Virginia 22161, Telephone No. (703) 487-4650. Rush orders may be placed for an extra fee by calling (800) 336-4700. LEW-13288

Pulling-Speed Control for Silicon-Web Growth

An automatic system promises to ensure high-quality silicon ribbon.

NASA's Jet Propulsion Laboratory, Pasadena, California

A proposed control system for the dendritic-web growth of silicon ribbons varies the ribbon speed according to the melt temperature. The system would prevent too fast or too slow withdrawal of the silicon web, which can cause pullout of the web or excessive web thickness, respectively. The system would also enable the semiautomatic startup of web growth by automatically increasing the web speed from zero to the optimum value.

A growth-control thermocouple is placed at a predetermined point (see figure) within the growth furnace but outside the crucible. The measured temperature determines ahead of time the temperature at the growing crystal. By a combination of prior temperature measurements and thermal modeling of the furnace, the relationship between the growth-control-thermocouple temperature and the crystal-growth-zone temperature is established and expressed as a time constant for exponential transient damping. Typically, the time constant is of the order of 2 minutes.

A single-crystal seed of silicon is inserted in the melt, as in the usual procedure, and the temperature of the melt is decreased so that the seed crystal grows outward. When the seed reaches a predetermined size, the system starts the motor to withdraw the seed, pulling with it a thin web of silicon. The system adjusts the motor speed continuously as the

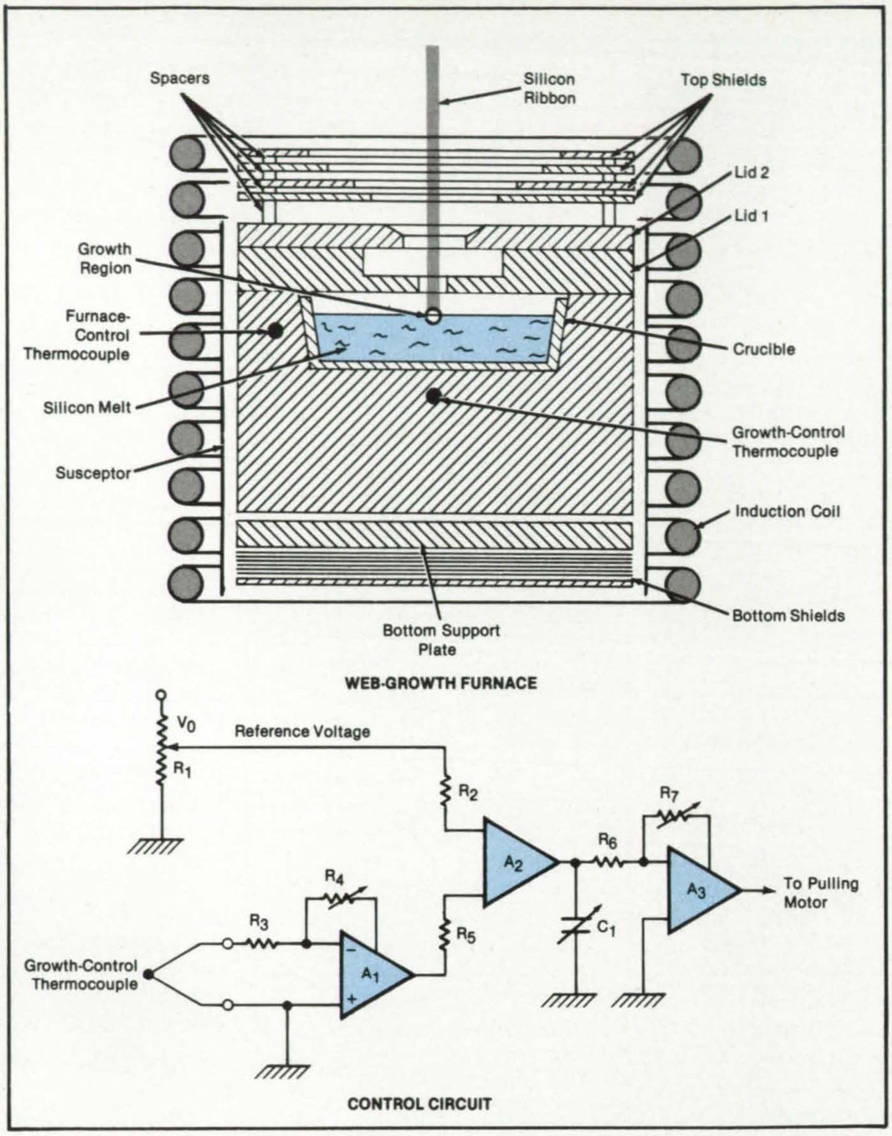

Temperatures Are Monitored at the furnace-control and growth-control points in the growth furnace. Capacitor C_1 in the control circuit takes into account the lag between a temperature change at the growth-control point and a temperature change at the site of the growing ribbon.

monitored temperature varies. This adjustment allows for the dip in melt temperature necessary to start the growth as well as for temperature variations during the subsequent growth.

As shown in the figure, the output of the growth-control thermocouple is amplified and inverted by operational amplifier A_1. The output of A_1 and a reference voltage are fed to differential amplifier A_2. The differential output of A_2 is fed to a final amplifier, A_3 that provides the control signal for the pulling motor.

When the surface of the melt is at the starting temperature (the melting point of silicon), the reference voltage is adjusted to produce a zero voltage from A_2 and thus also from A_3. The motor speed is thus initially set at zero.

The furnace control is then reset to a slightly lower temperature. When the temperature change reaches the growth-control thermocouple, the output of this thermocouple decreases, causing the output of A_1 to increase. The output of A_2 increases at a rate determined by the size of capacitor C_1, which takes into account the lag in the temperature drop in the web-growth region. The control signal from A_3 thus reflects the lag, gradually increasing the motor speed in accordance with the estimated current temperature at the growth front.

This work was done by Robert Richter of Caltech for **NASA's Jet Propulsion Laboratory**. *For further information, Circle 105 on the TSP Request Card.*
NPO-16685

Long-Term Electronic Timer

Power is turned on for intervals up to months.

Ames Research Center, Moffett Field, California

A timing circuit turns on a power source upon command, then turns it off again after a preset interval. In comparison with prior devices, the unit consumes little power and is smaller, lighter in weight, and less complicated.

The timer includes an oscillator and a counter in an integrated circuit (see figure). The timing interval equals the oscillator period multiplied by the number of cycles to be counted. The oscillator frequency depends upon resistor R_s and capacitor C_x. The number of oscillator cycles to be counted before the counter output changes state is determined by the selection of the counter output terminal, shown here as pin 3. The interval can be set anywhere in the range from fractions of a second to months; it is given by $T = 0.55R_sC_x2^n$, where n is an integer determined by the counter-output selection. Accuracy can be improved with a crystal.

Operation is initiated by the closure of momentary switch S_1 (or by a command signal having a similar effect). This grounds one side of relay K_1, thereby activating the relay and causing the closure of the switches that supply power to the timer and to the load. The turn-on of V_{cc} at the timer is coupled through C_1 to the counter-reset terminal, thus resetting the counter. The initial reset voltage transient is then drained away through R_1 to permit normal operation.

During the first half cycle of the counter operation, the counter output voltage (at pin 3 in this case) is low. This turns on transistor Q_1 so that relay K_1 latches on, enabling the timer to continue running even though switch S_1 has opened.

The oscillator runs while the relay is on. When the number of oscillator cycles reaches the limit, the counter output voltage at pin 3 goes high. This turns off Q_1,

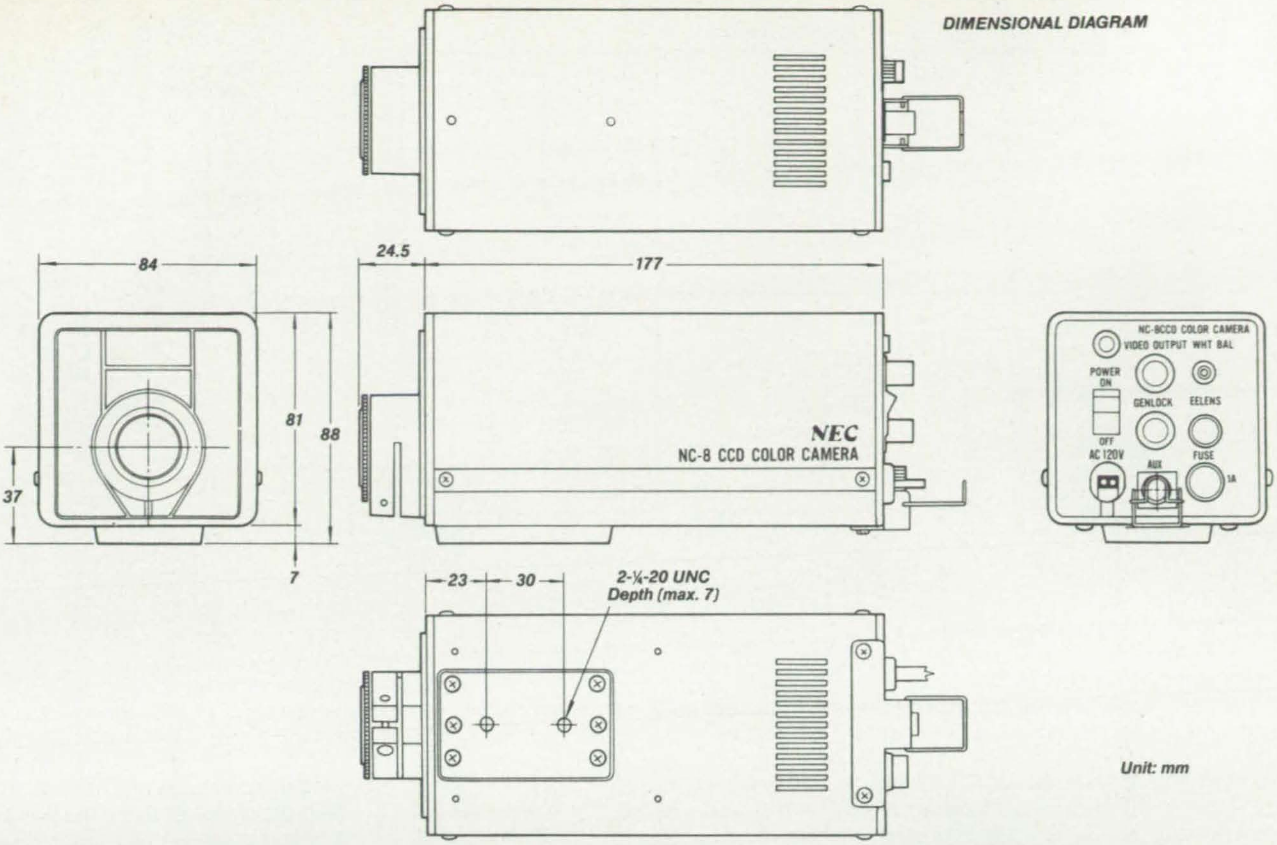

OUR DESIGN FITS YOUR SPECS.

NEC invites you to take a look inside the NC-8 single chip color camera — the camera designed with your specifications in mind. With the lightweight, flexible NC-8, you get high definition and resolution, very low lag and no burn in. It resists shocks, is immune to magnetic distortion, and because its pixels are arranged in a high precision matrix, there is no geometric distortion. It includes Gen Lock as a standard feature. It is equipped for any C-mount lens including auto iris.

This durable little camera is a match for any of your toughest video camera requirements and is easily adaptable to a wide variety of settings.

NEC, the world's largest manufacturer of semiconductors, offers an entire line of solid state industrial cameras — all high quality, hard-working products from a respected source.

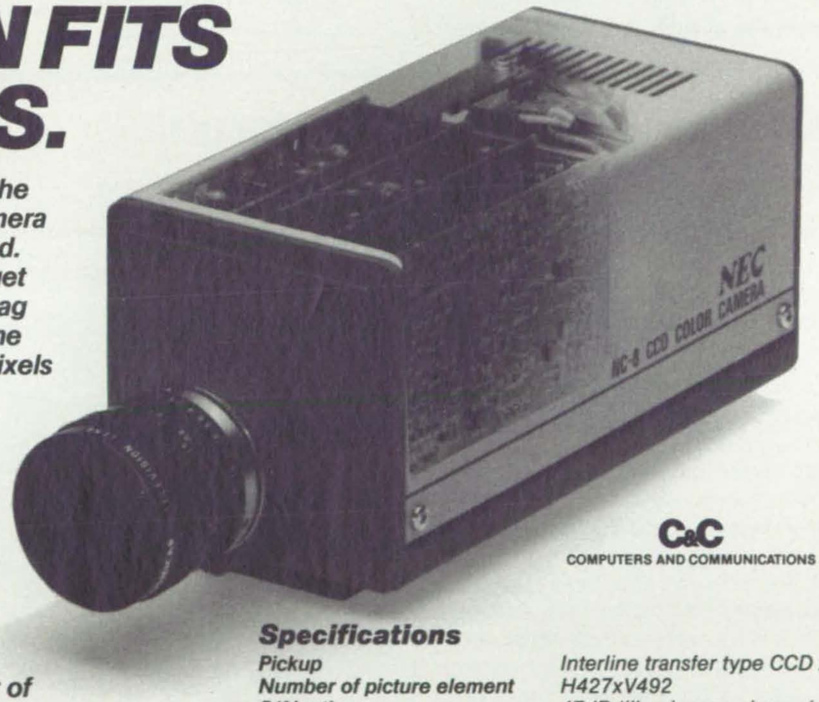

C&C
COMPUTERS AND COMMUNICATIONS

Specifications

Pickup	Interline transfer type CCD x1
Number of picture element	H427xV492
S/N ratio	47dB (illuminance channel, standard recording conditions, AGC: off)
Resolution	Horizontal: 280 lines Vertical: 350 lines
Sensitivity	1,600 Lux F4.0
Minimum illumination	10 Lux F1.4 AGC: ON (20% signal output level)
White balance adjustment	Manual/Remote
Lens mount	C-Mount
Power consumption	Approx. 6.5W (less than 9VA)
Weight	Approx. 1.4kg [3.1 lbs] (excluding lens)

NEC
IMAGINE WHAT WE'LL DO FOR YOU

For more information about the NC-8, TI-22AII, TI-22PII and TI-26A industrial cameras, contact the Industrial Video Group, Broadcast Equipment Division, NEC America, Inc., 1255 Michael Drive, Wood Dale, IL 60191 Toll free 1-800-323-6656. In Illinois phone 312/860-7600.

Circle Reader Action No. 369

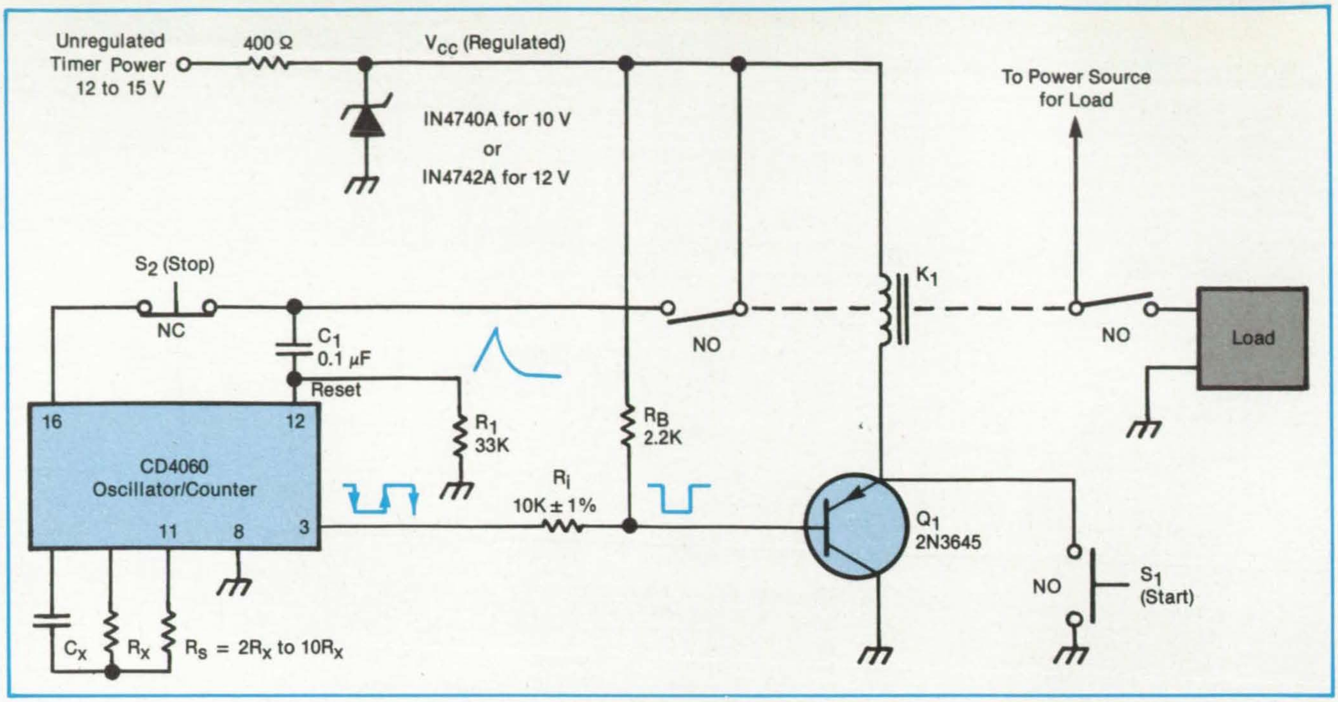

An **Oscillator and a Counter** in an integrated circuit package are combined with other commercially available parts to form a simple, reliable timing circuit. The timer is precise within 0.08 percent.

thereby turning off the relay and returning the system to the original "power-off" state to await the next starting command. The timing cycle can also be interrupted and the system turned off by opening normally-closed switch S_2.

This work was done by Gerald Temple and Tom Kalaskey of **Ames Research Center**. *For further information, Circle 1 on the TSP Request Card.*

Inquiries concerning rights for the commercial use of this invention should be addressed to the Patent Counsel, Ames Research Center [see page 29]. Refer to ARC-11590.

Electroabsorption Infrared Modulators

Compact monolithic arrays will operate at high speed.

NASA's Jet Propulsion Laboratory, Pasadena, California

New solid-state infrared modulator arrays have been fabricated and tested successfully. The arrays are based on electroabsorption, and because of the high speed inherent in small devices of this kind, they are expected to perform well at multigigahertz frequencies in such applications as multiplexing, demultiplexing, high-speed recording, and printing.

The modulator array includes eight parallel single-mode waveguides. Each waveguide is also a p-π-n heterojunction diode. To modulate the light in a waveguide/diode, a reverse voltage is applied at the diode contacts. Most of the applied voltage is developed across the π region, which is also the region of highest refractive index and, therefore, the region in which most of the optical radiation is guided. Thus, most of the radiation travels through the high-electric-field region, resulting in the optimum electroabsorption interaction.

Molecular-beam epitaxy is used to grow three $Ga_xAl_{1-x}As$ layers on an n+—GaAs substrate (see Figure 1). Next, groups of eight 5-µm-wide CrAu contact stripes with center-to-center spacing of 9 µm are depos-

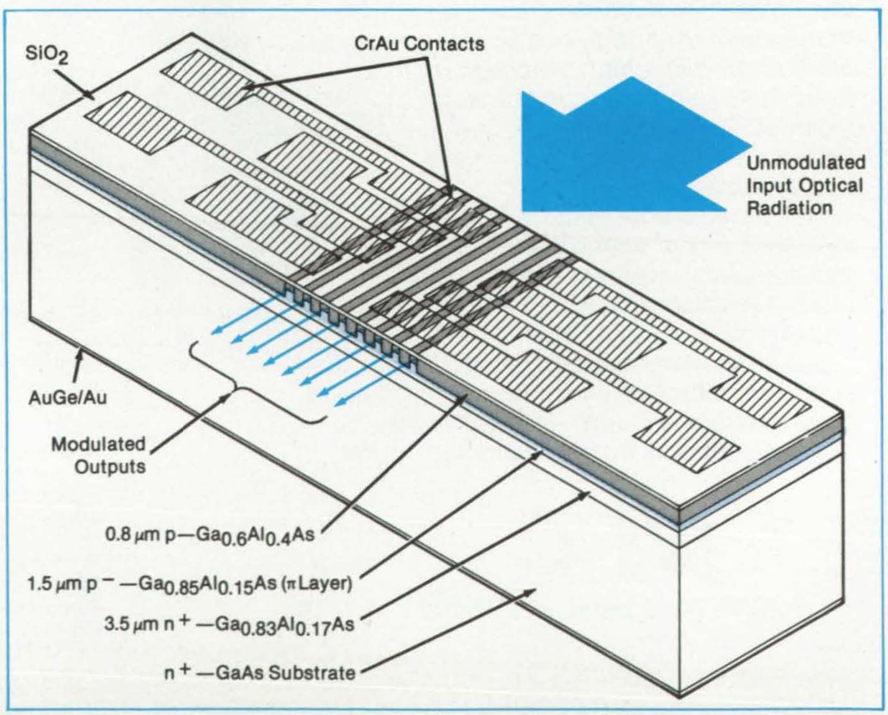

Figure 1. A **Monolithic Array of Modulating Waveguides** is fabricated in $Ga_xAl_{1-x}As$.

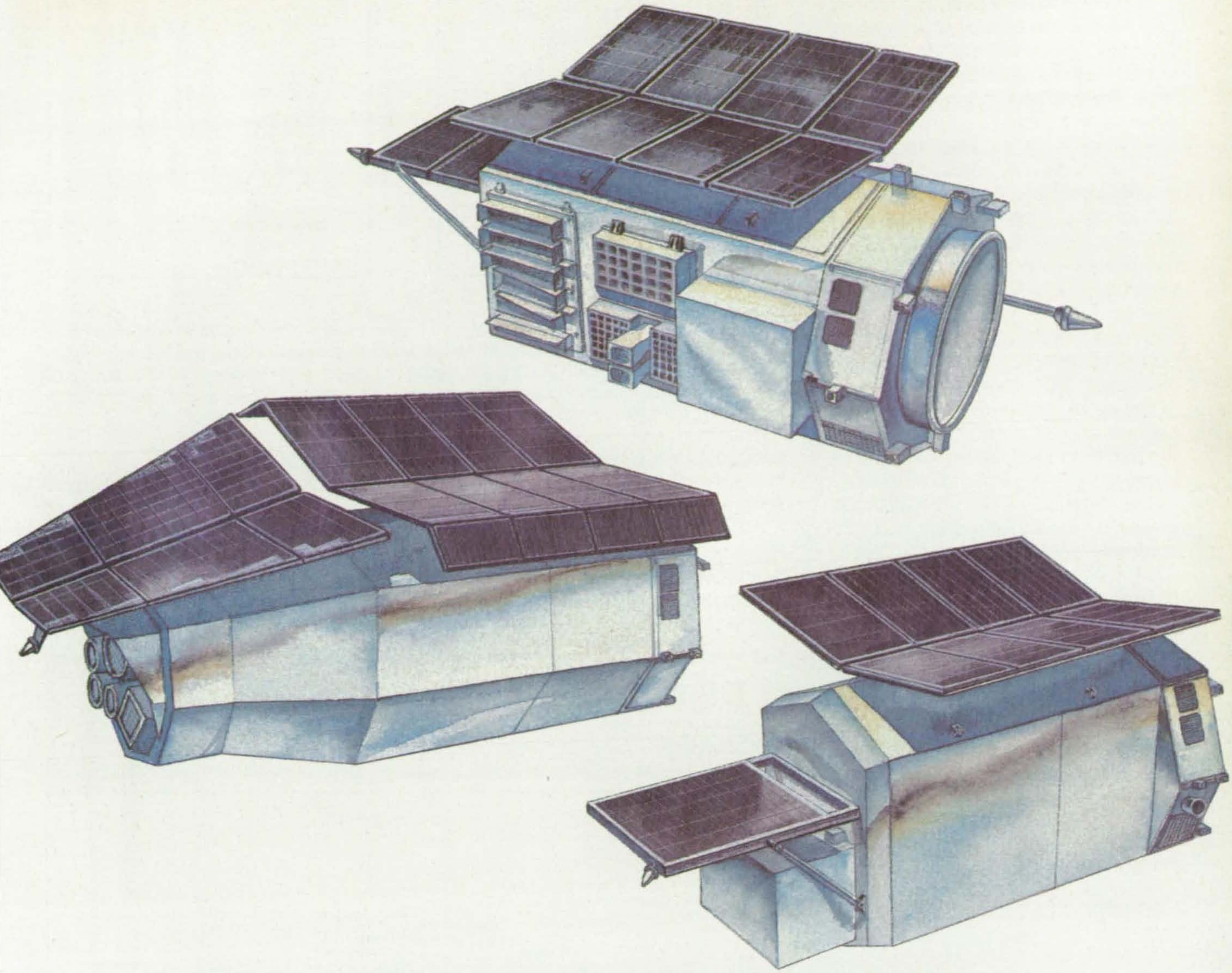

ited using a lift-off technique.

The waveguides are electrically and optically isolated from each other by proton implantation. Thick photoresist stripes on top of the CrAu stripes serve as the implantation mask. The proton energy is 160 keV, and the dose is 3×10^{15} cm^{-2}.

A film of SiO_2 is deposited, and contact holes are opened by standard photolithographic techniques. The second level of CrAu contacts is then evaporated onto the SiO_2. Finally, the wafer is lapped, a contact layer of AuGe/Au is evaporated onto the bottom, and the wafer is cleaved into individual devices.

In tests, arrays were illuminated by a beam focused from a semiconductor laser (wavelength 830 to 850 nm) on the entrance facets of the waveguides. When reverse bias was applied to individual waveguides, the outputs of those waveguides were reduced by electroabsorption (see Figure 2).

The magnitude of electroabsorption increases nonlinearly with voltage, becoming noticeable at higher levels (typically, 35 V for nearly complete extinction). The magnitude of electroabsorption also depends on the wavelength and polarization: It is higher in the TE than in the TM mode, and higher at 830 nm than at 850 nm.

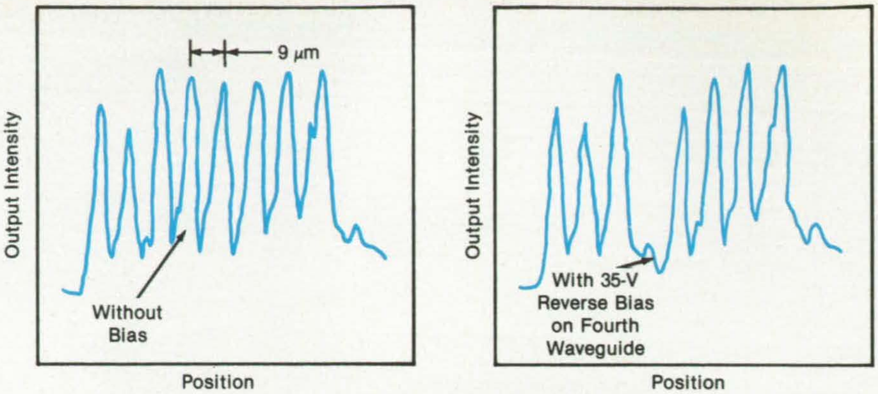

Figure 2. **Near-Field Scans** of the output of a modulator array show the suppression of output of the fourth waveguide from the left when 35-V reverse bias is applied to it. Residual electrical coupling with the fifth waveguide causes a slight diminution in the output of that unit as well. This defect should be curable in future devices by deeper ion implantation during manufacturing.

This work was done by Deborah L. Robinson, William K. Marshall, and Joseph Katz of Caltech for **NASA's Jet Propulsion Laboratory**. *For further information, Circle 48 on the TSP Request Card.*

Inquiries concerning rights for the commercial use of this invention should be addressed to the Patent Counsel, NASA Resident Office-JPL [see page 29]. Refer to NPO-16481.

Dual-Sampler Processor Digitizes CCD Output

Less bandwidth is required for processing.

NASA's Jet Propulsion Laboratory, Pasadena, California

A proposed circuit (see figure) for processing the output of a charge-coupled device (CCD) imager provides increased time for analog-to-digital conversion, thereby reducing the bandwidth required for video processing. Instead of the one sample-and-hold circuit of a conventional processor, the improved processor includes two sample-and-hold circuits that are alternated with each other.

To process a CCD signal in real time, the output of each pixel on the imager must be sampled, held, and converted to digital values during one pixel period — typically about 15 μs. A sample-and-hold circuit requires about 5 μs to acquire a sample with 0.01 percent accuracy, leaving only about 10 μs for analog-to-digital conversion. For some converters, this is not enough time. The new circuit makes more time available by

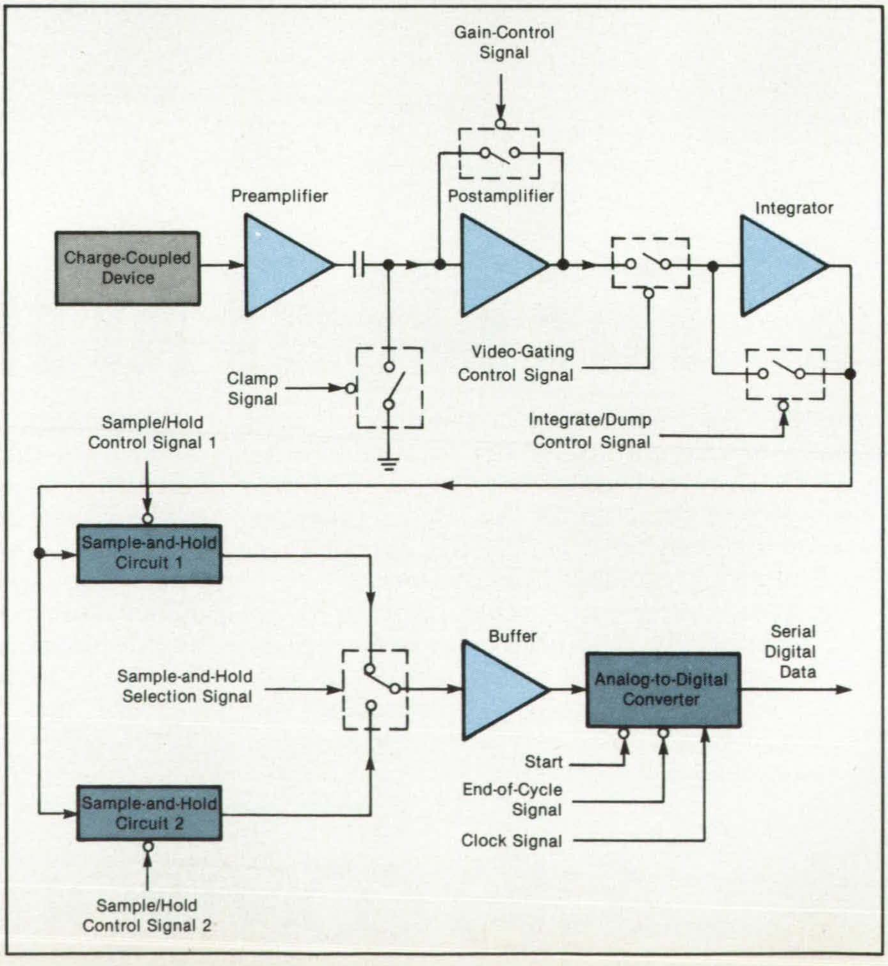

The **Dual-Sampler Processor** operates with lower bandwidth and with timing requirements less stringent than those of a single-sample processor.

Sensing the future.

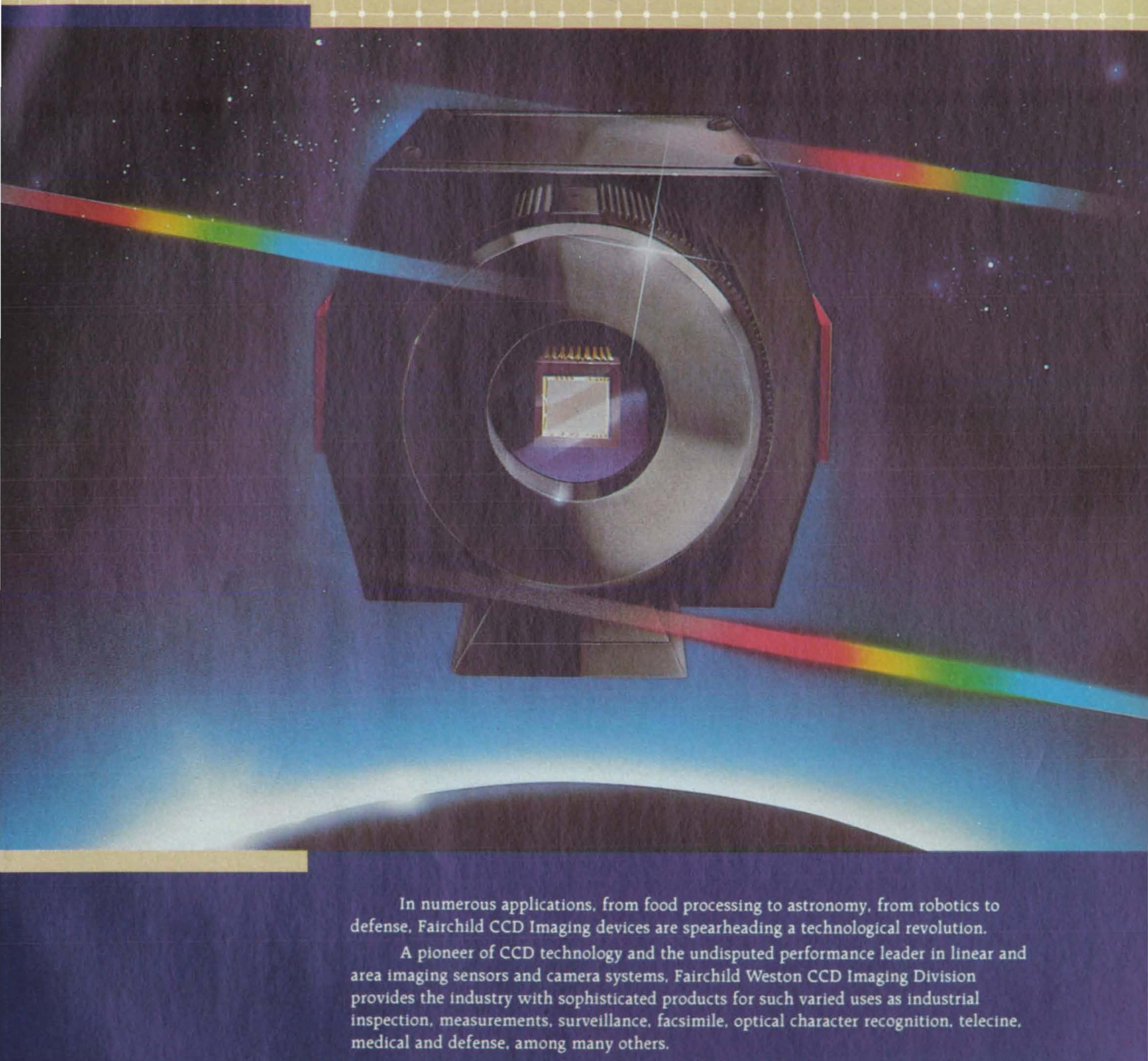

In numerous applications, from food processing to astronomy, from robotics to defense, Fairchild CCD Imaging devices are spearheading a technological revolution.

A pioneer of CCD technology and the undisputed performance leader in linear and area imaging sensors and camera systems, Fairchild Weston CCD Imaging Division provides the industry with sophisticated products for such varied uses as industrial inspection, measurements, surveillance, facsimile, optical character recognition, telecine, medical and defense, among many others.

As your imaging needs continue to change, we will be there with the right products for your application. Moreover, you can count on total support from the most experienced engineering staff in business, technically qualified field sales representatives and stocking distributor in your region.

To find out what we can do for you, or to receive our CCD catalog, please write us on your company letterhead: Fairchild Weston, CCD Imaging Division, 810 W. Maude Ave., Sunnyvale, CA 94086 or call us [408] 720-7600 or your local Hamilton/Avnet location.

FAIRCHILD WESTON SYSTEMS INC.
CCD IMAGING DIVISION

FAIRCHILD WESTON
Schlumberger

Excellence in Solid State Imaging Technology ... Worldwide

Circle Reader Action No. 411

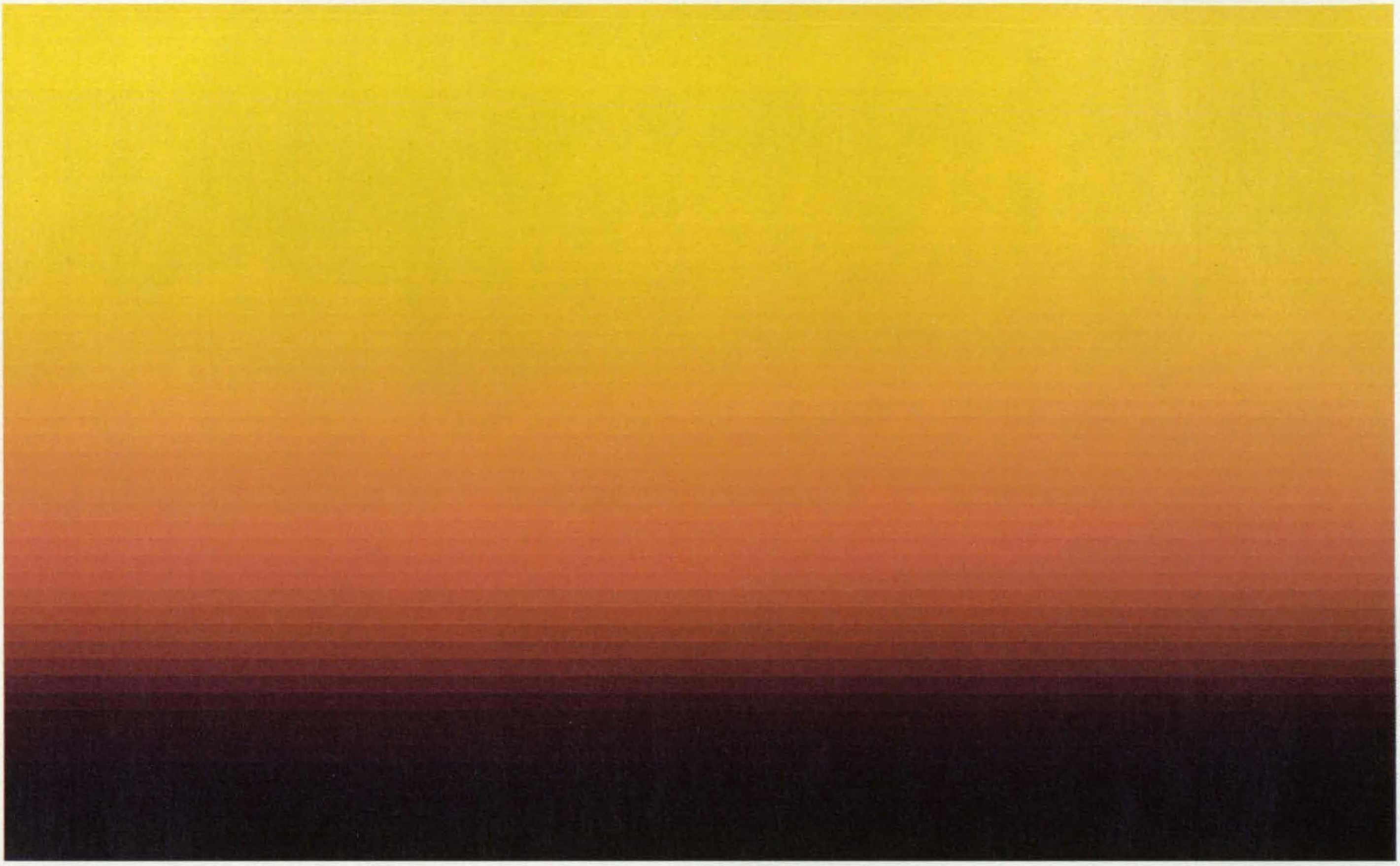

assigning part of the task to each of two sample-and-hold circuits: This allows a slower converter to be used, and each sample-and-hold circuit can be operated in a track-and-hold mode for additional accuracy of signal acquisition.

During a pixel interval, one sample-and-hold circuit samples while the other holds and provides input to the analog-to-digital converter. During the next pixel interval, the sample-and-hold circuits exchange roles. Each sample-and-hold circuit thereby prolongs the holding period beyond the pixel-sampling interval, well into the next pixel interval.

In the proposed design, the sampling interval is approximately 7 μs and the holding period approximately 23 μs. The time available for analog-to-digital conversion would be increased to approximately 12 μs, with a concomitant decrease in the required analog bandwidth and reduction of noise. An additional advantage is gained by the relaxation of speed and timing requirements of the clocking and signal-processing elements. Disadvantages include the increased complexity associated with the additional sample-and-hold circuit; the requirement of a single-pole, double-throw video switch with sufficient isolation between the sample-and-hold units; and an additional output delay of one pixel interval.

This work was done by Phil M. Salomon of Caltech for **NASA's Jet Propulsion Laboratory**. *For further information, Circle 45 on the TSP Request Card.* *NPO-16726*

Pulse-Width Proportional-Controller Circuit

A quad operational amplifier circuit yields full 0- to 100-percent pulse-width control.

Marshall Space Flight Center, Alabama

A proportional controller for motor speed provides full 0- to 100-percent linear control of the durations of motor-driving pulses. Conventional proportional controllers using phase-shift techniques provide a more-limited pulse-width range, typically 15 to 85 percent. As with any pulse-width proportional controller, the motor has high starting torque because the pulse height always equals the full supply voltage.

The controller (see figure) uses a commercially available LM3900 integrated circuit, which requires only a single supply voltage of 4 to 30 V. The pulse-repetition rate is set by a 1-kHz oscillator that incorporates amplifier A_1. The oscillator feeds ramp generator A_2, which generates a linear ramp voltage for each oscillator pulse. The ramp signal feeds the inverting input of comparator A_3; the speed-control voltage feeds the noninverting input.

Thus, the output of the comparator is a 1-kHz pulse train, the pulse width of which changes linearly with the control voltage. The control voltage can be provided by an adjustable potentiometer (as shown) or by an external source of feedback information such as a motor-speed sensing circuit. Depending on the control-voltage setting, the pulse duration can be set at any value from zero (for zero average dc voltage applied to the motor) to the full pulse-repetition period (for applied motor voltage equal to dc power-supply voltage).

An amplifier stage (A_4) with a gain of 10 acts as a pulse-squaring circuit. A TIP-31 medium-power transistor is driven by A_4 and serves as a separate power-amplifier stage. Additional power amplification may be required, depending on the motor being controlled. Since the power transistors that drive the motor are used essentially

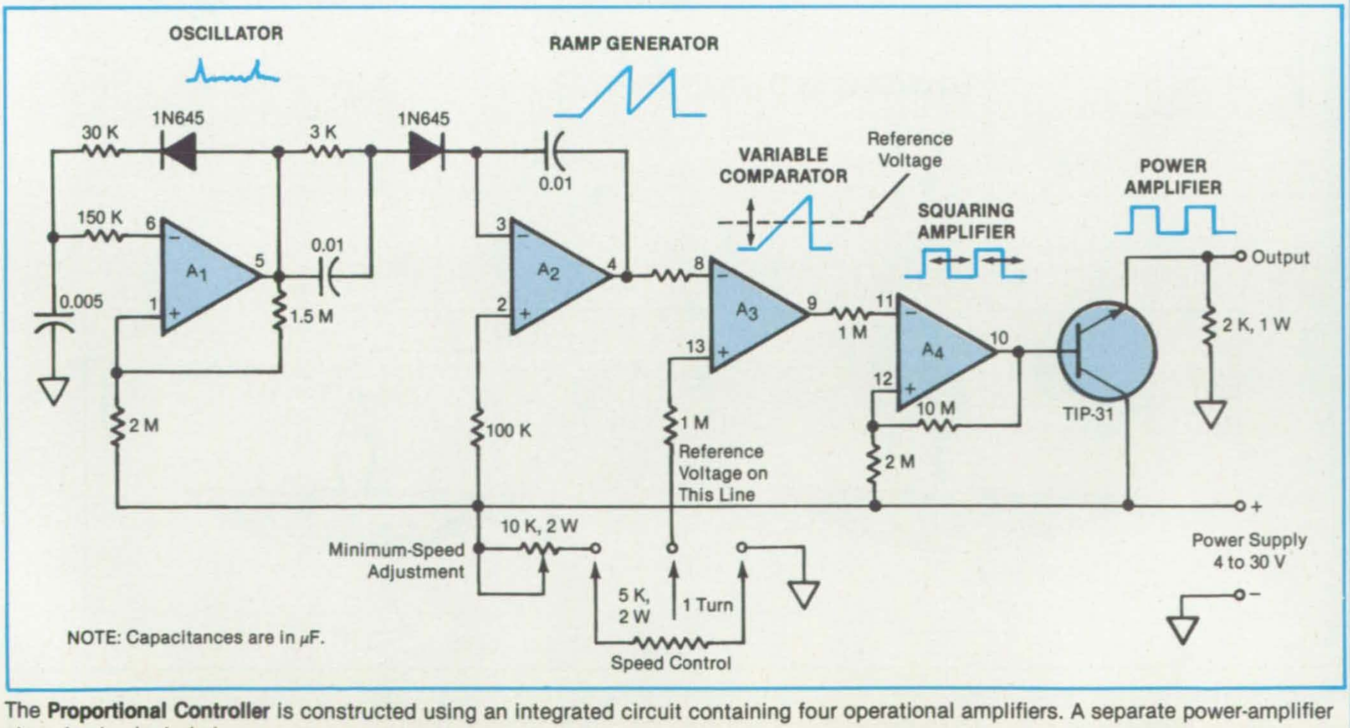

The **Proportional Controller** is constructed using an integrated circuit containing four operational amplifiers. A separate power-amplifier stage is also included.

as switches, transistor power dissipation is minimized. Thus the controller could also be used for the efficient control of such resistive loads as heaters.

This work was done by Rodney W. Clukey of Rockwell International Corp. for **Marshall Space Flight Center**. *For further information, Circle 10 on the TSP Request Card.* MFS-29102

A Combined Scanning Configuration for Near-Field Antenna Measurements

Combination of a cylinder and a plane enhances the customary configurations

NASA's Jet Propulsion Laboratory, Pasadena, California

A proposed scanning configuration for near-field antenna measurements uses cylindrical and plane-polar coordinate surfaces to guide the motions of the electromagnetic-field probes. Near-field measurements are needed especially to enable the determination of the far fields of large, low-sidelobe, multiple-beam antennas, for which the application of far-field measurements are often not suitable.

Prior near-field measurement coordinates were laid out on hemispherical, planar, or cylindrical surfaces (see top of figure). However, none of these configurations is suitable for measurements on large, multiple-beam antennas that may be sensitive to the orientation in the gravitational field: It is difficult to move the probes over such large surfaces, and the far-off-axis parts of the radiation patterns cannot be measured, even though they may contain important information on sidelobes.

The improved scanning arrangement (see bottom of figure) includes a vertical cylindrical coordinate surface topped by a horizontal plane-polar coordinate surface. This configuration surrounds the antenna with a pattern of measurement points more useful than do the other con-

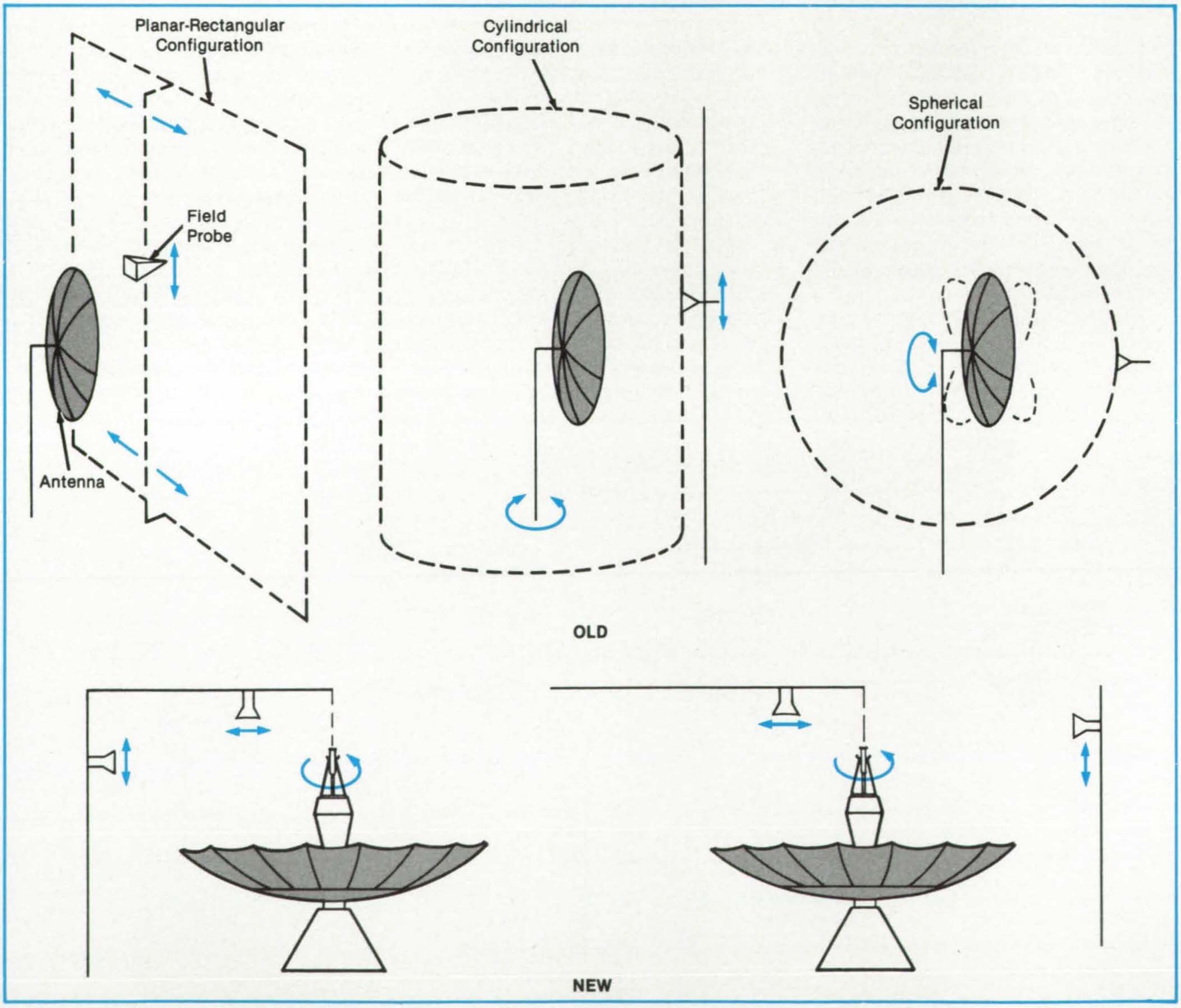

The **Old and New Scanning Configurations** differ in size and shape. The proposed new cylindrical/plane-polar scanning configuration requires less space, yet is expected to give complete measurements with fewer mechanical complications.

figurations. The overall dimensions of the vertical and horizontal scanning arms depend on the size of the antenna under test. However, this configuration lends itself to a modular mechanical design that can be adapted easily to antennas of different sizes and shapes.

Other advantages of the new configuration include the following:

- Reflector-dish and other antennas that are sensitive to gravitation can be pointed skyward to balance the weight.
- The scanning motions are simple; the antenna can be rotated on a stand, and each probe has to be moved only on a straight track. Alternatively, the probe tracks can be rotated about the antenna on a large stand.
- The plane-polar and cylindrical patterns can be scanned separately or together.
- Far-field patterns can be inferred from near-field measurements even for large beams that are scanned substantially away from the antenna axes. Both reflector antennas and arrays of radiating elements can be tested.
- It is not necessary to extend the planar area much beyond the projected antenna aperture because the cylindrical surface can be used to obtain the rest of the required near-field, large-angle data that would otherwise have to be obtained on the outer part of the plane. Thus, the planar-surface area required to test a large antenna is smaller than in a planar (only) configuration.
- With modifications of the computer programs for processing planar-polar and cylindrical measurements, a combined computer program can be generated.

This work was done by Yahya Rahmat-Samii of Caltech for **NASA's Jet Propulsion Laboratory**. *For further information, Circle 126 on the TSP Request Card.*
NPO-16644

Books and Reports

These reports, studies, and handbooks are available from NASA as Technical Support Packages (TSP's) when a Request Card number is cited; otherwise they are available from the National Technical Information Service.

Antenna Quadripod With Reduced Blockage

The net reflector gain is increased by 0.32 dB.

A design study for the subreflector support of a 64-m-diameter paraboloidal microwave antenna is described in a 19-page report. The objective of the study was to upgrade an existing antenna quadripod, subject to mechanical and electromagnetic design requirements and optimization criteria. The principal effort was directed toward reducing the signal blockage by the quadripod legs while minimizing structural weight.

The improved quadripod had to do the following:

- Support a larger, heavier subreflector at the quadripod apex;
- Accommodate lifting loads of the feedcone and subreflector hoists;
- Be stiff enough so that its vibrational frequencies exceed the minimums for compatibility with the antenna servocontrol system; and
- Resist gravitational bending at extreme tilt angles sufficiently to keep the lateral translation of the subreflector within the 9-in. (23-cm) range correctable by the subreflector positioner.

Ignoring diffraction, the blockage calculations were based solely on geometric optics. The quadripod legs were assumed to be opaque. With these assumptions, the blockage includes two components: (1) the shadow cast by the quadripod legs when the antenna is illuminated with a plane wavefront along the axis; and (2) the shadow cast by the legs when the antenna is illuminated by a spherical wavefront emanating from the focus in the subreflector assembly.

One way to reduce blockage is to increase the radius from the antenna axis to the leg-attachment points. Since this option requires excessive fabrication and erection costs, it was rejected. A somewhat more effective way is to make the legs more nearly parallel to the antenna axis. This increases the size of the assembly at the apex, but the assembly has to be enlarged anyway to accommodate the larger subreflector. The most effective way to reduce the blockage is to decrease the widths of the inner and outer faces of the legs, because these widths determine the widths of the shadows.

Various designs incorporating the two surviving changes were analyzed, using a finite-element, pin-jointed-truss mathematical model. The legs were made trapezoidal in cross section; the widths of the inner and outer faces were selected so that the outer faces lay within the spherical-wavefront shadow of the inner faces. Engineering tradeoffs were examined; for example, a reduction in the leg cross section reduces blockage and leg weight, but it also decreases the structural stiffness, as manifested in a decrease in the torsional-vibration frequency and an increase in the gravity displacement of the subreflector.

An optimal design that satisfied all of the competing criteria raised the gain 0.32 dB over that of the existing design. The analysis also lead to the following conclusions:

- Variations in the inner and outer face widths had significant effects on the fundamental torsional frequency as well as on the blockage.
- In all cases, the requirement on the gravity displacement of the subreflector was easily satisfied, and the torsional stiffness controlled the design.
- The pin-jointed mathematical model gives a torsional frequency much lower than that measured on a real structure. A rigid-jointed model, which accounts for the bending and torsional responses of the truss members, gives more realistic results.
- To achieve an adequate fundamental torsional frequency, it is necessary to increase the torsional rigidity of the legs by outrigger braces added at the lower ends.

This work was done by John J. Cucchissi of Caltech for **NASA's Jet Propulsion Laboratory.** *To obtain a copy of the report, "A New Microwave Antenna Quadripod With Reduced Blockage," Circle 75 on the TSP Request Card.*
NPO-16704

Electronic Systems

Hardware, Techniques, and Processes

Books and Reports

Computer Programs

Switching System for Redundant Power Supplies

Reliability increases as power is made more nearly uninterruptible.

Ames Research Center, Moffett Field, California

A load-transfer unit connects an airborne computer to a standby power supply in case the primary supply fails. The concept is adaptable to systems in which power interruptions cannot be tolerated; for example, computers with volatile memories, safety equipment, and precise timers.

The load-transfer unit (see figure) operates with four power inputs, any of which can supply all the power required by the load. In the absence of other indications, the unit selects the input to connect to the load according to a priority list that matches the numerical order of the power-supply designations (supply 1 is the first choice, and supply 4 is the last choice). When it is necessary to switch to a different input, the unit does so in half the time it takes for the load functions to begin deteriorating for a lack of power.

Each input source is provided with overvoltage protection in the form of transient-suppressing filters and voltage sensors. When the unit senses an overvoltage on the active input line, it switches the load to the input line of next lower priority that has a voltage within specification. The unit acts similarly when it senses undervoltage at the load. When the power supply in use is not of the highest priority and a higher priority supply returns to the correct voltage, the unit switches the load back to the higher priority supply.

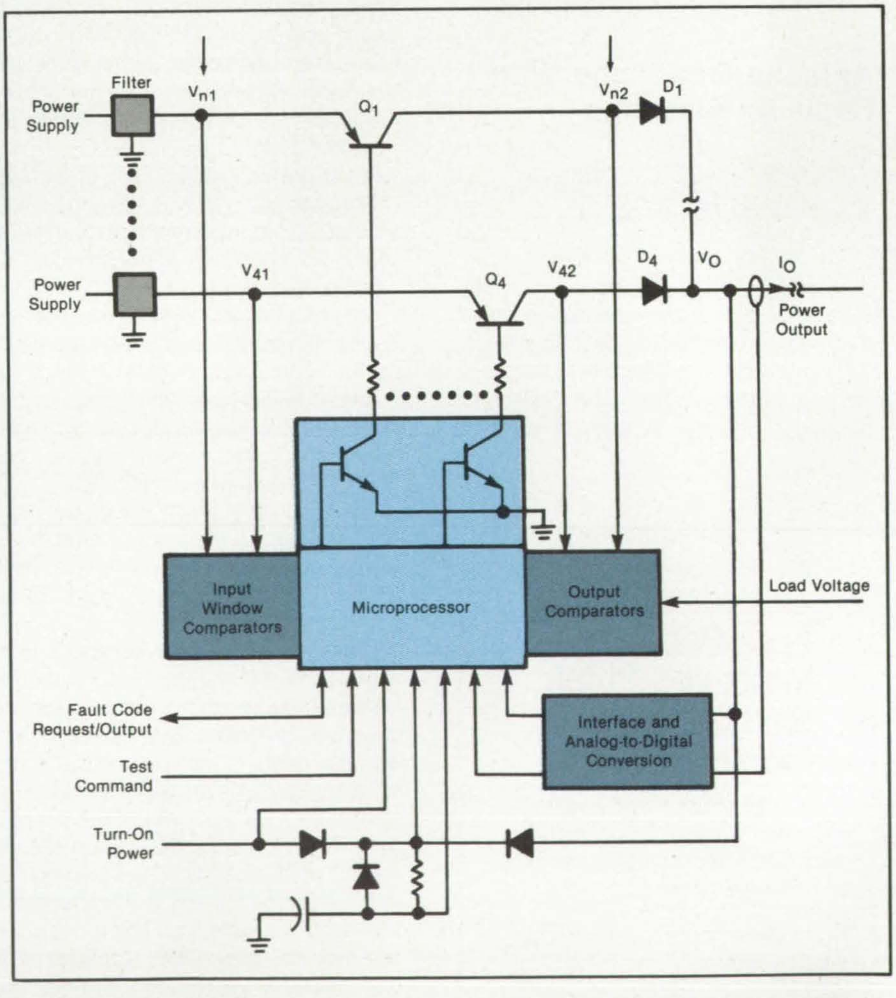

The **Load-Transfer Unit** monitors voltages and load current. The microprocessor controls transistor switches that connect the load to whichever power supply has the highest priority and the correct voltage.

The unit monitors the output current for overload. If an overload persists for a specified time, the unit latches off until all power is removed, then resets so that it can be energized when power is restored.

The unit is provided with a testing program that exercises each monitoring and switching circuit to verify its proper operation and the isolation of the unit. The test is initiated by a command signal and can be done at any time without degrading the output voltage significantly.

All load-transfer-unit circuits are initially supplied by an internal or external power source that can be turned off subsequently. After the four power supplies are turned on, the turn-on source is disconnected, and the unit is powered by the supply connected to the load. A capacitor stores enough charge to maintain all functions through load-transfer interruptions. If power is lost for enough time to allow the capacitor to discharge, the unit latches off until another turn-on pulse is received.

Upon receipt of a turn-on pulse, the processor checks all sensors for proper status before connecting a power supply to the load. The output and V_{n2} sensors should all give "low" indications, and the V_{n1} sensors should indicate input voltages within specification. If any sensor shows an incorrect condition, the processor removes the affected power supply from the priority list. The remaining operable supplies are then listed in the turn-on priority sequence. The highest priority supply is turned on gradually to prevent excessive inrush currents that would be difficult to distinguish from short-circuit currents. From this point onward, operation proceeds as described above, and the priority list is updated at each pass of the microprocessor program.

This work was done by M. Bradford, R. Grant, and G. Parkinson of United Technologies for **Ames Research Center**. *For further information, Circle 12 on the TSP Request Card.*
ARC-11545

Fade-Free Mobile Communication

A mostly digital system would offer high-quality mobile telephony.

NASA's Jet Propulsion Laboratory, Pasadena, California

A scheme for mobile communication would reduce multipath fading and interference between adjacent channels. The proposed communication system lends itself to an almost completely digital implementation, eliminating costly and bulky crystal filters. The scheme is suitable for satellite-aided or terrestrial mobile communication, including cellular mobile telephony, at frequencies in the 150-to-900-MHz range.

The scheme allows improved modulation, demodulation, and signal processing in an amplitude compandored single-sideband (ACSB) system. In the past, the ACSB technique has been hampered by random amplitude and phase variations caused by the motion of the vehicle through a stationary or nearly stationary pattern of communication signals. The new approach would detect and automatically correct for these unwanted variations and thereby reduce signal fading.

In ACSB, the audio signal is compressed before single-sideband modulation takes place. To provide a reference for the automatic gain control and automatic frequency control at the receiving end, a pilot signal is transmitted with the single-sideband signal. The problem is that, as the channel frequency is increased above about 150 MHz, the pilot tone becomes spread because of the random amplitude- and phase-modulation effects of the propagation medium. The higher the frequency, the greater the spreading, and it therefore becomes increasingly difficult for the receiver to separate the signal from the pilot.

The new system would solve this problem by using a Weaver modulator and demodulator with additional signal processing in the receiver for phase and amplitude correction. The Weaver method for generating and detecting single-sideband signals was first described in 1956 but has found little application until now. Component technology was not up to its requirements for accurate quadrature phase shifts at both radio and audio frequencies and close matching of gain, phase, and delay between its two signal channels. However, recent improvements in components make the Weaver method a practical and economical alternative to the conventional method employing narrow, steep-skirted intermediate-frequency crystal filters for rejecting unwanted sidebands and signals occupying adjacent

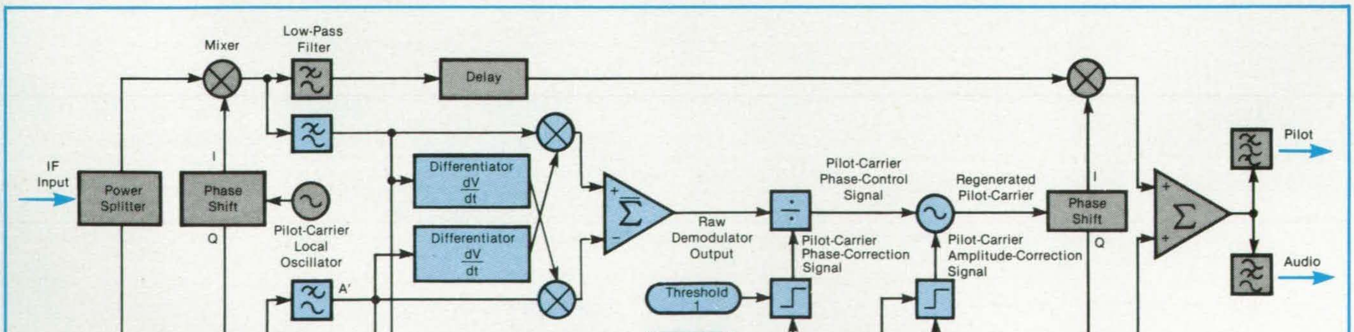

The **Receiving Portion** of a modified amplitude-companding single-sideband system compensates for the multipath fading and Doppler shift that hamper mobile communication. Colored blocks in this diagram represent circuitry added to the basic Weaver demodulator for fading correction. The transmitting portion of the system is a basic Weaver modulator.

Just what the DoD ordered! An embedded, parallel multicomputer with run-time Ada for less than $50,000.

The new Series 600 and 1200 Flex/32 MultiComputers offer system integrators and OEMs the best price/performance available in fifth generation, parallel systems. The Flex/32's concurrent software provides an Ada real-time, run-time environment as well as an Ada development environment. The Series 600 and 1200 come in 21-inch high, standard rack mountable chassis ready for embedding, or in desk-high cabinetry.

And all of this for less than $50,000 in OEM quantities.

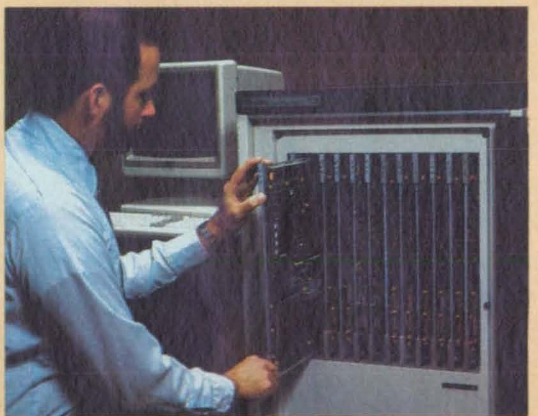

The Series 1200 configured with 8 super minicomputers and 33 mb of memory.

APPLICATIONS

Command/Control and Communications
Multi-target Radar/Sonar
Flight/Combat/Weapon Simulation
Test Systems
Signal/Image Processing
Artificial Intelligence/Expert Systems

PARALLEL HARDWARE

Multiple Super Minicomputers
Multiple Memories
Multiple Data Paths
Multiple Instruction Paths
Multiple VMEbus I/O Paths
Multiple Built-In-Test

CONCURRENT SOFTWARE

Ada
ConCurrent C
ConCurrent FORTRAN
UNIX System V
Real-time Operating System
Concurrency Simulator

Flexible Computer Corporation

P.O. Box 299005; Dallas, Texas USA 75229-9005; (214) 929-6000; TX: 5106001569

Sales Offices: Philadelphia (215) 648-3916; Chicago: (312) 654-1125; Los Angeles (213) 640-3322; San Jose (408) 292-7335; Washington D.C. (703) 356-8882; Florida (305) 344-0808.

A New Dimension in Portable, Digital Spectrum Analyzers!

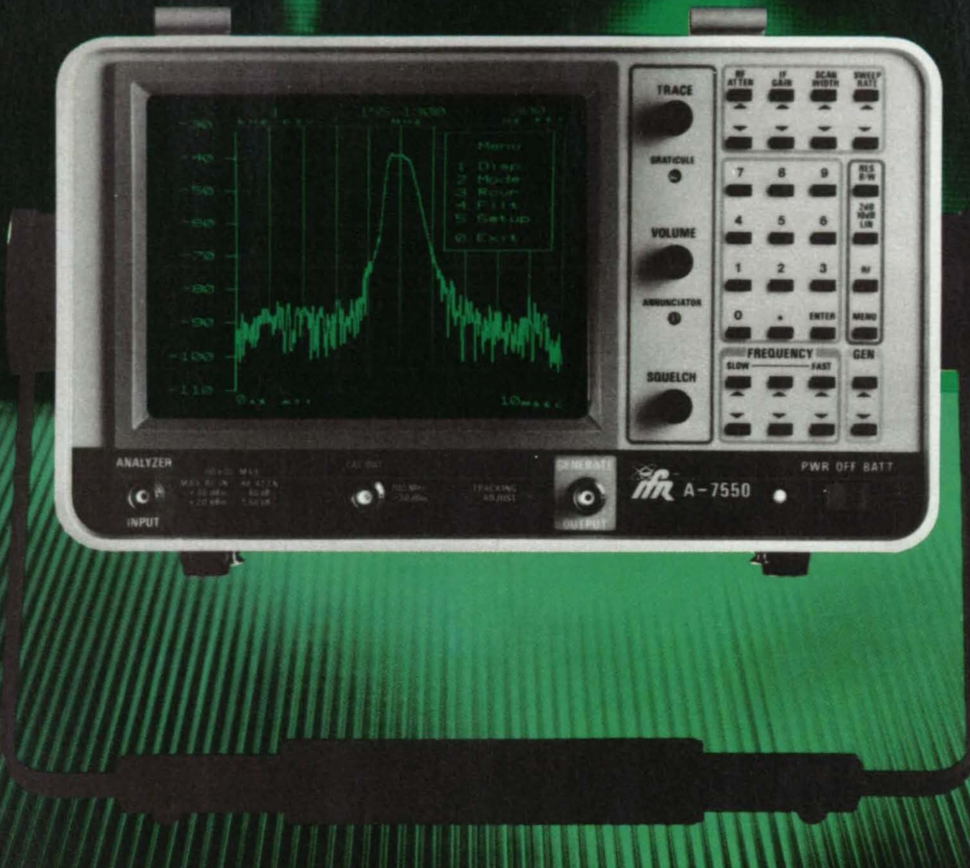

The A-7550 Spectrum Analyzer

The A-7550 Spectrum Analyzer by IFR is the most advanced, low cost, portable spectrum analyzer on the market today.

Two powerful microprocessors, menu driven display modes and single function keyboard entry aid the user in the operation of all analyzer functions.

To further enhance the operational simplicity of the A-7550, the microprocessor system automatically selects and optimizes the analyzers bandwidth, sweep rate, center frequency display resolution and the rate of the frequency slewing keys. An operator override is also provided when non-standard settings are required.

Features...Performance...Dependability... The A-7550 portable Spectrum Analyzer by IFR—innovative accomplishments in design.

Impressive Standard Features Include:

▪ 100 kHz to 1 GHz frequency coverage ▪ VRS™ (Vertical Raster Scan) CRT display ▪ Single function keyboard entry ▪ Menu driven display modes ▪ Automatic amplitude calibration ▪ Selectable linear/log display modes ▪ Digital storage of all displayed parameters ▪ 70 dB dynamic range ▪ 300 Hz resolution bandwidth ▪ 16 selectable scan widths ▪ Accurate center frequency readout ▪ Direct center frequency entry ▪ Automatically scaled electronic graticule ▪ Variable top scale reference (+30 to −95 in 1 dB steps) ▪ IF gain in 1 dB steps ▪ Line, bar, average and compare display modes ▪ 300 Hz and 30 kHz video filters

Optional Features Include:

▪ Internal rechargeable 5 APH battery for portable operation ▪ Tracking generator with 10 dB step attenuator ▪ Tracking generator with 1 dB step attenuator ▪ FM/AM/SSB receiver ▪ IEEE-488 interface bus ▪ RS-232 interface bus ▪ 75Ω adaptor ▪ Quasi-peak detector

ifr → Contact your authorized IFR distributor for a demonstration.

IFR SYSTEMS, INC.
10200 West York Street / Wichita, Kansas 67215 U.S.A.
316 / 522-4981 / TWX 910-741-6952

Circle Reader Action No. 317

channels.

The updated ACSB system would be a hybrid pilot-carrier, tone-in-band system in which the pilot tone is actually the radio-frequency carrier. The received signal is amplified and converted to the intermediate frequency (IF) in a conventional way. After mixing identical samples of the faded IF signal with quadrature components of a local-oscillator pilot signal, the receiver produces the pilot and the folded sideband (see figure). This composite signal is band limited and delayed by an amount equal to the delay through the pilot processor before it is applied to a second set of mixers.

The pilot spectrum in the folded baseband at the output of the first set of mixers is contained within a bandwidth equal to the Doppler frequency shift created by the vehicle speed. The pilot spectrum is recovered by low-pass filters with a corner frequency somewhat greater than the maximum expected Doppler frequency. This separates the faded pilot from the sideband information and allows the pilot to be processed by an amplitude-normalized sine/cosine detector so that fading can be detected and corrected.

This work was done by Carl R. Stevenson of Caltech for **NASA's Jet Propulsion Laboratory**. *For further information, Circle 34 on the TSP Request Card.*

This is the invention of a NASA employee, and a patent application has been filed. Inquiries concerning license for its commercial development may be addressed to the inventor, Mr. Carl R. Stevenson, 845 North Woods Avenue, Fullerton, CA 92632. Refer to NPO-16441.

Monolithic 20-GHz Transmitting Module

Phase shifts are digitally controlled by a compact and relatively inexpensive unit.

Lewis Research Center, Cleveland, Ohio

A 20-GHz monolithic microwave/millimeter-wave integrated circuit (MMIC) with amplification and phase-shift (time-delay) capabilities has been developed. The use of this MMIC module technology promises to make feasible the development of weight- and cost-effective phased-array antenna systems. Advanced phased-array antenna systems have been identified as a major factor in achieving minimum cost and efficient use of the frequency and orbital resources of future generations of communication satellite systems. The use of MMIC transmitting modules provides for a relatively simple method for phase-shift control of the many separate radio-frequency (RF) signals that are required for phased-array antenna systems. Other methods of providing a large number of controlled RF signals suffer in areas of cost, complexity, weight, and overall system efficiency.

This MMIC module uses microelectronic-fabrication techniques that incorporate a microstrip approach, in which all the active and passive devices required for the various module functions are fabricated on a gallium arsenide semiconductor substrate. The module functions include a phase-shifting circuit with controls that provide a digitally-selectable module phase-shift capability of 0 to 360° in increments of 11.25°. A two-stage buffer amplifier follows the phase shifter to compensate for the phase-shifter losses. Finally, a three-stage power amplifier completes the module.

A photograph of the module is shown in the figure. The module size is 4.8 by 6.4 mm. However, a final version is expected to be smaller. The initial version on the MMIC module has demonstrated all of the desired module functions. The predicted overall module performance specifications are as follows: bandwith 17.7 to 20.2 GHz, gain 16 dB, output power 200 mW, and efficiency 15 percent.

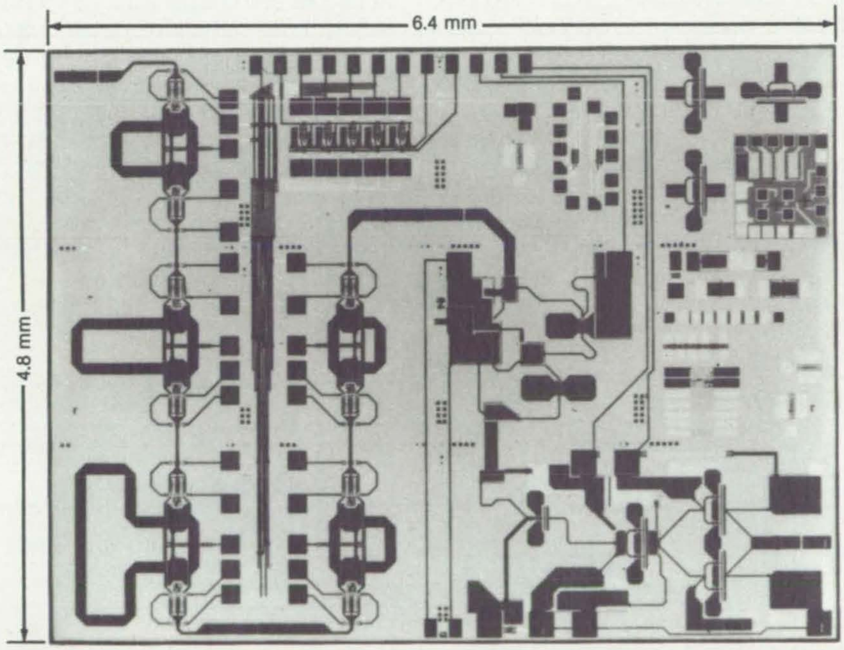

The **Monolithic 20-GHz Transmitting Module** contains a 5-bit phase shifter, a two-stage buffer amplifier, and a three-stage power amplifier.

An important feature of the MMIC module is its relatively large scale of the integration of many and varied devices. The types of devices include the following: transistors (FET's) used both as switches and in amplifying circuits, capacitors, microstrip transmission lines, resistors and diodes. At the high frequency of 20 GHz, this capability to incorporate monolithically many electronic-circuit functions into a single module provides for the consistency of performance.

The MMIC module does not require external tuning. Such other problems as parasitics and device-value uncertainties, normally associated with non-monolithic techniques are minimized. Also, the use of microelectronic-fabrication methods promises to offer the cost-effective manufacture of the large number of MMIC modules that would be required for an advanced phased-array antenna system.

This work was done by T. J. Kascak of **Lewis Research Center** *and G. R. Kaelin and A. K. Gupta of Rockwell International Corp. Further information may be found in NASA TM-83518 [N84-13399/NSP], "Microwave Monolithic Integrated Circuit Development for Future Spaceborne Phased Array Antennas."*

Copies may be purchased [prepayment required] from the National Technical Information Service, Springfield, Virginia 22161, Telephone No. (703) 487-4650. Rush orders may be placed for an extra fee by calling (800) 336-4700.
LEW-14285

Simulator Tests Controller Performance

A computer model imposes reaction torques on a motor, imitating a dynamically changing real load.

NASA's Jet Propulsion Laboratory, Pasadena, California

A compact servosystem applies simulated dynamic loads, enabling realistic appraisal of a motor and its control system without the inconvenience of attaching a real load. The system can simulate moments of inertia, rotational vibrations, changing load torques, and other characteristics of large or complex loads, without the loads themselves and without the awkwardness (and inaccuracy) of gravity-compensating devices that may have to be used with such loads.

The system compares the actual shaft rate and shaft position of the motor under test with the corresponding data from a complete nonlinear real-time computer model of the dynamic performance of the load to be simulated. The system controls a load-simulating motor, which is mounted concentrically on the shaft of the motor under test.

The system includes hybrid analog and digital control (see figure). An analog circuit differentiates the rate signal from a gyroscope on the shaft to determine the actual acceleration, from which it develops a primary torque signal that closely approximates the load-inertia reaction torque. Meanwhile, a digital controller develops a small secondary torque that adds noninertial torques and compensates for most of the error in the primary torque. This brings the total torque close to the value needed to simulate the load dynamics.

The simulator includes stability and drift compensation of the analog loop. It also includes automatic safety devices.

The actual shaft inertia can be kept much smaller than the inertia being simulated: a ratio of more than 10 to 1 has been achieved. Changing inertia loads can be simulated without interruptions to rearrange the apparatus: the system simply follows changes in the driving dynamic model.

Torque transducers are not required. There is implicit verification of the accuracy of the conversion from the command signal to the torque exerted by the motor under test because conversion errors show up in the angular tracking error and are automatically taken into account. The test-control computer monitors the angular tracking error to determine whether the motor under test is converting properly.

This work was done by Michael F. Lembeck and Robert D. Rasmussen of Caltech for **NASA's Jet Propulsion Laboratory**. *For further information, Circle 76 on the TSP Request Card.*
NPO-15744

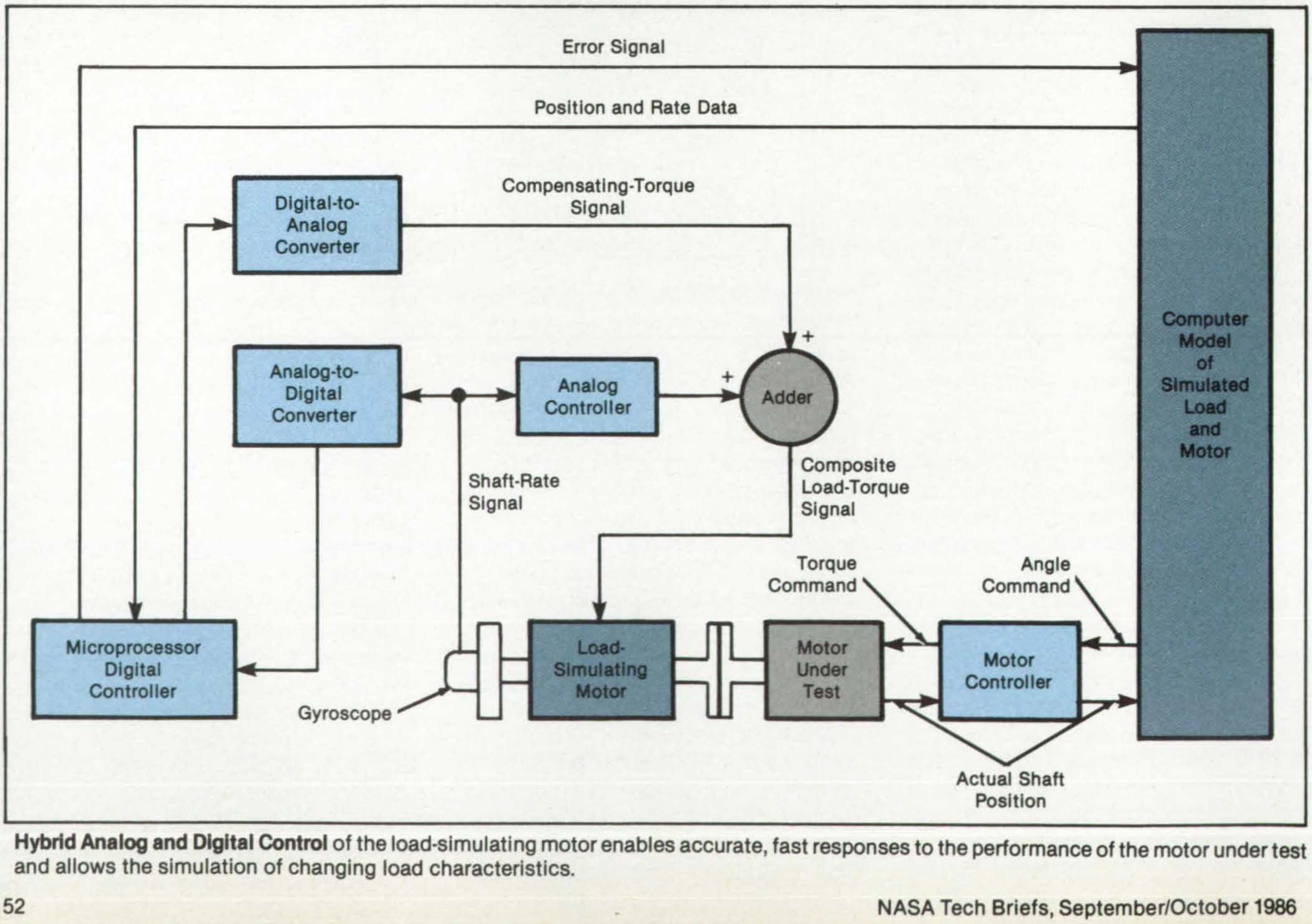

Hybrid Analog and Digital Control of the load-simulating motor enables accurate, fast responses to the performance of the motor under test and allows the simulation of changing load characteristics.

Transponder System for High-Frequency Ranging

Distances are measured by phase differences at convenient frequencies.

Lyndon B. Johnson Space Center, Houston, Texas

A transponder system (see figure) uses the phase difference between transmitted and reflected high-frequency radio waves to measure the distance to a target. To suppress spurious measurements of reflections from objects near the target at the transmitted frequency and its harmonics, the transponder at the target generates a return signal at half the transmitted frequency. The system should be useful in such applications as surveying, the docking of ships, and short-range navigation.

The outgoing signal could be sent at any convenient frequency. In the experiments 30.01 MHz was the chosen value because it is well suited for the generation and processing of reference, offset, and intermediate-frequency signals.

The transponder target includes a short dipole antenna with a frequency-halving circuit at its middle. This circuit consists of a varactor and two inductor/capacitor circuits, one resonant below 15 MHz and one resonant above 30 MHz.

The 15.005-MHz return signal generated by the transponder is locked in phase to the 30.01-MHz transmitted signal that impinges on the antenna. As measured at 15.005 MHz, the total phase shift sustained by the signal as it travels from the transmitter to the transponder, then back to the receiver is $2\pi d/\lambda \pm\pi$, where d = the distance to the target and λ = the wavelength at 15.005 MHz. The $\pm\pi$ ambiguity arises from an inevitable uncertainty in the initial phase state of the frequency-halving circuit. The ambiguity can be resolved by an initial calibration at turn-on or by the introduction of suitable amplitude, frequency, or phase modulation.

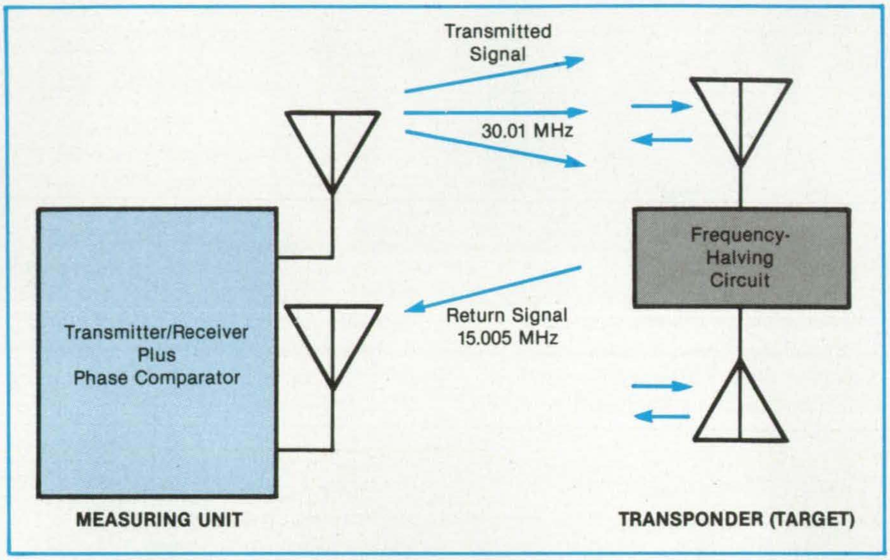

The **Transponder Ranging System** measures distances in terms of the phase difference between the return signal and a phase-locked reference signal. The return signal generated by the transponder is phase-locked but at half the transmitted frequency.

In the receiver the 15.005-MHz return signal is mixed with a 15.000-MHz signal derived from the master oscillator. After low-pass filtering, the mixer output is proportional to

$$\cos\left(\frac{\omega t}{2} - \frac{2\pi d}{\lambda} \pm \pi\right)$$

where $\omega = 2\pi \times 5$ kHz. The receiver also generates a 5-kHz reference signal locked to the master oscillator, proportional to $\cos(\omega t/2)$.

The two 5-kHz signals are separately filtered, amplified, and limited, using standard FM limiters. The limiting process conditions the signals for use in a start/stop counter that counts the delay (typically a few nanoseconds) between the zero crossings of the two signals. When corrected for the phase ambiguity, this delay gives the distance to the target.

An experimental version of the system has been tested with some success. Range measurements were made out to about 350 ft (107 m).

This work was done by Christopher L. Lichtenberg, Paul W. Shores, and Herbert S. Kobayashi of **Johnson Space Center**. *For further information, Circle 69 on the TSP Request Card.*

Inquiries concerning rights for the commercial use of this invention should be addressed to the Patent Counsel, Johnson Space Center [see page 29]. Refer to MSC-20912.

A Priority Protocol for Token-Ring Networks

Key messages are guaranteed access to a local-area network during peak loads.

NASA's Jet Propulsion Laboratory, Pasadena, California

A new priority protocol controls access to a token-ring local-area network (LAN) of digital-communication stations over a widely ranging mix of low- and high-priority traffic. The protocol, called a round-robin priority scheme (RRPS), introduces only a small overhead and therefore degrades system performance only minimally.

The RRPS accommodates the different response requirements of a variety of users and applications (see figure). In an

Data Acquisition

Which recorder is more accurate ?

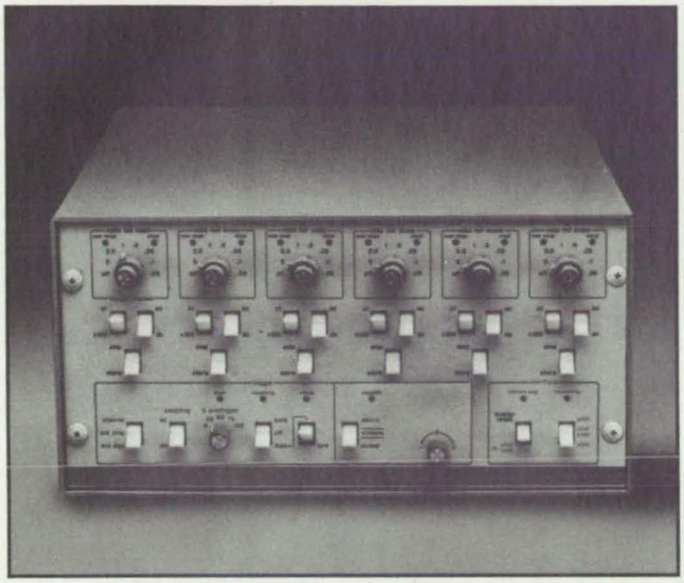

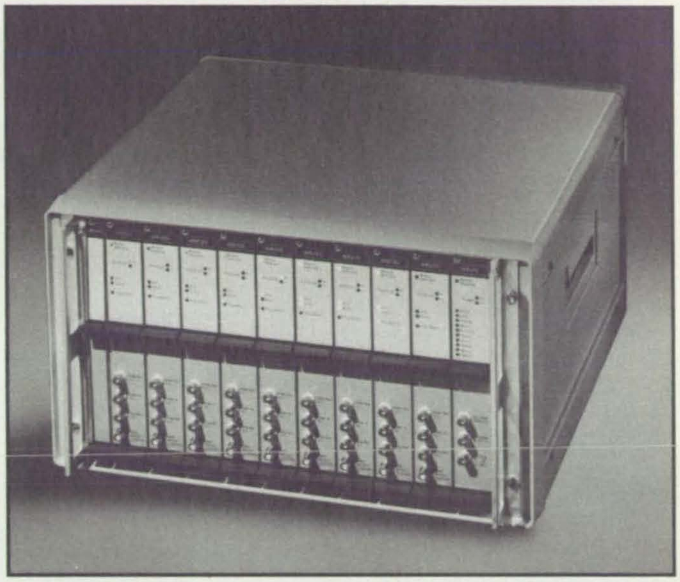

One like this ?

OR, Datalab's versatile, fully programmable multitrap™ with NO dials, NO switches?

multitrap relies on menu-driven software to select the triggering options, sampling rates and data handling required for your application, with 8 or 12 bit ADC. Standard I/O interfaces include 16 bit parallel, GPIB, and RS232 at rates up to 19,200 bauds.

INQUIRE TODAY, get full details PLUS an easy to use selection guide. Call 203-582-3898 for an immediate response, or Fax: 203-583-0748.

Datalab

Data Laboratories, Inc.
44 Dell Manor Drive
Bristol, CT 06010

academic environment, for example, it will ensure that the network responds more rapidly to a service request from a network manager than to a request from a user and that faculty users get faster responses than student users during periods of heavy message traffic. In real-time service, RRPS will provide a constant response delay for voice channels so that intelligibility of conversations is guaranteed. In production applications, it will make sure that control signals from a central computer have preference over routine bulk traffic, such as transfers of file or image data.

Ordinarily, a token-ring network is vulnerable to overloading and unreliable because each station is an active element in network operation; the failure of any station halts the entire network. The RRPS, however, employs distributed priority control so that operation does not depend on any single station. Any station can be assigned dynamically to be the monitor station to poll the status of all the other stations. A high-priority data packet can be sent out by any station.

Any station can send packets of a single priority level or of mixed priorities. The potential for sending a packet of any given priority is equally distributed among all stations regardless of their positions in the ring.

The access algorithm of the RRPS operates in the following way:

- Every message packet has a priority level for gaining access to the ring.
- The priority level of a station is the same as the highest priority of the packets in that station.

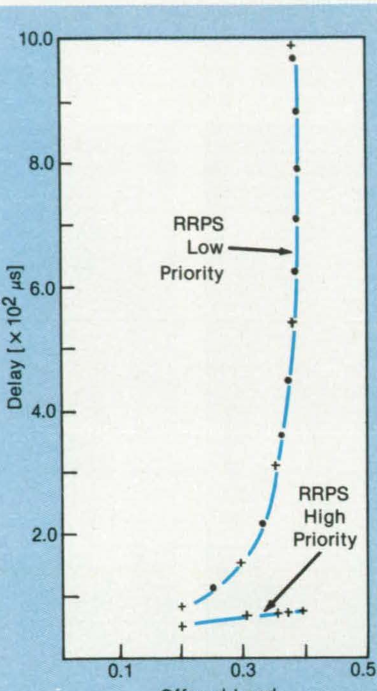

Delay-Throughput Characteristics in RRPS Scheme

- A station can capture a free token having the same or lower priority level.
- If the priority level of a requesting station is higher than the level of a free token, the requesting station marks its level on the token. A free token of the same priority will then be issued after the current transmission is completed. The free token will bypass low-priority stations and be seized by the requesting station; however, an intermediate requesting station with equal or higher priority may capture the token before it reaches the original requesting station.
- If the priority level of the requesting station is equal to the level of a busy token, the station will mark the round-robin bit in the token.
- A destination station sends an acknowlegment back to the source station after receiving a packet. A new free token with the new priority-requesting

The **Round-Robin Priority Scheme** ensures that high-priority stations gain access to the local-area network, regardless of the load imposed on the network. These curves result from the mathematical model of a typical LAN. As the load increases, high-priority requests are delayed hardly at all beyond the normal delay. The prompt service is at the expense of low-priority requests, which can be delayed substantially at high loads.

level is put back into the ring.

- The token returned by a requesting station is checked to see whether it has the same requesting priority as that of the source station and whether the round-robin bit is set. If both conditions are met, a new free token with the requesting-priority level is put on the ring, and the round-robin bit is reset. If the round-robin bit of the old token was not set, then the same station continues to be served.
- If no more packets need to be served, a new free token with zero priority and round-robin bits is put on the ring.

This work was done by Howard T. Liu of Caltech for **NASA's Jet Propulsion Laboratory**. *For further information, Circle 97 on the TSP Request Card.*
NPO-16683

Books and Reports

These reports, studies, and handbooks are available from NASA as Technical Support Packages (TSP's) when a Request Card number is cited; otherwise they are available from the National Technical Information Service.

Global Timing With Low- and High-Orbiting Satellites

Clocks would be synchronized within nanoseconds.

A report summarizes a method for synchronizing clocks at intercontinental distances employing satellites of the Global Positioning System (GPS) in high Earth orbit and a transit satellite in orbit at the relatively low altitude of about 1,300 km. When fully implemented, the method is expected to supply precise time measurements for worldwide communication and navigation.

The comparison of distant clocks is based on differences in the arrival times of signals from the GPS satellites. These differences contain information about the offset between the clocks and the propagation and instrument delays suffered by the signals. Synchronization can be performed if the positions of the two Earth stations and the satellite orbits are known and if the delays are properly calibrated.

When two sites are widely separated, the intervals during which both have a view of the same GPS satellite are often too short for accurate synchronization. Furthermore, the satellite must often be observed near the horizon, so the signals acquire additional delay errors from long paths through the troposphere.

In the proposed system, each ground station looks at a different GPS satellite, which is chosen to be far enough above the horizon so that the tropospheric delay error is minimal. The GPS includes 18 satellites, several of which are usually accessible to the ground stations and simultaneously in view from the transit satellite. Thus, the intervals available for intercontinental time comparison are longer than with a single GPS satellite.

A differential GPS pseudorange measurement is made between the transit satellite and each of the ground sites. A second difference is then taken between the GPS measurements. A precise clock is not needed on the transit satellite because the second difference cancels the transit-clock error.

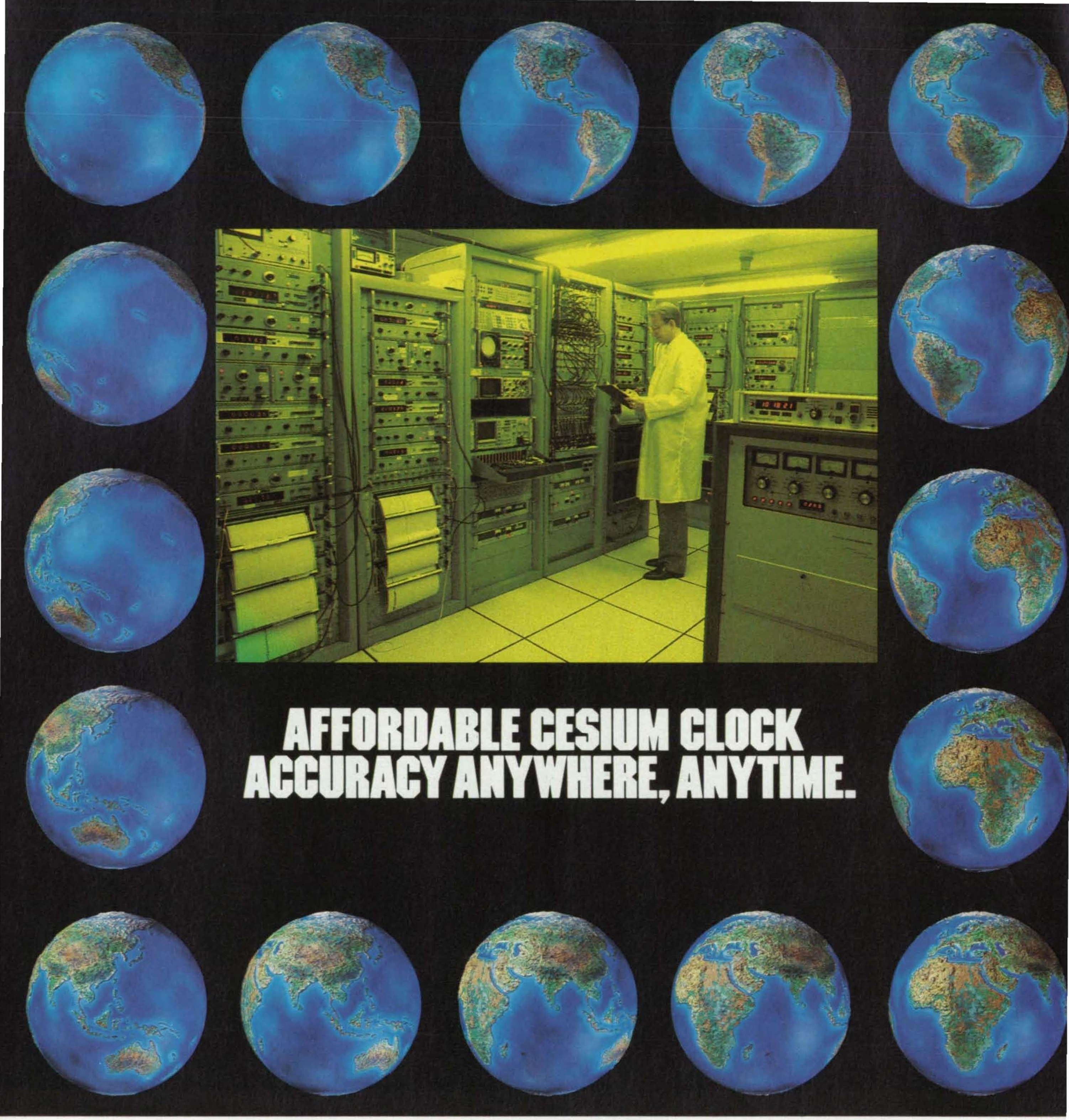
AFFORDABLE CESIUM CLOCK
ACCURACY ANYWHERE, ANYTIME.

Although in principle the transit station could be on the ground, placing it in orbit is advantageous because of the following:

- The ground track covers a large part of the Earth in a short time, thereby providing transit service for a worldwide community.
- The station is above the troposphere and therefore does not introduce the additional tropospheric delay error of a ground station.
- The rapidly changing geometry of the low orbit improves the precision of the GPS orbital-position measurements, thereby improving the accuracy of time measurements.

The 1,300-km altitude was chosen to minimize the combined effect of two error sources: A lower orbit would introduce uncertainty due to atmospheric drag and imprecise knowledge of the slightly aspherical geopotential field. In a higher orbit, time measurements would be more sensitive to GPS position errors. Considering all error sources and using conservative assumptions, a computer simulation showed that times at distant points on Earth can be compared within 1 to 2 ns.

This work was done by Sien-Chong Wu and V. John Ondrasik of Caltech for **NASA's Jet Propulsion Laboratory.** *To obtain a copy of the report, "Method and Means for Low-Cost Intercontinental Time Synchronization," Circle 39 on the TSP Request Card.*
NPO-16407

Advanced Transceivers for Firefighters

Improvements in convenience and dependability are based on user preferences and propagation studies.

A report presents the concept of an improved portable radio transceiver for firefighters. The concept was based in part on a study of the propagation of radio waves in such environments as high-rise buildings, ships, and tunnels. Communications devices currently in use and the regulations affecting them were considered. The study also took into account the possible health hazard posed by personal transceivers and the needs and wishes expressed by firefighters in interviews.

The interviews were held with fire-service officials in 10 diverse cities in the United States. The officials were asked about fire-ground communications problems and were encouraged to offer suggestions for improvements.

In the propagation study, extensive measurements were made in various structures at frequencies of 46, 154, 458, and 809 MHz. The sites were the Conrad Hilton Hotel, Chicago; the MGIC Plaza East office building, Milwaukee; the Washington (D.C.) Metro tunnel near the L'Enfant Plaza station; and the U.S. Navy heavy cruiser *Des Moines* at the Philadelphia Naval Base.

Additional design guidance came from a study of the possible health hazard of personal radio transceivers. The study found that the energy-absorption rates of the body for a representative radio were well within standards. Caution is needed, however: the highest internal fields (measured in simulated human tissue in a dummy) were found in the area of the central nervous system. This means that further experimentation is needed before health implications can be fully assessed.

The conceptual radio would be attached to clothing to allow hands-free use; it would be voice-actuated with the microphone worn at the throat. The speaker would be placed near the wearer's shoulder. The flexible antenna would be placed either horizontally across the shoulders, vertically at one shoulder, or on the transceiver itself.

The 450-MHz uhf band was selected for transmission on the basis of the propagation experiments. Although a radio with this frequency band would be more expensive and less energy efficient than others, its performance would be superior. Each radio would be able to operate at six frequencies in the band. The user would be assigned one of these frequencies, which would be selected by locking it in with a key or by some other simple adjustment. The range would be 600 meters under relatively unimpeded conditions — enough for fire-ground communication in all but the most exceptional situations. The range would be less when buildings or other obstacles interfere.

This work was done by Benjamin D. Blood, Om P. Gandhi, and Robert E. Radke of REMIC Corp. for **Marshall Space Flight Center.** *To obtain a copy of the report, "Firefighters Communication System — Final Report," Circle 35 on the TSP Request Card.*
MFS-27040

Digital Control of Durability-Testing Burner Rigs

Surface temperatures are controlled more precisely than before.

A report describes hardware and software that implement the hybrid digital control of two Jet A-1-fueled, mach-0.3 burners from startup to completion of a preset number of hot-corrosion/flame-durability cycle tests of materials at 1,652 °F (900 °C). Material-durability testing in dynamic flame combustion products is in common use in the gas-turbine and high-temperature-alloys industries. Heretofore, the determination and control of the true surface temperature has been a continuing problem and a source of uncertainty in the results obtained from such tests.

In the reported system, the determination and control of the surface temperature were accomplished by the use of a microcomputer programmable in the BASIC language and of a data-acquisition and -control unit; the two components were connected together by an IEEE-488 bus. The absolute specimen temperature was controlled to ± 3 °F (± 1.7 °C) by digital adjustment of the fuel flow using a proportional-integral-derivative control algorithm. The specimen temperature was within ± 2 °F (± 1.1 °C) of the set point more than 90 percent of the time. Pressure control was achieved by digital adjustment of the combustion airflow using a proportional control algorithm. The burner pressure was controlled at 1.0 ± 0.02 psig (6.9 ± 0.14 kPa gauge).

Logic schemes were incorporated into the system to protect the test specimen from abnormal test conditions in the event of a hardware or software malfunction. Also, the special and difficult problem of the transitions from heating to cooling and back to heating, presented by cyclic testing, can be easily handled in a positive way through software by using a hardware-generated burner-position signal.

The digital control avoids some of the problems associated with the analog control systems commonly used in such tests. The fuel and air valves are adjusted by small incremental steps, as opposed to the large, rapid variations possible with analog control. The result is a more accurate control of the test conditions, especially during long-term tests, which are unattended much of the time. The interpretation of test results for specimens tested under varying and sometimes questionable conditions is greatly suspect. The more accurate control of parameters possible with a digital control greatly reduces the uncertainty of the results.

This work was done by Daniel L. Deadmore of **Lewis Research Center**. *Further information may be found in NASA TM-86959 [N85-21321/NSP], "Digital Temperature and Velocity Control of Mach 0.3."*

Copies may be purchased [prepayment required] from the National Technical Information Service, Springfield, Virginia 22161, Telephone No. (703) 487-4650. Rush orders may be placed for an extra fee by calling (800) 336-4700.
LEW-14362

Low-Concentration-Ratio Solar-Cell Arrays

Many compact, lightweight concentrators would be combined to produce about 100 kW.

A paper presents a design concept for mass-producible arrays of solar electric batteries and concentrators that can be tailored to individual requirements. The arrays are intended primarily for space stations needing about 100 kW of power. However, the modular, lightweight, compact, and relatively low-cost design may also fulfill the requirements of some terrestrial applications.

An array would consist of sunlight-concentrator modules with a geometric concentration ratio of about 6. Either silicon or gallium arsenide solar cells could be used with the concentrators.

The idea behind the concentrator array concept is to substitute cheaper reflecting surfaces for a large portion of the more-expensive solar-cell material. The low concentration ratio makes accurate Sun pointing unnecessary; a deviation of $\pm 8°$ to $\pm 10°$ off axis produces only a modest drop in power, but as little as 1° of error in a high-ratio concentrator causes a drastic drop. For the low-concentration-ratio approach to be successful, however, the concentrator must be lightweight and be fairly efficient.

Each concentrator in an array would be an inverted truncated pyramid formed by four reflector panels with a top opening of about 0.5 m square to collect sunlight and a 20-cm-square bottom lined with solar cells. The panels would be made of aluminized plastic film.

Two arrays would extend like paddles on opposite sides of the space station. Each array would be 34 m long and 648 m wide. Articulated rotary booms, each having two degrees of freedom would point the arrays to the Sun. A system of hinges, pulleys, cables, springs, slides, and latches folds the arrays into compact rectangular solid blocks for storage and transportation, then unfolds them for service.

The arrays can be built with currently available materials. Pultrusions, injection-molded parts, and composite materials can be used extensively to keep weight low. For added flexibility in design and construction, the silicon and gallium arsenide solar-cell panels are interchangeable.

This work was done by Michael S. Biss and David A. Reed, Jr., of Rockwell International Corp. for **Marshall Space Flight Center**. *For further information, Circle 139 on the TSP Request Card.*
MFS-28022

Physical Sciences

Hardware, Techniques, and Processes

Books & Reports

Increasing the Deposition Rate of Silicon

A hollow cylinder is the key to a fourfold increase in the deposition rate.

NASA's Jet Propulsion Laboratory, Pasadena, California

A modified Siemens reactor enables chemical vapor deposition (CVD) of silicon to occur simultaneously on the inner and outer surfaces of a hollow cylinder, resulting in an increase in the mass of silicon deposited per unit time. The conventional Siemens process uses a single solid cylindrical rod, initially of a small radius, with silicon deposition occuring on the outer surface only.

The new outer reactor for silicon deposition shown in the figure would be made from quartz or stainless steel. The hollow cylinder could be either a single resistance-heated hollow cylinder about 5 to 10 cm or greater in diameter or 1-cm-diameter rods aligned in circular channels at the top and bottom, the initial circles being 5 to 10 cm in diameter or greater. The cylinder is resistance-heated throughout the deposition period to about 1,000 to 1,200 °C. A reactor may contain one or more of the hollow cylinders. The reactant gases are introduced through gas ports or jets into the interior and exterior spaces of the hollow cylinders. Any one of the chlorosilanes, with hydrogen or without hydrogen, or silane itself can be used as the feedstock.

The mixture of unreacted gases is allowed to escape from the outer reactor through exit ports. One or more components of this mixture can be sepa-

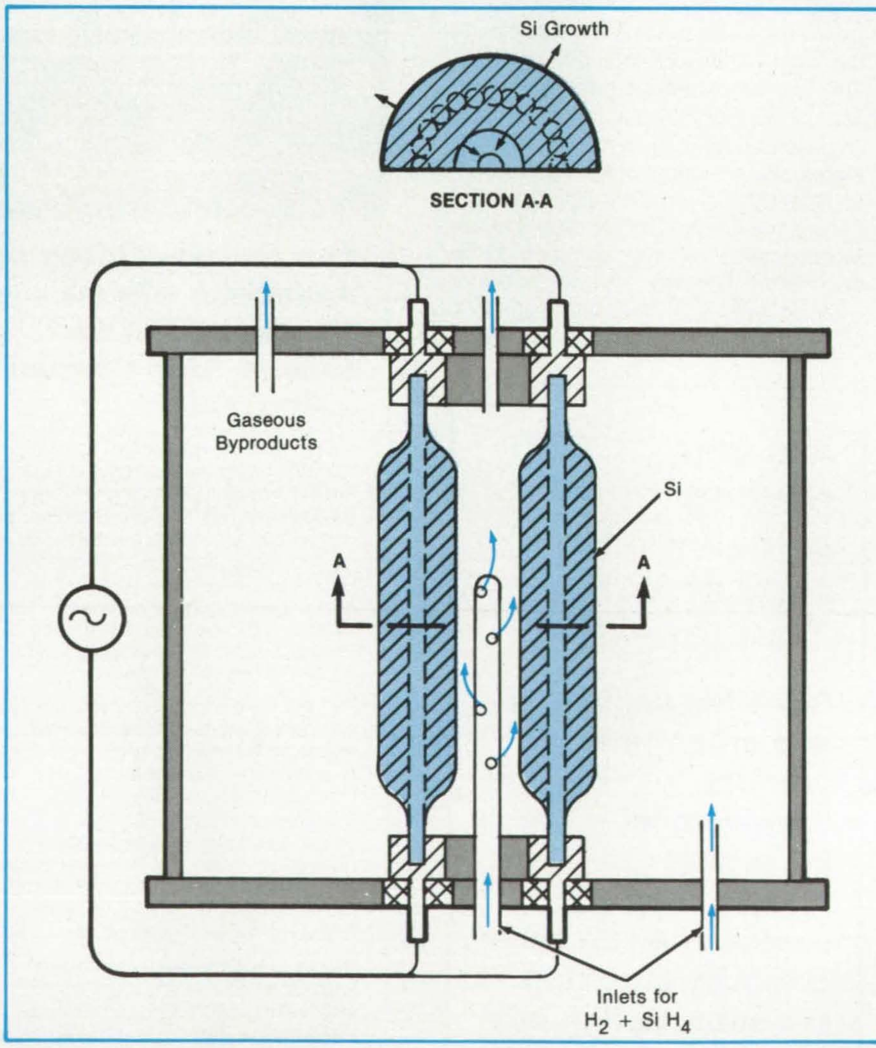

The **New Siemens Chemical-Vapor-Deposition Reactor** uses a 5- to 10-cm-diameter hollow cylinder made of 1-cm-diameter solid silicon rods. The tightly-packed resistance-heated rods are aligned in circular channels at the top and bottom. Silicon deposition occurs simultaneously on the inner and outer surfaces of the hollow cylinder.

rated and recycled in the process.

At the end of the growth, the hollow cylinder has been filled to a cylinder of radius R/2 inward and outward to form a solid rod of radius R. As a result, during this time period, the production rate with the hollow tube is four times that obtained with the conventional rod.

This work was done by Ralph Lutwack and K. Allan Yamakawa of Caltech for **NASA's Jet Propulsion Laboratory.** *For further information, Circle 22 on the TSP Request Card.* *NPO-15911*

Tandem-Mirror Ion Source

Ions are produced in a broad range of energies.

Marshall Space Flight Center, Alabama

An improved ion source produces a beam of ions at any kinetic energy from 1 to 1,000 eV, with little spread in energy or angle. Such ion beams are useful in studies of the surface properties of materials, surface etching, deposition, and the development of plasma-diagnostic instrumentation.

In the source (see figure), a heated, negatively biased filament supplies electrons that produce ions by collisions with atoms of a working gas. The electrons spiral about the lines of a magnetic field generated by five segmented solenoidal field coils. The spiral motion lengthens the path that the electrons must travel before leaving the ionization chamber; this increases the probability of collisions with the gas atoms, thereby increasing the ionization efficiency.

The currents in the coil segments are adjusted so that the field at the extraction end is about 5 times that at the ionization end and about twice that of the adjacent segment. The exact taper of the magnetic field depends sensitively on the desired ion energy and current. The field taper effectively spreads the electrons over the ionization chamber (for beam uniformity). The field-line constriction at the high-field (extraction) end constitutes a magnetic mirror that has little effect on the ions but reflects many electrons back into the chamber, where they undergo additional ionizing collisions.

In prior ion sources, the variation of potential along the filament caused excessive beam-energy spread. In this source, the filament is placed outside the ionization chamber. The chamber thus becomes an equipotential region; consequently, all ions are created at the same potential and emerge with little energy spread.

The other of the two tandem mirrors is an electrostatic grid placed behind the filament. The grid is biased at the same potential as (or at a slightly more negative potential than) that of the filament so that electrons launched back from the filament are repelled forward into the ionization chamber instead of being lost to the walls. This makes more electrons available for ionizing collisions; with a planar grid, the output is increased by about 50 percent. (The additional output gained by the negative bias of this grid is only a few percent so that the expense of this bias power supply may not be justified.)

Previously, a grid was seldom placed beyond the extraction grid. Without the grid, a series of concave equipotentials that formed spontaneously in the output beam caused the beam to diverge. Some prior source designs included a shielding

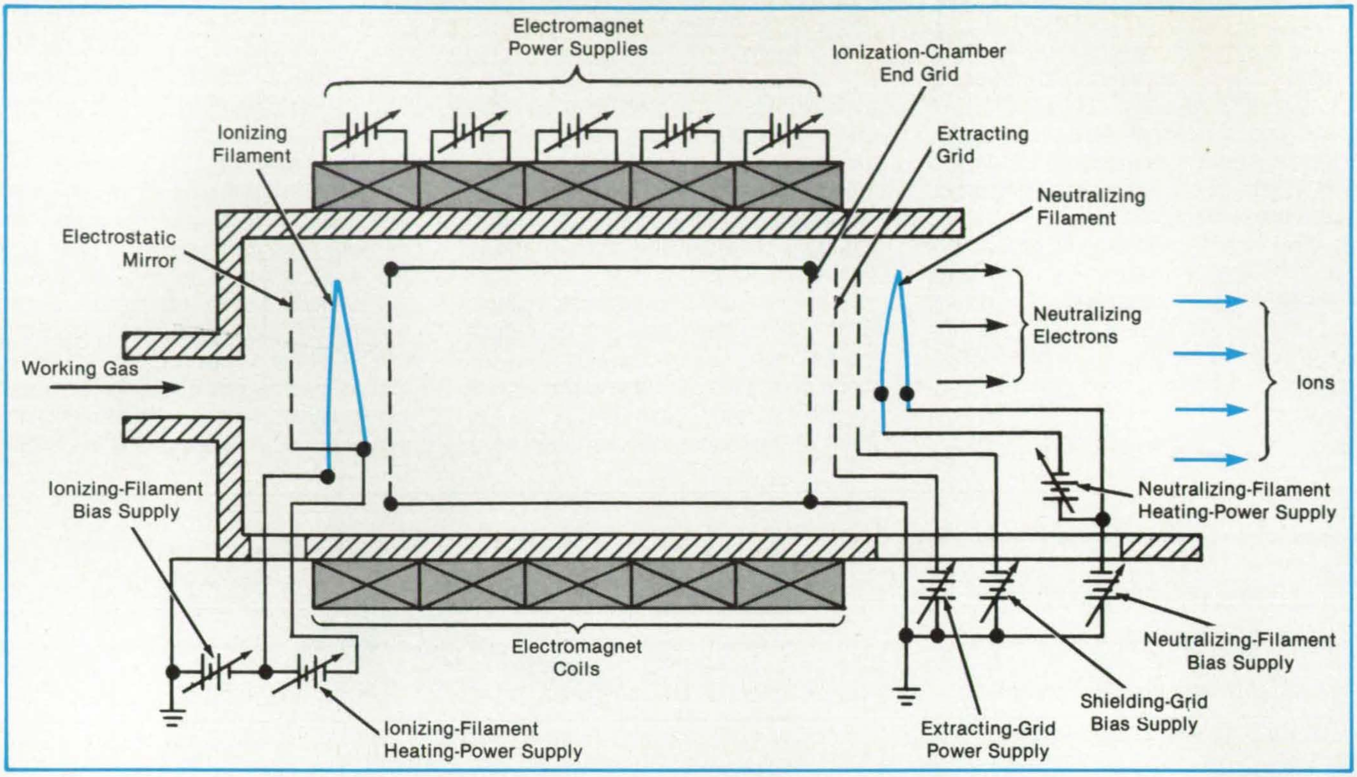

The **Tandem-Mirror Ion Source** uses electrostatic and magnetic fields to keep electrons in the ionization chamber and to assure a uniform output ion beam having low divergence in energy and angle.

grid at ground potential to establish a planar reference-potential surface, thereby reducing the beam divergence. In this source, additional flexibility is obtained by operation of the shielding grid at a slight bias. A small bias does not distort the reference surface greatly but does enable the output to be maximized by matching electrically the grid-hole sizes to the intergrid spacing. The effect of this bias is especially pronounced at energies below 10 eV, where the output is critical.

This work was done by A. P. Biddle, N. H. Stone, D. L. Reasoner, W. Chisholm, and J. Reynolds of **Marshall Space Flight Center.** *No further documentation is available.*

Inquires concerning rights for the commercial use of this invention should be addressed to the Patent Counsel, Marshall Space Flight Center [see page 29]. Refer to MFS-28122.

Field Funneling and Range Straggling in Silicon Detectors

Conditions for operation as charged-particle detectors are tentatively established.

NASA's Jet Propulsion Laboratory, Pasadena, California

The magnitudes of field funneling and range straggling have been determined in silicon-surface-barrier (Schottky-barrier) charged-particle detectors (SSBD's) through the measurement of charges collected from alpha-particle tracks. The method used may be extended to the straightforward measurement of charge collection from heavy-ion tracks in these and other semiconductor devices. Such measurements can be used to assess single-event upsets in integrated-circuit chips, with a view toward making them resistant to radiation.

Field funneling in SSBD's is the extension of the electric field along the ion track, beyond the depletion region. This field funneling can be observed by the measurement of the charge collected from ions of known energy and range (penetration distance) as a function of detector bias. Differential-capacitance measurements yield the depletion width as a function of the bias potential. The

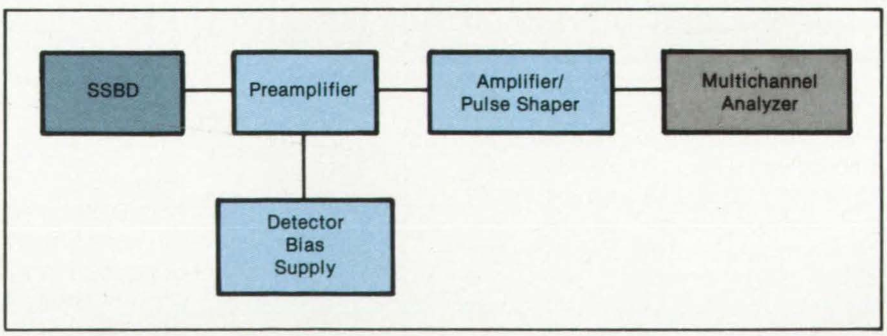

Figure 1. **Field Funneling and Range Straggling** are measured with the electronic system shown above, in which charge collected from individual ions is measured and recorded by the multichannel analyzer.

Multiple Pages Intentionally Left Blank

generated charge is fully collected, even when the depletion width is somewhat less than the ion range. However, as the depletion width is diminished further (by lowering the detector bias) beyond a certain point, the narrow collected-charge (energy) peak in the energy spectrum of a beam of ions begins to decrease in amplitude and to be dispersed in energy.

Under these narrow-depletion-width conditions, the end-of-range charge is being collected by diffusion rather than by a drift field. Because diffusion is isotropic some of the charge is lost (observed as a decrease in signal amplitude), and the charge collected from individual ions is dispersed by range straggling, which is a variation in the distance traveled by individual ions, manifesting itself as dispersion in the energy spectrum.

To measure the funnel length, (the distance the electric field extends beyond the depletion region along the ion track) and to observe the dispersion of charge collection due to range straggling, data were obtained by collecting 8.78-MeV alpha particles from a Th^{228} emitter in an Au/N-type Si SSBD, using the electronic system of Figure 1. The charge collected from individual ions was measured and recorded by the multichannel analyzer. As the particles were counted, the number of counts within the energy-range intervals were recorded and displayed.

The top of Figure 2 shows the complete alpha-particle emission spectrum at a bias of 58 V. In this case, the depletion width, W, was 61 μm, which was greater than the 59 μm range of the most-penetrating 8.78-MeV alpha particles in Si. Therefore, all of the ionization charge was collected.

When the bias was 30 V, the depletion width of 44 μm was 15 μm less than the range. Since the peak was not appreciably lowered or dispersed, little or no charge was lost from the 15 μm portion of the ion track beyond the original depletion range. Consequently, the electric field must have been extended by that distance, which thus represents the funnel length for the 8.78-MeV alpha particles at a bias of 30 V.

When the bias was reduced to 20 V so that the depletion width was 36 μm, the 8.78-MeV peak moved lower on the energy axis by an amount equivalent to $\delta E = 0.21$ MeV. The energy spread of this peak increased to $\Delta E = 0.4$ MeV. The spectrum taken at a bias of 11 V shows the further decrease in the collected charge. The value of δE represents the amount of charge lost at the end of the ion track, because of diffusion away from the Schottky barrier. The energy dispersion, ΔE, reflects range straggling at the end of the ion track.

This type of data clearly indicates the roles of field funneling and range straggling in the collection of charge from ion tracks in Si solid-state devices. This technique is superior to that of observing individual-particle responses (i.e., output voltage as a function of time), because the individual tracks exhibit different charge losses by diffusion due to range straggling.

This work was done by John A. Zoutendyk and Carl J. Malone of Caltech for **NASA's Jet Propulsion Laboratory.** *For further information, Circle 71 on the TSP Request Card.*

Inquiries concerning rights for the commercial use of this invention should be addressed to the Patent Counsel, NASA's Resident Office-JPL [see page 29]. Refer to NPO-16584.

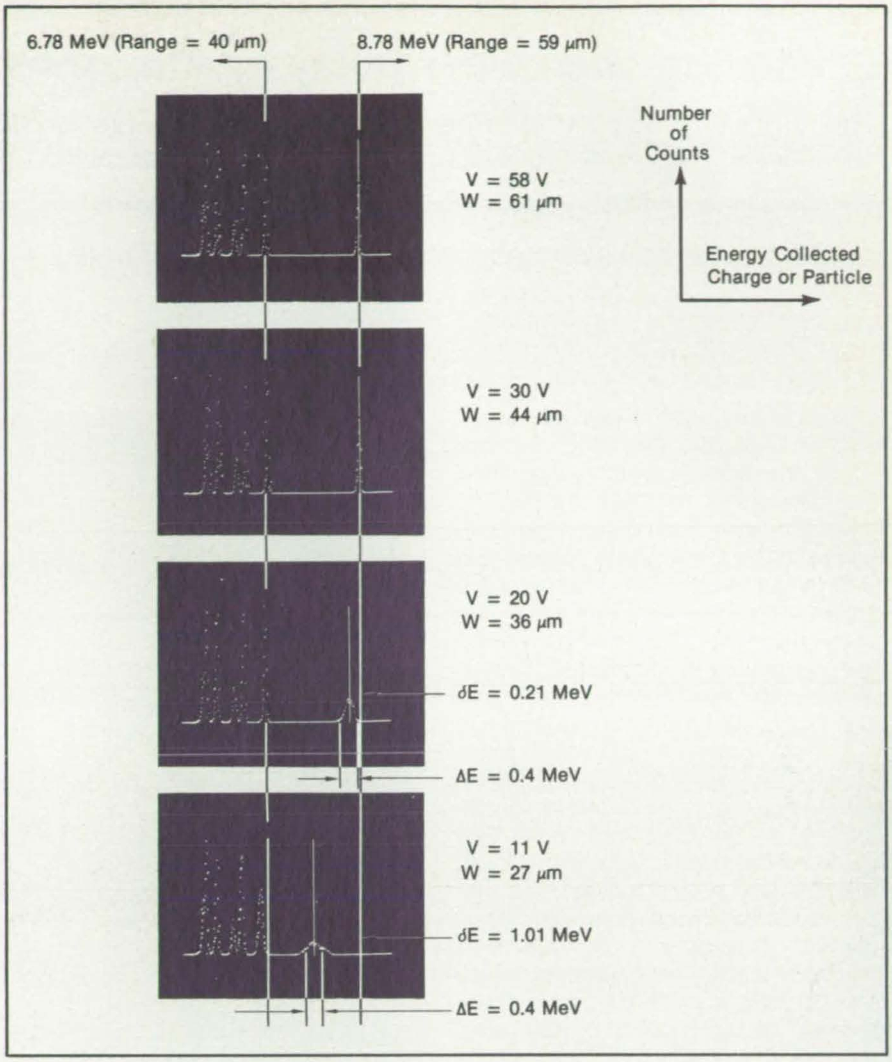

Figure 2. **Charge-Collection Data** are shown as energy spectra of particles in an Si SSBD under different bias potentials.

Estimating Microwave Delay by Atmospheric Water

This algorithm accommodates changes in the observation conditions, the emission model, and radiometer hardware.

NASA's Jet Propulsion Laboratory, Pasadena, California

Tropospheric path delays for microwave very-long-baseline interferometry (VLBI) are estimated with an algorithm that determines and then explicitly integrates a simple water-vapor distribution based on temperature data from a water-vapor radiometer (WVR) and an emission model. Although computationally complex, this method readily accommodates even dramatic changes in observation conditions, the emission model, and the WVR equipment.

One of the most intractable error sources for microwave VLBI is tropospheric water vapor, which can contribute up to 30 cm of excess zenith delay. Because the water distribution varies strongly with time, the surface location, and the altitude, surface meteorology alone does not yield tropospheric models capable of producing the desired 0.5-cm accuracy. Consequently, as part of the calculation of wet-path delays, many VLBI observers now infer water distributions from data obtained by WVR's, which usually detect thermal emission at two frequencies near the 22-GHz rotational transition of water.

The new algorithm yields an optimized simple humidity-versus-altitude profile (see figure) that is the product of two functions, the first of which consists of the vapor pressure of the water normalized by the total pressure as a function of altitude. The second function, which specifies the vertical profile of the relative humidity, is defined in altitude by linearly connecting values at three altitudes.

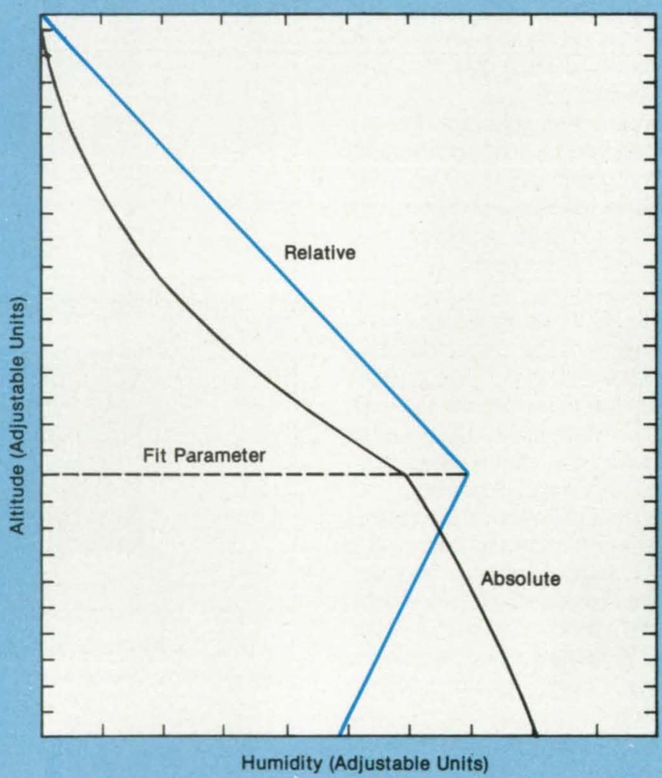

A **Simple Humidity-Versus-Altitude Profile** obtained from surface meteorology, water-vapor radiometer temperature data, and the assumption of zero humidity above a certain elevation, is integrated with other factors when calculating the portion of the microwave signal-path delay due to water in the atmosphere.

At the surface of the Earth, the relative humidity is provided by surface meteorology, and at some high altitude, usually 10 km, the relative humidity can be taken as zero. The third point is an intermediate altitude around 2 km, where the relative humidity is estimated by the algorithm. Once the values at the three altitudes are known, the vapor profile is considered to be completely specified. The liquid-water profile, which normally has a much smaller effect, is assumed to be proportional to the vapor profile.

The actual vertical water distribution may be somewhat different from that specified by the profiles. However, in integrating the vapor distribution with other factors to calculate the wet delay, vapor-distribution variations of high spatial frequency average out, making a smooth function (that is, the profiles) an adequate representation.

Because the algorithm first establishes the profile parameters instead of proceeding directly to the delay, the mean height of the water-vapor distribution is effectively varied to make a best fit to the data. This allows for variations in the emission characteristics that arise from changes in the vertical distribution of the water. Therefore, the accuracy of the profile algorithm is not strongly influenced by site and seasonal variations. In addition, the necessary incorporation of a tropospheric-emission model into the formulation gives the ability to prescribe all parameters describing the WVR configuration and delay integrals with minimal effort for any data set. The price paid for these advantages is an increase in complexity and added computation time.

Simulations using radiosonde data from a number of locations show that intrinsic accuracy of the algorithm is better than 2 mm in clear weather. This level of error is competitive with the most accurate of the more conventional linear algorithms, which use retrieval coefficients tailored to specific sites.

This work was done by Steven E. Robinson of Caltech for **NASA's Jet Propulsion Laboratory.** *For further information, Circle 31 on the TSP Request Card. NPO-16642*

Measuring Sodium Chloride Contents of Aerosols

Particle analysis by mass spectrometry enables mass measurements of individual aerosol particles in real time.

NASA's Jet Propulsion Laboratory, Pasadena, California

The amount of sodium chloride in individual aerosol particles can be measured in real time by an analyzer that includes a mass spectrometer. The analyzer can be used to determine the mass distributions of active agents in therapeutic or diagnostic aerosols derived from saline solutions and in analyzing ocean spray.

A beam of aerosol particles is formed by expanding the aerosol through a capillary nozzle into the vacuum in a particle-beam generator (see figure). The region between the nozzle and the skimmer is differentially pumped.

The particles in the beam are individually introduced into a miniature Knudsen-cell oven at 1,600 K. The oven, made from rhenium sheet 0.018 mm thick, is situated inside the ion source of a quadrupole mass spectrometer. Once inside the oven, a particle is trapped and completely vaporized. This is an improvement over conventional filament sources, in which particles bounce off the filaments and, therefore, are only partially vaporized.

The oven is located 6 cm downstream from the particle-beam generator. At this position, the particle beam is wider than the 1.50-mm-diameter oven opening. Particles in the outer ring of the beam striking the outside surface of the oven are likely to be only partially vaporized and, therefore, would cause errors in the measurements. Accordingly, a collimator is placed at the oven orifice. Particles hitting the collimator are reflected without appreciable vaporization or ionization and are therefore not analyzed.

Some of the atoms in the vapor are ionized. Each vaporized particle thus produces a pulse of ions that effuses out of the oven through the same opening by which the particles entered. The ions are swept into the quadrupole mass spectrometer, which is set to measure the intensities of the sodium-ion components of the vapor pulses. It has been determined by measurements that the sodium-ion-pulse amplitude is proportional to the mass of the vaporized salt particle raised to the 0.86 power.

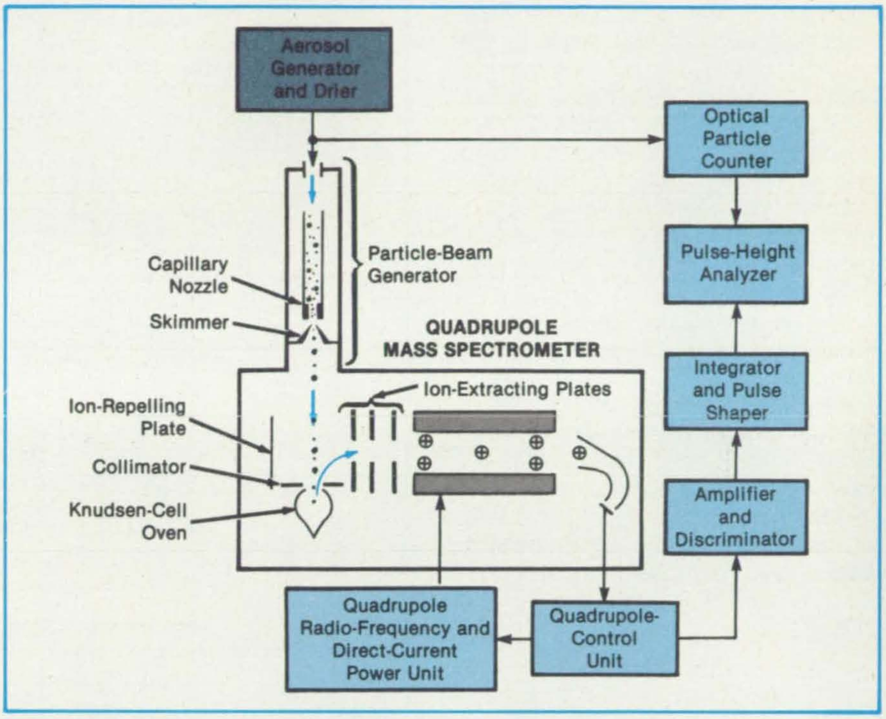

Aerosol Particles Composed of Sodium Chloride are introduced into an oven, where they are individually vaporized on the hot wall. The vapor molecules are thermally dissociated, and some of the resulting sodium atoms are ionized on the wall. These ions leave the oven in a burst and are analyzed by the spectrometer, which is set to monitor the sodium-ion intensity.

This work was done by Mahadeva P. Sinha and Sheldon K. Friedlander of Caltech for **NASA's Jet Propulsion Laboratory**. *For further information, Circle 95 on the TSP Request Card.*
NPO-16722

Quiet Plasma Source

Synthesis of plasma from separate ion and electron emitters suppresses electromagnetic interference.

NASA's Jet Propulsion Laboratory, Pasadena, California

A plasma source operates at low pressure and generates little or no electromagnetic interference. The peak plasma density is 2×10^6 particles per cubic centimeter, and the background natural pressure is less than 10^{-5} torr ($\sim 10^{-3}$ N/m^2). Previously, plasma sources have utilized impact-ionization-discharges in neutral gases to produce ions and electrons. Such discharge sources generate a high level of electromagnetic interference and must use differential pumping to reduce the pressure of the neutral gas.

The new source (see figure) employs separate emitters for electrons and ions. The ion emitter is a β-eucryptite ($Li_2O \cdot Al_2O_3 \cdot 2SiO_2$) source that yields lithium ions without a gaseous electrical

discharge. The potential difference between the grid and the case controls the ion current. The ion energy is determined by the potential of the case with respect to ground.

The electrons are emitted by a grounded, conventional oxide-coated cathode or by tungsten filaments. In either case, the positive space potential created by the ions increases the electron emission by a factor of 5 to 10 so that the plasma density is high. The electron temperature is the same as the cathode temperature. Relatively cold electrons are needed for the original application of the plasma source — studying the effects of plasmas on high-voltage solar arrays. Consequently, the oxide cathode temperature was set at 1,460 °C (0.15 eV). The tungsten filaments produce electrons of higher temperature — about 3 eV: The higher temperature is attributed to the voltage drop along the filaments.

The plasma source can be used to simulate a variety of astrophysical phenomena and space-plasma effects. For example, it can be used in studies of the propagation of electromagnetic waves in plasmas. It can also serve as an interference-free charge neutralizer.

This work was done by Philip L. Leung of Caltech for **NASA's Jet Propulsion Laboratory**. *For further information, Circle 25 on the TSP Request Card.*
NPO-16215

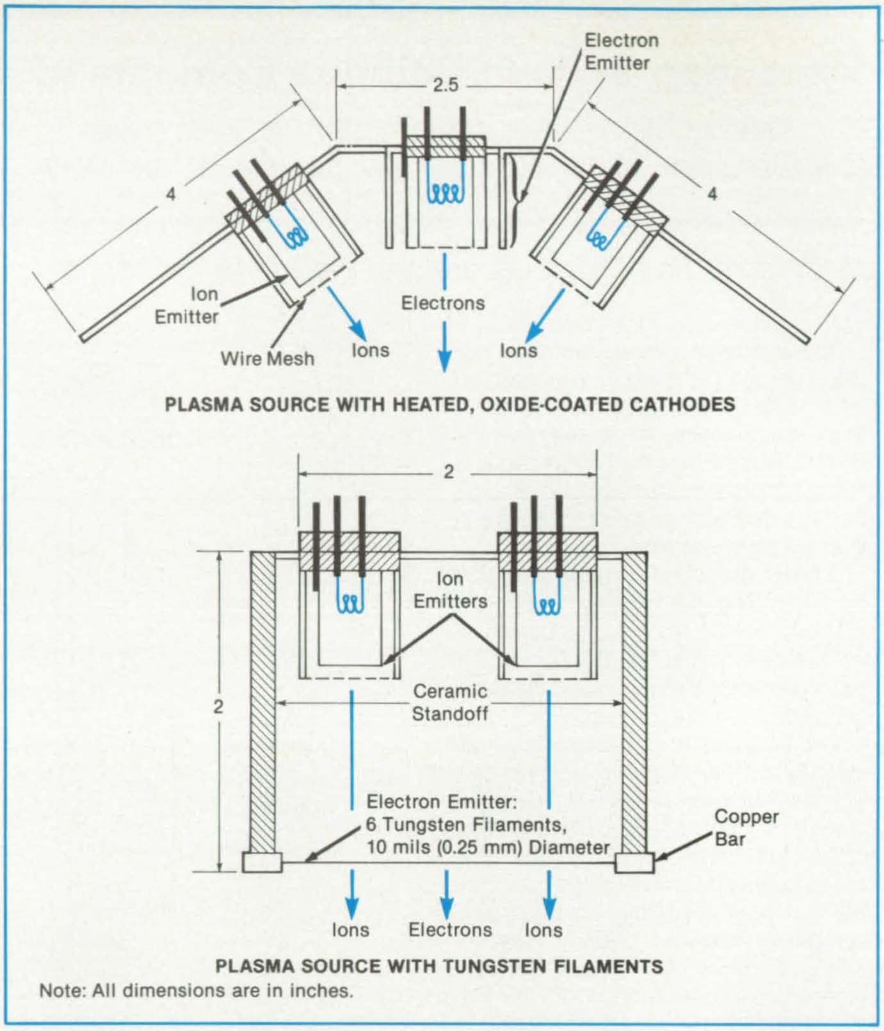

Ions and Electrons Are Generated Separately in the plasma synthesizer. Two alternative configurations are depicted — with electrons generated either by an oxide-coated cathode or by tungsten filaments. In either case, the ion source is β-eucryptite, a hexagonal crystalline lithium aluminum silicate mineral.

Measuring Combustion Advance in Solid Propellants

The propellant forms a dynamic part of capacitors.

NASA's Jet Propulsion Laboratory, Pasadena, California

A set of gauges on a solid-propellant rocket motor with an electrically insulating case measures the advance of the combustion front and the local erosion rates of the propellant and insulation. The data furnished by the gauges aid in motor design, failure analysis, and performance prediction. The technique is also useful in determining propellant uniformity and electrical properties of the exhaust plume. The gauges can be used both in flight and on the ground. The foil-gauge technique may also be useful in basic research on pulsed plasmas or the combustion of solids.

Each gauge consists of a small metal foil on the outside of the rocket motor case (see figure). Each gauge constitutes one electrode of a capacitor, while the combustion products constitute the other electrode. Since the flame in the motor cavity is extremely hot — 2,000 to 3,000 K — the gaseous combustion products are ionized and, therefore, electrically conductive.

An ac electrical signal is applied to the gases, which induce a voltage signal in the foil electrodes through the intervening dielectric media of the propellant and motor casing. The induced pulses become larger as the propellant (and eventually part of the insulator) is consumed, thereby reducing the dielectric thickness. The outputs of the electrodes thus provide a profile of the moving combustion front. The detail of the profile depends on the number and locations of electrodes applied to the case.

Each electrode is connected by a separate wire and by a resistor and ground wire to electronic monitoring circuitry. The resistors could be thin chips on the surface of the motor case. The wires can be either thin, twisted pairs or flat transmission lines. For further protection, these components can be covered by a thin layer of epoxy resin, which protects them and en-

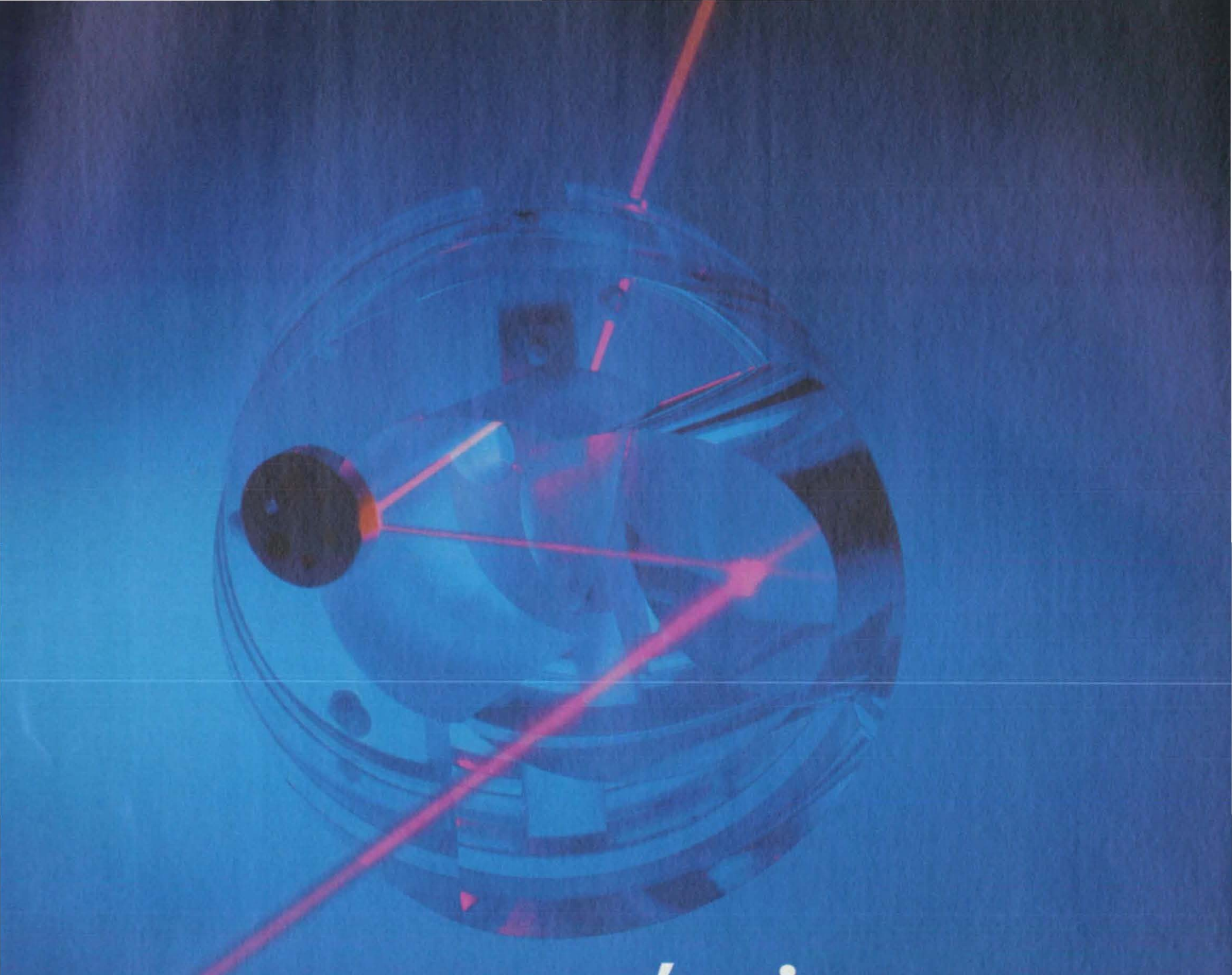

ca·top′-tric

(kə·tap′-trik) optical systems dealing with the reflection of light from mirrors.

PNEUMO PRECISION leads the industry in state of the art optical systems.

We offer design and fabrication of multi-mirrored optical systems for your prototype, pre-production or production needs. Our aspheric and plano components can be made from metals, crystals & polymers. Finish coating, plating, polishing and a variety of additional capabilities make Pneumo your first choice in optics.

PNEUMOPRECISION
An Allied-Signal Company

PRECISION PARK, BOX 543 KEENE, NEW HAMPSHIRE 03431 603/352-5242 TWX 710 366 7619
OPTICS WEST DIVISION, 5981 GRAHAM CT., LIVERMORE, CA 94550 415/443-0200

Circle Reader Action No. 366

sures that they add only minimally to the aerodynamic resistance of the rocket.

Because the components are located outside the combustion chamber, they do not affect the combustion process. Preliminary estimates show that the amplitude of the applied voltage pulse can be made low enough so that it does not significantly perturb the combustion products.

If the motor case is made from electrically conductive materials, such as metals or carbon fiber composite, the electrodes can be placed inside the motor and insulated from the case. The gauge operates in a similar manner, except miniature cables are required for the gauge connection from the interior to the outside of the motor.

This work was done by Lien C. Yang of Caltech for **NASA's Jet Propulsion Laboratory**. *For further information, Circle 6 on the TSP Request Card. NPO-16585*

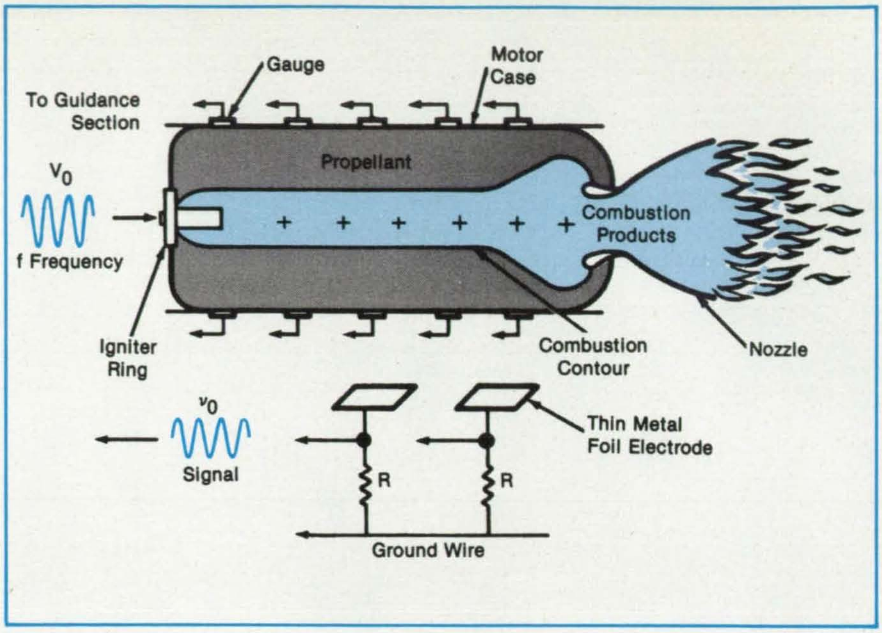

Metal-Foil Electrodes form capacitors with the plasma at the core of a motor engine, the propellant and motor case being the capacitor dielectric. Electrical pulses applied to the plasma thus appear on the electrodes.

Books and Reports

These reports, studies, and handbooks are available from NASA as Technical Support Packages (TSP's) when a Request Card number is cited; otherwise they are available from the National Technical Information Service.

Determining Monthly Mean Humidities From Satellite Data

Radiometric measurements over oceans are analyzed statistically.

A report describes a statistical study to estimate the monthly average humidity of the marine surface layer of the atmosphere from measurements by radiometers on satellites. The study is part of a continuing effort to determine the flux density of the latent heat due to evaporation at the ocean surface. Such observations and measurements are important because the latent-heat flux affects the weather and the temperature and salinity of the upper ocean layers.

The temperature and humidity of the atmospheric layer in contact with the ocean affect the exchanges of heat and momentum between the ocean and the atmosphere. The flux density, E, of water vapor can be estimated by the bulk parameterization formula: $E = \varrho C_E U(Q_S - Q)$, where ϱ is the density of the surface air, C_E is the transfer coefficient, Q_S is the saturation humidity at the surface temperature of the sea, U is the windspeed, and Q is the specific humidity. (U and Q are measured at a reference altitude near the surface.) The latent heat flux can be determined by multiplying E by the latent heat of vaporization L. The objective of this study is to determine Q.

At present, the number of meteorological reports from merchant ships and fishing vessels over vast areas of the equatorial and southern oceans are only adequate to determine the long-term averages; satellite data are needed to generate the evolving monthly averages over these areas.

A radiometer measurement gives the total amount of water vapor in the vertical atmospheric column under observation. In this investigation, mid-ocean vertical humidity distributions measured by radiosondes were statistically surveyed for correlations between the surface humidity and the total precipitable water content as measured by spaceborne radiometers.

The radiosonde soundings showed that Q can be estimated with an accuracy of 0.4 g/kg by applying a local statistical regression to a satellite observation. With a global regression, Q can be estimated within about 0.8 g/kg. These accuracies correspond to about 10 and 20 W/m^2, respectively, in the flux density of latent heat as determined by the bulk parameterization method, provided that the parameters other than humidity are also known.

This work was done by Wing-Yuen T. Liu and Pearn P. Niiler of Caltech for **NASA's Jet Propulsion Laboratory**. *To obtain a copy of the report, "Determination of Monthly Mean Humidity in the Atmospheric Surface Layer Over Oceans From Satellite Data," Circle 116 on the TSP Request Card. NPO-16529*

Reflective Shields for Artificial Satellites

Mirror facets would disperse radiant energy in many directions.

A report proposes a reflective shield that would protect a spacecraft from radiant energy. It would also give some protection against particle beams and cosmic rays.

The conceptual shield is essentially an advanced version of the decorative multifaceted mirror balls that are often hung over dance floors. A portion of a spheri-

cal surface — usually a hemisphere or an entire sphere — would be covered with flat, second-surface mirrors, each about 1 to 2 in. (2.5 to 5 cm) square. Because the number of facets is large and each faces in a different direction, there is only a small probability that incident visible or microwave radiation would be specularly reflected back to the signal source.

Each mirror segment would be made of fused borosilicate or fused aluminosilicate glass of a type previously developed for the mirrors of solar-energy systems. The glass would be about 0.040 to 0.06 in. (1.0 to 1.5 mm) thick, with high specularity and minimal diffuse reflectance or reradiation. The rear surface would be coated with a reflective layer of silver and copper, followed by a special backing paint. It is expected that such a mirror facet would reflect 96 to 98 percent of the incident solar electromagnetic energy; the remainder would be absorbed in the glass and metal layers.

The spherical shield support would preferably be made of aluminum; such alternatives as titanium, coated steel, or coated composites might also be used. A layer of acrylate, polycarbonate, or polyimide would be bolted or riveted onto the support to serve as a substrate for the mirror facets. The facets would be attached to the polymer substrate with a semirigid adhesive that allows for differences in thermal expansion. The spaces between facets would be filled with a sealant of butyl rubber with an outer layer of silicone that has been blackened to prevent reflections from the facet edges. Such a sealant also protects against ultraviolet, water vapor, and other environmental effects.

The shield can be mounted on hinges or other mechanisms to move it into place for different operating modes; for example, a spherical shield might be made in two hemispherical parts that are brought together to protect the satellite in all directions and moved apart to allow the satellite to communicate with other satellites or with ground stations. The shield could be a single hemisphere (or slightly more than a hemisphere) that protects the satellite from radiation from the ground, while allowing it to communicate with satellites in higher orbits. In this case, the entire satellite or the shield could be rotated to protect against radiation from above, while allowing communication with the ground.

This work was done by Frank L. Bouquet of Caltech for **NASA's Jet Propulsion Laboratory**. *To obtain a copy of the report, "Energy Reflecting Spacecraft Shield and Concealment System," Circle 2 on the TSP Request Card.*
NPO-16428

Materials

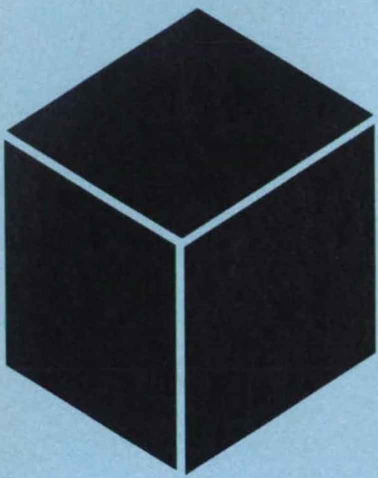

Hardware, Techniques, and Processes

Books and Reports

Lightweight, Fire-Resistant Graphite Composites

Paneling for aircraft interiors could be made safer.

Ames Research Center, Moffett Field, California

Aircraft safety could be improved with interior paneling made of a new laminate with good thermophysical properties. Featuring a lightweight graphite composite, the laminate is more heat- and flame-resistant and produces much less smoke in fire than the commonly used epoxy-resin-containing laminates.

In current paneling, an epoxy-resin-preimpregnated bond ply serves to bind the outer glass/polyvinyl fluoride decorative laminate to a honeycomb core. Upon exposure to fire or heat, the polyvinylfluoride and the glass/epoxy-resin substrate yield large quantities of smoke, a particular hazard in the close confines of an aircraft.

The new laminate (see figure) is prepared without the epoxy resin. A graphite unidirectional cloth is preimpregnated with a blend of vinyl polystyrylpyridine and bismaleimide (VPSP-BMI). Either of two types of VPSP-BMI blend is used, depending on the method of preparation of the chemicals and the technique used to fabricate the panel. For use in the hot-melt method, VPSP (30 parts by weight) might be mixed with BMI (70 parts by weight) and tetrahydrofuran (10 parts by weight). The graphite fiber is coated by a conventional hot-melt method at 70 °C, then dried at 80 °C.

In the wet method, the resin proportions are the same, but 70 to 150 parts of tetrahydrofuran are used to obtain a solution with a suitably low viscosity. The graphite cloth is passed through the solution, then led between a steel roller and a wiper blade to assist impregnation and remove the excess solution. In both the hot-melt and wet methods, the impregnated cloth is stored in a plastic bag at -10 to 5 °C.

The impregnated cloth is cured at 180 °C and 100 psi (0.69 MPa) for about 1 hour; this curing schedule can be varied somewhat to suit the fabrication method. A decorative polyetherketone film can be applied with a polyamide or silicone adhesive. The laminate is joined to the honeycomb core with a pressure of 100 psi at 177 °C.

Composite panels 1 in. (2.5 cm) thick made in this manner have a density of 75 to 85 kg/m^3, which is 20 to 25 percent less than the density of panels made from the conventional epoxy/glass composites. In addition, the new laminates have processing and curing parameters comparable to those of the epoxy/glass composites, making their manufacturing costs lower than those of such other high-temperature- and fire-resistant resins as the polyimides.

This work was done by Demetrius A. Kourtides and John A. Parker of **Ames Research Center** *and Ming-Ta-Hsu of H.C. Chemical Corp. For further information, Circle 42 on the TSP Request Card.*

This invention is owned by NASA, and a patent application has been filed. Inquiries concerning nonexclusive or exclusive license for its commercial development should be addressed to the Patent Counsel, Ames Research Center [see page 29]. Refer to ARC-11615.

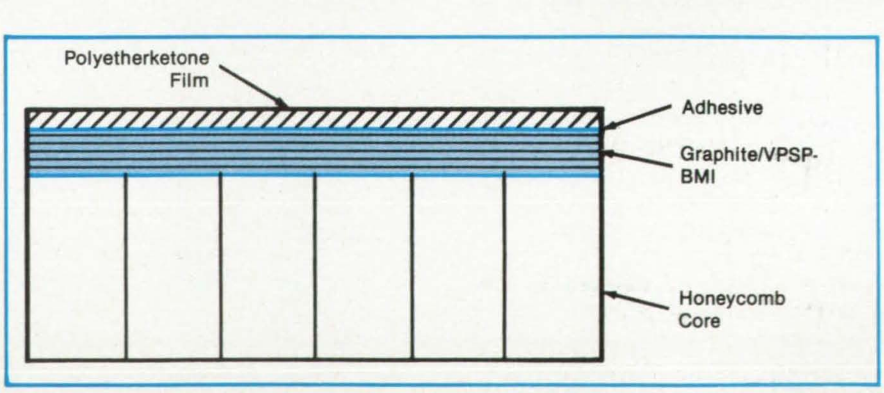

An **Aircraft Panel** is made with the graphite/VPSP-BMI laminate on a honeycomb core. The graphite/VPSP-BMI is safer than epoxy/glass-fiber laminates because when heated it emits less smoke.

THE CHALLENGE: "REPLACE OUR 50-INCH, FABRICATED TURBINE REAR FRAME WITH AN ADVANCED TECHNOLOGY, ONE-PIECE INVESTMENT CASTING."

Impossible? It would be for most. But because of our advanced technology in large structural castings, Howmet's Hampton Casting Division was able to cast General Electric's 50-inch TF39 turbine rear frame. And, since this one-piece casting replaced an eight-piece fabricated design, General Electric now has a more reliable component.

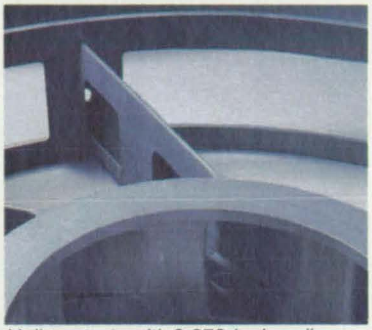

Hollow struts with 0.070-inch walls are lighter and more cost-effective.

Howmet has the capability to produce superalloy investment castings with outside diameters up to 50 inches. These large castings replace many fabrications and weldments and achieve smoother internal contours. And because we are able to cast walls to 0.070-inch thickness, we can produce lighter, more cost-effective components.

Howmet's Hampton vacuum furnace can pour 1,500 pounds and produce castings up to 57 inches long with a 50-inch outside diameter in nickel and cobalt-based superalloys. For titanium alloys, Hampton can pour over 1,200 pounds, producing castings over 50 inches in diameter and length. When specified, Howmet can subject castings to Hot Isostatic Pressing in one of four HIP vessels. All of our titanium castings are HIP'ed to enhance metallurgical integrity.

At Howmet, we will work closely with you, engineer to engineer, from concept through design and finished product. Whether your problem requires a simple but cost-effective solution or state-of-the-art technology for complex applications, you'll find Howmet able to help.

For more information on large structural castings and the potential this holds for your company, write our Marketing Department, Howmet Turbine Components Corporation, 475 Steamboat Road, Greenwich, CT 06836-1960.

Or phone Sales Manager Richard Thompson of the Hampton Casting Division at (804) 838-4680. Telex 710 882-0076.

IMPOSSIBLE? CHALLENGE US.

Howmet

TURBINE COMPONENTS CORPORATION
Hampton Casting Division, Hampton, VA

Circle Reader Action No. 335

50 inches in diameter, this nickel-based superalloy GE TF39 turbine rear frame is near-net shape.

THE ONLY ALL-AMERICAN IN THE FIELD. THORNEL® CARBON FIBERS.

If your field is aerospace and you're looking for carbon fiber products that are made in the U.S.A., there's only one way to fly.

THORNEL pitch and PAN based carbon fibers. And THORNEL Advanced Composite Systems high modulus prepregs.

We offer carbon fibers and prepregs that are made solely from domestically produced materials and manufactured here in the States. In fact, we have two fully integrated plants in Greenville, South Carolina.

Our THORNEL carbon fibers and prepregs provide you with a consistently high quality product. Backed by unmatched on-the-spot technical support, continuing R&D and a resins technology background unequaled in the industry.

You'll appreciate the light weight and superior stiffness, as well as the high thermal conductivity, dimensional stability and rapid vibration damping ability of our THORNEL pitch fibers.

For consistent properties in strength critical applications you'll want to look into THORNEL PAN fibers.

There's no reason to be up in the air about any of our THORNEL products. For more information write to Amoco Performance Products, 39 Old Ridgebury Road, Dept. F-2311, Danbury, CT 06817.

We'll show you how to get your designs off to a flying start without leaving home.

Amoco Performance Products

Circle Reader Action No. 336

Ion-Plated Soft Metallic Films Reduce Friction and Wear

Self-lubricating surfaces protect sliding and rotating parts.

Lewis Research Center, Cleveland, Ohio

Ion plating is an ion-assisted or glow-discharge surface-deposition technique. In this process, ions or energetic atoms transfer energy, momentum, and charge to the substrate and the deposited surface film. This process can be controlled to modify the physical characteristics of the surface, the subsurface chemical conditions, and the surface and subsurface microstructures as well. Ion plating with such soft, thin metallic films as gold, silver, or lead has great potential for producing self-contained lubricating surfaces. Such films can reduce friction, wear, and corrosion on sliding or rotating mechanical surfaces used in a wide range of environments.

The difference between the ion-deposited surface and the substrate results in a gradient interface. The graded interface not only guarantees an excellent adherence but also induces a surface-strengthening effect which improves the mechanical properties, such as tensile and fatigue strengths. These ion-plated films, unlike the more conventionally formed films, are normally very thin (about 0.2 μm) and exhibit distinct, improved film structures with equiaxed, small grains, which are responsible for the high density and a minimum degree of lattice misfit. As a result, continuous, uniform films are obtained at lower nominal thicknesses, which have a favorable effect on the coefficient of friction, as shown in the figure for the gold and lead films. The minimum critical film thickness is responsible for the lowest coefficient of friction and decreased steady-wear rate.

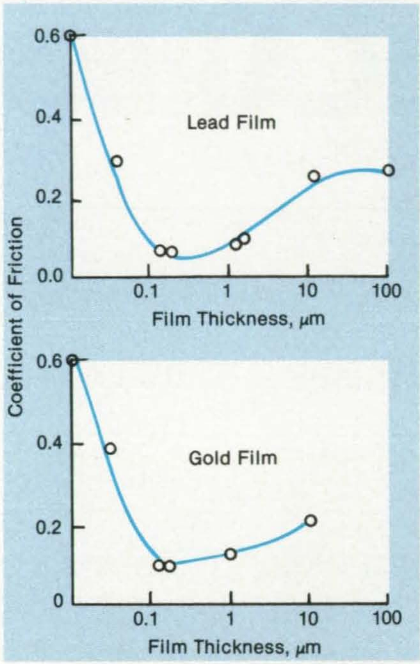

The **Coefficient of Friction** varies with the thicknesses of the ion-plated films.

The frictional and wear behavior is correlated with the coating structure and the coating/substrate adherence. Consequently, three distinct improvements exist over the conventionally deposited films: (1) increased endurance life, (2) lower coefficient of friction and reduced wear, and (3) the avoidance of catastrophic failure after film depletion. Much additional work remains to be done in the field, and vast improvements in surface properties are possible in the future.

This work was done by Talivaldis Spalvins of **Lewis Research Center.** *Further information may be found in NASA TM-87055 [N85-29085/NSP], "The Structure of Ion Plated Films in Relation to Coating Properties."*

Copies may be purchased [prepayment required] from the National Technical Information Service, Springfield, Virginia 22161, Telephone No. (703) 487-4650. Rush orders may be placed for an extra fee by calling (800) 336-4700.
LEW-14311

Detecting Pores in SiC Coatings

A nondestructive testing method produces images of inadequately covered areas.

Lyndon B. Johnson Space Center, Houston, Texas

A liquid-penetrant/fluorescence technique reveals cracks and pinholes in protective coatings. The technique was developed for checking the quality of overcoatings on silicon carbide layers on advanced carbon/carbon substrates. The difference in thermal expansion rates between the substrate and the silicon carbide tends to crack the silicon carbide layer. The silicon carbide coating prevents the exposed substrate from oxidizing, but the effectiveness of the coating is greatly reduced if it is cracked or porous.

The new technique is similar to other liquid-penetrant/fluorescence techniques used to make pores visible. If porosity is excessive, the material can be recoated or perhaps subjected to a healing process that would close the pores.

The penetrant is a suspension of organic fluorescent particles, 3 to 50 μm in diameter, in isopropyl alcohol. The part can be dipped in the suspension, or the suspension can be brushed or poured on the part. After about 5 min, the part is viewed in ultraviolet light. Porous areas absorb more of the suspension and therefore accumulate more fluorescent particles. They therefore fluoresce more brightly than their surroundings.

The absorption does not adversely affect the protective characteristics of the coating or the ability of the part to accept a recoat. The technique could be automated by using spray nozzles to apply the suspension and a scanning laser and photodetectors to find the pores.

This work was done by Anthony B. Hamilton, Kenneth L. Tummons, and James W. Lawton of LTV Aerospace and Defense for **Johnson Space Center.** *No further documentation is available.*
MSC-21041

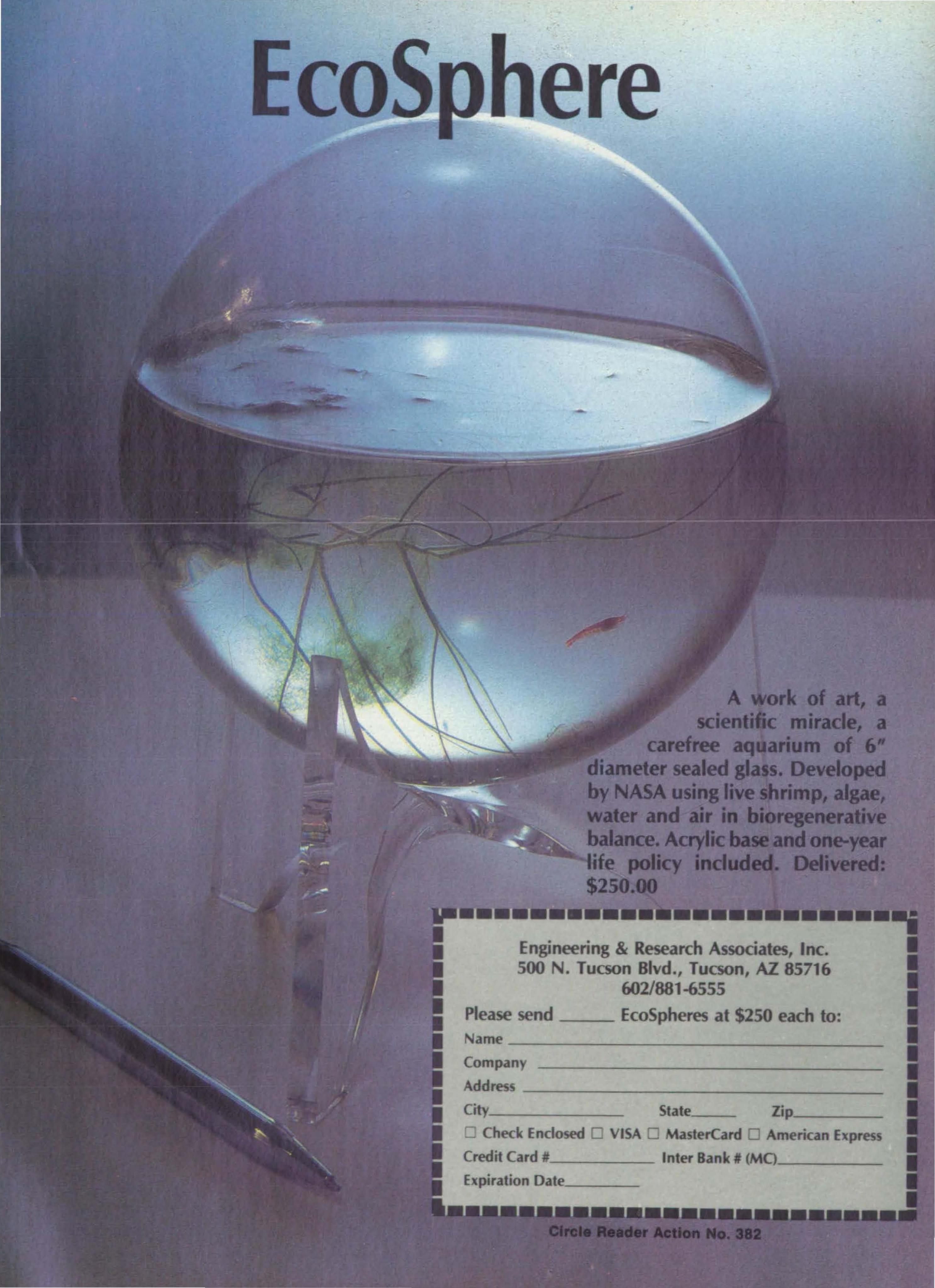
EcoSphere
A work of art, a scientific miracle, a carefree aquarium of 6" diameter sealed glass. Developed by NASA using live shrimp, algae, water and air in bioregenerative balance. Acrylic base and one-year life policy included. Delivered: $250.00
Engineering & Research Associates, Inc.
500 N. Tucson Blvd., Tucson, AZ 85716
602/881-6555
Please send _____ EcoSpheres at $250 each to:
Name
Company
Address
City_____ State_____ Zip_____
☐ Check Enclosed ☐ VISA ☐ MasterCard ☐ American Express
Credit Card #_____ Inter Bank # (MC)_____
Expiration Date_____
Circle Reader Action No. 382

Chemical Fracturing of Refractory-Metal Vessels

Localized reactions could cause refractory-metal vessels to break up at predetermined temperatures.

NASA's Jet Propulsion Laboratory, Pasadena, California

A concept that might assist in the breaking-up of nuclear reactors of spacecraft power systems upon re-entry into the atmosphere could be used in safety devices that would disintegrate whenever the temperature exceeds a predetermined value. A device following this concept can be designed to break up along predetermined lines into smaller pieces at a temperature significantly below the melting point of the metal from which it is made. Possible applications may include fire extinguishers that could breakup to release extinguishing gas in enclosed areas, pressure vessels that could otherwise burst dangerously in fire, and self-destroying devices. The technique is particularly suitable as a modification to already existing structures.

Current nuclear power systems of spacecraft are constructed of such relatively low-melting-temperature materials as stainless steel (melting point about 1,800 K). Advanced power systems that are now being developed include materials that require dispersion and are encased by walls made of such refractory metals as tungsten, molybdenum, niobium, or tantalum. The melting points of these metals range from 2,740 to 3,680 K. Such temperatures cannot be reached easily by aerodynamic heating alone.

According to the new concept, tubes containing a metal or an oxidizing agent would be welded into the walls along the desired lines of failure. The metal or oxidizing agent would be solid and nonreactive at normal reactor temperatures. When heated above the designated failure temperature, the material in the tubes would react rapidly with the refractory metal to form a liquid alloy or oxide. The walls of the vessel would thereby be liquefied and parted at the tube locations, causing the vessel to break up and its content to be dispersed.

For example, niobium tubes filled with beryllium could be welded to niobium vessel walls. During normal service, the reactor might operate at 1,100 K, which is more than 500 K below the beryllium melting point and 1,640 K below the niobium melting point (2,740 K). However, when the temperature approaches the beryllium melting point, the beryllium begins to alloy with the niobium tube to form a liquid along the line of the tube. (A 90Nb/10Be alloy melts at 1,873 K.) Alternatively, the tubes could contain an oxidizing agent like WO_3 or V_2O_4, which would melt and oxidize the Nb to Nb_2O_5 (melting point 1,785 K).

This work was done by Robert J. Campana of GA Technologies Inc., for **NASA's Jet Propulsion Laboratory.** *For further information, Circle 13 on the TSP Request Card.*
NPO-16541

Abrasion-Resistant Coating for Flexible Insulation

A two-step process increases the ruggedness of fragile quartz fabric.

Lyndon B. Johnson Space Center, Houston, Texas

A ceramic coating increases the durability and heat resistance of flexible high-temperature insulation. The coating is compatible with the quartz-fabric insulation and allows it to remain flexible during and after repeated exposures to temperatures of 1,800 °F (982 °C). It prevents the fabric from becoming brittle while increasing its resistance to aerodynamic abrasion and loading.

The coating consists of a penetrating precoat and a topcoat. The major ingredients are high-purity colloidal silica binder and ground silica filler, which ensure stability and compatibility with the fabric at high temperatures. The ratio of binder to filler must be carefully controlled to ensure erosion resistance. Also essential to erosion resistance is adhesion to the fabric; this is provided by the precoat, which penetrates the waterproofing on the fabric and interlocks with the fibers.

The precoat consists of a solution of 80 parts by volume of colloidal silica in 20 parts isopropyl alcohol. The ingredients are mixed by adding the alcohol to the silica while stirring.

The topcoat consists of a mixture of 47 percent by weight colloidal silica and 53 percent ground silica. The ingredients are mixed on a rolling mill in a porcelain grinding jar containing Alundum (or equivalent) aluminum-oxide pebbles. Both the precoat and the topcoat should be stored in sealed polyethylene containers. The materials have long shelf lives, provided that the precoat is agitated once per week and again just before use.

The precoat is brushed or sprayed on the fabric so as to coat it completely and uniformly. About 0.12 lb/ft^2 (0.59 kg/m^2) of precoat should be applied per 100 ft^2. It should be allowed to dry for at least 4 hours before the topcoat is applied.

The topcoat is similarly brushed or sprayed, with special care taken that the slurry is worked into the spaces between fibers. About 12 lb should be applied per 100 ft^2. The topcoat should be dried for 24 hours before the fabric is used. Both the precoat and topcoat can be cured at room temperature.

This work was done by Daniel Mui and Ronald E. Headding of Rockwell International Corp. for **Johnson Space Center.** *For further information, Circle 50 on the TSP Request Card.* *MSC-20799*

Polyimide of Modified Melt Flow and Toughness

End capping improves process-flow properties.

Langley Research Center, Hampton, Virginia

A linear aromatic polyphenylene ether sulfideimide (BDSDA/APB) polymer has been molded, used as a resin, and cast into thin films. According to recent experiments to synthesize and characterize this polymer, the polymer is well suited for processing by conventional thermoplastic methods. In an effort to improve further both the use properties and the amenability to process BDSDA/APB, the molecular weight of the polymer was varied by variations in the percentage of end capping. The effect of end capping BDSDA/APB was determined by the measurement of the polymer melt viscosity and fracture-energy values for the different number-average synthesized molecular weights.

When the ends of the molecules were capped with varying amounts of phthalic anhydride, the molecular weight of the polymer was lowered from 13,900 to 8,660. This decrease resulted in a concomitant decrease in the melt viscosity, as shown in Figure 1. At 250 °C there was no deviation from linearity, but at the higher extrusion temperature of 280 °C, the viscosity dropped steeply for polymers with molecular weights below 10,000. This information should prove valuable in optimizing the amenability of the polymer to processing.

When moldings were prepared from the polymers of different molecular weights, the fracture-energy values showed that a considerable loss in fracture resistance occurs as the molecular weight decreases; this is shown in Figure 2. Of particular interest was the fact that, over the range tested, the fracture energy was related linearly to the molecular weight.

When mixtures of the low and high molecular weight polymers were evaluated, it was found that the flow properties were controlled by the low molecular weight portion and the toughness (fracture energy) obeyed a simple rule of mixtures.

This approach of limiting molecular weight to improve the flow properties of BDSDA/APB has proven successful. From the results obtained concerning the variation of the melt viscosity and the fracture energy with the change in number-average molecular weight, it is obvious that tradeoffs can be made between process optimization and final mechanical properties, when polymer formulations are developed.

This work was done by Terry L. St. Clair and Harold D. Burks of **Langley Research Center**. *For further information, Circle 68 on the TSP Request Card.*

This invention has been patented by NASA (U.S. Patent No. 4,552,931). Inquiries concerning nonexclusive or exclusive license for its commercial development should be addressed to the Patent Counsel, Langley Research Center [see page 29]. Refer to LAR-13135.

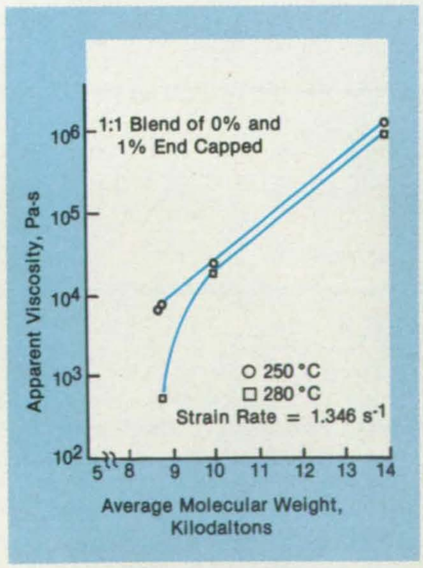

Figure 1. The **Viscosity of BDSDA/APB** increases with increasing average molecular weight; thus, end capping improves the flow characteristics in processing.

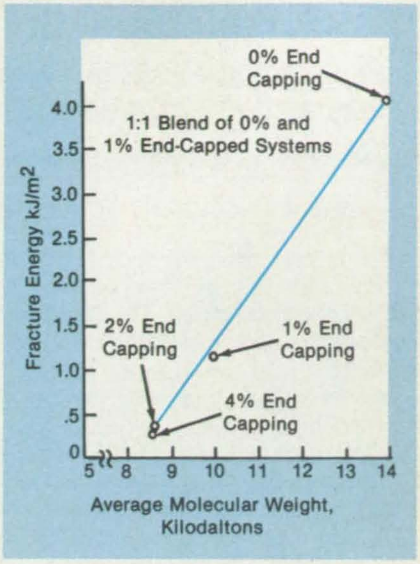

Figure 2. The **Fracture Energy of BDSDA/APB** increases with increasing average molecular weight; thus, end capping decreases the resistance to cracking.

Batch Gas-Sampling System

Specimens are kept in a stable form until they can be recovered and examined.

Lyndon B. Johnson Space Center, Houston, Texas

A sampler collects air or other gases in a consistent way and stabilizes them for later chemical analysis. The device can be used for concentrations ranging from a few parts per million to 100 percent. It also separates and collects particles in the gas for analysis.

The sampler is gas specific; that is, a separate sampler is needed for each component of the gas to be analyzed. Each sampler contains a material selected expressly to react irreversibly with a given component. The amount of the new compound thus formed is proportional to the concentration of the component in the sampled air. Because the new compound is inert, it can be stored in the sampler for long periods without deteriorating and causing an erroneous analysis.

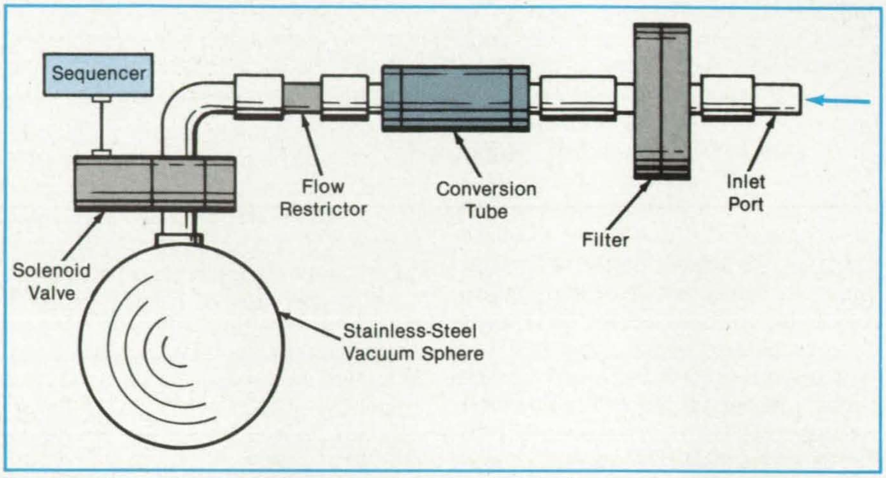

Gas Flows Into a Vacuum Sphere when the solenoid valve is opened. As it passes through the conversion tube, a constituent of the gas forms a stable compound that remains in the conversion tube for analysis at a later time. The sampler parts are made of glass, polytetrafluoroethylene, and stainless steel so that they do not react with the sample.

To start the collection of a sample, a sequencer sends an electric current to a solenoid valve (see figure). The valve opens, and gas from the surroundings is immediately drawn by the vacuum in a stainless-steel sphere into an inlet port, where particles are trapped in a filter. The gas continues into a conversion tube, where the component of interest reacts and is changed into a stable compound in proportion to its concentration. At the end of a preset collection period or when the vacuum is exhausted, the sequencer closes the valve.

An attendant recovers the sample by removing, tagging, and sealing the conversion tube and the filter and sending them to a laboratory for analysis. The attendant evacuates the sphere with a vacuum pump and installs a new conversion tube and filter. The sampler is then ready to collect again.

The sequencer can be a microprocessor that operates an assembly of samplers on a programmed long- or short-term schedule. Alternatively, the valves can be operated manually. The assembly of samplers may be fixed or portable.

With a 500-milliliter capacity, each sphere on an assembly draws in the same volume of gas every time. If the velocity of the in-rushing gas affects measurement accuracy, it can be controlled by the configuration and size of the inlet port.

This work was done by Vernon Diaz, Jr., Eric L. Miller, and Fred P. Rollins of Lockheed Engineering and Management Services Co., Inc., for **Johnson Space Center.** *For further information, Circle 57 on the TSP Request Card.*

Inquiries concerning rights for the commercial use of this invention should be addressed to the Patent Counsel, Johnson Space Center [see page 29]. Refer to MSC-20977.

Producing Silicon Carbide/Silicon Nitride Fibers

Promising reinforcement fibers for composites are made from extruded resin.

Marshall Space Flight Center, Alabama

An experimental manufacturing process makes $C_xSi_yN_z$ fibers. Precursor fibers are spun from an extruding machine charged with a polycarbosilazane resin. When pyrolyzed, the resin is converted to a cross-linked mixture of silicon carbide and silicon nitride, still in fiber form. The $C_xSi_yN_z$ fibers are promising substitutes for carbon fibers in high-strength, low-weight composites where high electrical conductivity is unwanted.

The extruding machine is basically a cylinder-and-piston assembly. A variable-speed dc motor, acting through a differential-screw mechanism, pushes the piston into the cylinder cavity at a controlled rate. The piston pushes hot resin from the cavity through fine holes in a plate at the end of the cavity. The resin emerges from the holes as continuous fibers, which are wound on a variable-speed takeup wheel. The fibers can be extruded directly into the air; a controlled-atmosphere cabinet is not needed.

In one of several experiments under various conditions, the machine extruded molten resin at 225 °F (107 °C) through a 32-mil (0.81-mm) orifice into fibers of 25 to 30 μm diameter. About 3,000 ft (900 m) of fiber were drawn on the takeup wheel

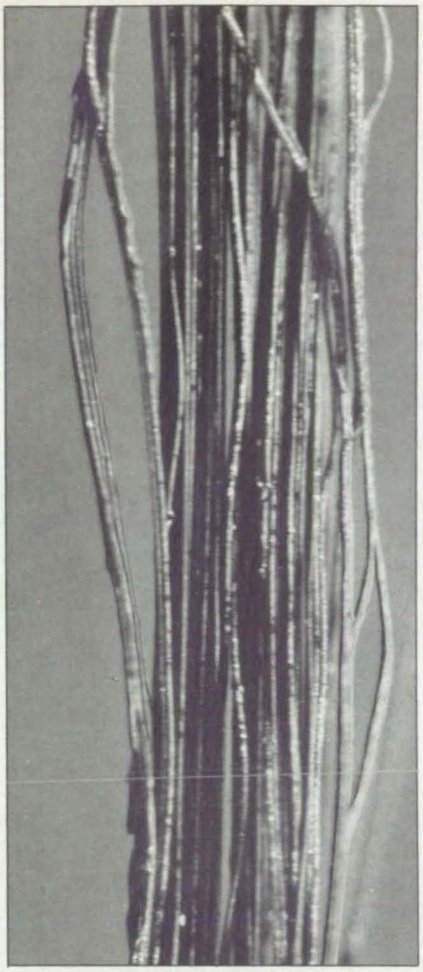

A **Bundle of Pyrolyzed Fibers** is composed mainly of cross-linked silicon carbide and silicon nitride molecules. Like carbon fibers, these $C_xSi_yN_z$ fibers can reinforce composite materials. However, $C_xSi_yN_z$ has higher electrical resistivity, and therefore may be usable where the lower resistivity of carbon cannot be tolerated.

in 3 minutes.

The fiber is crosslinked in a hydrolysis reaction: It is heated to 50 °C at 100 percent relative humidity for several days. During this time, the fiber strength and melting point increase, and its brittleness decreases. After 9 days, the softening temperature reaches 800 °C.

The crosslinked fiber is pyrolyzed to drive out the more-volatile organic components, leaving $C_xSi_yN_z$. In this process, fibers are gradually heated to 1,000 °C during 3 hours in a nitrogen atmosphere. The product (see figure) has a shiny, black metallic appearance.

This work was done by Bjorksten Research Laboratory, Inc., for **Marshall Space Flight Center.** *For further information, Circle 59 on the TSP Request Card.*
MFS-27123

Oxygen-Concentrating Cell

High-purity oxygen is produced electrolytically from breathing air.

John F. Kennedy Space Center, Florida

High-purity oxygen is produced from breathing air or from propellant-grade oxygen in an oxygen-concentrating cell. A full-scale concentrator having a total apparent electrode area of 27.9 m^2 would produce 5,606 kg per week. The operating economics of the concentrator are attractive: The energy consumption would be about 4 Wh per liter of oxygen, slightly lower than that of conventional electrochemical oxygen extractors.

The oxygen-concentrating cell operates by the reduction of oxygen in the feed gas flowing past the cathode, according to the reaction

$$O_2 + 2H_2O + 4e^- \rightarrow 4OH^-$$

The hydroxide ions migrate through an asbestos matrix soaked with saturated potassium hydroxide electrolyte toward the anode, where the reverse reaction releases oxygen. Because of activation, diffusion, and ohmic losses, the bias voltage required for this process using breathing air is two orders of magnitude larger than the theoretical open-circuit value of 0.01 V calculated from the Nernst equation.

In an experimental version of the cell, the anode consisted of nickel cobalt oxide, 20 mg/cm^2, bonded with polytetrafluoroethylene on a gold-plated 100-mesh (wire diameter 0.11 mm) nickel screen. The cathode consisted of platinum black, 10 mg/cm^2, bonded with polytetrafluoroethylene on an identical screen. The asbestos matrix was 20 mils (0.5 mm) thick. The current collectors were made of perforated expanded-metal material (EXMET or equivalent), with a sheet thickness of 10 mils (0.25 mm) and a strand width of 58 mils (1.5 mm). The anodic current collectors were gold-plated to prevent oxidation. Silver wires were attached to the current collectors to serve as electrical leads out of the cell. The cell housing was made of acrylic plastic and sealed with a two-part epoxy

resin.

The cell was operated with a dc power supply. To prevent electrode degradation, the bias was not allowed to exceed 1.2 V. To prevent the loss of electrolyte and carbonate poisoning of the electrodes, the feed gas was scrubbed with an alkaline solution before entering the cell. To eliminate CO_2 poisoning, experiments were conducted immediately after the addition of the electrolyte through the oxygen-collecting port.

Impedance measurements were taken as the bias voltage was increased incrementally from the minimum up to the maximum of 1.2 volts. Cathodic measurements were taken immediately after anodic measurements, and as soon as reasonably steady states were reached. Taken in 5-h runs, polarization measurements were repeatable. Taken in 12-h runs, measurements of oxygen purity showed a level of 99.996 percent.

This work was done by Kurt Buehler of **Kennedy Space Center**. *For further information, Circle 86 on the TSP Request Card.*

Inquiries concerning rights for the commercial use of this invention should be addressed to the Patent Counsel, Kennedy Space Center [see page 29]. Refer to KSC-11335.

Lubricants and Additives Affect Spur-Gear Fatigue

Additives increase gear life considerably.

Lewis Research Center, Cleveland, Ohio

Surface-fatigue tests conducted with AISI 9310 steel spur gears have shown that the surface-fatigue life of AISI 9310 steel spur gears can be increased by as much as 400 percent by the addition of a small amount of a phosphorus-type extreme-pressure (EP) additive in the lubricant.

Research was conducted at the NASA Lewis Research Center to investigate the effects of lubricant base stock and additive content on the spur-gear surface-fatigue (pitting) life. Spur-gear endurance tests were conducted with six lubricants, using a single lot of AISI 9310 gear-test specimens. The sixth lubricant was divided into four batches, each of which had a different additive content. The lubricants used in the investigation can be classified into three basic types: synthetic hydrocarbon, mineral oil, and ester-based lubricants. The ester-based lubricants meet the MIL-L-23699 specification and were aircraft type II lubricants.

Gear failure by surface fatigue is affected by the physical and chemical properties of the lubricant. Lubricant additives are normally used in gear lubricants to increase the load-carrying capacity of the gears. The EP additives can prevent or minimize wear and surface damage (scoring) to gears when the load-carrying surfaces operate under very-thin-film or boundary-lubrication conditions. There are many gear systems that operate with this thin-film condition.

The antiwear or EP additives either are adsorbed onto the surface or react with the surface to form a protective coating or surface film. The boundary film provides a barrier that prevents contact of the metal surfaces and provides a low shear strength, which reduces the friction coefficient below that of the base metal.

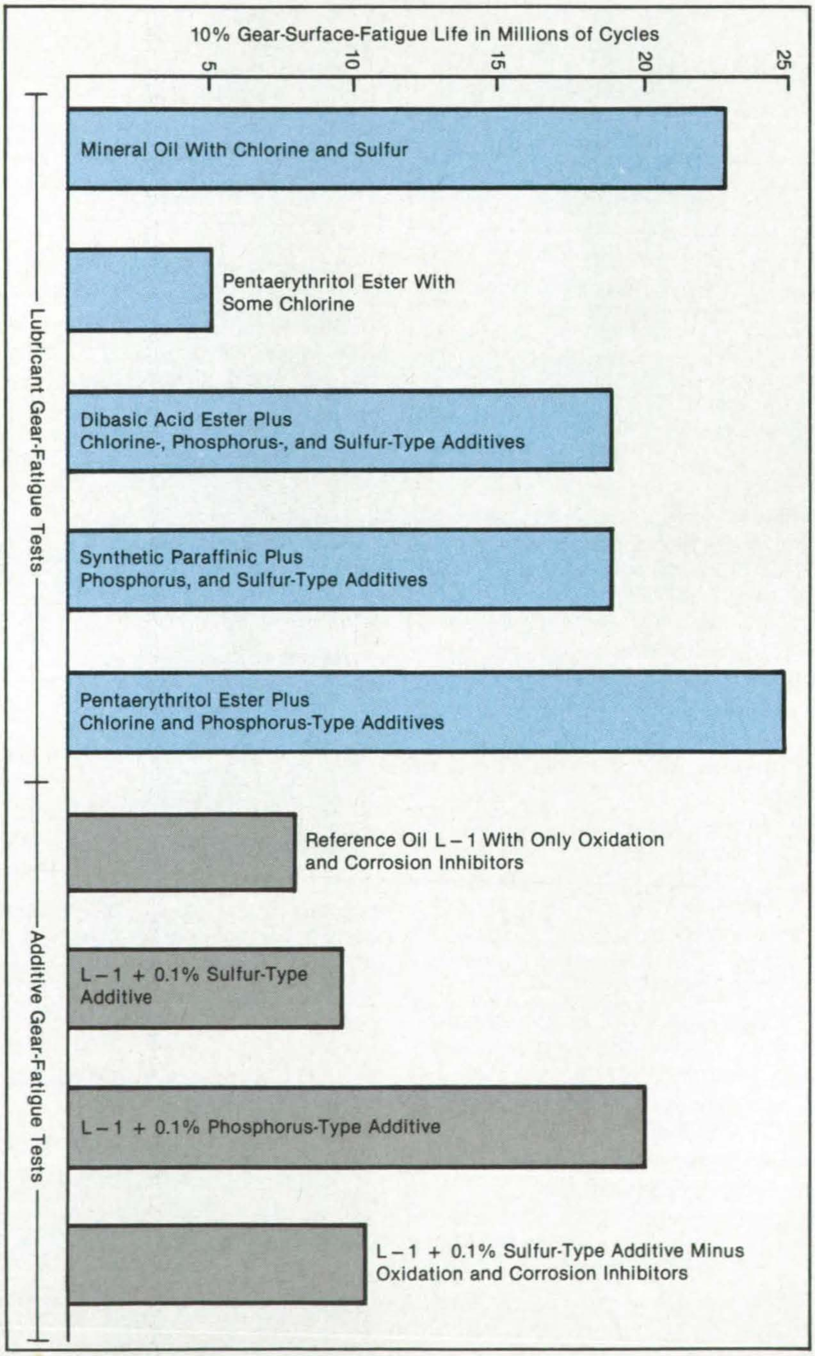

The **Surface-Fatigue Lives of AISI 9310 Gears** were measured while using them with nine different lubricants.

A summary of the gear-test results is shown in the figure. One lubricant tested with a phosphorus-type EP additive showed a fatigue-life increase of 400 percent over a similar lubricant without this additive. EP and antiwear additives in the lubricant appear to control the resultant surface-fatigue life of the gears. The surface films were 200 to 400 Å (0.8 to 1.6 μin.) thick. These results reveal that the type II aircraft lubricants with phosphorus-type EP additive can produce fatigue-life results equivalent to those of mineral-oil lubricants formulated specifically for gear applications.

This work was done by H. W. Scibbe, D. P. Townsend, P. R. Aron, and E. V. Zaretsky of **Lewis Research Center**. *Further information may be found in:*

NASA TP-2408 [N85-13234/NSP] "Effect of Lubricant Extreme-Pressure Additives on Surface Fatigue Life of AISI 9310 Spur Gears,"

NASA TP-2419 [N85-16099/NSP], "Effect of Five Lubricants on Life of AISI 9310 Spur Gears," and

NASA TM-87044 [N85-28373/NSP], "Lubricant and Additive Effects on Spur Gear Fatigue Life."

Copies may be purchased [prepayment required] from the National Technical Information Service, Springfield, Virginia 22161, Telephone No. (703) 487-4650. Rush orders may be placed for an extra fee by calling (800) 336-4700.
LEW-14314

Polyimide Film of Increased Tear Strength

A new process incorporates an elastomer into the polymer to increase this strength.

Langley Research Center, Hampton, Virginia

A high-temperature linear aromatic polyimide with improved resistance to tearing is made by a new process that incorporates an elastomer into the polyimide. Linear aromatic condensation polyimides are materials of prime choice for use as films and coatings on advanced spacecraft and aircraft where durability at temperatures in the range of 200 to 300 °C is required. The tendency of these films to tear upon impact by meteors or other space debris limits their usefulness in space applications. It is anticipated that elastomer-containing polyimide film with improved toughness will prove useful for applications where resistance to tearing and long-term thermal stability are necessary.

The elastomeric phase is provided by the addition of an aromatic-amine-terminated butadiene/acrylonitrile (AATBN) rubber into the polyimide. The AATBN is dissolved with a diamine such as 4, 4'-oxydianiline in amide solvent. A dianhydride such as benzophenone tetracarboxylic dianhydride is then added to the mixture to produce an intermediate polyamic acid. In summary, the entire process involves the preparation of the amic acid prepolymer into which a specific amount of AATBN elastomer has been chemically reacted, the preparation of the elastomer-containing polyamic acid film, and the conversion of the film to the polyimide by heating at 250 °C.

The desired resistance to tearing is achieved by careful control of the amount and chemical composition of the added elastomer. The concentration of the AATBN in the elastomer-containing polyimide film is critical. Various samples prepared show that the tear strength of the film is at a maximum (a 50-percent improvement over the polymer containing no elastomer) when the concentration of the elastomer is 10 percent by weight of the polymer. At concentrations of 5 percent and 15 percent of elastomer, the tear strength is improved by approximately 25 percent. At a concentration of 20 percent AATBN, there is no improvement of tear strength at all.

The acrylonitrile content of the AATBN is also a critical factor. The three examples cited above had AATBN with 18 percent acrylonitrile content. A polymer system prepared with 15 percent AATBN having no acrylonitrile content produced the largest increase in tear strength (50 percent), while one having 10 percent acrylonitrile content produced very little increase in tear strength.

This work was done by Anne K. St. Clair and Jeffrey A. Hinkley of **Langley Research Center** *and Stephen A. Ezzell of Virginia Polytechnic Institute and State University. For further information, Circle 51 on the TSP Request Card.*

This invention is owned by NASA, and a patent application has been filed. Inquiries concerning nonexclusive or exclusive license for its commercial development should be addressed to the Patent Counsel, Langley Research Center [see page 29]. Refer to LAR-13491.

High-Temperature Alloys for Automotive Stirling Engines

Alloys are chosen for availability, performance, and manufacturability.

Lewis Research Center, Cleveland, Ohio

NASA and DOE have investigated the Stirling engine (see Figure 1) as an alternative to the internal-combustion engine. The Stirling engine is an external-combustion engine that offers fuel economy, low emissions, low noise, and low vibrations. One of the most critical areas in the engine development concerns material selection for component parts.

Alloys CG-27 and XF-818 have been identified after an extensive research program at NASA's Lewis Research Center to be capable of withstanding the rigorous requirements of the automotive Stirling engine. For potential mass production and customer satisfaction, alloys were required to be low in cost and to contain a minimum of such strategic materials as cobalt and chromium. Further requirements imposed on the heater-head alloys included good high-temperature strength, oxidation/corrosion resistance, compatibility with hydrogen and resistance to hydrogen permeation, capability to be fabricated, weldability, and long-term cycle operation.

Alloy CG-27 was chosen for the heater-head tubes because of its high strength (see Figure 2, top) achieved by precipitate strengthening and its resistance to hydrogen permeation achieved by forming an aluminum-rich oxide on the tube internal diameter (see Figure 2, middle). Alloy XF-818 was chosen for the cylinder

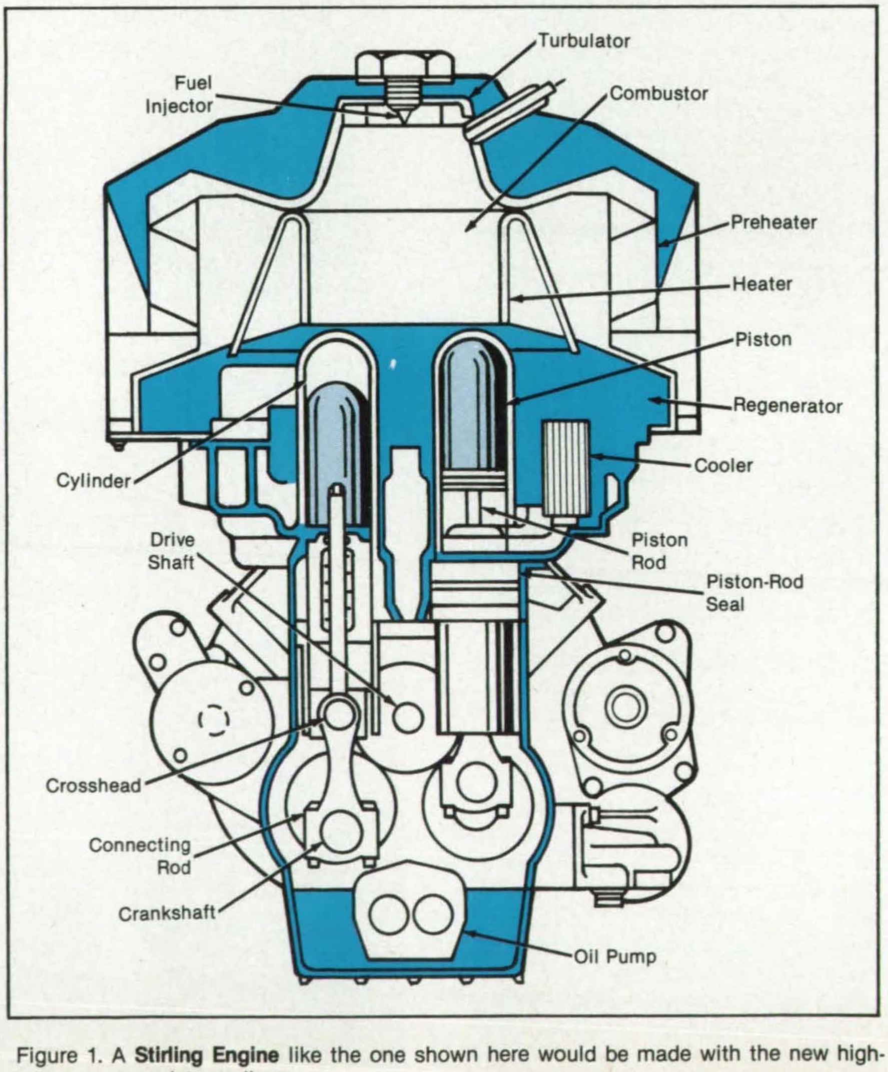

Figure 1. A **Stirling Engine** like the one shown here would be made with the new high-temperature-resistant alloys.

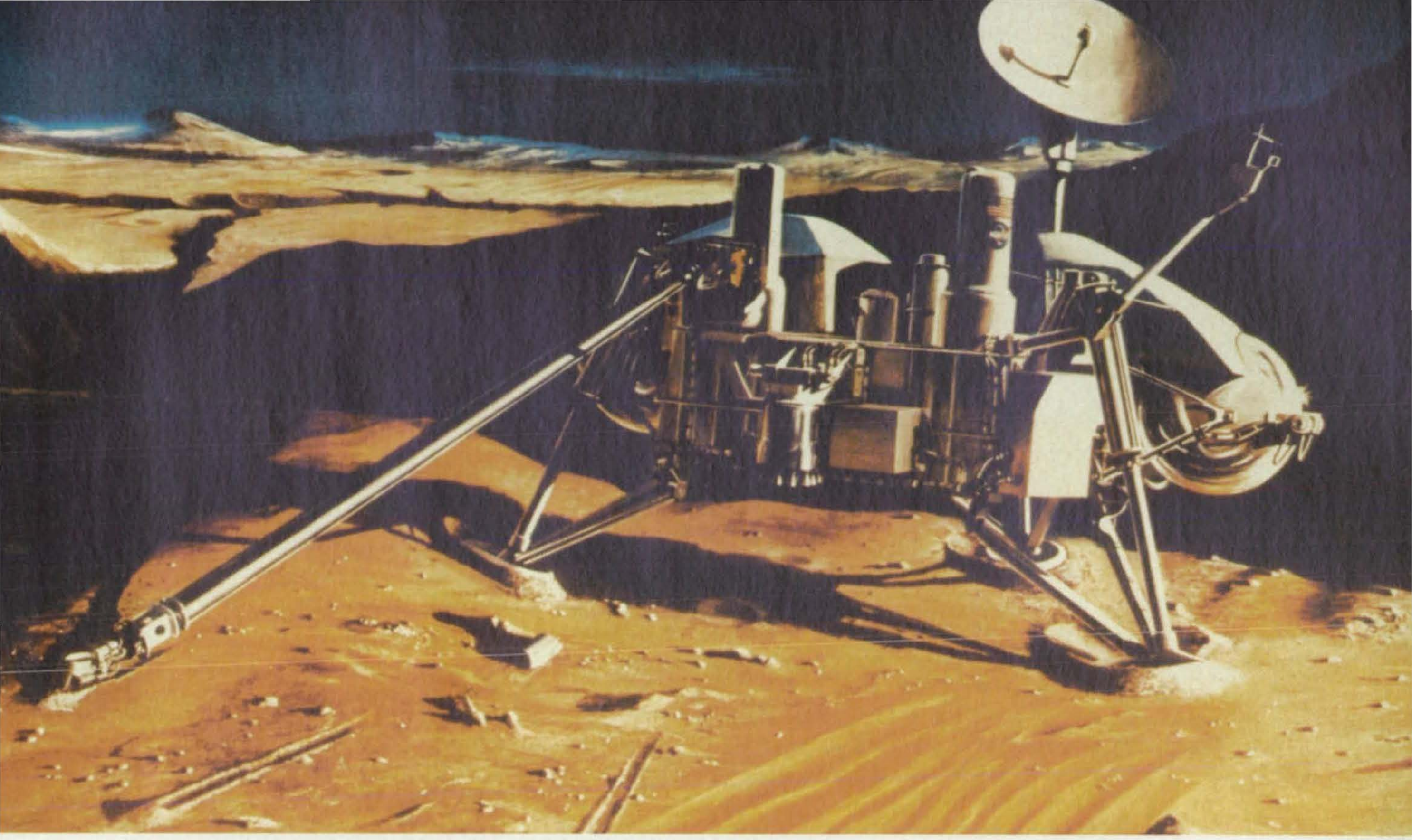

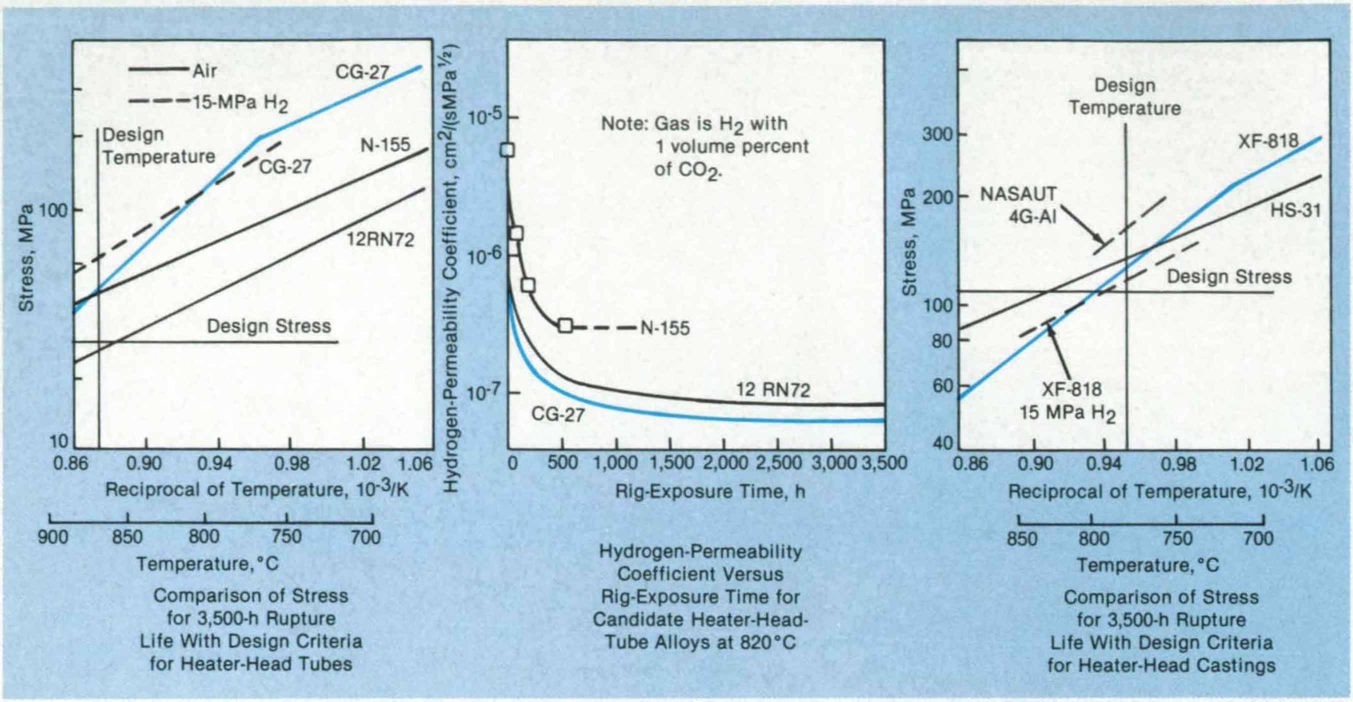

Comparison of Stress for 3,500-h Rupture Life With Design Criteria for Heater-Head Tubes

Hydrogen-Permeability Coefficient Versus Rig-Exposure Time for Candidate Heater-Head-Tube Alloys at 820°C

Comparison of Stress for 3,500-h Rupture Life With Design Criteria for Heater-Head Castings

Figure 2. Some **Properties of Alloys** are compared to show the special utility of the new alloys.

and regenerator housing because of its good castability, strength (see Figure 2, bottom), ductility, and weldability. These advanced iron-base alloys have the potential for a variety of applications, including stationary solar-power systems.

This work was done by Joseph R. Stephens and Robert H. Titran of **Lewis Research Center**. *Further information may be found in NASA TM-83659 [N84-28963/NSP], DOE/NASA/51040-54, "Advanced High Temperature Materials for the Energy Efficient Automotive Stirling Engine."*

Copies may be purchased [prepayment required] from the National Technical Information Service, Springfield, Virginia 22161, Telephone No. (703) 487-4650. Rush orders may be placed for an extra fee by calling (800) 336-4700.
LEW-14325

Books and Reports

These reports, studies, and handbooks are available from NASA as Technical Support Packages (TSP's) when a Request Card number is cited; otherwise they are available from the National Technical Information Service.

Responses of Dielectrics to Space Radiation

The nature, extent, and possible prevention of radiation damage are discussed.

A report summarizes the likely effects of high-energy radiation in outer space on a variety of commercially-available dielectric materials used in spacecraft. The effects are reported on the basis of recent Galileo tests, unpublished tests involving proton or electron irradiation, and published information.

The types of particles and electromagnetic radiation encountered in space are complex and depend upon the particular mission trajectory. Radiation-induced changes result from ionization processes or atomic displacements, which can lead to both chemical reactions and changes in local microscopic structure. The size of a radiation-induced change can depend upon the total amount, intensity, composition, energy spectrum and impingement angle of the radiation, the composition of the immediate surroundings, the presence or absence of shielding, and the amounts of such other stresses as temperature, humidity, and electric fields.

In general, organic materials with carbon or inorganic fillers are most resistant to radiation. Moreover, the response of a given material to radiation can be modified by surface contamination or erosion by atomic oxygen, especially in orbits near the Earth.

Materials used in the Galileo orbiter (designed for the exploration of Jupiter, Saturn, and beyond) were selected for proton/electron irradiation tests. Some samples showed small amounts of surface cracking in the proton tests. In the electron tests, some adhesives lost strength, and some dielectrics changed in color. The major result was that zinc orthotitanate (used as a thermal-control coating) underwent a significant change when exposed to the maximum Galileo mission proton-radiation test level of 2.8 $\times$ 10^{10} rad. Although its emissivity increased by only 9.22 percent, its white absorptance increased from 0.13 to 0.42, or 249 percent.

The radiation-induced conductivity of a variety of dielectrics was investigated. Conductivity phenomena are numerous and complicated, involving many poorly-understood chemical and physical damage mechanisms, both in the bulk material and on the surface.

Charge buildup is related to conductivity. Experimental data on charge buildup and release are nearly in agreement with the predictions of a model based on the trapping of electrons in insulators. The response of the charge buildup and release depends on the ratio of the material relaxation time constant to a release rate from traps.

Certain organic additives increase the radiation resistances of polymers. Any additive material that would absorb or otherwise eliminate free radicals might reduce the vulnerability to radiation by blocking the damaging action of excited radicals. Conductive polymers should be useful in the prevention of charge buildup that could lead to deleterious results.

This work was done by Frank L. Bouquet of Caltech for **NASA's Jet Propulsion Laboratory**. *To obtain a copy of the report, "Response of Dielectrics to Space Radiation," Circle 3 on the TSP Request Card.*
NPO-16687

Thermal Conductances of Pressed Copper Contacts

Measurements at liquid-helium temperatures are reported.

A report describes an investigation of the thermal conductivities of smooth copper contacts pressed together at liquid-helium temperatures. The investigation was prompted by the need for accurate thermal models for infrared detectors and other cryogenic instruments.

Previous studies of pressed contacts had shown that they do not obey the Wiedemann-Franz law, according to which the ratio of thermal to electrical conductivity is proportional to the absolute temperature. In addition, the thermal conductances of contacts are difficult to predict because even the smoothest surfaces have irregularities that limit the touching area to as few as three small spots, regardless of sample size. In fact, experiments have shown that the contact conductance depends on the force of contact rather than on the nominal contact area.

As the contact force increases, the material deforms. Thus, the touching area increases, and new spots develop. Heat flow is constricted in the vicinity of the touching locations by the narrowness of the touching spots. This constriction is responsible, in large part, for the contact thermal resistance.

For lack of an adequate theory to predict the contact thermal conductance as a function of the temperature and contact force, measurements were taken on pairs of lapped, flat samples of oxygen-free, high-conductivity copper. Each sample pair was tested at temperatures from 1.6 to 4.2 K while squeezed together with forces ranging from 0 to 670 N. With both samples cooled by liquid helium, one was heated slightly by an electrical-resistance heater, and the heat flow and temperatures were measured in the two samples.

The experimental data were fitted to the equation

$$\dot{Q} = \alpha \left(\frac{T_u^{n+1} - T_l^{n+1}}{n+1} \right)$$

where $\dot{Q}$ = the rate of heat flow across the contact, and T_u and T_l represent the upper- and lower-sample temperatures, respectively. The experimental results are presented in tables and a graph. For fixed values of the contact force, n ranges from 1.9 to 2.2, suggesting that the contact conductance varies approximately as the square of the absolute temperature.

The report does not present a quantitative evaluation of the increase in the contact conductance with the contact force. However, it appears from a cursory examination of the graph that, at a fixed temperature, the conductance is roughly proportional to the force to the 2/5 power.

This work was done by L. J. Salerno and P. Kittel of **Ames Research Center** *and A. L. Spivak of Trans Bay Electronics. For further information, Circle 37 on the TSP Request Card.*

Inquiries concerning rights for the commercial use of this invention should be addressed to the Patent Counsel, Ames Research Center [see page 29]. Refer to ARC-11572.

Computer Programs

COSMIC: Transferring NASA Software

COSMIC, NASA's Computer Software Management and Information Center, is the one central office established to distribute software that is developed with NASA funding. COSMIC's role as part of NASA's Technology Utilization Network is to ensure that NASA's advanced software technology is made available to industry, other government agencies, and academic institutions.

Because NASA's software development efforts are dynamic and ongoing, new programs and updates to programs are added to COSMIC's inventory on a regular basis. *Tech Briefs* will continue to report information on new programs. In addition, the 1986 edition of the *COSMIC Software Catalog* is available with descriptions and ordering information for available software. Several new programs for control systems/robotics, expert systems, thermal analysis, turbomachinery design, structural analysis, and computer graphics are offered.

For additional information on any programs described in this issue of *Tech Briefs*, circle the appropriate number on the TSP card at the back of the publication. If you don't find a program in this issue that meets your needs, you can call COSMIC directly at (404) 542-3265 and request a review of programs in your area of interest. There is no charge for this information review.

COSMIC®
Computer Services Annex, University of Georgia, Athens, GA 30602; Phone (404) 542-3265
John A. Gibson, Director

Computer Programs

These programs may be obtained at a very reasonable cost from COSMIC, a facility sponsored by NASA to provide tested and reliable software to the public. For information on program price, size and availability, circle the reference number on the TSP and COSMIC Request Card in this issue.

Electronic Components & Circuits

Analyzing Millimeter-Wave Mixers

An indepth analysis of the electrical characteristics will pave the way to improved mixers.

A series of computer programs have been developed to serve as a tool in understanding the behavior and the subsequent optimization of millimeter-wave mixers. The major program in the collection is a general mixer-analysis program that performs a complete large- and small-signal analysis of a mixer with known diode and mount characteristics. One program analyzes the performance of varactor-diode multipliers, and two programs analyze channel-waveguide transformers.

The primary objective behind developing these programs was to gain a better understanding of the factors that affect the performance of room-temperature, single-ended Schottky-diode mixers operating above 100 GHz. However, these programs are general enough to be applied to a wide variety of mixer problems.

In the mixer-analysis program, the large-signal voltage and current waveforms produced in the diode by the local oscillator (LO) and the available mixer LO power are determined by a nonlinear circuit analysis based on the multiple-reflection technique. This approach can handle a diode with any given current-versus-voltage and capacitance-versus-voltage relationships.

The Fourier coefficients of the large-signal waveforms are used in a small-signal analysis to obtain the mixer input and intermediate-frequency (IF) output impedances and the conversion losses between any two side-band frequencies. Both the thermal noise produced in the diode series resistance and the shot noise from the periodically pumped current in the diode conductance are determined. The effects of intervalley scattering and hot-electron noise can be included as approximations.

The multiplier-analysis program is a variation of the mixer-analysis program. The analysis is performed for a particular input frequency, available output power, bias voltage, and a given set of embedding impedances.

Two programs are provided to analyze a stepped or tapered transformer of the

type often used to minimize the mismatch between the mixer or multiplier and an impedance-matching, reduced-height waveguide. The first program finds the cutoff wavenumbers along the length of the transition from the method of transverse resonance, and then uses the characteristic-impedance method to calculate the reflection coefficient as a function of frequency. The second program solves the wave equation to find the cutoff wave numbers, then uses the characteristic-impedance method.

This series of programs is written in FORTRAN IVH for batch execution and has been implemented on an IBM 370-series computer. The largest program has a central-memory requirement of approximately 74K of 8-bit bytes. The programs were developed in 1983.

These programs were written by P.H. Siegel and A.R. Kerr of **Goddard Space Flight Center** *and W. Hwang of Columbia University. For further information, Circle 43 on the TSP Request Card.*
GSC-12940

Electronic Systems

Interface Program for Reliability Predictions

The user is assisted by numerous menus and prompts.

CARE3MENU generates an input file for the CARE III program. CARE III is used to predict the reliabilities of complex, redundant, fault-tolerant systems, including digital computers, aircraft, and nuclear and chemical control systems. The CARE III input file often becomes complicated and is not easily formatted with a text editor. CARE3MENU provides an easy interactive method of creating an input file by automatically formatting a set of user-supplied inputs for the CARE III system. CARE3MENU provides detailed online help for most of its screen formats.

The reliability-model input process is divided into sections, using menu-driven screen displays. Each stage, or set of identical modules comprising the model, must be identified and described in terms of the number of modules, the minimum number of modules for stage operation, and the critical fault threshold. The fault-handling and fault-occurrence models are detailed in several screens by such parameters as transition rates, propagation and detection densities, Weibull or exponential characteristics, and model accuracy.

The system fault-tree and critical pairs fault-tree screens are used to define the governing system-failure logic resulting from component failures and to specify pairs of nearly coincident component failures that will cause system failure when they exist. Additional CARE3MENU screens prompt the user for output options and run-time control values, such as mission time and truncation values. There are 14 major screens, many with default values and HELP options.

The documentation includes the following: (a) a user's guide with several examples of CARE III models, the dialog required to insert them into CARE3MENU, and the output files created and (b) a maintenance manual for assistance in changing the HELP files and modifying any of the menu formats or contents.

CARE3MENU is written in FORTRAN II for interactive execution and has been implemented on a DEC VAX-series computer operating under VMS. This program was developed in 1985.

This program was written by Salvatore J. Bavuso of **Langley Research Center** *and John L. Pierce of Research Triangle Institute, Paul L. Petersen of Kentron International, Inc., and Alan Roberts of Tesserract Systems. For further information Circle 134 on the TSP Request Card.*
LAR-13514

Mechanics

Hardware, Techniques, and Processes

Acoustic Coupler for Monitoring Bearing Wear

Coupler ensures efficient transfer of sound energy while protecting a piezoelectric sensor.

Marshall Space Flight Center, Alabama

A concept for an acoustic coupler would allow sound to be efficiently conveyed from bearings to an external sensor. Noise from bearings in a bearing test machine can be monitored for signs of incipient failure.

The proposed coupler (see figure) would extend in a straight line from a bearing. The feedthrough and seal allow a constant axial load to be applied to the coupling rod.

The electrical connection to the coaxial cable connector at the top of the assembly is made through a solid rod that passes through the packing gland. An adjustable force is applied through a compression spring to the piezoelectric element and the anvil between the element and the coupling rod. The force also holds the rod in contact with the bearing-race surface, maintaining constant contact pressure over a wide range of temperatures.

The anvil guide — a polytetrafluoroethylene tube — provides electrical insulation and acoustic isolation for the piezoelectric element. The rod guide provides further acoustic isolation, since it prevents direct contact between the coupling rod and the narrow channel between the feedthrough and the bearing-race surface.

The coupling rod passes through instrumentation ports in the bearing housing but not through coolant channels. It is therefore isolated from the turbulence in the flowing coolant that surrounds the bearing. The turbulence otherwise would vibrate, bend, or break the coupler.

The coupler is designed to pass sound frequencies between 100 kilohertz and 1 megahertz. This passband minimizes the lower frequency turbulence noise that reaches the piezoelectric element while transmitting the higher-frequency, bearing-damage noise.

This work was done by W. D. Jolly of Southwest Research Institute for **Marshall Space Flight Center**. *For further information, Circle 4 on the TSP Request Card.*
MFS-27077

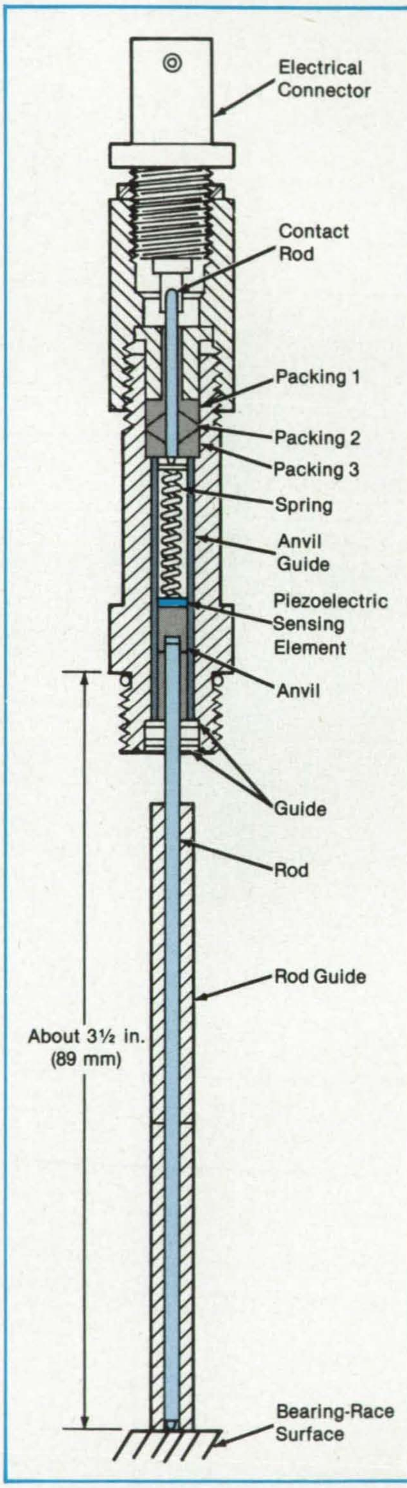

The **Straight-Through Acoustic-Coupler Assembly** can be inserted through existing ports in the housing of a bearing-testing machine. The threaded electrical connector at the top can be rotated to adjust the force applied to the sensing element and the contact bearing.

Testing Gimbal Axes Before Complete

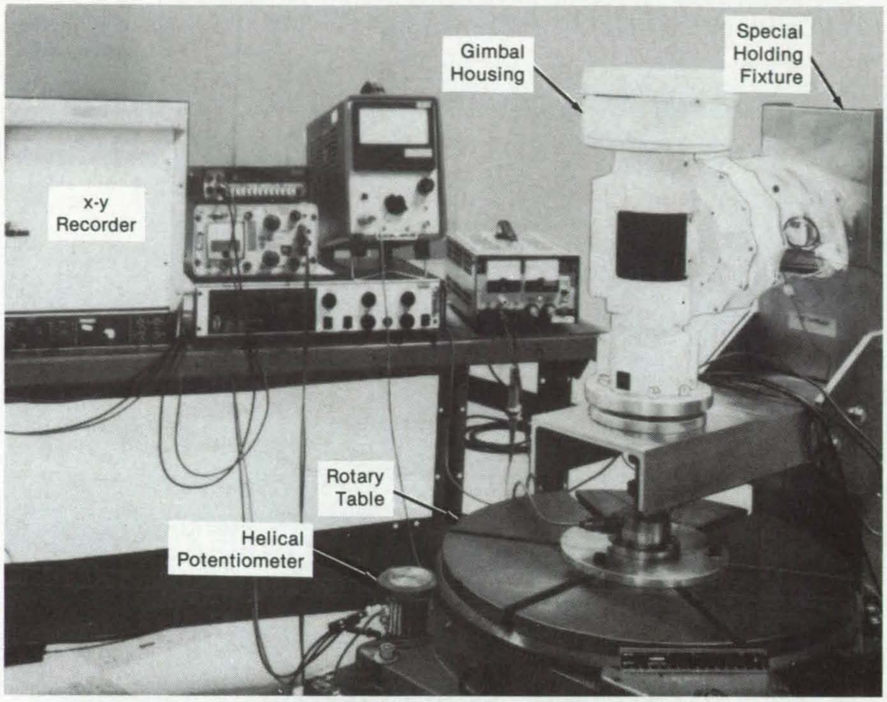

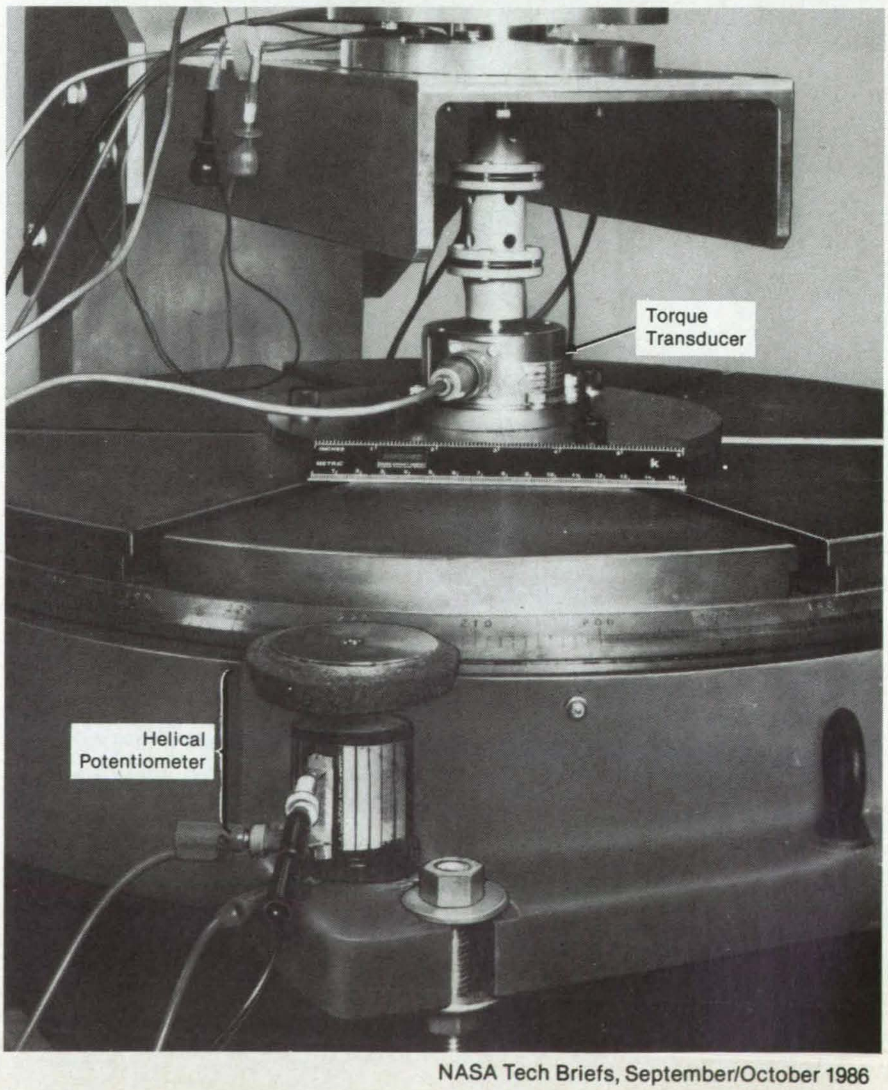

Assembly

Early testing increases chances that the assembly will function well without expensive rework.

Lyndon B. Johnson Space Center, Houston, Texas

A preassembly test ensures that a gimbal axis functions properly before further time and work are invested in assembling the entire gimbal. Developed for antenna gimbals, the test eliminates the delay and costs that ensue when a fully assembled antenna fails because of excessive torque and friction in the gimbal. The time required to disassemble, repair, reassemble, and retest a defective unit is about 7 working days. With the new test, gimbal motors can be installed and the test can be performed in about 1 day. If performance is unsatisfactory, corrections can be made before any further assembly is done.

A special fixture was developed to hold the gimbal housing with the axis to be tested coinciding with the axis of a rotary table (see Figure 1). A torque transducer is mounted on the rotary table. A flexible torque coupling connects the gimbal-axis shaft with the torque transducer. Standard instrumentation furnishes power and monitors and records the test.

A constant direct current is supplied to the axis motor. The rotary table is turned from one stop of the gimbal to the other and back to the original position. Meanwhile, the output of the torque transducer is recorded on the vertical (y) axis of an x-y recorder (see Figure 2). The shaft of a helical potentiometer is coupled to the rotary table, and the potentiometer output is fed to the horizontal (x) input of the x-y recorder to indicate the rotary-table position. The dc voltage supplied to the potentiometer can be increased to expand the horizontal scale.

Plots are made for two directions of motor current. Suspect portions of a plot can be examined further by repeating the test with the horizontal scale expanded in the area of interest.

Any corrections needed in the gimbal are made, and the test is repeated. After the test is completed successfully, assembly can proceed with high confidence that the final unit will meet its requirements.

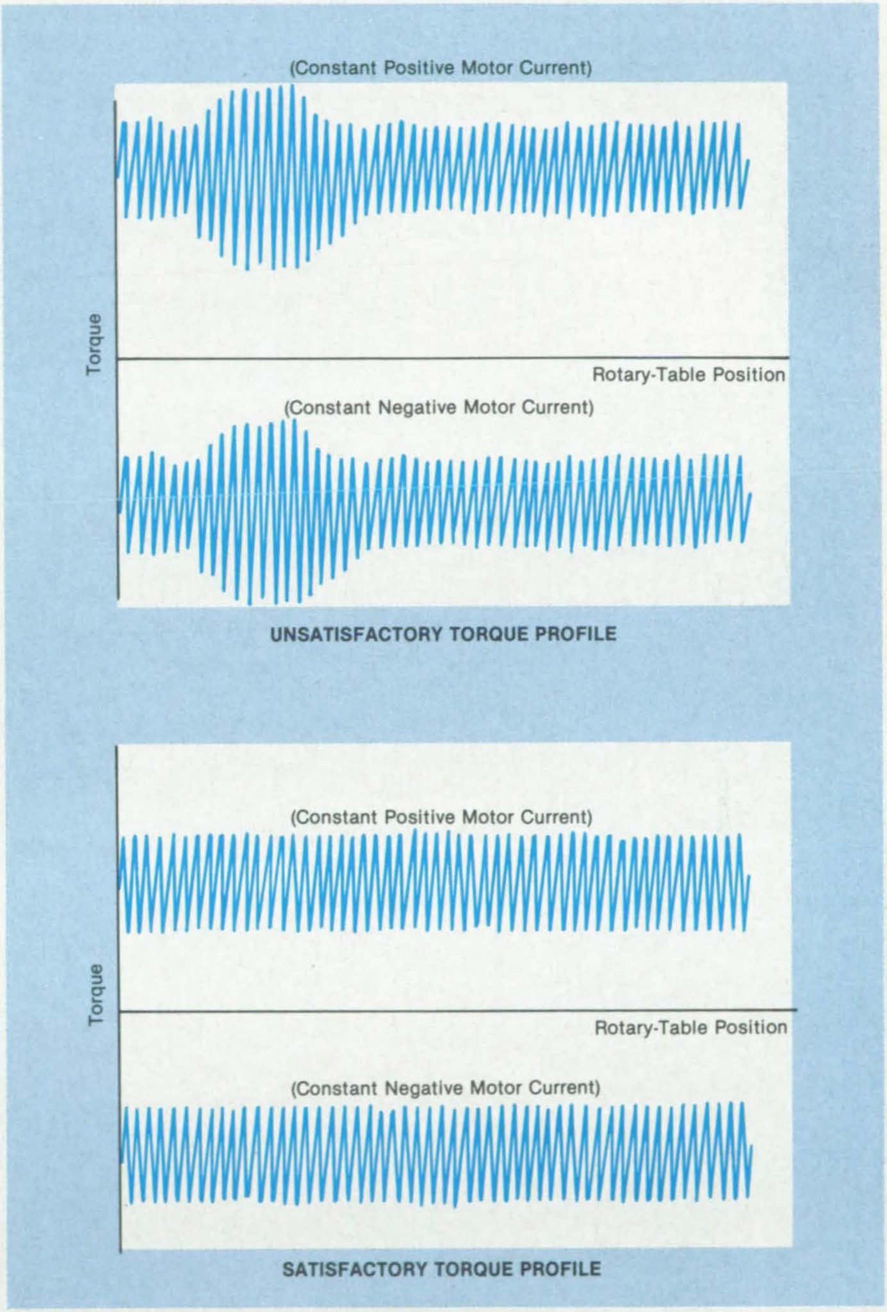

Figure 2. **Unacceptably High Bearing Friction** is reflected in the bulge in the upper plot of the torque on the alpha axis of a gimbal for a K_u-band antenna. The bulge appears for both positive and negative directions of motor current.

This work was done by W. Babis of Hughes Aircraft Co. for **Johnson Space Center**. *No further documentation is available. MSC-20809*

◄ Figure 1. The **Gimbal Housing Is Mounted** above a rotary table. The gimbal axis to be tested is connected to a torque transducer on the table. With the exception of the special holder for the gimbal housing, all of the testing instruments are commercially available items.

Perturbation Method for Computational Fluid-Dynamical Equations

This technique reduces the grid-point density required for accurate results.

Ames Research Center, Moffett Field, California

A perturbation technique yields accurate flow solutions using as few as one-fourth the number of grid points required by finite-difference methods. While the technique was originally developed to solve the Euler equations of two-dimen-

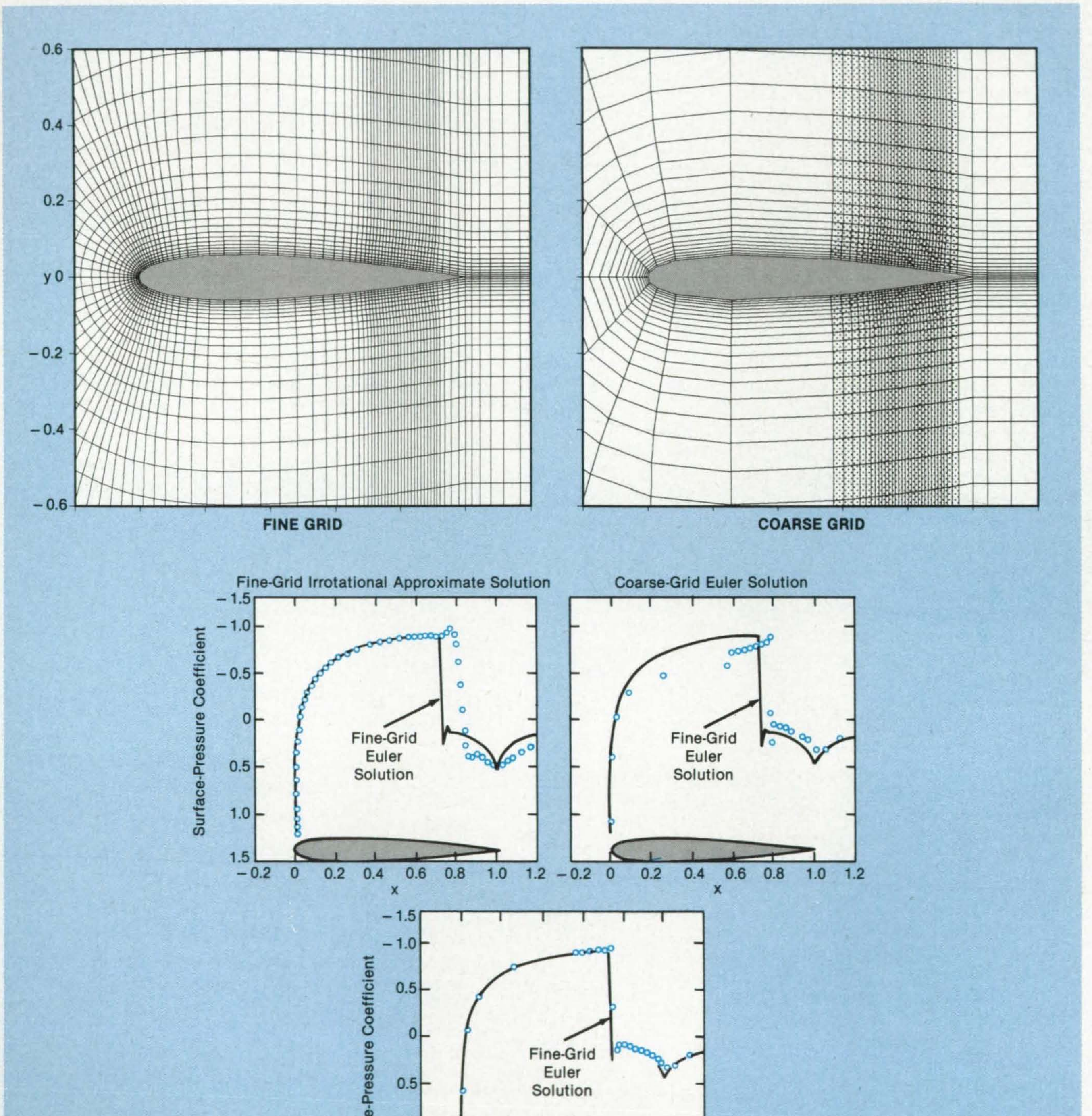

A **Coarse-Grid Perturbation Euler Solution** for a transonic, nonlifting airfoil operating at a free-stream mach number M_∞ of 0.85 and an attack angle α of 0° are compared here with both fine- and coarse-grid Euler solutions.

Multiple Pages Intentionally Left Blank

sional, steady, inviscid transonic flow about airfoils, it is applicable to arbitrary equation sets and higher dimensions.

A smooth, gradually varying function can be resolved accurately with fewer grid points than can a rapidly varying one. To exploit this fact, the governing equations are rewritten in terms of a perturbation about a known nearby or approximate base solution. The base solution should be easily obtainable and must be a good approximation over most of the flow domain. In most of the flow domain, the perturbation quantity (the difference between the two solutions) will then be a smooth, gradually varying function, and the computation grid can be coarsened without appreciable loss of accuracy.

The figure shows the results of one of a series of calculations of transonic, rotational flow about an airfoil. As is typical in the flow-speed range studied, the irrotational approximate solution overpredicts the shock strength and places the shock about 10 percent of chord further downstream.

The 91-by-33-point coarse grid is a subset of the fine grid. It was obtained by discarding grid points in the nose and wake regions. The coarse-grid conventional Euler solution computed with the standard Euler algorithm agrees poorly with the fine-grid Euler solution. (The coarseness of the grid and the discontinuous spacing degrade the solution considerably.) However, the perturbation Euler solution computed on the same coarse grid agrees well with the fine-grid Euler solution. In this and all the other cases studied, the perturbation Euler solutions accurately capture steady, two-dimensional transonic solutions on very coarse grids.

For the airfoil cases studied, the computation time required for the coarse-grid Euler perturbation calculations is only about one-quarter to one-half that for fine-grid Euler calculations of comparable accuracy. (In three-dimensional applications, the grid coarsening would reduce computation time even more dramatically.) The perturbation scheme requires 26 to 70 percent less array storage. Moreover, traditional means of accelerating iterative convergence can still be used, and the required perturbation source terms appear to be readily embeddable into any existing finite-difference code.

The new perturbation scheme could be used in a design cycle where potential solutions are generated routinely; the Euler perturbation method could be used in a second-cut analysis. The method could also be used to couple other equation sets. For instance, the Navier-Stokes (viscous-flow) equations could be perturbed about a full-potential/boundary-layer solution. Further investigation is warranted for other applications.

This work was done by Leslie J. Chow and Thomas H. Pulliam of **Ames Research Center** *and Joseph L. Steger of Stanford University. For further information, Circle 72 on the TSP Request Card.*

Inquiries concerning rights for the commercial use of this invention should be addressed to the Patent Counsel, Ames Research Center [see page 29]. Refer to ARC-11550.

Capacitive Gauge Measures Film Thickness

Continuous readings are obtained with minimal disturbance to flow.

Ames Research Center, Moffett Field, California

A rugged capacitive transducer measures the thickness of a film of liquid flowing over a wind-tunnel model or other object. The transducer is mounted flush with the surface of the model to preserve the model outline, thus minimally disturbing the wind-tunnel and film flows. Additional uses could include thickness control of paint or nonmetallic solid films.

The coaxial arrangement is easy to fabricate (see figure). The capacitance between the inner and outer electrodes increases with the dielectric constant and thickness of the liquid layer and is measured with a capacitance bridge or other suitable circuit.

A transducer of this type has been used to measure liquid film thicknesses in the submillimeter range. Other ranges could be measured with the proper choice of transducer dimensions and capacitance-bridge components. For each liquid of interest, the capacitance-bridge output can be calibrated directly in terms of the liquid depth: Depth measurements for calibration might be obtained, for example, with a depth micrometer equipped with a pointed stylus. The change of capacitance with depth will be approximately linear over a portion of the total depth range.

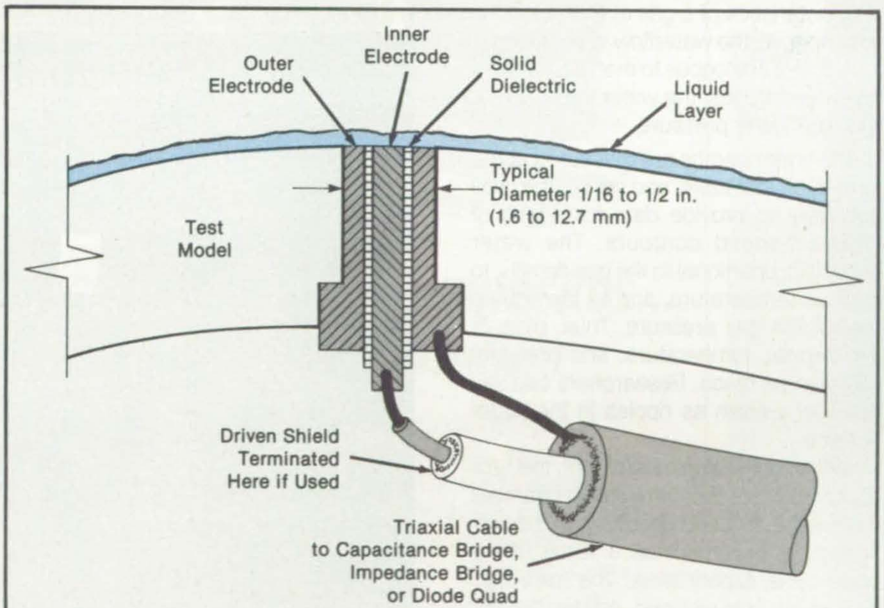

The **Capacitance Between the Inner and Outer Electrodes** varies with the depth of liquid on the model surface. The liquid depth is inferred from the capacitance reading.

This work was done by H. Lee Seegmiller of **Ames Research Center.** *No further documentation is available.*

Inquiries concerning rights for the commercial use of this invention should be addressed to the Patent Counsel, Ames Research Center [see page 29]. Refer to ARC-11449.

Studying Transonic Gases With a Hydraulic Analog

A water table has been adapted to gas dynamics.

Marshall Space Flight Center, Alabama

A water table for hydraulic-flow research can yield valuable information about gas flow at transonic speeds. The water table has been used to study fuel and oxidizer flow in high-pressure rocket engines, in particular to study transonic flow at the walls of a combustion chamber. The chamber allowed new wall geometries to be evaluated quickly by visual observation.

The method can be applied to gas flows in such equipment as furnaces, nozzles, and chemical lasers. It is especially suitable when wall contours are nonuniform, discontinuous, or unusually shaped. Wall shapes can be changed quickly for study and evaluated on the spot. The method can be used instead of computer simulation when computer models are unavailable, inaccurate, or costly to run.

A full-scale, two-dimensional wall, representing one-half the flow chamber, is placed on the water table (see figure). A sheet of water flows over the table and around the wall. The depth of the sheet at any point is analogous to some of the characteristics of a gas at that point. For example, as the waterflow is accelerated to a speed analogous to that of a transonically flowing gas, the water depth falls to indicate lower pressure.

The water depths are measured at the center of the table and along the wall boundary to provide data for a grid of constant-speed contours. The water depth is proportional to the gas density, to the gas temperature, and to the square root of the gas pressure. Thus, plots of the density, temperature, and pressure can also be made. Researchers can see the flow pattern as ripples in the water surface.

In the rocket-engine problem, the radii of curvature of the combustion-chamber walls were reduced upstream and downstream of the throat as a result of the water-table experiments. The transonic-flow length was reduced, and the coolant pressure loss was decreased.

This work was done by W. R. Wagner and F. F. Lepore of Rockwell International Corp. for **Marshall Space Flight Center.** *For further information, Circle 8 on the TSP Request Card.*
MFS-29100

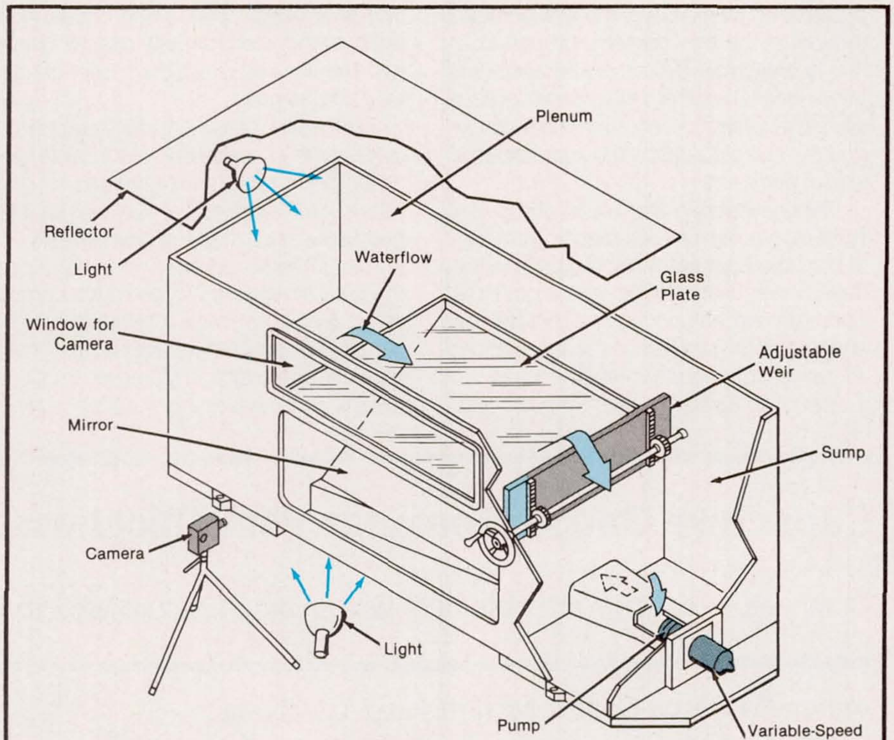

WATER TABLE

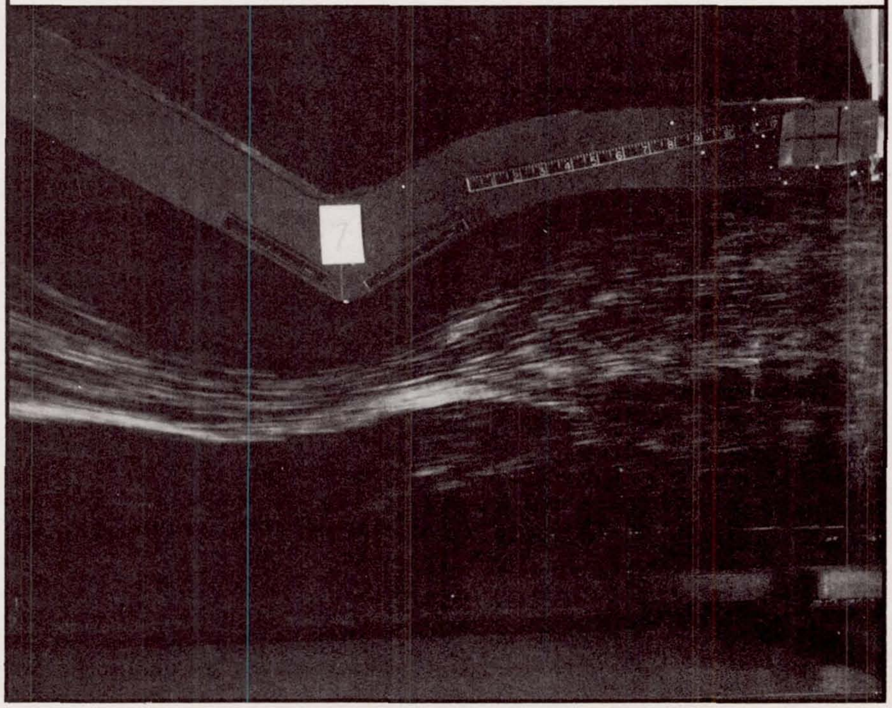

MODEL OF A FLOW-CHAMBER WALL ON THE WATER TABLE

Water Flows Over the Transparent Glass Plate of the water table. Flow patterns around objects on the table are clearly visible through windows, and the depth of the flowing water at various points can be readily measured.

Sealing a Loosely Fitting Valve Assembly

A double-ring seal avoids the expense of remachining or redesigning valve parts.

Marshall Space Flight Center, Alabama

An O-ring and a backup ring are combined to seal high-pressure hydrogen gas in a fitting that has loose clearances. The fittings are part of a valve on a hydrogen compressor.

Originally, bolt loading through a flange was used to create enough yield in metal sealing parts to form a leak-tight seal. With hydrogen and with the normal wear of the sealing surfaces, however, the bolt torque required for tight sealing became excessive and caused structural problems in the cast iron of the compressor housing.

The solution was to redesign the seal and use a totally captured O-ring and a glass-filled polytetrafluoroethylene backup ring. (The loose manufacturing tolerances of the valve components made it useless to machine a standard O-ring groove.) When the rings are installed in the valve, the O-ring forces the backup ring to conform to the gap between mating metal parts (see figure). At the same time, the backup ring prevents the O-ring from being extruded into the gap. The combination of rings thus ensures a tight seal and makes it unnecessary to remachine the parts or fabricate new ones to maintain tighter clearances. With the double-ring seal, the leakage of gaseous hydrogen is undetectable at a pressure of 850 lb/in.^{2} (5.9 MPa).

This work was done by L. R. Goff and G. F. Tellier of Rockwell International Corp. for **Marshall Space Flight Center**. *No further documentation is available.*
MFS-29051

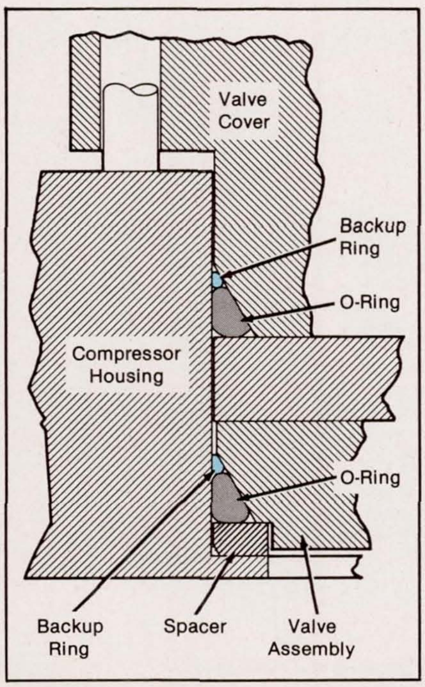

Mating Fittings on a Valve are sealed by a pair of rings — one an O-ring and the other a backup ring. The backup ring fills the relatively large gap between parts. This prevents the softer O-ring from being pushed into and through the gap.

Machinery

Hardware, Techniques, and Processes

Books & Reports

Continuous Removal of Coal-Gasification Residue

Ashes would flow from a reactor in a continuous stream instead of in batches.

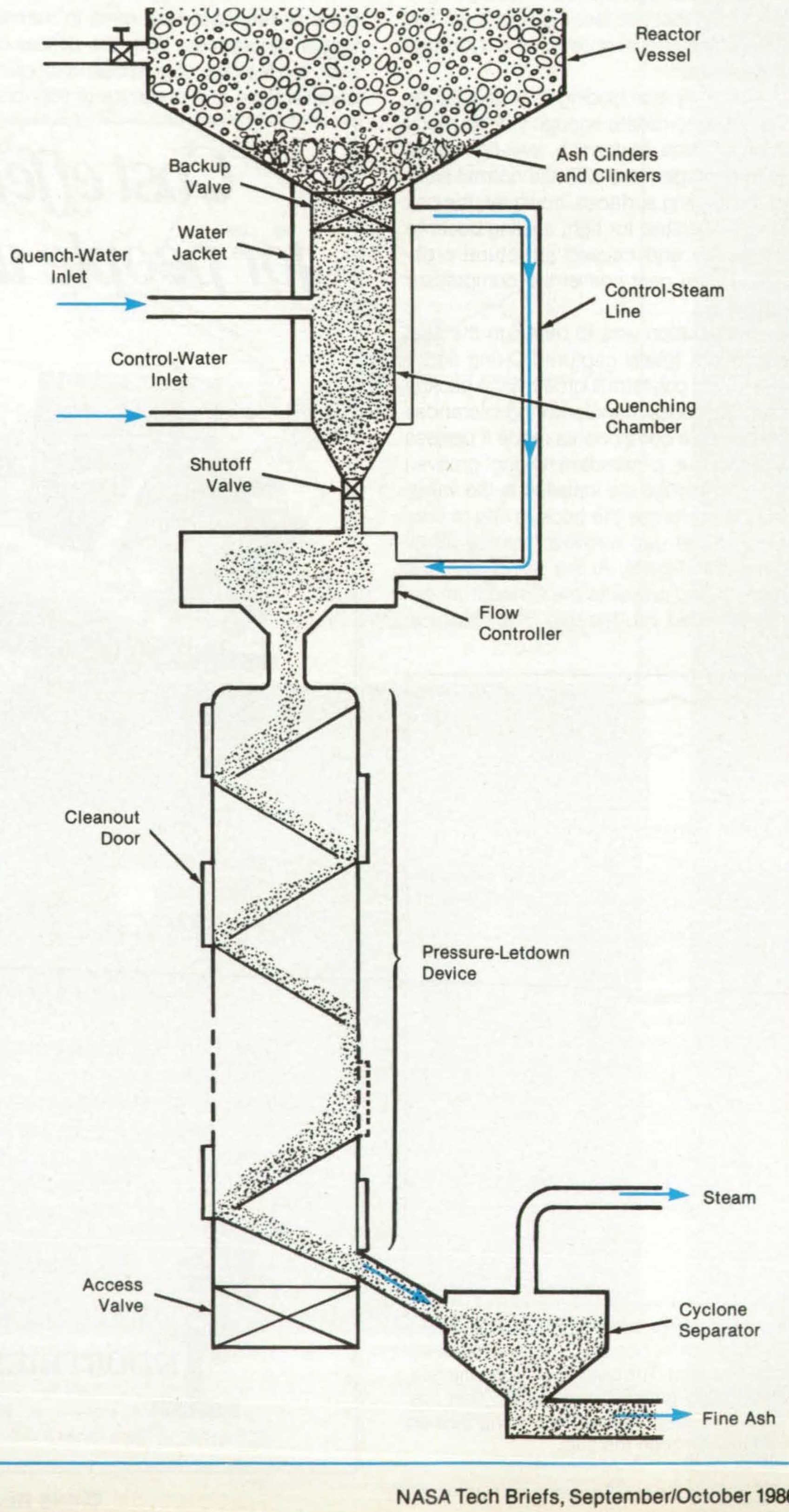

NASA's Jet Propulsion Laboratory, Pasadena, California

A proposed continuous-flow hopper would process the solid residue from coal gasification, converting it from ashes, cinders, and clinkers to particles the size of sand granules. Unlike conventional ash lockhoppers, which operate on batches of materials, the proposed unit would not require repeated depressurization of the lockhopper to admit and release materials. It therefore would consume less energy. Because the unit has no airlock valves to be opened and closed repeatedly on hot, abrasive particles, it will be subjected to lesser wear.

According to the concept, as the hot ashes, cinders, and clinkers leave the reactor, a stream of quenching water hits them (see figure). The water flashes to steam on contact and explosively destroys the cinders and clinkers, reducing them to small particles. The ash and steam enter the flow controller where the flow is throttled to keep a high pressure in the reactor. A water jacket surrounding the quenching chamber absorbs enough heat from the ash to vaporize the water flowing through it. The resulting steam operates the flow controller.

The stream enters the pressure-letdown device, where the ashes move slowly from chamber to chamber, with minimal abrasion. In each chamber, the pressure drops slightly, reaching atmospheric pressure at the outlet. The openings between chambers are made progressively larger to accommodate the expanding volume of gas as the stream cools and depressurizes.

Finally, the stream feeds into a cyclone separator, which separates steam and coal gas, if any, from the ash. The steam can be used for heating. Alternatively, the steam can be used to drive a low-pressure turbine to generate electrical power. In this case, the steam would be separated before the ash is completely depressurized.

This work was done by Earl R. Collins, Jr., Jerry Suitor, and David Dubis of Caltech for **NASA's Jet Propulsion Laboratory**. *For further information, Circle 9 on the TSP Request Card.*
NPO-16605

◄ **Coal-Gasification Residue Flows** slowly through a pressure-letdown device. Material enters and leaves continuously. A cleanout door on each pressure-letdown chamber allows access for maintenance and emergencies.

Effects of Structural Flexibility on Aircraft-Engine Mounts

A design technique is used to decouple linear and rotational oscillations of the engine.

Langley Research Center, Hampton, Virginia

A new analysis extends a technique for the design of a widely used type of vibration-isolating mounts for aircraft engines, in which rubber mounting pads are located in a plane behind the center of gravity of the engine-propeller combination. Such mounts are frequently designed to decouple the linear and rotational motions of the engine. The present study extends the decoupling analysis to account for the flexibility of the mount structure.

The overall problem of vibration oscillation of an aircraft powerplant is a problem in dynamics, which can be exactly solved only by accounting for the distribution of mass and stiffness throughout the structure as well as for such factors as the gyroscopic effects of the engine and propeller. This new analysis, however, treats a problem in statics. The results of this simple approach are useful in providing equations for the design of the vibration-isolating mounts. The equations are believed to be applicable in the usual situation in which the engine-mount structure itself is relatively light and is placed between the large mass of the engine and other heavy components of the airplane.

In the engine-mount system illustrated in the figure, the engine is supported by m equally spaced mounting pads. The axis of each pad intersects the centerline of the engine at a common point and makes an angle α with the centerline. The vertical and pitching motions of the powerplant are considered. The same analysis is applicable to the lateral decoupling of engine vibrations (lateral movement and yawing rotation) by redefining axes.

From the relative displacements of the front and rear faces of each mounting pad, the axial, radial, and tangential forces produced on the engine by each pad are calculated. The forces are re-

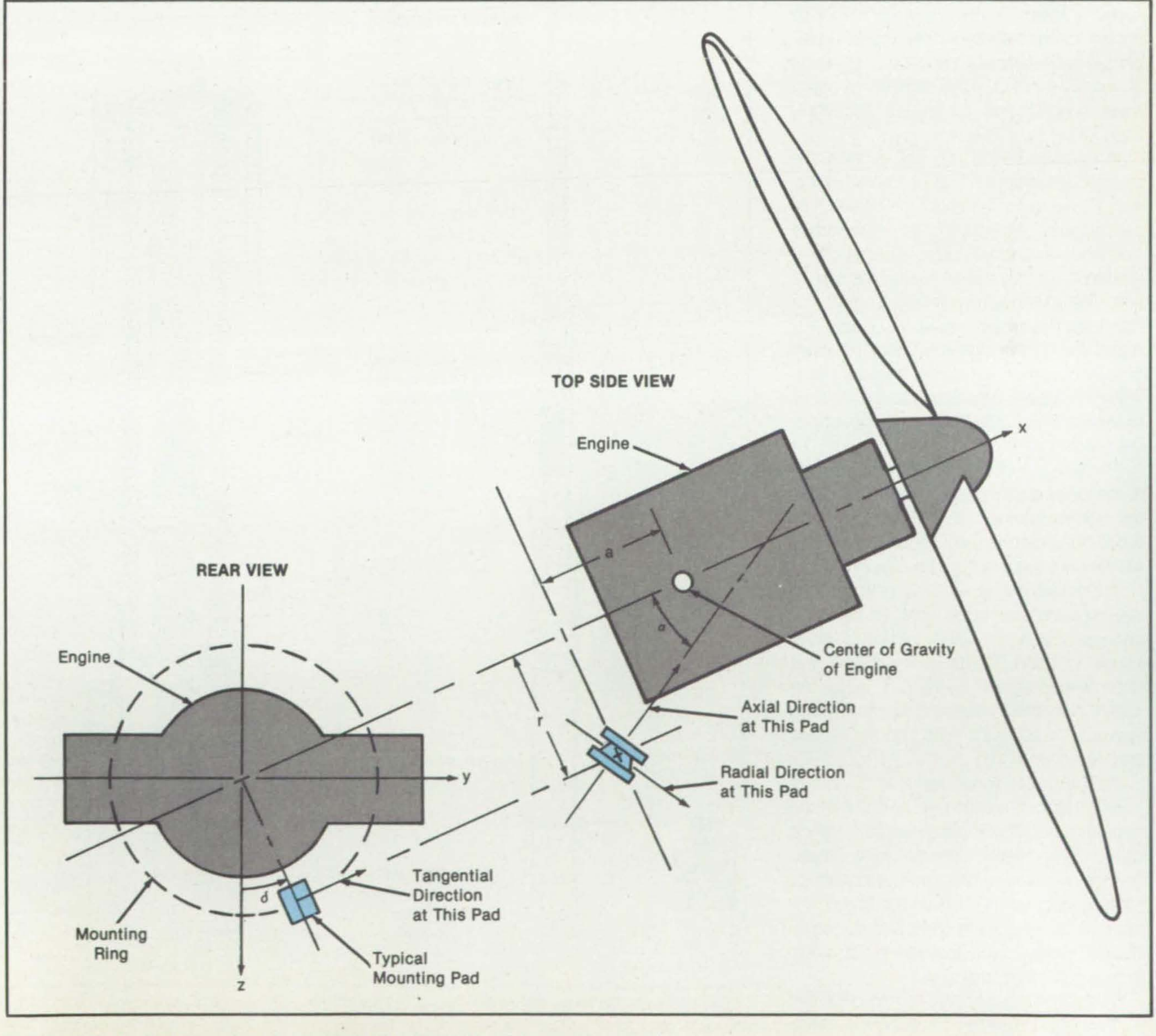

This **Coordinate System** is used in analyzing the flexibility of the engine mounts.

solved along the powerplant axes, allowing the total vertical force and the moment about the center of gravity of the powerplant to be calculated. The stiffness components of the mount can be determined, and an equation can be obtained to express the decoupling in terms of α, the overhang ratio a/r, and the stiffness parameters of the system.

Equations and curves were developed to enable the design of mount systems and to illustrate the results for a range of design conditions. Arrangements of mounting pads other than those involving equal spacing around the mount ring may be analyzed by the equations developed. The results of this analysis show that the structural flexibility has a relatively small effect when the center of gravity of the engine is close to the plane of the mounting points, but it becomes more important as the distance between the center of gravity and the plane of the mounting points increases.

This work was done by William H. Phillips of **Langley Research Center**. *Further information may be found in NASA TM-85725 [N84-16590/NSP], "Effect of Structural Flexibility on the Design of Vibration-Isolating Mounts for Aircraft Engines."*

Copies may be purchased [prepayment required] from the National Technical Information Service, Springfield, Virginia 22161, Telephone No. (703) 487-4650. Rush orders may be placed for an extra fee by calling (800) 336-4700.
LAR-13305

Shock-Absorbent Ball-Screw Mechanism

End-of-travel impacts are safely absorbed, increasing the service life.

Ames Research Center, Moffett Field, California

An actuator containing two ball screws in series employs Belleville springs to reduce impact loads, thereby increasing its life expectancy. This new application of Belleville springs can increase the reliability of equipment in which ball screws are commonly used.

In addition to the two ball screws, the mechanism employs two ball nuts, a tube, and a drive motor (see figure). The two nuts are mounted at the tops of the lower screw and tube, respectively. The upper screw is held so that it may move only in axial translation. The lower screw is free to rotate or translate. The tube is held so that it may only rotate. When the tube is rotated, the lower screw rotates or translates, thereby translating the upper screw axially so that it raises or lowers a part attached to the upper tip of the mechanism.

Previously, a circular plate was attached to the lower end of each ball screw to strike the corresponding nut and thus limit the travel of the mechanism. The impact tended to wear out the mechanism rapidly.

In the new mechanism, the striking plates are replaced by three sets of Belleville springs. When the upper screw is in its lowest position, the uppermost spring is compressed against surface B. When the motor is started counterclockwise facing upward, it rotates the tube and the screws start to ascend.

As the upper screw reaches its limit of travel, surface A comes in contact with the upper ball nut. The upper spring is thus once again compressed, absorbing the kinetic energy released as the lower screw stops rotating and starts translating. When the lower screw reaches its upper limit, surface C makes contact with the lower nut, compressing the middle spring.

When the drive motor is reversed, the screws start to descend. The lower screw is stopped in its descent when surface D

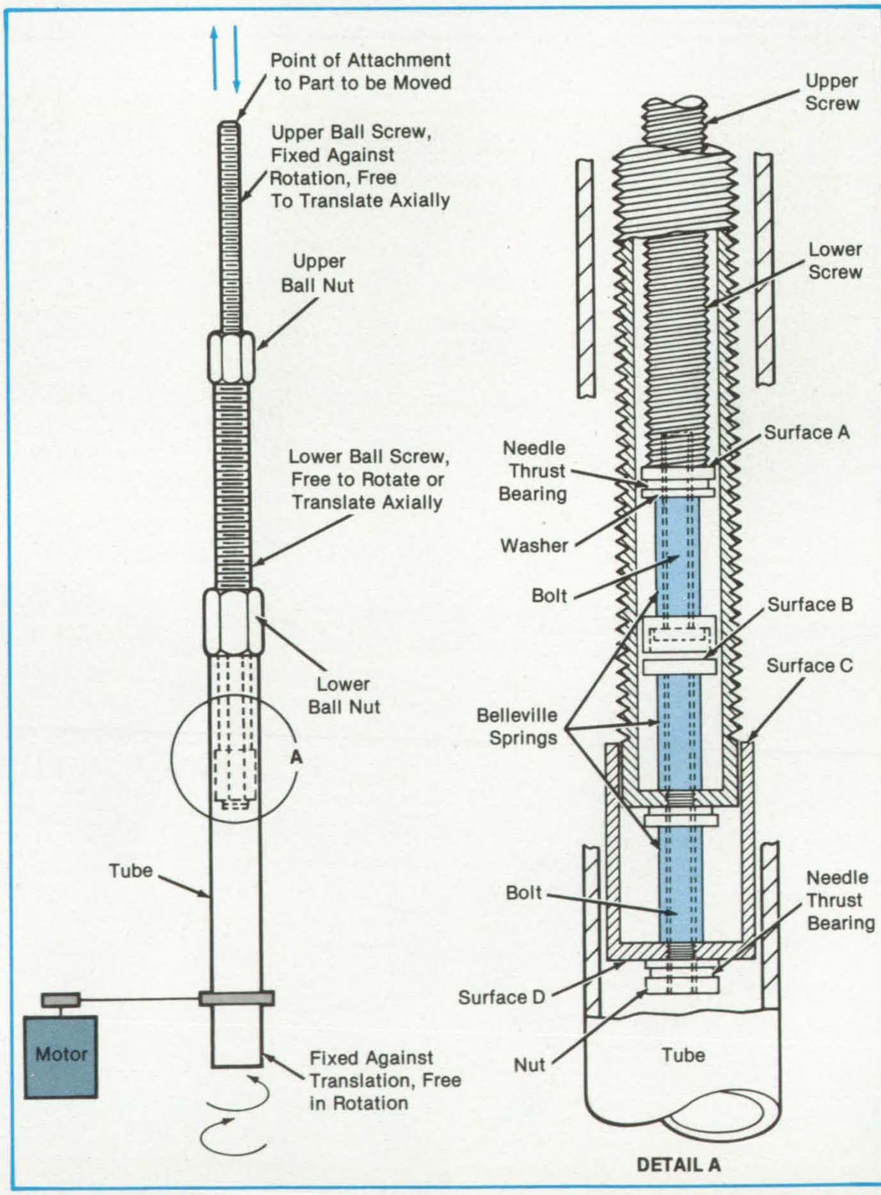

A **Set of Three Springs** within the lower screw of the ball-screw mechanism absorbs the impacts that result when the parts reach their upper and lower limits of movement. The mechanism is shown near its lowest position.

strikes the bottom of the tube. When this happens, the lower spring absorbs the kinetic energy. The upper screw is stopped in its descent when contact is made at surface B.

The compression forces are applied to the springs through needle-thrust-bearing-and-washer assemblies. If the forces were applied directly, the screws would tend to lock because of friction between the spring ends and the contact surfaces.

The mechanism was designed with Belleville springs as the shock-absorbing elements because Belleville springs have a good energy-to-volume ratio and are easily stacked to attain any stiffness and travel.

This work was done by Otto A. Hirr, Jr., and Robert W. Meneely of **Ames Research Center**. *For further information, Circle 29 on the TSP Request Card.*

Inquiries concerning rights for the commercial use of this invention should be addressed to the Patent Counsel, Ames Research Center [see page 29]. Refer to ARC-11366.

Improved Orifice Plate for Spray Gun

Spray patterns are made repeatable.

Marshall Space Flight Center, Alabama

The erratic spray pattern of a commercial spray gun is changed to a repeatable one by a simple redesign of two parts. Such an improvement may be useful in many industrial applications requiring repeatable spray patterns. These might include the spraying of foam insulation, paint, other protective coatings, detergents, abrasives, adhesives, process chemicals, or fuels.

In the unmodified spray gun (see figure), the orifice plate lies between the gasket and the nozzle. The gasket, orifice plate, and nozzle are held together inside a specially shaped nut. The inside diameter of the nut is 0.625 in. (15.88 mm), while the outside diameters of the nozzle and orifice plate are both 0.590 in. (14.99 mm). The nozzle and orifice plate thus fit loosely in the nut and can slide laterally up to a maximum misalignment of 0.035 in. (0.89 mm).

The spray pattern depends critically on the alignment between the orifice and the nozzle. In the unmodified gun, the looseness of these critical parts causes the spray angle to vary several degrees in an unrepeatable manner. In the modified gun, alignment is assured by reworking the polytetrafluoroethylene bushing, providing the orifice plate with a shank that fits in the bushing, and increasing the outer diameter of the orifice plate to 0.620 in. (15.75 mm). This combination of changes assures a repeatable spray pattern.

This work was done by W. C. Cunningham of Martin Marietta Corp. for **Marshall Space Flight Center**. *For further information, Circle 91 on the TSP Request Card.*

This invention is owned by NASA, and a patent application has been filed. Inquiries concerning nonexclusive or exclusive license for its commercial development should be addressed to the Patent Counsel, Marshall Space Flight Center [see page 29]. Refer to MFS-28110.

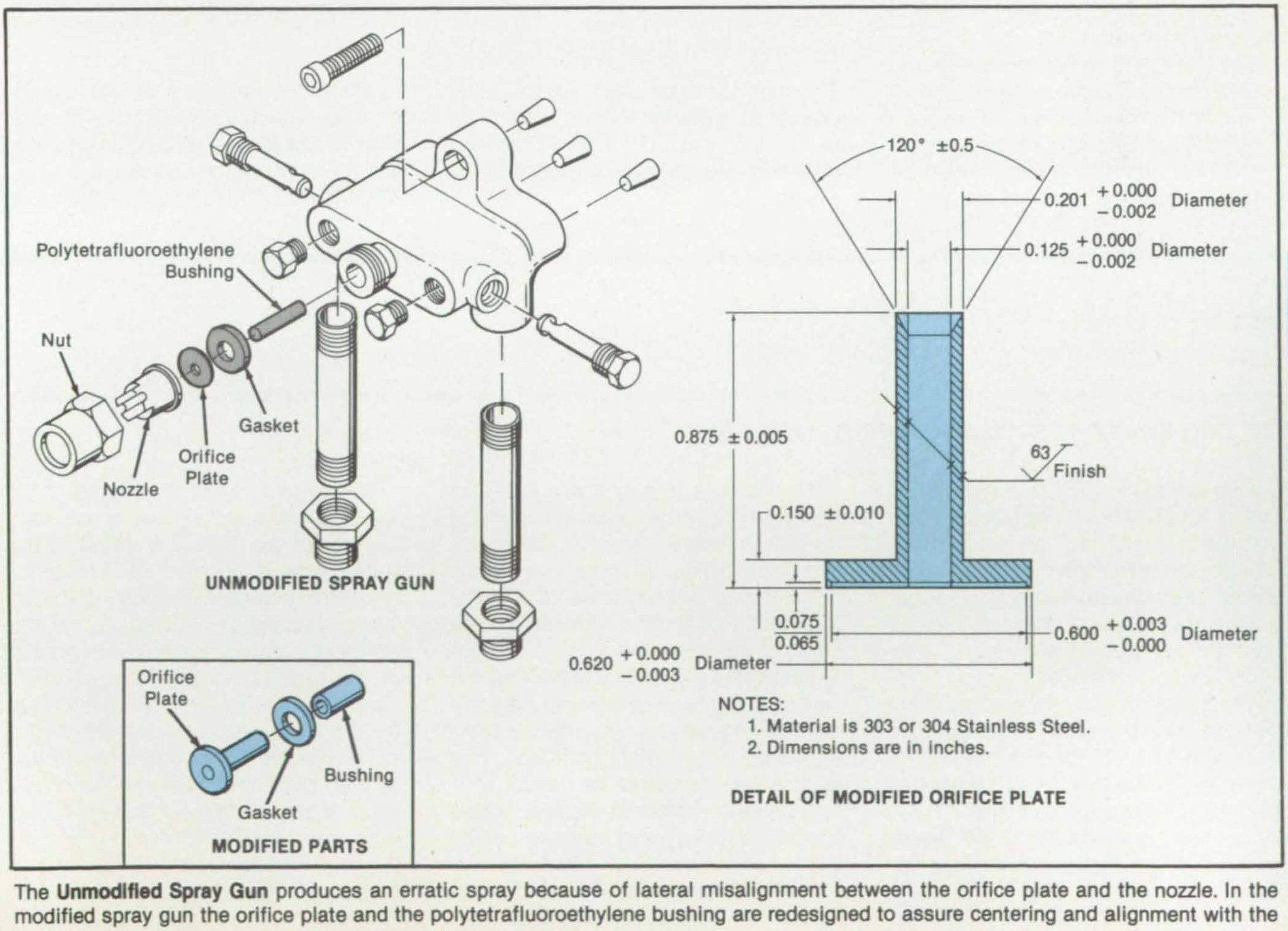

The **Unmodified Spray Gun** produces an erratic spray because of lateral misalignment between the orifice plate and the nozzle. In the modified spray gun the orifice plate and the polytetrafluoroethylene bushing are redesigned to assure centering and alignment with the nozzle.

Flow Injector Would Keep Slurry From Settling

Costly pipeline choking would be reduced or prevented.

NASA's Jet Propulsion Laboratory, Pasadena, California

A proposed ring nozzle may help to prevent the choking of coal-slurry pipelines. Intended originally for use in coal mines, the nozzle concept should be generally applicable to short-haul slurry pipelines where high-pressure water (or other slurry fluid) is available.

Where the flow rate is insufficient, the particles of a slurry tend to settle out of the fluid, forming a solid slug that blocks the pipeline. In some instances, it is necessary to break the pipeline open to remove the blockage.

The ring nozzle helps to prevent such blockages by enabling the injection of extra water or other fluid to augment the flow near the wall. A relatively small volume of water at high pressure is accelerated through an annular slit into the pipe (see figure), forming a laminar-flow boundary layer that entrains a large volume of slurry. Helical fins in the accelerating slit impart a rotation to the injected and entrained flows, thereby enhancing the ability to prevent settling of the slurry particles.

The injection concept is expected to be efficient in energy and applicable to coal-slurry conduits at any angle from horizontal to vertical. For maximum effectiveness, injection nozzles would be placed at intervals along a slurry line.

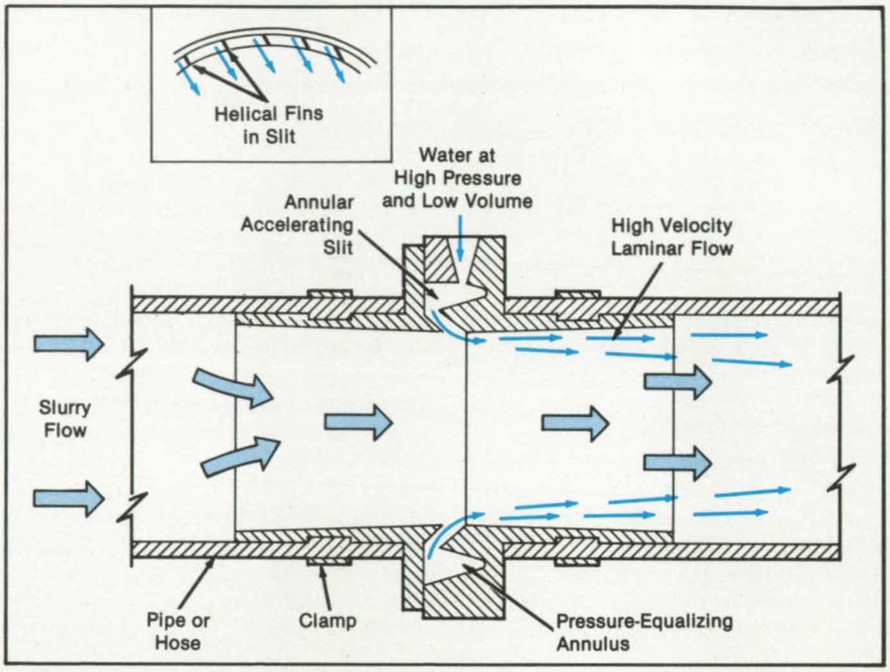

Extra Water is injected into the flow near the wall of a slurry pipe to keep the slurry particles from settling and blocking the pipe.

The separations between nozzles, water pressures, injection angles, and other parameters would be chosen in accordance with the haulage conditions of the slurry system.

This work was done by Edward V. Lewis of Caltech for **NASA's Jet Propulsion Laboratory.** *For further information, Circle 90 on the TSP Request Card. NPO-16186*

Liquid/Gas Vortex Separator

Gas is removed from a liquid in a tank.

Lyndon B. Johnson Space Center, Houston, Texas

A liquid/gas separator vents gas from a tank of liquid that contains gas randomly distributed in bubbles. The device, which resembles a cyclone separator, was conceived for use in zero gravity. On Earth an augmented version could be used to separate gas from a liquid when gravitation alone is insufficient.

The separator includes a spinning impeller to impart rotation to the liquid/gas mixture in a tube in the tank (see figure). In the resulting vortex, liquid is thrown to the tube wall by centrifugal force. The gas in the center of the tube is almost free of liquid. The gas is withdrawn from the center through a vent pipe.

A three-way solenoid-operated valve at the outlet end of the vent pipe either lets the gas escape or else closes the outlet and diverts the flow back into the tank through a venturi tube in the liquid-recirculation path. The main liquid flow in the venturi causes the suction that drives this secondary flow. An ultrasonic transducer detects such liquid as might remain in the gas and be drawn into the vent pipe and sends a signal to the valve controller to turn the valve to the recirculating, nonventing position. This feature reduces loss of the liquid.

A pressure sensor in the tank is also connected to the valve controller. When the pressure has been reduced to a preset level, the controller stops the venting by turning the valve to the recirculating position.

The vortex tube has slits through which the liquid/gas mixture flows to and from the rest of the tank. The inside of the vortex tube is polished or coated for smoothness to minimize friction between it and the liquid, thus increasing the efficiency of vortex generation. The outside of the tube is coated with polytetrafluoroethylene to make it unwettable, thereby facilitating the movement of gas.

The impeller is powered by an encapsulated permanent-magnet rotor; the stator is outside the tank and separated from the rotor by a pressure barrier. Leakage through rotary seals is thus eliminated. The impeller could also be turned through a magnetic drive like those used commonly on industrial

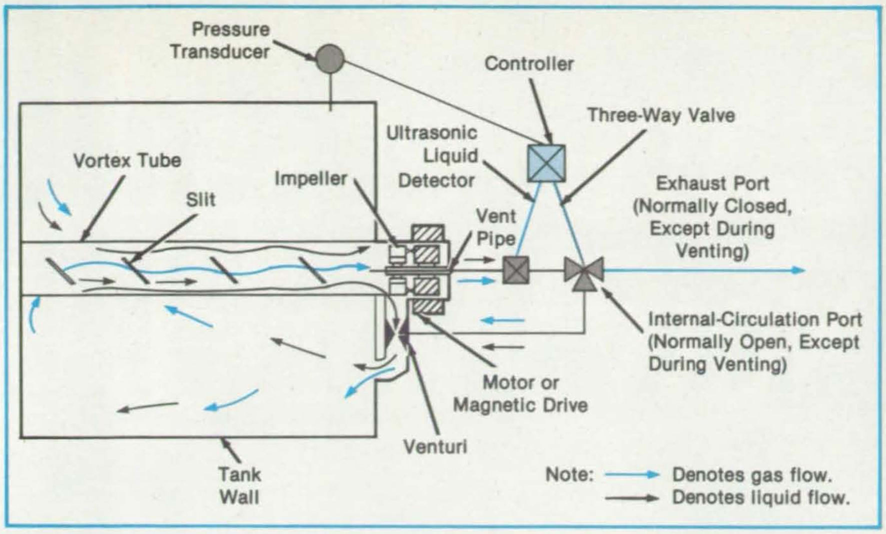

A **Centrifugal Force** separates liquid and gas, forcing the liquid out of the vortex tube through the venturi tube. Gas is vented through the exhaust port. When liquid is detected in the vent tube, the exhaust port is closed, and the liquid/gas mixture in the vent tube is drawn back into the tank through the venturi.

pumps.

The continuous circulation of the liquid tends to produce a uniform temperature throughout the tank. Liquid-quantity gauges will therefore produce more accurate readings.

This work was done by Brian G. Morris of **Johnson Space Center**. *No further documentation is available.*

Inquiries concerning rights for the commercial use of this invention should be addressed to the Patent Counsel, Johnson Space Center [see page 29]. Refer to MSC-21058.

Automated Rotating-Machinery Analysis

System provides data and plots of motion.

Marshall Space Flight Center, Alabama

A computer-controlled automatic system processes accelerometer data from rotating machines, producing a mathematical description and graphical display of shaft motion. The program saves processing time, readily identifies the type of motion (circular, looped, or elliptical), provides annotated assessments to assist in failure analysis, alerts the user to look for distinctive characteristics of the machinery, and creates informative plots.

The system digitizes the data from two orthogonally positioned transducers, thereby obtaining histories of motion along the transducer axes. It calculates the time required for one shaft orbit and determines the oscillation frequencies above and below the shaft rotational speed, while compensating for distortions

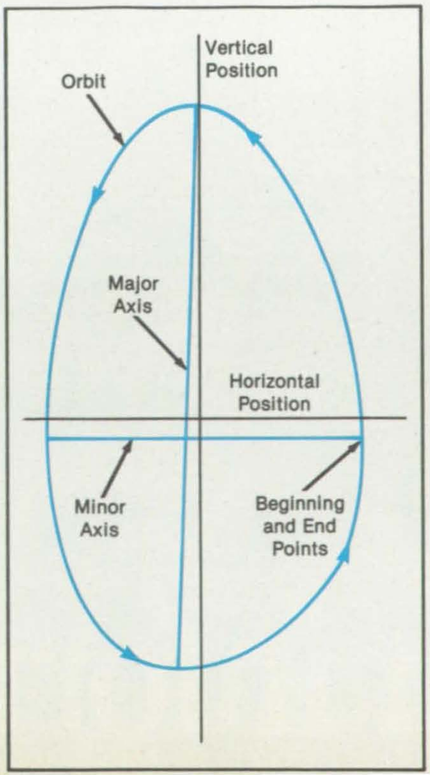

A **Shaft Orbit** is printed out as a plot of successive positions computed from accelerometer measurements. Additional plots (not shown) are of power versus frequency and rotational cycle.


J.Harrelson
our name is Harris.

introduced by low signal-to-noise ratios. The program finds the major and minor axes of the shaft orbit. It prints out single and multiple orbits (see figure) and shows the motion history and the power spectrum of the dynamic data. With the system, the user can analyze rotor stability and evaluate unbalance response, impact, and rubbing caused by nonrotating machinery.

This work was done by J. E. Clark of Rockwell International Corp. for **Marshall Space Flight Center**. *No further documentation is available.*
MFS-19912

Bidirectional, Automatic Coal-Mining Machine

Deadheading and other inefficiencies would be eliminated.

NASA's Jet Propulsion Laboratory, Pasadena, California

A proposed coal-mining machine would operate in both the forward and reverse directions along a mine face. The new design would increase efficiency and productivity, because it would not stop cutting as it retreated to the starting position after completing a pass along the face. To further increase efficiency, the automatic miner would carry its own machinery for crushing the coal and feeding it to a slurry-transport tube.

According to the concept, the mining machine cuts coal with two cutting drums as it advances on crawler tracks. The aft drum is elevated above the forward drum so that it has access to fresh material (see figure). With this arrangement, the machine frame must be no higher than the forward-drum cutting diameter; since the machine will be automatically controlled, there will be no difficulty in designing it for a low profile — no cab for an operator will be necessary.

The coal cut by the aft drum falls on a loading apron at the rear of the machine. The apron simply feeds coal by gravity to crushing screws at the center of the machine.

The coal cut by the forward drum falls to the mine floor, where oscillating gathering arms scoop and push it up the forward-loading ramp of the machine into the crushing screws. The screws crush the coal from both forward and aft cutters to a size that can be handled by the slurry-transport system. The machine adds water at low pressure to the crushed particles, and the lower screws convey the mixture into a slurry-haulage tube on the side of the machine opposite the mine face.

When the machine reaches the end of a pass, the relationship of the drums is reversed. The aft drum is lowered, and the forward drum and its loading ramp are raised so that they can continue cutting and feeding the slurry tube as the miner reverses direction and retreats. The only interruption is that for the machine to maneuver in the entry passage to cut farther into the face; this maneuver would be controlled automatically or remotely by human operators.

This work was done by Earl R. Collins, Jr., of Caltech for **NASA's Jet Propulsion Laboratory**. *For further information, Circle 26 on the TSP Request Card.*
NPO-15860

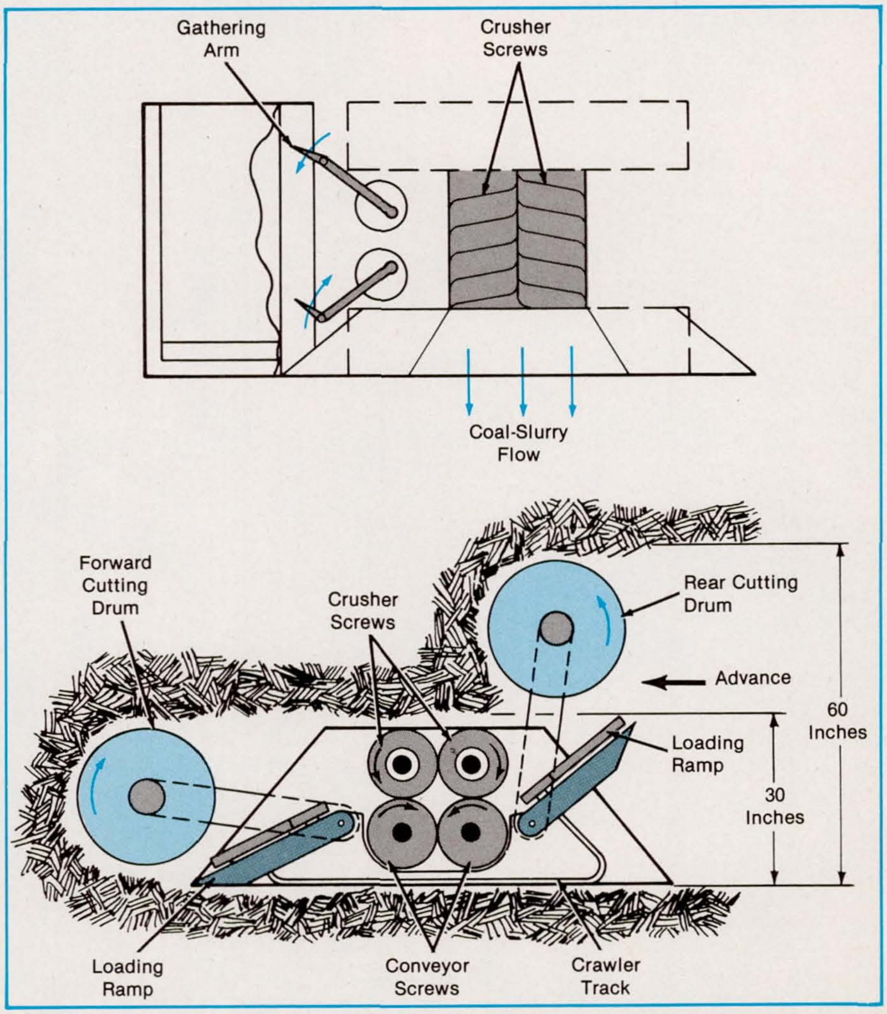

The **Dual-Drum Mining Machine** cuts coal in two layers, crushes it, mixes it with water, and feeds it as a slurry to a haulage tube. At the end of a pass, the forward drum is raised so that it becomes the rear drum, and the rear drum is lowered, becoming the forward drum for the return pass.

Heat Radiators for Electromagnetic Pumps

Carbon/carbon composite radiators withstand high temperatures.

A report proposes the use of carbon/carbon composite radiators in the electromagnetic coolant pumps of nuclear reactors on spacecraft. Carbon/carbon composite materials can function well at temperatures in excess of 2,200 K. Aluminum, which would normally be used, has a melting temperature of only 880 K.

Two configurations have been proposed. In the first case, the composite radiator structure would be bolted and clamped to the three outer ends of the stator-core laminations of a polyphase, annular linear induction pump. The operating temperature would be about 600 K. The radiator structure would conduct heat from the stator core and windings to an outside shield, from which the heat would be radiated into space.

Heat from the portion of the core away from the radiator would be conducted circumferentially around the core in the copper stator windings and into the part of the core near the radiator. Heat that leaks into the stator from the heat-transfer fluid being pumped, including heat induced by the oscillating magnetic field of the pump, joins the thermal flux conducted from the stator to the radiator. In the second case, a composite structure would serve as the waste-heat radiator of an integral thermoelectric generator that supplies power to a thermoelectromagnetic coolant pump. The maximum operating temperature would be 825 K. In both cases, the radiators would be made large enough, not only to radiate heat adequately, but also to shield the equipment from meteorites and other debris.

This work was done by Robert J. Campana of GA Technologies, Inc., for **NASA's Jet Propulsion Laboratory**. *To obtain a copy of the report, "Electromagnetic Pump Heat Radiators," Circle 81 on the TSP Request Card.*
NPO-16458

Long, Thin, Deployable Mast

The mast extends to 25 times its original length.

A report describes a 15-m-long deployable mast and discusses the design and development that went into making the product. Only 0.6 m long when stowed, the mast extends itself to its full length. Although the extended mast is long and narrow, with an aspect ratio of 67:1, it resists bending. Its predicted bending strength and bending stiffness are 4,700 N-m and 1.3×10^6 N-m^2, respectively. Its mass per unit length is 3.43 kg/m.

The mast consists of longerons braced by battens and diagonal filaments. The components are made of glass-reinforced epoxy. In the stowed condition, the 15-m-long longerons are coiled in a tight helix, with the battens and filaments nested between coils. When restraining rods are released, the longerons uncoil and the mast extends. A lanyard controls the rate of uncoiling so that the longerons do not snap immediately to their full length and overstress the structure. The lanyard is also used to retract the mast by pulling the tip toward the base; the longerons again coil and compress the structure to its drumlike stowed form.

A base support, end plate, and winch were built for testing the mast in a 1 g environment. In such testing, the mast should be mounted with its base up and should be extended downward to avoid damage.

This work was done by Laurence A. Finley of Astro Research Corp. for **Marshall Space Flight Center**. *To obtain a copy of the report, "Large-Diameter Astromast Development, Phase II — Final Report," Circle 11 on the TSP Request Card.*
MFS-27088

Circle Reader Action No. 328

Fabrication Technology

Hardware, Techniques, and Processes

Books and Reports

Making Highly Pure Glass Rods

A quasi-containerless process might be used to make optical fibers.

Marshall Space Flight Center, Alabama

A proposed quasi-containerless method for making glass rods or fibers would minimize the contact between the processing equipment and the product. The method would allow a greater range of product sizes and shapes than have thus far been achieved in experiments on containerless processing.

Most research and development on containerless processing involves levitating materials by aerodynamic or acoustic forces or allowing materials to fall through long tubes while their temperatures are varied. With these methods, the specimens assume a spherical shape becuse of surface tension in the molten materials. In addition, the specimens are necessarily small because of the physical limitations of the equipment and the low thermal conductivities of the melts, which limit the heating and cooling rates in the containerless environment.

In contrast, the new quasi-containerless concept would enable the formation of glass rods. The rod diameter would be limited only by the amount of power available to melt through the polycrystalline raw material. To a large extent, the method would retain the advantages of true containerless processing. It would

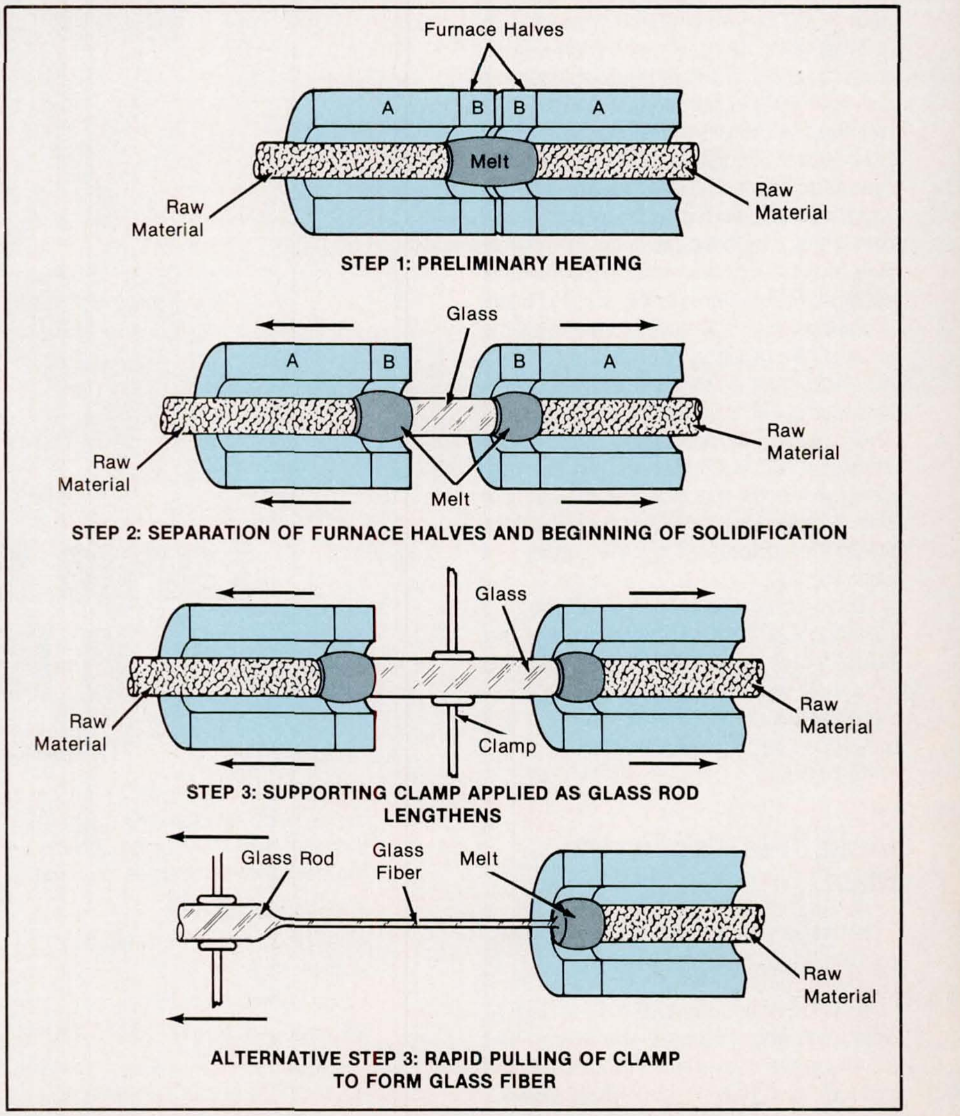

A **Molten Zone Is Established** in a polycrystalline rod. Furnace sections are separated, and a glass rod solidifies between them. A clamp then supports the solid glass as it grows in length. Pulling the clamp rapidly away from the melt draws a glass fiber. The fiber diameter could be controlled by adjustment of the pulling rate.

eliminate contamination of the melt by a crucible. It would also eliminate premature nucleation by contact with a container and would thus permit deep undercooling and unusual glass compositions.

According to the concept, the starting material is a rod of either a polycrystalline or gel precursor of the amorphous glass product. In rod form, the precursor is placed in a furnace of two movable halves, each containing two temperature zones (see figure). The walls of zones A are heated to just below the melting point of the rod. The walls of zones B are adjusted at the junction of the halves so that they melt a short zone of the rod. (As in standard floating-zone refining, the rod may be pulled through the furnace a few times to become purified and have uniformly distributed dopants.)

The sections of the furnace are slowly separated, moving the molten regions outward along the rod. The central melt cools by radiation and gradually solidifies as a glass. Premature nucleation is avoided because nothing contacts the cooling material except the molten zones, which have the same composition as that of the cooling material.

In most glasses, increasing temperatures cause the surface tensions to decrease. Therefore, bubbles in the newly formed glass melt would ordinarily tend to migrate out of the cooler solidifying rod toward the hotter melts in zones B.

Initially, the solidified glass must be supported by the surface tension of the molten zones. If the process is conducted in low gravity, longer unsupported regions are possible. External clamps may be extended to brace the glass rod after it has begun to solidify. Such a clamp may be used to draw the rod into an optical fiber, as shown in the figure.

This work was done by Robert J. Naumann of **Marshall Space Flight Center**. *For further information, Circle 17 on the TSP Request Card.*

This invention is owned by NASA, and a patent application has been filed. Inquiries concerning nonexclusive or exclusive license for its commercial development should be addressed to the Patent Counsel, Marshall Space Flight Center *[see page 29].* *Refer to MFS-28090.*

Improved Joint Design for Box-Stiffened Panels

Photoelastic models are used to visualize stress concentrations.

Langley Research Center, Hampton, Virginia

An aircraft fuselage structure must contain an internal pressure and carry the fuselage compressive loads. Optimization techniques can be used to find efficient stiffened structures to carry the compressive loads, but the internal pressure induces cyclic tensile loading transverse to the stiffeners that will determine the structural fatigue life. Therefore, in addition to carrying the compressive loads without buckling, an efficient stiffened fuselage wall must demonstrate an adequate cycle life. Mass and strength analyses and system requirements have identified a titanium-box-stiffened-skin wall (see Figure 1) as a candidate for the lightweight fuselage of a pressurized vehicle.

Test results identified a severe stress concentration at the junction of the box stiffeners with the panel skin. The stress concentration would limit the number of cycles to failure below the desired service life of 10^6 cycles at 50,000 psi (340 MPa). Photoelastic models of the stiffener-to-skin joint were used to identify quickly modifications to the joint that would lower the severity of the stress concentration. Results with various photoelastic models cut from polyurethane sheet led to a novel diffusion-bond joint with a reduced stress concentration. For verification, titanium test specimens of this joint indicated that the desired cycle life could be achieved at the desired stress level with the box-stiffened-skin panel.

Photoelastic model A in Figure 2, of the standard doubler under a tensile load, shows a severe stress concentration at the bottom of the notch. Model B of the flanged doubler shows a stress concentration that also is unacceptable. Model C, a chemically milled transition with a generous radius, shows a

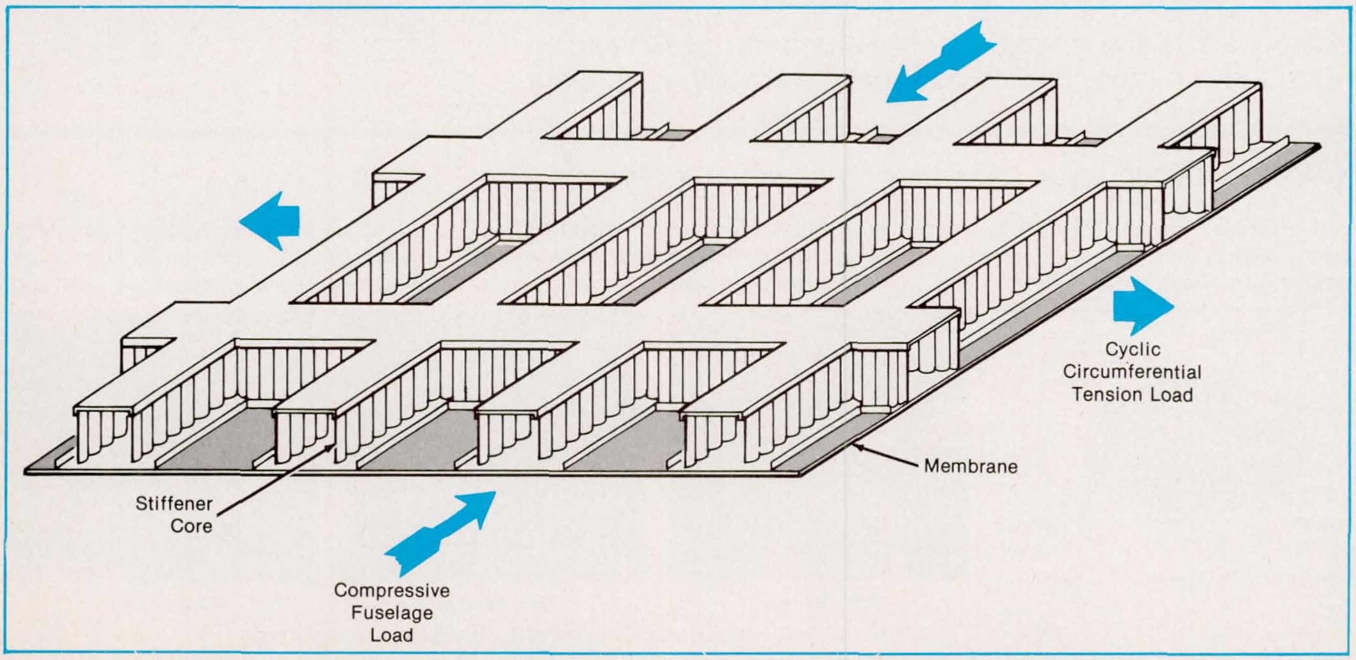

Figure 1. **The Titanium-Box-Stiffened Skin** is a candidate for use in the walls of pressurized fuselages.

stress concentration that is greatly reduced by the large radius transition, with an area of nearly zero stress at the raised corner of the land.

Model D duplicates a proposed joint in which the stiffener lower cap would be diffusion bonded to the chemically milled transition such that the bond line ends at the corner of the land, where the stresses are the lowest. Results from model D show that this location for the sharp notch of the lower cap-to-skin joint is out of the area of stress concentration that affects the cycle life. Additionally, the photoelastic-model results show that decreasing the thickness of the land under the stiffener reduces the induced bending stresses caused by a discontinuous load path and reduces the stress concentration for this improved doubler-joint design.

Titanium-fatigue-coupon test results demonstrated a potentially significant loss in fatigue life associated with the stress concentrations found in the photoelastic models. Titanium fatigue specimens with varying geometric details for the improved doubler-joint design show that increased land depth and no flange overhang increase bending stresses in the joint, adversely affecting cycle life. A refined joint with a flange overhang and a thin land gives a design that provides the desired 10^6-cycle life at 50,000 psi (340 MPa). Results from symmetric specimens show that further reductions in load-path discontinuity could improve this cycle life at even higher stresses.

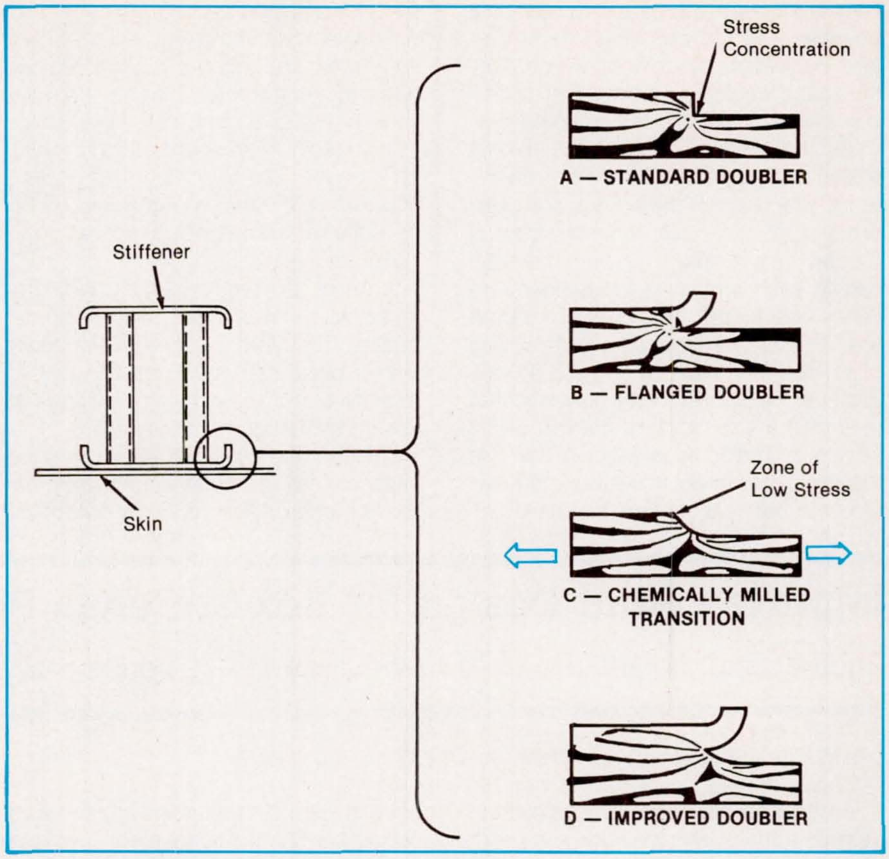

Figure 2. **Photoelastic Models** make visible the stress-concentration patterns in the stiffener-to-skin junctions.

This work was done by Randall C. Davis of **Langley Research Center** *and Paul L. Moses of PRC Kentron, Inc. Further information may be found in NASA TP-2480 [N85-33537/NSP], "Joint Design for Improved Fatigue Life of Diffusion-Bonded Box-Stiffened Panels."*

Copies may be purchased [prepayment required] from the National Technical Information Service, Springfield, Virginia 22161, Telephone No. (703) 487-4650. Rush orders may be placed for an extra fee by calling (800) 336-4700. *LAR-13460*

Smoother Scribing of Silicon Wafers

Ethanol alters the normally brittle character of the silicon wafers into a more ductile material for smoother scribing.

NASA's Jet Propulsion Laboratory, Pasadena, California

A proposed new tool may be used to scribe silicon wafers into chips more smoothly than was possible before. The new scriber produces a surface that appears ductile. The scribed groove cuts have relatively smooth walls.

The scriber would consist of a diamond pyramid point on a rigid shaft. Ethanol would flow through the shaft and

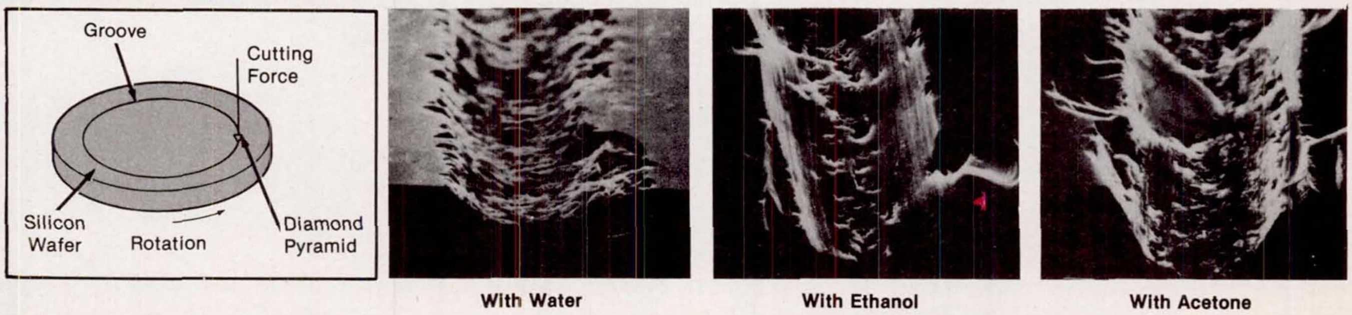

A **Groove Is Cut** in a 3-in. (7.62-cm) wafer by a diamond point. With water as a lubricant, the groove is rough and uneven; with ethanol, the groove is smoother and more sharply defined. Intermediate results are obtained with acetone.

around the point, like ink in a ballpoint pen.

Ethanol has a significantly different effect for scribing silicon than water, which is used in conventional diamond scribers. The ethanol apparently adsorbed by the silicon surface softens it for cutting. The effectiveness of ethanol as a scribing lubricant was discovered in a study of abrasion mechanisms in silicon. Wafers of polished silicon were rotated under a stationary diamond pyramid while im-mersed in various fluids (see figure). The resulting grooves were examined with a scanning electron microscope. For a given cutting speed and force on the diamond, the water-lubricated groove showed rougher, uneven walls, as compared with the ethanol-lubricated groove.

This work was done by Steven Danyluk of the University of Illinois for Caltech and **NASA's Jet Propulsion Laboratory**. *For further information, Circle 19 on the TSP Request Card.* *NPO-16568*

Robotic Vision for Welding

The view from the welding head is used to control the welder.

Marshall Space Flight Center, Alabama

A vision system for a robotic welder looks at a weld along the axis of the welding electrode. The vision system gives the robot a view of most of the weld area, including the yet-unwelded joint, the weld pool, and the completed weld bead.

The viewing optics are contained within the gas cup of a gas/tungsten arc welder (see figure). The optical components are thus protected from the heat, corrosive gas, and spattered metal just outside the cup. Moreover, the components do not interfere with the workpiece or hinder tool movement. Although the optical components are shielded by the electrode from the intense, direct light rays from the core of the arc, they nevertheless view the bright light cast on the weld area and from it produce a detailed image. A control computer analyzes the changing image in real time to guide the robot and adjust such welding parameters as current and wire feed.

A lens in the gas cup focuses an image of the weld area onto the end of a fiber-optic bundle. The torch lens is mounted in a ring having 30-mm outside diameter. A filter window protects the lens and the fiber-optic bundle from the welding environment; the window passes wavelengths around 800 nanometers. It absorbs the visible and ultraviolet radiation from the arc and the longer infrared wavelengths from the incandescent weld pool. Cooling water flowing through the torch body removes the heat of the absorbed radiation. The window also blocks fumes and spattered metal.

The fiber-optic bundle is composed of more than 100,000 glass fibers, each 10 to 12 μm in diameter and 7 ft (2.1 m) long. The fibers are arranged in a circular matrix. At each end, the bundle is encased in a stainless-steel ferrule, and the end surfaces are ground and polished. The bundle is sheathed in an oil-filled plastic tube. The packaged bundle is highly flexible to allow fast and wide-ranging movement of the robot arm and torch.

The bundle carries the image to a video camera atop the robot-manipulator boom. A cable carries the video signal to a control console, where the raw signal is processed into analog and digital video signals for the computer.

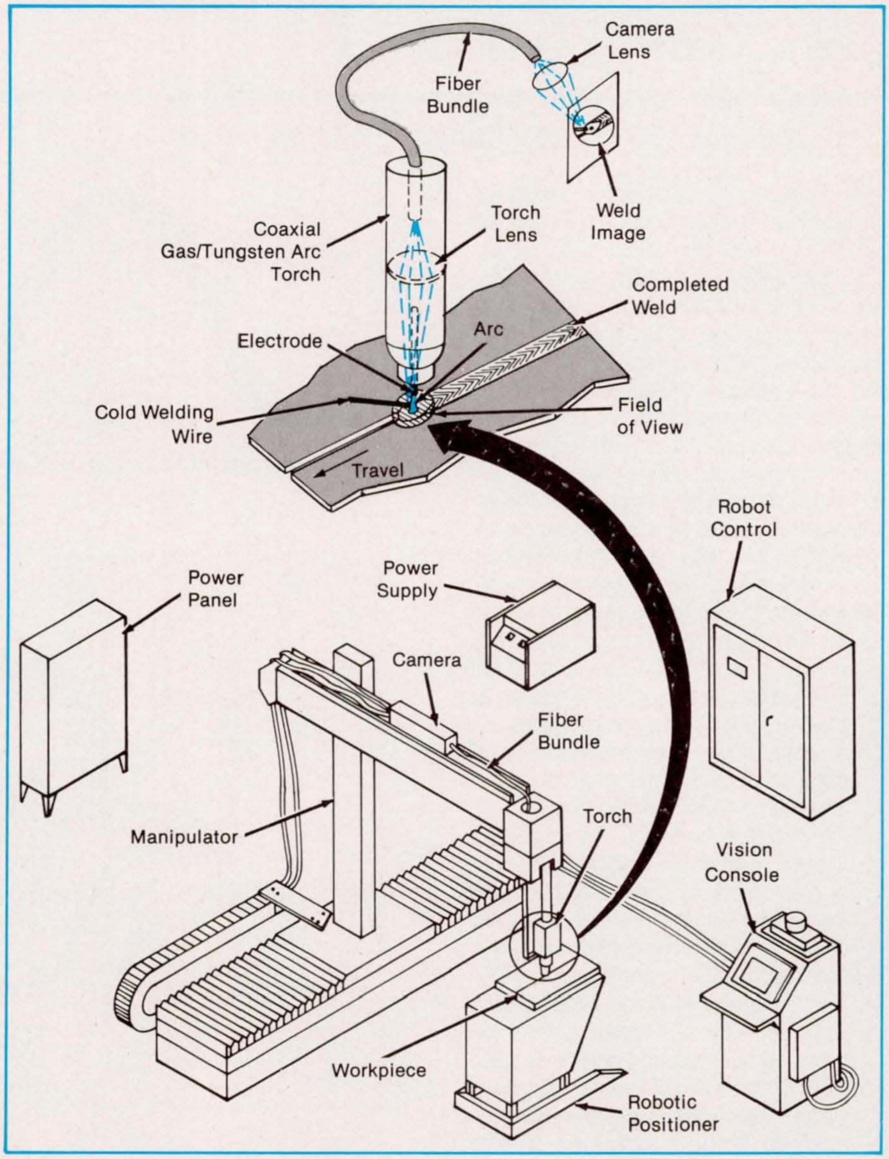

Protected Within a Welding-Torch Body, a lens and fiber bundle give a robot a closeup view of a weld in progress. Relayed to a video camera on the robot manipulator frame, the weld image provides data for automatic control of the robot motion and the welding parameters.

The computer is based on an 8-bit, 1-MHz microprocessor. It has 96 kilobytes of memory and uses 54 kilobytes of software, written in Assembler language. The software includes 30 kilobytes of specially written programs for processing images, controlling the robot, and interacting with users. The software consists of the following four modules:

1. The vision-system module supports basic system operation.
2. The image-processing system module provides real-time processing of video images to extract the locations of the weld features.
3. The "weld teach" module handles programming of the robot for specific welding jobs.
4. The vision-utilities module accommodates communication with remote systems, controls video recording of welding, and handles other supporting functions.

From the processed image data, cross-seam control commands are generated for one-dimensional control of the robot path to center the pool on the weld joint. A signal representing the width of the joint is generated and used to control the feed of welding wire into the weld. A signal representing the weld-pool width is used to control the welding current.

This work was done by Richard W. Richardson of the Ohio State University Research Foundation for **Marshall Space Flight Center.** *For further information, Circle 121 on the TSP Request Card.*

In accordance with Public Law 96-517, the contractor has elected to retain title to this invention. Inquiries concerning rights for its commercial use should be addressed to:

James B. Wilkens, Patent Administration
The Ohio State University Research Foundation
1314 Kinnear Road
Columbus, OH 43212.

Refer to MFS-27119, volume and number of this NASA Tech Briefs issue, and the page number.

Flexible Diaphragm Withstands Extreme Temperatures

This diaphragm seals and retains its flexibility from −200 to +600 °F (−129 to +316 °C).

Lyndon B. Johnson Space Center, Houston, Texas

A diaphragm seal retains flexibility throughout the temperature range of −200 to +600 °F (−129 to +316 °C). The diaphragm is durable, simple, versatile, and relatively inexpensive to manufacture. Developed specifically for the Space Shuttle orbiter, the diaphragm should be suitable for refrigeration seals, autoclaves, storage lockers, and other sealing applications subjected to extreme temperature differentials.

The diaphragm (see figure) consists of two outer layers of silicone rubber on an inner layer of glass fabric impregnated with an adhesive. The fabrication process involves the following sequence of steps:

1. An aluminum male layup mold, machined 2 percent oversize to allow for the shrinkage of the silicone rubber, is cleaned with 1,1,1-trichloroethane.
2. A continuous coat of adhesive is sprayed on the working surface and allowed to develop a good tack.
3. To aid the removal of air during vacuum bagging, a first bleeder layer of glass fabric is applied smoothly to the adhesive, with the warp in the long direction of the mold and extending beyond the diaphragm edge.
4. The bleeder fabric is coated and saturated with a release agent; for example, a fluorocarbon parting agent.
5. The first layer or sheet of calendered, uncured silicone rubber is applied without wrinkles to the bleeder fabric. Good results have been obtained with calendered, uncured methyl phenyl siloxane polymer sheet 0.030 in. (0.076 cm) thick.
6. The inner layer of continuous glass-

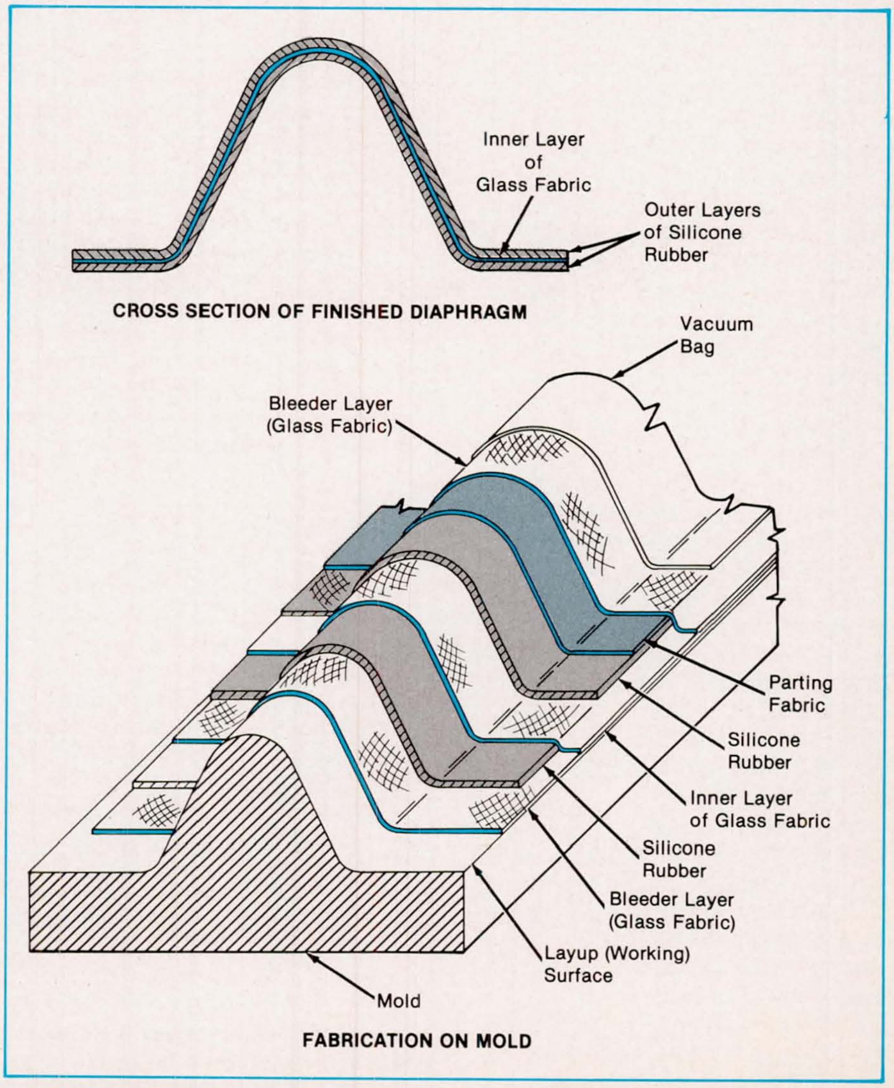

The **Flexible Diaphragm** contains a glass-fabric layer sandwiched between two silicone-rubber layers.

fabric reinforcement is applied without wrinkles, splices, or folds to the first layer of silicone rubber, maintaining the warp direction and extending beyond the edge of the silicone rubber.
7. The reinforcing layer is impregnated with diluted silicone-rubber adhesive primer.
8. The second silicone-rubber layer is applied.
9. A layer of fluorocarbon-coated or other parting fabric is applied to the second layer of silicone rubber.
10. The parting fabric is covered with a layer of bleeder fabric extending beyond the edge of the silicone rubber.
11. A vacuum bag is sealed to the layup mold over the preceding layers.
12. A vacuum is slowly applied between the vacuum bag and the mold, and the assembly of layers is cured at 345 °F (174 °C) with a pressure of 75 psi (520 kN/m^2) applied externally to the vacuum bag.
13. The assembly is cooled, the vacuum and pressure are released, and the finished diaphragm is removed from the first bleeder layer and the parting layer.
14. The diaphragm flanges are trimmed to the finished dimensions.

This work was done by Guillermo Lerma of Rockwell International Corp. for **Johnson Space Center**. *For further information, Circle 5 on the TSP Request Card.*

This invention is owned by NASA, and a patent application has been filed. Inquiries concerning nonexclusive or exclusive license for its commercial development should be addressed to the Patent Counsel, Johnson Space Flight Center [see page 29]. Refer to MSC-20797.

Repairing Foam Insulation

Holes are filled without introducing voids.

Marshall Space Flight Center, Alabama

Large holes in polyurethane foam insulation are repaired reliably by a simple method. Little skill is needed to apply the method, and it can be used for overhead repairs as well as for those in other orientations.

The method was developed for replugging pull-test holes in the insulation on a tank: After the insulating polyurethane foam has been applied, it must be tested to determine its adherence to the tank. This is a destructive test in which a plug of foam is removed.

In the previous repair procedure, liquid foam was placed in a hole and covered with tape while it cured. The resulting plug usually contained large voids of entrapped air. This was particularly true for holes in overhead and sidewall insulation because air could not escape through the solid surroundings in these orientations.

In the new repair method, a two-piece plug of foam insulation is inserted in the hole and held in place with a mounting fixture (see figure). A fresh batch of foam is mixed and, while still liquid, is injected through the plug. The liquid foam is allowed to cure and harden into a contiguous mass that joins the plug to the surrounding insulation and the substrate. After about 2 hours, the mounting fixture is removed. The protruding end of the plug and excess foam are trimmed away.

The method was demonstrated by filling 40 holes in foam 1 ½ to 2 in. (3.8 to 5.1 cm) thick. All repaired holes met the inspection requirement that a repair area contain no more than seven voids, with no more than one void greater than 0.3 in. (0.8 cm) and none greater than 0.5 in. (1.3 cm).

This work was done by J. M. Corbin and D. F. Buras of Martin Marietta Corp. for **Marshall Space Flight Center**. *For further information, Circle 61 on the TSP Request Card.*

Inquiries concerning rights for the commercial use of this invention should be addressed to the Patent Counsel, Marshall Space Flight Center [see page 29]. Refer to MFS-28109.

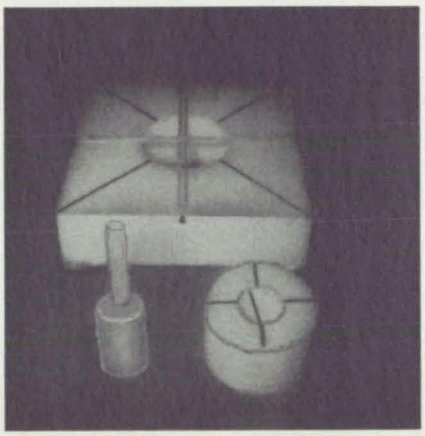

Two-Piece Plug and Mounting Fixture

Plug and Fixture Installed Over Hole

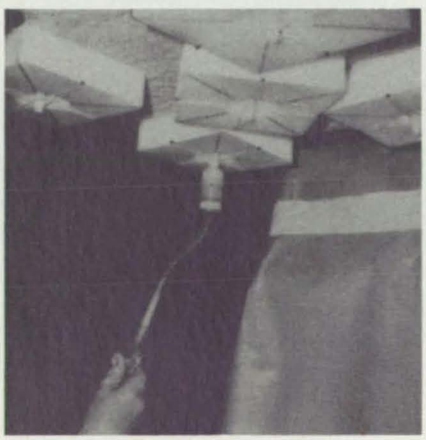

Injection of Foam

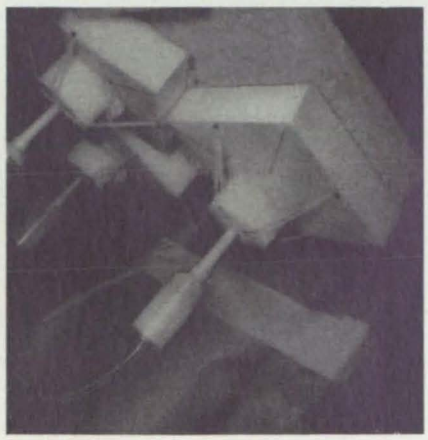

Curing of Completed Repair

A Plug Is Positioned in the Hole to Be Filled and held in place with a mounting fixture. Fresh liquid foam is injected through the plug to bond it in place. As the foam cures and expands, it displaces the plug outward. This protrusion is later removed.

Liquid-Dopant Fabrication of Solar Cells

Cells are as efficient as those produced by gaseous diffusion.

NASA's Jet Propulsion Laboratory, Pasadena, California

Liquid dopants and liquid masks are used to produce the front and back junctions of solar cells. The resulting cells are equal in efficiency to those fabricated by the more-expensive gaseous-diffusion technique.

To begin the fabrication of the back junction, liquid boron dopant is applied to the back of dendritic-web silicon, and a liquid mask is applied to the front. Then the wafer is baked at 200 to 400 °C for 15 minutes to remove excess solvents. The dopant is then thermally diffused into the silicon from the back surface. After diffusion, the mask and the excess dopant (now in the form of a glass) are removed.

To begin the fabrication of the front junction, liquid phosphorus dopant is applied to the front of the wafer, and a liquid mask is applied to the back. Again, the wafer is baked at 200 to 400 °C for 15 minutes to remove excess solvents. The phosphorus dopant is then thermally diffused into the silicon. The diffusion glass is then removed.

This work was done by Paul Alexander, Jr., of Caltech for **NASA's Jet Propulsion Laboratory** *and Robert B. Campbell of Westinghouse Corp. For further information, Circle 100 on the TSP Request Card.*
NPO-16652

Books and Reports

These reports, studies, and handbooks are available from NASA as Technical Support Packages (TSP's) when a Request Card number is cited; otherwise they are available from the National Technical Information Service.

Development of Graphite/Epoxy Corner Fittings

Various layup patterns are evaluated.

A report documents a development project aimed at improving the design and load-carrying ability of a complicated corner fitting for an optical bench. The new fitting is made of graphite filaments in an epoxy-resin matrix. The composite material was selected as a replacement for titanium because it is lighter and because its dimensions change little with temperature variations. Previous efforts to use graphite/epoxy had to be abandoned in favor of titanium because the composite material was too weak.

The objectives of the project were to evaluate layup changes to increase the ultimate strengths of the parts, to develop basic data on the material, to establish analysis methods, and verify the design and analysis by testing full-size parts. Four different fitting designs were executed, each differing from the other by the arrangement, or layup of the composite material.

The unsuccessful graphite/epoxy fittings that preceded the titanium version failed by fracture along the laminate splice lines. These lines lay along the edges of the fitting. In the new graphite/epoxy fittings, the same laminate material, fiber orientation, resin content, and basic dimensions were used. The layup patterns, however, were modified to relocate the splice lines away from the corners.

Strain-gauge measurements were made while the fittings were subjected to static-load tests. The ultimate failure load varied from a low of 2,229 lb (9,915 N) to a high of 4,492 lb (19,981 N). The test results did not correlate closely with the predictions of finite-element structural analysis using classical laminate theory. Test results also did not correlate closely among different fittings of the same configuration. The low correlation has been tentatively attributed to the lack of quality control in fabrication. This kind of variation among units is typical of composite materials.

This work was done by Gwyn Faile, Rose Hollis, Frank Ledbetter, Juan Maldonado, Jim Sledd, Jim Stuckey, Gerald Waggoner, and Erich Engler of **Marshall Space Flight Center**. *Further information may be found in NASA TM-86512 [N85-32147/NSP], "Development and Test of Advanced Composite Components."*

Copies may be purchased [prepayment required] from the National Technical Information Service, Springfield, Virginia 22161, Telephone No. (703) 487-4650. Rush orders may be placed for an extra fee by calling (800) 336-4700. The report is also available on microfiche at no charge. To obtain a microfiche copy, Circle 101 the the TSP Request Card.
MFS-27129.

Mathematics and Information Sciences

Hardware, Techniques, and Processes

Estimating Wall-Induced Velocities in Wind Tunnels

Wall effects are calculated from upwash distributions.

Ames Research Center, Moffett Field, California

Estimates of wall effects in a two-dimensional wind tunnel are obtained using upwash measurements on two contours near the test model. The method is derived from a combination of prior techniques that correct for wall effects.

The improved method is limited to flows describable by linear equations. Measured flow perturbations are assumed to be superpositions of the perturbations resulting from the model in free air at a corrected airspeed and angle-of-attack, plus perturbations produced by the tunnel walls. The mathematical assumptions are valid if wall-induced velocities are uniform near the model: Test conditions become increasingly uncorrectable as wall-induced velocity gradients grow near the test model.

The wind-tunnel geometry is shown in the figure. The model is enclosed by two integration contours, each consisting of two horizontal lines extending an infinite distance upstream and downstream, joined at their ends by vertical lines. Since the contribution of the vertical lines to the flow field is infinitesimal due to their infinite distance from the model, the contours are treated as consisting of the horizontal lines alone. The lines closest to the model are called "source levels," while the outer lines are called "field levels."

The Schwarz formula (which is a linear transformation) enables the calculation of the wall-induced upwash along the tunnel axis ($y = 0$) from the symmetric component of the wall-induced upwash at either the source or the field level. Similarly, the streamwise velocity perturbation at the axis due to the walls is obtained from equations that involve the antisymmetric upwash components measured at the source and field levels. Model-induced upwash is then expressed as the difference between the total upwash and the wall-induced upwash.

The Schwarz operators are determined from potential-flow theory, in which it is assumed that the wall-induced flow within the control contour is governed by Laplace's equation. The resulting velocity-transformation equations give the upwash and streamwise perturbations at the axis in terms of integrals of weighted upwash values along the contours. In practical situations, continuous upwash distributions are approximated by sets of upwash measurements at discrete points, the integrals therefore being replaced by sums.

The method was tested in a mathematical simulation of a wind tunnel with simple singularities. In another test, data from an adaptive-wall wind-tunnel experiment were analyzed. The method accurately predicted the wall-induced velocities along the centerline of the theoretical wind tunnel and confirmed that the wall adjustments substantially reduced wall interference.

This work was done by Edward T. Schairer of **Ames Research Center**. *For further information, Circle 27 on the TSP Request Card.*

Inquiries concerning rights for the commercial use of this invention should be addressed to the Patent Counsel, Ames Research Center [see page 29]. Refer to ARC-11586.

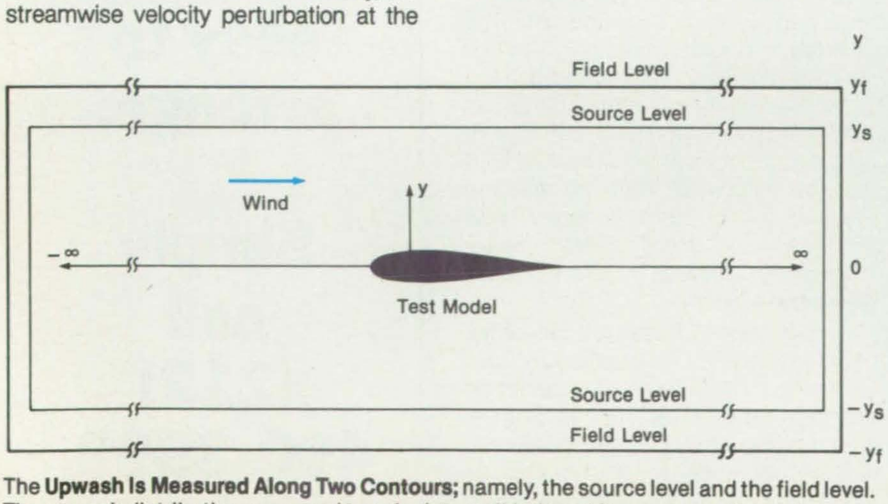

The **Upwash Is Measured Along Two Contours;** namely, the source level and the field level. The upwash distributions are used to calculate wall-induced flow perturbations along the tunnel axis.

Life Sciences

Books and Reports

These reports, studies, and handbooks are available from NASA as Technical Support Packages (TSP's) when a Request Card number is cited; otherwise they are available from the National Technical Information Service.

Estimating Crop Yields From Multispectral Reflectance

Progress in developing an economical way of predicting yields is reported.

Three reports describe research on a proposed method for estimating crop yields by combining meteorological data with satellite measurements of reflected radiation to estimate crop-absorbed radiation. The concept, when tested over large areas, could form the basis for evaluating crop conditions and estimating yields over regions where ground observations would be too costly or too difficult.

The research involves the terrestrial measurement and analysis of the multispectral reflectance and the amount of radiation intercepted by corn, soybeans, and wheat grown under several different management systems. In principle, the terrestrial radiation measurements can be correlated with satellite spectral reflectance measurements for use in the crop-yield model.

One of the papers, "Spectral Estimation of Absorbed Photosynthetically Active Radiation in Corn Canopies," discusses methods of incorporating multispectral data into mathematical models for crop conditions and yields. It concludes that the absorbed photosynthetically active radiation (PAR), cumulated through the growing season, is a better indicator of yield than is the cumulated-leaf-area index. It suggests that the absorbed PAR may be estimated from the spectral reflectances of corn canopies with large areas, where direct measurements of leaf-area indices would be prohibitively costly.

Another paper, "Spectral Estimates of Solar Radiation Intercepted by Corn Canopies," describes experiments on combining spectral and meteorological data. Agronomic data collected to coincide with the spectral data included the leaf-area index, biomass, development stage, and final grain yields. The paper concludes that the concept of estimating the intercepted solar radiation from spectral data represents a viable approach for merging spectral and meteorological inputs.

The third paper, "Techniques for Measuring Intercepted and Absorbed PAR in Corn Canopies," describes a study of several techniques in which a line sensor that spatially averages the photosynthetic-photon flux density is used to measure the transmitted and absorbed PAR in corn canopies. The effects of the orientation and length of the sensor upon measurements of the transmitted PAR and the errors induced by using the intercepted PAR (the total incoming radiation minus the transmitted PAR) as an estimate of the absorbed PAR, were examined. The measurements of the intercepted PAR generally resulted in less than a 4-percent overestimate of the absorbed PAR throughout most of the growing season. Thus, the intercepted PAR appears to be a reasonable measure of the absorbed PAR.

This work was done by C. S. T. Daughtry of Purdue University for **Johnson Space Center**. *To obtain copies of the reports, Circle 82 on the TSP Request Card.*
MSC-21060

Letters

The "Letters" column is designed to encourage a wide exchange of ideas among *NASA Tech Briefs* readers. To contribute a request for information or to respond to such a request, use the feedback cards in this issue, or write or call: Manager/Technology Transfer Division, P.O. Box 8757, Baltimore/Washington International Airport, MD 21240; (301) 859-5300. While we can print only a small number of letters, we will endeavor to select those that are of varied and wide interest.

FREE PUBLICITY

I have developed a VDT, CRT radiation antiglare product. Also a new printer silencer. Your polymer articles and acoustical pieces have helped my product R & D immensely, and your polymer rust VV effect articles, also. What is the procedure for publicity in Spinoffs? *I can send R & D reports at your request. Absolutely wonderful articles. Thank you!*

Christopher B. Veleke
President
Data Research
Portland, OR

To find out if you qualify for publication in *Spinoff*, NASA's annual report on commercial applications of NASA-developed technology, contact Linda Watts at NASA Spinoff, Technology Transfer Division, P.O. Box 8757, BWI Airport, MD 21240.

ECHOES OF THE ECO-SPHERE

My first issue—it looks great! Where can I get a reprint of the EcoSphere technology transfer?

D.B. Jensen
Cons. Engineer
Realtime Consulting
Mansfield, OH

Engineering Research Associates, Inc., 500 N. Tucson Blvd., Tucson, AZ 85716 (602/881-6555) is the exclusive licensee of the EcoSphere technology, which was developed and patented at NASA's Jet Propulsion Lab. For more information, contact ERA, Inc., in Tucson, or the Patent Counsel at JPL. His name and address are on page 29.

WITH THE NAVY

I was especially intrigued by the Oil-Free Compressor (NTB, p. 130, March/April 1986). This would solve a major shipboard problem which occurs with maddening frequency in heavy seas. No compressor was ever designed for shipboard use, regardless of what is written. The oil-free compressor should be standard gear on Navy ships. I intend to investigate this problem further. Tech Briefs has helped.

Christopher P. Sagovac
Lt. J9
U.S. Navy
FPO San Francisco, CA

NASA Tech Briefs is a very informative publication. You are doing a great job of providing information on what your labs and consultants are doing. I wish your concept of providing this type of information could be expanded to other government agencies. I work for the Air Force at Hill AFB, Utah, doing electronic failure analysis. I feel isolated from other government labs doing similar work, with the exception of the information I receive through Tech Briefs.

Scott M. Edwards
Ogden, UT

The U.S. Navy publishes a free monthly technology transfer fact sheet. For more information about becoming a subscriber, write: The Navy Domestic Technology Transfer Fact Sheet, Code E211, Naval Surface Weapons Center, Dahlgren, VA 22448-5000.

WITH THE SCOUTS

Would it be at all possible to obtain copies of the report of the National Commission on Space and the report of the investigation of the shuttle failure for use as background for the Boy Scout Space Exploration Merit Badge?

Neal E. Wilson
Boy Scouts of America
Newington, CT

The report of the National Commission on Space has been published by Bantam Books. It is available for $14.95 plus $1.00 handling from Science News, Book Order Service, 1719 N Street N.W., Washington, DC 20036.

The report by the Presidential Commission on the Shuttle Challenger Accident is on sale for $18 a copy from the Government Printing Office, 710 North Capitol Street, Washington DC 20401. The order number is 040-000-00496-3.

WITH THE WEEDS

The article on NSTL plant-based purification systems (NTB, May/June, p. 18) caught my eye. I would appreciate any additional information available on its application to individual homeowners.

Gerald A. Loignon, Jr.
Assoc. Mgr.—Performance & Results
South Carolina Electric & Gas Co.
Jenkinsville, SC

You can contact NSTL's technology utilization officer for more information on applying plant-based purification technology. His name, address and phone number are listed on page 29.

"FRAMEWORK" FOLLOW-UP

The "Framework for Action" series (May/June 1986, pp. 157-161 and preceding installments) was excellent. It would be nice if reprints were available.

George D. Uffenorde
Senior Specialist Engineer
Boeing Commercial Airplane Co.
Seattle, WA

For information concerning the availability of "Framework for Action" reprints, contact the Office of NASA Productivity Programs, NASA Headquarters, Code ADA, Washington, DC 20546; (202) 453-8437.

Information concerning the 1986 NASA Symposium on Quality and Productivity "Strategies for Revitalizing Maturing Organizations," to be held December 2-3, 1986, in Washington, DC, can also be obtained by contacting the Office of Productivity Programs.

CHANGE OF PLANS

I am writing to comment on a photograph in the July/August issue of NASA Tech Briefs. On pages 12 and 13, you show an aerial view of Kennedy Space Center, including the Vehicle Assembly Building, Launch Control Center, and Orbit Processing Facility. I would like to call attention to the fact that this photograph is reversed.

When viewing the VAB from the south (the side with the American flag and bicentennial emblem), the LCC should be on the right, while the OFP would appear on the left. I have enclosed a copy of the map of the VAB area at KSC, which should clarify this. I hope that this was simply an oversight on the part of your staff and does not mean major facility modifications are being planned here at KSC.

Arlan G. Cage
McDonnell Douglas Astronautics Company
Kennedy Space Center, FL

Clyde Pennington asked us in what mirror we took that photo of the VAB. For the many who wrote or called to tell us the picture was "flopped," don't worry—the bulldozers aren't on the way. We regret the error.

MORE MAILBAG

No direct application yet, but it give me interesting ideas and is a prize publication in my periodicals library. I also think the selected commercial advertisements are a plus over the former (no ads) version.

A couple of page article on COSMIC would be useful in a future edition.

Jeffrey S. Katz
Design and Development Engineer
Advanced Computer Applications
Windsor, CT

Computer Previews '87, a special issue to be sent to all NASA Tech Briefs subscribers in December, will contain articles on COSMIC,® as well as other information on NASA's computer capabilities.

Subject Index

Advertiser's Index

*RAC stands for **Reader Action Card.** For further information on these advertisers, please circle the RAC number on the Reader Action Card elsewhere in this issue. This index has been compiled as a service to our readers and advertisers. Every precaution is taken to ensure its accuracy, but the publisher assumes no liability for errors or omissions.

Mission Accomplished

Through the technology transfer process, many of the systems, methods and products pioneered by NASA are re-applied in the private sector, obviating duplicate research and making a broad range of new products and services available to the public.

To the inventor, the challenge faced time and again is to push back the gates of that which is known and enter uncharted territory, to unlock the imagination and discover its secret trails. The trick is to find the key, the muse, the spark of an idea that will burst open the gates, clear the fog, and lead to creative solution.

In February 1986, Joseph King, a 27-year-old engineering associate for RCA's Automated Systems Division, was standing before the gates of the unknown. Working on an intrusion detection system that had already reached the fabrication stage, Mr. King was faced with a problem. The test system, designed to detect simulated targets, was just too large and clumsy.

"In addition to the typical constraints of time and board space, our available power was extremely limited," explained Mr. King. "We had to strive for simplicity."

His goal was to replace the existing circuitry with a new design that would minimize the number of switches on the console and simplify operation of the equipment, consequently bringing down skyrocketing costs. The solution? Experience provided the engineer with a notion where it might be found—in the pages of NASA Tech Briefs.

"I first started receiving NASA Tech Briefs in 1982 while working for Northrop Corporation," Mr. King said. "It's quite a useful and informative magazine. I save all my old copies, never throw one out. If any kind of problem comes up, I have somewhere to turn."

In 1985, his final year at Northrop, Mr. King redesigned a cooling system used to control the temperature of an inertial navigation system. His design was based on a process described in NASA Tech Briefs. "I read in Tech Briefs how scientists working on the Space Shuttle would intentionally frost fluid lines to improve insulation," stated Mr. King. "This gave me an idea. I found that by pre-cooling, by letting the lines frost, we could get down to the temperature we wanted in one hour, halving the amount of time it took to reach the desired temperature."

But for Joseph King this was only the beginning, a warmup exercise. In February 1986, when his test system became a big and growing headache, Mr. King sought out his muse.

"With thoughts of the circuit in mind, I was looking through an old issue of NASA Tech Briefs (Spring 1984) when I came across the 'Digital Sequence Controller' article," Mr. King recalled. "I said to myself, 'That's just it. That's exactly what we want.' "

This brief, by James O. Lonborg of Caltech, gave the resourceful engineer three ideas. First, the sequencing controller would eliminate several switches on the system's console, simplifying operation. Second, the circuit's power consumption was low enough to allow battery operation, which alleviated Mr. King's power supply concerns. And because of its versatility, the 555 IC described in the brief would provide an ideal initial building block. It could be used as the systems clock, as the various timing elements to provide necessary delays, and, since it could source 200 mA, as the driving stage.

While the sequencing controller would provide many answers, one problem yet remained—lack of space. The chip count required to provide even a single output was well beyond Mr. King's available space. His solution? The invention of the "Multiple Output Sequencing Controller" (see accompanying article), an improvement over Mr. Lonborg's model.

"With the numerous types of PLDs (Pro- ►

RCA Engineers John Carvalho (left) and Joe King.

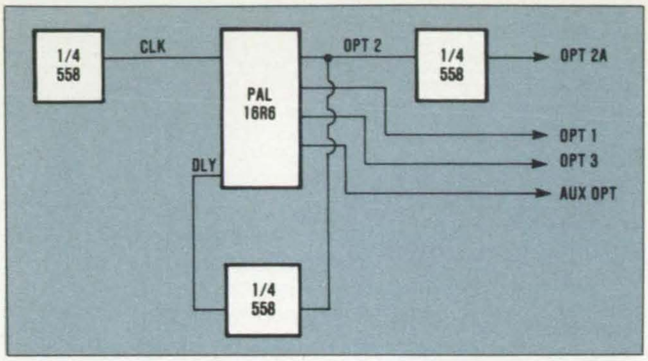

Block diagram of Joseph King's Multiple Output Sequencing Controller

grammable Logic Devices) on the market," stated Mr. King, "I thought a much more eloquent approach could be taken. After a little more research, I discussed the subject with our local PLD expert, John Carvalho (a senior project member at RCA). Together we decided that by using the concept of finite state machines as applied to MMI's series of PALs and integrated with a network of 555s, a powerful multiple output sequencing controller could result."

Within days the engineers had developed a two-chip version. A tremendous advantage of the design was an over 66% reduction in IC population from the original circuit, resulting in even lower power consumption and, in Mr. King's words, "considerably less real estate." This versatile sequencing controller is now being applied to two other pieces of test equipment in the developmental stage at RCA.

Joseph King has always been a man who gets results. During a term in the Marine Corp (1978-1982) in which he worked on radar jammers, Mr. King established a 95% repair rate, the highest in Marine Corp history. He has no thoughts of resting on his laurels. Currently, he and Mr. Carvalho are developing a device that will allow power current sensing without introducing a power loss into the system. Whether or not the final product succeeds, Mr. King is already ahead of the game, because the next time he walks up that winding path and approaches the gates of uncertainty, he carries with him an invaluable secret: He knows just where the key may be hidden. ☐

MULTIPLE OUTPUT SEQUENCING CONTROLLER

by Joseph D. King
RCA Automated Systems Division
Burlington, MA 01803

A new multiple output sequencing controller has been designed with only two integrated circuits and a total current consumption of less than 50 mA (see Fig. 1). It operates as an eight-state, gray-encoded machine utilizing combinatorial and registered logic as implemented in a programmable logic device (see Fig. 2).

This new circuit generates clock pulses capable of controlling sequential devices by using a 558 to supply both a system clock and the various timing elements to a PAL 16R6. The two-chip design, made possible by applying the concept of finite state machines, provides several distinct advantages. First, it allows for a variable output pulse width that is not only independent of the system clock, but is also independent of the other additional output pulses. The pulse width is varied by keeping an output high or low for more than one state through the Boolean expressions that define the different states (see Figs. 2 and 3).

A second advantage of this new circuit design is a clocked output that is available only during one or more of the delay stages. The output frequency is a user variable, independent of the ►

system clock. A possible application of this output is to drive a step motor that supports a video camera. The conventional output pulses could then be used to trigger the camera at each static position.

A third advantage is that the sequencing controller is nonretriggerable, which is achieved by not including the enable switch in the Boolean expression for states 1 through 7. The controller operates in the non-stable mode, requiring a manual switch actuation to start operating the system. Upon completion of the sequencing period, the controller returns to the idle state and awaits retriggering. In a later application, the state equations were modified to allow the machine to free-run until reset. ☐

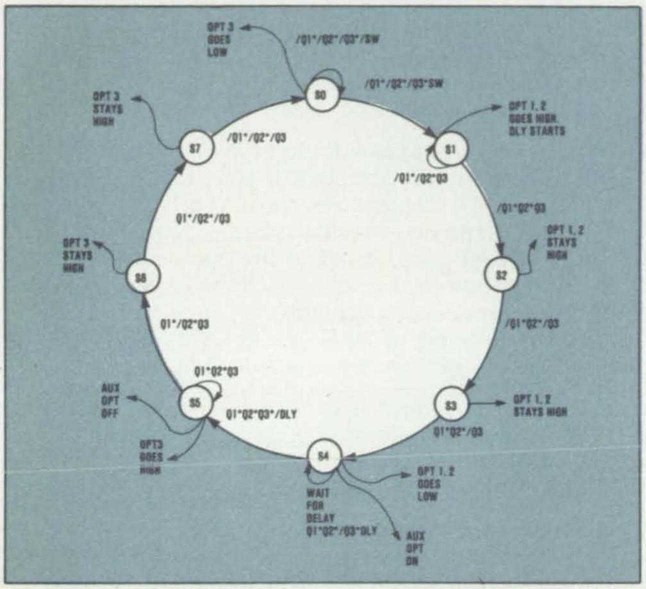

Multiple Output Sequencing Controller state diagram

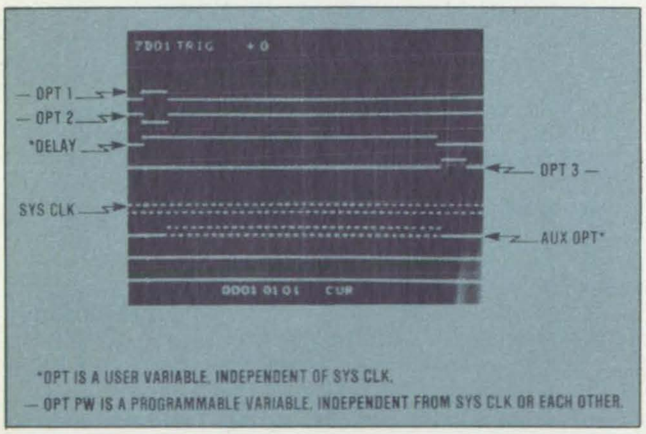

Multiple Output Sequencing Controller timing diagram

This device generates the control signals for the Sequencer. The count sequence is as follows:

Q1	Q2	Q3		
0	0	0	S0	Idle state waits for switch to be pressed
0	0	1	S1	Generates output 1 pulse for f = 3 * 1/1200 Hz
0	1	1	S2	
0	1	0	S3	Waits in this state for end of long delay
1	1	0	S4	Generates output 2 pulse for f = 3 * 1/1200 Hz
1	1	1	S5	Return to idle state
1	0	1	S6	
1	0	0	S7	
0	0	0	S0	

Multiple Output Sequencing Controller count sequence

ABOUT THE NASA TECHNOLOGY UTILIZATION PROGRAM

This document was prepared under the sponsorship of the National Aeronautics and Space Administration. NASA Tech Briefs is published bi-monthly and is free to engineers in U.S. industry and to other domestic technology transfer agents. It is both a current-awareness medium and a problem-solving tool. Potential products...industrial processes...basic and applied research...shop and lab techniques...computer software...new sources of technical data...concepts...can be found here. The short section on New Product Ideas highlights a few of the potential new products contained in this issue. The remainder of the volume is organized by technical category to help you quickly review new developments in your areas of interest. Finally, a subject index makes each issue a convenient reference file.

Further information on Innovations—Although some new technology announcements are complete in themselves, most are backed up by Technical Support Packages (TSP's). TSP's are available without charge and may be ordered by simply completing a TSP Request Card, found at the back of this volume. Further information on some innovations is available for a nominal fee from other sources, as indicated. In addition, Technology Utilization Officers at NASA Field Centers will often be able to lend necessary guidance and assistance.

Patent Licenses—Patents have been issued to NASA on some of the inventions described, and patent applications have been submitted on others. Each announcement indicates patent status and availability of patent licenses if applicable.

Other Technology Utilization Services—To assist engineers, industrial researchers, business executives, Government officials, and other potential users in applying space technology to their problems, NASA sponsors Industrial Applications Centers. Their services are described on pages 28-29. In addition, an extensive library of computer programs is available through COSMIC, the Technology Utilization Program's outlet for NASA-developed software. See special section on computer programs on page 74.

Applications Program—NASA conducts applications engineering projects to help solve public-sector problems in such areas as safety, health, transportation, and environmental protection. Two applications teams, staffed by professionals from a variety of disciplines, assist in this effort by working with Federal agencies and health organizations to identify critical problems amenable to solution by the application of existing NASA technology.

Reader Feedback—We hope you find the information in *NASA Tech Briefs* useful. A reader-feedback card has been included because we want your comments and suggestions on how we can further help you apply NASA innovations and technology to your needs. Please use it; or if you need more space, write to the Manager, Technology Transfer Division, P.O. Box 8757, Baltimore/Washington International Airport, Maryland 21240.

Advertising Reader Service—Reader Action Card (RAC): For further information on the advertisers, please circle the RAC number on the separate Reader Action Card in this issue.

Change of Address—If you wish to have *NASA Tech Briefs* forwarded to your new address, use the Subscription Card enclosed at the back of this volume of *NASA Tech Briefs*. Be sure to check the appropriate box indicating change of address, and also fill in your identification number (T number) in the space indicated.

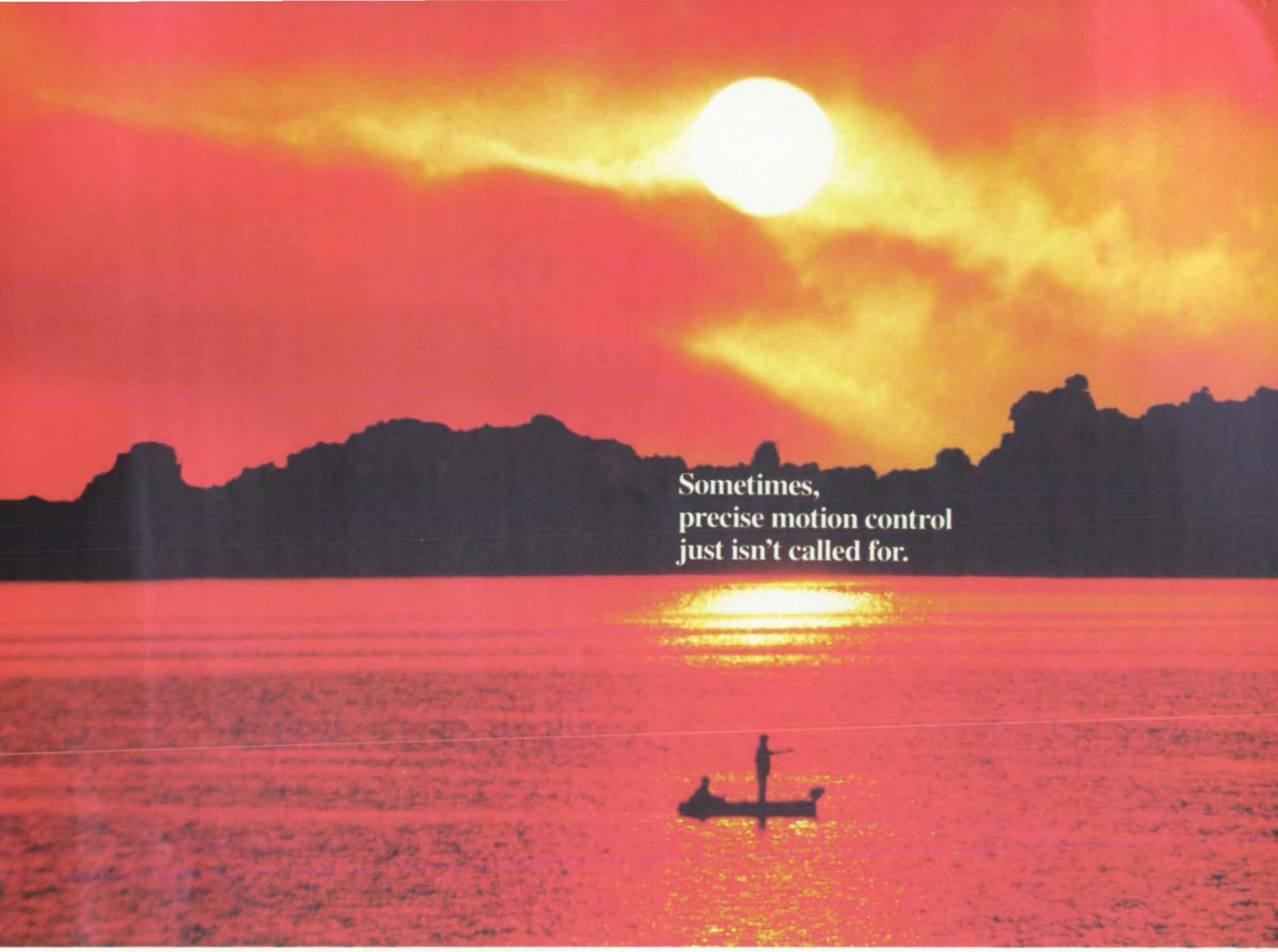

But when it is, call BEI. We offer you the most complete line of accurate, high-reliability motion control components and systems anywhere in the world.

Standard and custom motion components from BEI are applied to advanced products in a broad variety of markets and industries. These include computer and office automation machines, light and heavy-duty industrial equipment, and the world's most accurate, high-resolution, and reliable components for space and military systems.

BEI Divisions are dedicated to being the best in their respective motion component specialties. Look to BEI for:

- Optical Rotary Encoders
- Brushless Motors, Actuators, Commutators and Drive Electronics
- Precision Servo Drives for Controlling Rate, Position, and Instrumentation Indexing
- Integrated Drive or Motion Control Assemblies

When accurate, reliable motion components are essential to your product or program, call BEI at (619) 931-1500. Or write to us at the address below.

BEI Motion Systems Company
2111 Palomar Airport Road • Suite 250 • Carlsbad, CA 92008

BEI

When reliable motion control is essential.

Circle Reader Action No. 337

CHIPS TO GO.

If you're hungry for some of the new MIL-STD-1750A chips, we've got them. Fact is, we can serve 'em up right now. Full MIL temperature range, low power, high speed. No waiting. Our MDC281 is the first microprocessor chipset to gain MIL-STD-1750A (Notice I) verification. It's a general-purpose, 16-bit module consisting of three CMOS/SOS Large Scale Integrated Circuits on a single plug-in assembly.

The MDC281 is ideal for embedded applications in small systems where there are size, weight and power limits. It performs across the full MIL temperature range (−55° C to +125° C) on less than two watts, and is available in several speed and screening grades. If you need MIL-STD-1750A chips, call (314) 234-8040. Or write: McDonnell Douglas Microelectronics Center, Marketing, MOO2/111, P.O. Box 516, St. Louis, MO 63116.

We serve orders to go.

MCDONNELL DOUGLAS

Circle Reader Action No. 372